

Griffiths, D.M. (1975) Infrared studies of the rutile surface. PhD thesis, University of Nottingham.

**Access from the University of Nottingham repository:**

<http://eprints.nottingham.ac.uk/12307/1/457457.pdf>

**Copyright and reuse:**

The Nottingham ePrints service makes this work by researchers of the University of Nottingham available open access under the following conditions.

This article is made available under the University of Nottingham End User licence and may be reused according to the conditions of the licence. For more details see:  
[http://eprints.nottingham.ac.uk/end\\_user\\_agreement.pdf](http://eprints.nottingham.ac.uk/end_user_agreement.pdf)

**A note on versions:**

The version presented here may differ from the published version or from the version of record. If you wish to cite this item you are advised to consult the publisher's version. Please see the repository url above for details on accessing the published version and note that access may require a subscription.

For more information, please contact [eprints@nottingham.ac.uk](mailto:eprints@nottingham.ac.uk)

INFRARED STUDIES OF THE  
RUTILE SURFACE

by

D. M. GRIFFITHS B.Sc.

Thesis submitted to the University  
of Nottingham for the degree of  
Doctor of Philosophy, October, 1975

**BEST COPY**

**AVAILABLE**

Variable print quality

To my Father

## ACKNOWLEDGEMENTS

The work described in this thesis was carried out under the supervision of Dr C H Rochester whose help and advice have been invaluable during the project. I should like to thank British Titan Products Co. Ltd. for the award of a research grant and for their technical assistance. I am indebted to the glass-blower, Mr A Buckland, and to Mr K Rigley and the workshop staff, who not only built much of the apparatus used in this work but helped in its design. The thesis was typed by Mrs K Kennedy to whom I am very grateful for her care and patience.

Many thanks are due to my wife for her endless help and encouragement during the writing of the thesis.

## ABSTRACT

The thesis describes infrared spectra recorded during the adsorption of water, acetone, acetic acid and hexafluoroacetone onto oxidized and reduced rutile, and the development of a technique for recording the infrared spectrum of a solid immersed in a liquid.

Bands observed on the hydroxylated rutile surface have been assigned to hydroxyl groups on the (110) plane and water molecules adsorbed onto strong and weak Lewis sites on all exposed planes. The hydroxyl groups exist as isolated or hydrogen bonded groups on surface titanium ions or as hydrogen ions on bridging oxygen ions. Reduction of the rutile surface considerably decreased the amount of molecular water adsorbed on the hydroxylated surface.

The adsorption of acetone onto the hydroxylated surface took place in three consecutive stages, the first involved acetone molecules Lewis-bonding to weak sites, the second resulted in the formation of mesityl oxide on strong surface sites and occurred with stage one in the absence of surface water molecules. In the third stage acetate molecules were formed as a result of the decomposition of mesityl oxide.

Adsorption of acetic acid onto rutile resulted in the formation of water and appearance of bands due to acetate groups and Lewis-bonded complexes on the weak sites.

Hexafluoroacetone reacted with surface hydroxyls to produce a salt of the gem-diol hexafluoropropane-2,2-diol, which decomposed on the removal of water to form trifluoroacetate species.

An infrared cell has been developed enabling solid discs to be treated and immersed in a solution under inert conditions. The cell, of path length 0.7cm, has been used to study the adsorption of ether, from a solution in carbon tetrachloride, onto silica. Designs of variable path length cells for use under vacuum are included.

## CONTENTS

### SECTION 1

	<u>Page</u>
PREFACE	i
<u>CHAPTER 1 INTRODUCTION</u>	
1.1 TITANIUM DIOXIDE	1
1.2 BULK PROPERTIES	3
1.3 CATALYTIC ACTIVITY	
1.3.1 Theories of Catalysis	5
1.3.2 Catalytic Properties of Rutile	7
1.4 STUDIES OF SURFACE CHARACTERISTICS	
1.4.1 Electron Spin Resonance Studies	8
1.4.2 Electrical Measurements	9
1.4.3 Infrared Spectroscopy	10
1.4.4 Raman Spectroscopy	11
1.5 INFRARED STUDIES OF TITANIUM DIOXIDE	
1.5.1 Previous Work	13
1.5.2 The Present Work	13
<u>CHAPTER 2 EXPERIMENTAL</u>	
2.1 INTRODUCTION	
2.1.1 General Requirements of the Apparatus	15
2.1.2 The Vacuum Frame	15
2.1.3 Design of an Infrared Cell	16



	<u>Page</u>
2.1.4 The Cryostat	18
2.1.5 The Infrared Spectrometer	19
2.1.6 The Pretreatment of Rutile	22
2.2 APPARATUS	
2.2.1 The Vacuum Frame	24
2.2.2 The Cells	
A. Cell used by Ramsbotham	26
B. Cell used by Jackson	27
2.2.3 The Cryostat	
2.2.4 The Infrared Spectrometer	30
2.2.5 Operation	32
2.3 REAGENTS	
2.3.1 Rutile	34
2.3.2 H <sub>2</sub> O and D <sub>2</sub> O	36
2.3.3 Acetone h <sub>6</sub> and d <sub>6</sub>	37
2.3.4 Hexafluoroacetone	37
2.3.5 Acetic acid d <sub>4</sub>	36
2.3.6 Oxygen and Hydrogen	38

CHAPTER 3 ADSORPTION AND DESORPTION OF WATER AND  
DEUTERIUM OXIDE

3.1 INTRODUCTION	39
3.2 RESULTS	
3.2.1 Desorption of Water from Oxidized Rutile	41
3.2.2 Adsorption of H <sub>2</sub> O and D <sub>2</sub> O onto Oxidized Rutile	44

	<u>Page</u>
3.2.3 Adsorption of H <sub>2</sub> O and D <sub>2</sub> O onto Reduced Rutile	48
3.2.4 Summary	51
3.3 DISCUSSION AND CONCLUSIONS	
3.3.1 Preliminary Assignments	53
3.3.2 Surface Structure	54
3.3.3 Adsorption onto the Rutile Surface	
A. Infrared Studies of Water Adsorption	58
B. Other Studies of the Adsorption of Water onto Rutile	63
C. Lewis and Brønsted sites on Rutile	66
D. Conclusions	
3.4 BEHAVIOUR OF OBSERVED BANDS	71
3.4.1 to 3.4.8 Behaviour of Individual Bands	
3.4.9 Summary	86
3.4.10 Reactions occurring on the adsorption and desorption of water	
A. Oxidized Rutile	87
B. Reduced Rutile	89
 <u>CHAPTER 4 ADSORPTION OF ACETONE AND HEXADEUTEROACETONE</u>	
4.1 INTRODUCTION	91
4.2 RESULTS	
4.2.1 Adsorption of acetone and acetone d <sub>6</sub> onto oxidized rutile	93

	<u>Page</u>
4.2.2 Adsorption of Acetone d <sub>6</sub> onto Reduced Rutile	98
4.3 DISCUSSION AND CONCLUSIONS	
4.3.1 Properties of Acetone	
A. Enolization	100
B. Aldol condensation	101
C. Other reactions	103
4.3.2 Adsorption of acetone onto oxides	103
4.3.3 Behaviour of Bands	106
4.3.4 Surface Reactions	121
 <u>CHAPTER 5 ADSORPTION OF DEUTEROACETIC ACID</u>	
5.1 INTRODUCTION	128
5.2 RESULTS	129
5.3 DISCUSSION AND CONCLUSIONS	
5.3.1 Properties of Acetic Acid	133
5.3.2 Adsorption of Carboxylic acids onto oxides	134
5.3.3 Assignment of Observed Bands	135
5.3.4 Surface Reactions	142
 <u>CHAPTER 6 ADSORPTION OF HEXAFLUOROACETONE ONTO                     OXIDIZED AND REDUCED RUTILE</u>	
6.1 INTRODUCTION	
6.1.1 Aim	145
6.1.2 Experiments	146

Page

6.2	RESULTS	147
6.3	DISCUSSION AND CONCLUSIONS	
6.3.1	Properties of hexafluoroacetone and derivatives	152
6.3.2	Behaviour of Bands	153
6.3.3	Surface Reactions	158

CHAPTER 7 SUMMARY

7.1	EXPERIMENTAL PROCEDURES	161
7.2	THE RUTILE SURFACE	162
7.3	FURTHER WORK	164

SECTION 2

CHAPTER 8 A TECHNIQUE FOR THE STUDY OF THE SOLID/LIQUID INTERFACE USING INFRARED SPECTROSCOPY

8.1	INTRODUCTION	
8.1.1	Aim of this work	165
8.1.2	Other studies of the solid liquid interface using infrared spectroscopy	166
8.1.3	Initial Experiments	168
8.2	EXPERIMENTAL	
8.2.1	Design of the cell	169
8.2.2	Description of the cell	171

	<u>Page</u>
8.2.3 Vacuum Frame	173
8.2.4 Reagents	173
8.2.5 Spectrometer	174
8.2.6 Operation	174
8.3 RESULTS AND DISCUSSION	178
8.4 FURTHER WORK	
8.4.1 Disc immersed in a liquid	180
8.4.2 Powder immersed in a liquid	183

## PREFACE

The work described in this thesis continues that reported by Jackson<sup>1</sup> and Ramsbotham<sup>2</sup> on the surface properties of rutile. It differs from these studies in that infrared spectroscopy is the only technique used, Jackson and Ramsbotham using both electrophoresis and infrared spectroscopy to study the surface of rutile.

The basic aims of this work have been the study of the rutile surface by the adsorption of molecules containing carbonyl groups and the development of an infrared cell in which to measure the spectrum of the solid-liquid interface. The thesis has therefore been divided into two sections, the first reporting and discussing the results from the adsorption of water, acetic acid, hexafluoroacetone and acetone onto oxidized and reduced rutile, and the second considering the design and construction of a suitable cell for measuring the infrared spectrum of a solid immersed in a liquid.

The introduction to Section 1 contains information concerning the catalytic and surface properties of rutile. Detailed consideration of the bulk and catalytic properties would be out of place in this thesis but the study of reduced rutile and the condensation reactions of acetic acid and acetone on the surface require that a brief description of these properties is included. Results from the study of surface properties of rutile using a variety of techniques including infrared are considered. The theory

and applications of infrared are not included in the introduction as it is a well known technique on which many books have been written<sup>3,4</sup>. Similarly, no detailed survey of infrared spectroscopy applied to the study of surfaces is included, two books<sup>5,6</sup> and several reviews<sup>7</sup> having been published on the subject. Relevant references are cited and discussed where necessary. A brief survey of infrared work on anatase and rutile has been included in the introduction but as the study of the adsorption and desorption of water (Chapter 3) forms a basis for discussion of the rutile surface detailed consideration of this work is included in Chapter 3 and subsequent chapters.

The requirements and design of apparatus for the measurement of spectra produced by gas or vapour phase adsorption onto oxide discs are considered in the introduction to the experimental work (Chapter 2). Details of the apparatus and reagents used in this work are included in the sections that follow.

The four succeeding chapters (3-6) consider the adsorption of each of the reagents and have the same basic structure: introduction, results, discussion and conclusions. All spectra and graphs are included in an appendix at the end of the thesis to permit easy reference and prevent separation of the text. The properties of the adsorbate are included in the discussion of the results, together with a summary of the behaviour of the individual bands observed. Bands are then assigned and a reaction mechanism proposed.

The final chapter (7) of Section 1 summarizes the conclusions drawn from the results discussed in the previous chapters.



## CHAPTER 1

### INTRODUCTION

#### 1.1. TITANIUM DIOXIDE

Titanium dioxide exists in three crystalline modifications<sup>8,62</sup>, anatase, rutile and brookite, the first two of these being the most common and commercially important. It is manufactured<sup>8,9</sup> from two mineral ores, ilmenite ( $\text{FeTiO}_3$ ) and natural rutile.

The hydrated oxide may be prepared in the laboratory by the hydrolysis of many titanium compounds, the tetrachloride being commonly used, although this may result in contamination of the surface by chloride ions<sup>1,10,11</sup>. An alternative method, used by Jones and Hockey<sup>11</sup>, is the burning of a titanium isopropoxide-hydrogen mixture in a diffuse flame. Single crystals of rutile may be made by the Verneuil flame method<sup>12</sup>.

Titanium dioxide is non-toxic, inert to most reagents and is white in the pure crystalline form. These properties, together with the high opacity derived from its very high refractive index, combine to make it an ideal pigment, particularly for paints<sup>9</sup>. In common with many other transition metal oxides it may also be used as a semiconductor<sup>13</sup> or catalyst<sup>14</sup>.

Studies of the oxide may be divided into three broad,

overlapping categories consistent with its uses. These categories being: properties of the bulk structure; catalytic activity; and surface characteristics, other than those studied by catalytic reactions. Much work has been published on the electrical properties<sup>13</sup> of the bulk structure, particular reference being given to the defect structure, and on the catalytic activity<sup>14</sup>, usually in relation to other transition metal oxides. Although much of this work falls outside the scope of this thesis the relevant fundamental properties are discussed below.

Characteristics of the surface, which include the groups present on the surface and the surface structure, are important factors in the manufacture of paints as they determine the interaction between the pigment and dispersing liquid. Hence they have been widely studied with a variety of techniques including electrophoresis, heats of adsorption, electron spin resonance and infrared spectroscopy.

Detailed comparison of results and conclusions from studies of titanium dioxide is not usually possible because of differences in the samples used. Not only may the samples' crystalline structure differ but as the extent of reduction varies considerably with the pretreatment (Section 1.2.4.) the observed properties may also vary. A further consideration, particularly with samples obtained from titanium tetrachloride, is the absence in many studies of attempts to establish the purity of the starting surface which might be contaminated and hence produce unreliable results.

## 1.2 BULK PROPERTIES

Rutile has a tetragonal structure<sup>8,13,15</sup> with each titanium (IV) ion coordinated to six oxygen ions in a distorted octahedron, and each oxygen ion coordinated to three titanium ions. Four of the oxygen ions are in a plane round the titanium ion, 0.1944 nm from it, while the other two oxygen ions are perpendicular to this plane, 0.1988 nm above and below the central ion<sup>15</sup>.

The bonding in rutile is not purely ionic. There is strong evidence for some degree of covalent bonding<sup>13</sup>, electronegativity measurements indicating a value of 43% ionic character for the Ti-O bond<sup>13</sup>.

Under vacuum at room temperature rutile is a non stoichiometric oxide with a deficiency of oxygen ions<sup>16</sup>. There is disagreement concerning the position of the resultant excess titanium ions which may be in interstitial sites associated with an equivalent number of electrons or on lattice sites as a Ti<sup>3+</sup> ion associated with an oxygen vacancy<sup>14,17</sup>. The excess Ti<sup>3+</sup> ions cause n-type semiconductivity in rutile<sup>13,18</sup> which varies with the extent of reduction<sup>18</sup>. The band structure of rutile has been considered by Goodenough<sup>19</sup>.

Reduction of rutile by evacuation at elevated temperatures or in reducing atmospheres<sup>13</sup> results in an increase in the number of Ti<sup>3+</sup> ions in the surface and subsurface layers<sup>17</sup> and darkening of the sample to a blue-grey colour<sup>20</sup>. Sandler<sup>20</sup>

has determined the concentration of the  $Ti^{3+}$  ions on the surface to be 0.3% (white rutile) and 1.0% (blue rutile) while Richardson et al<sup>17</sup>. found that approximately 40% of  $Ti^{3+}$  ions were on the surface of their sample, the remainder occupying subsurface levels.

On mild reduction to  $TiO_{2-\delta}$  ( $\delta \sim 0.005$ ) randomly spaced and orientated  $\{132\}$  shear planes appear on the rutile surface<sup>21</sup> together with  $\{101\}$  planar defects. Greater reduction leads to an increase in the number of  $\{132\}$  shear planes.

## 1.3 CATALYTIC ACTIVITY

### 1.3.1 THEORIES OF CATALYSIS

Only a brief description of the electronic theory of catalysis is given here, detailed discussions are to be found in two reviews<sup>22,23</sup>.

#### A. Boundary Layer Theory

The majority of the first row transition metal oxides are either n-type, due to a stoichiometric excess of metal, or p-type due to a stoichiometric excess of oxygen ions probably in anion vacancies. The majority carriers in n-type oxides are conduction band electrons and in p-type oxides valence band holes.

In the boundary layer theory chemisorbed species are assumed to accept electrons from the semiconductor or donate electrons to it. Changes in conductivity may now occur, depending on the chemisorbed species and oxide, as shown in Table 1.1.

TABLE 1.1Changes of Conductivity on Chemisorption onto Semiconductors

Type of Oxide	Increase in conductivity (cumulative chemisorption)	Decrease in conductivity (depletive chemisorption)
n-type	electrons from chemisorbed species to conduction band	electrons from conduction band to chemisorbed species
p-type	electrons from valence band to chemisorbed species	electrons from chemisorbed species to valence band

Depletive chemisorption results in a charge transfer which is limited by the space charge barrier (boundary layer) formed and is characterized by equilibrium coverage less than 1% of monolayer and a decreasing heat of chemisorption with coverage. Cumulative chemisorption results in adsorption to a monolayer and a constant heat of adsorption.

Wolkenstein<sup>24</sup> has enlarged the above concept and defines two types of chemisorption "weak" and "strong". "Strong" chemisorption involves donation or capture of electrons by the chemisorbed species and results in changes of conductivity and work function. "Weak" chemisorption does not involve transfer of electrons and no changes in conduction occur. The chemisorbed species remain electrically neutral, unlike those involved in "strong" adsorption which become ionic. This theory is further discussed in Section 1.4.2. with reference to the adsorption of water on rutile.

## B) Correlation of catalytic activity with d-electron configuration

Dowden<sup>25</sup> found for the reaction  $\text{H}_2 + \text{D}_2 \rightleftharpoons 2\text{HD}$  that the catalytic activity was high for  $3d^3$ ,  $3d^6$ ,  $3d^7$ , and  $3d^8$  cationic configurations and low for  $3d^0$ ,  $3d^5$ ,  $3d^{10}$  and concluded that, for this reaction, the presence of a partially filled d-shell was necessary for the bonding of the adsorbed species to the cation.

### 1.3.2 CATALYTIC PROPERTIES OF RUTILE<sup>14</sup>

Rutile is an inactive catalyst compared with other transition metal oxides. In oxidizing atmospheres (e.g. homomolecular exchange of oxygen,  $\text{CO}_2/\text{O}_2$  exchange, decomposition  $\text{N}_2\text{O}$ ) and oxidizing-reducing atmospheres (oxidation  $\text{H}_2$ ,  $\text{CO}_2$  and  $\text{CH}_4$ ) the low activity is consistent with the bulk electrical properties. In reducing atmospheres ( $\text{H}_2/\text{D}_2$ , hydrogenation of ethylene) the low activity is consistent with the  $d^0$  configuration of the cation, the reactivity being due to the  $\text{Ti}^{3+} [d^1]$  ions produced by the reduction of the surface during the pretreatment or reaction<sup>26</sup>.

The reduction of rutile increases the number of  $\text{Ti}^{3+}$  ions in the surface<sup>17</sup> and the number of electrons in the conduction band<sup>13,18</sup>, hence the catalytic activity increases.

## 1.4 STUDIES OF SURFACE CHARACTERISTICS

### 1.4.1 ELECTRON SPIN RESONANCE STUDIES

Recent studies<sup>27,28</sup> of rutile have shown that two types of  $\text{Ti}^{3+}$  species are present on the reduced rutile surface. On moderate reduction  $\text{Ti}^{3+}$  ions are formed in lattice sites or interstitial positions which exhibit low reactivity towards oxygen at 77 K<sup>27</sup>. Further reduction creates  $\text{Ti}^{3+}$  ions in lattice or interstitial positions associated with one or two anionic vacancies.

Adsorption of oxygen onto reduced rutile produces two triplet signals of differing thermal stability<sup>28</sup> which are assigned to  $\text{O}_2^-$  species adsorbed on two different sites. These species may also be produced by the ultra-violet irradiation of unreduced rutile in the presence of oxygen<sup>27</sup>. The adsorbed  $\text{O}_2^-$  species are thought to exist as ions with the internuclear axis parallel to the plane of the surface and perpendicular to the axis of symmetry.

Adsorption of tetracyanoethylene (TCNE) and sym-trinitrobenzene (TNB) onto unreduced titanium dioxide<sup>29</sup> produces the radical anions  $(\text{TCNE})^-$  and  $(\text{TNB})^-$ . At temperatures below 573 K it is proposed that the electron donor centres are the OH groups while above this temperature the OH groups condense to form  $\text{O}^{2-}$  ions which are responsible for the reducing properties of the oxide.



#### 1.4.2 ELECTRICAL MEASUREMENTS

Figurovskaya<sup>30</sup> determined the change in electrical conductivity and work function when water was adsorbed onto titanium dioxide surfaces pretreated at 293 K to 673 K. Adsorption of water onto a hydrated surface evacuated at room temperature caused a decrease in the work function and increase in conductivity. Adsorption of water onto surfaces evacuated at temperatures from 293 K to 673 K also caused a similar effect, however the change in work function increased while the change in conductivity decreased. On evacuation of the water the values coincided with the initial values indicating the process to be reversible. Adsorption onto the 473-673 K evacuated surfaces resulted in a decrease of conductivity after evacuation.

The increase of conductivity does not result from the loss of an electron from water molecules due to its high ionization potential. A donor-acceptor mechanism is proposed in which the oxygen lone pair interacts with the empty Ti d-orbital to form a donor-acceptor complex. This results in an effective dipole with a negative charge on the titanium and a positive charge on the oxygen which decreases the work function but does not change the conductivity. This complex corresponds to Wolkenstein's<sup>24</sup> "weak" chemisorption. It is further proposed that the presence of this dipole affects the surrounding crystal field and might cause a charge defect (eg.  $\text{Ti}^{3+}$ ) to lose its electron<sup>31</sup> so increasing the conductivity.

Two forms of water are proposed to exist on the surface

of rutile which has been heated at 293–473 K, a neutral reversible form leading to a decrease in the work function and not changing the electrical conductivity, and a charged reversible form, accompanied by a decrease in the work function and an increase in the conductivity.

Above 473 K evacuation causes loss of the surface OH groups and adsorption of water correspondingly results in a dissociation of some water molecules into  $\text{OH}^-$  and  $\text{H}^+$  ions. This dissociation may cause an irreversible negative charge either by localization of the holes and electrons by OH and H groups or an elimination of donor defects resulting in a surface negative charge and decrease in conductivity.

### 1.4.3 INFRARED SPECTROSCOPY

Infrared and Raman spectroscopy are valuable techniques for the investigation of surface characteristics as they offer a direct method of examining surface groups and species adsorbed on the surface. The surface structure and properties may be investigated by recording spectra of the surface after evacuation at different temperatures, after the adsorption of 'inert' compounds, and after the adsorption of compounds which react with the surface.

Infrared transmittance spectroscopy, in which the solid is placed between the source and detector, is the most popular method of determining the vibrational spectrum of the surface as

commercial spectrometers may be used without modification. The solid is usually in the form of a pressed disc of the oxide powder and is contained in a cell connected to a vacuum frame. Details of the experimental technique are given in Section 2.1.

Transmittance spectroscopy is not suitable for solids of low surface area as the number of active groups in the beam is low, nor is it usually suitable for powders as scattering greatly reduces the intensity of the radiation reaching the detector. The use of discs to reduce this scattering can cause interparticulate contact which may affect the spectrum of the oxide<sup>32</sup>.

Reflectance spectroscopy<sup>33</sup> is a relatively new technique which may be used to record the spectra of low surface area solids in powder<sup>34</sup> or crystal<sup>35,36</sup> form. The technique requires modification of the spectrometer and the resolution is inferior to that of transmittance spectroscopy. Reflectance spectra have been determined for titanium dioxide<sup>37</sup>, silica<sup>34,35,38</sup>, magnesium oxide<sup>37,38</sup>, zinc oxide<sup>37</sup>, tin (IV) oxide<sup>37</sup> and germanium (IV) oxide<sup>37</sup>. The bands observed for  $\text{TiO}_2$  are reported at 3690 and 3350  $\text{cm}^{-1}$ .<sup>37</sup>

#### 1.4.4 RAMAN SPECTROSCOPY

The introduction of lasers and more sophisticated instruments has made Raman spectroscopy<sup>3</sup> a technique suitable for the study of adsorbed species. Hendra<sup>39</sup> has recently published a

review describing the experimental techniques and discussing the spectra which have been obtained. Raman spectroscopy has several advantages compared with infrared, the most important being the relatively low intensity of bands due to the bulk adsorbent. These usually obscure at least part of the useful infrared region, for example rutile completely absorbs infrared radiation below  $1000\text{ cm}^{-1}$  due to the Ti-O-Ti vibrations of the lattice. The recorded spectra, however, usually have a low signal:noise ratio and consequently weak bands are difficult to detect although computer averaging techniques may be used to eliminate much of the noise.

Raman spectroscopy is not suitable for recording bands in the  $3800$  to  $3200\text{ cm}^{-1}$  region in which OH stretching frequencies occur due to the insensitivity of detectors in the region and the weak absorbance of OH bands in the Raman caused by the low polarizability of the bond. The use of Argon-ion lasers, instead of the usual, less powerful He/Ne, to overcome this problem may result in overheating of the sample. Hendra<sup>39</sup> reports a blackened thermometer in an evacuated cell reaching  $673\text{ K}$  in the argon-ion beam and, although he records a temperature rise of  $\sim 5^\circ$  for a PTFE sample in the same beam, it is possible that the temperature rise for an opaque oxide would be too high for studying adsorption. Immersion of the solid in a liquid would reduce the temperature rise and consequently Raman spectroscopy might be used for the study of the solid-liquid interface.

No detailed study of the Raman spectrum of titanium dioxide has been reported, Hendra<sup>40</sup> observed bands below  $1100\text{ cm}^{-1}$  due to the adsorption of pyridine on the oxide.

## 1.5 INFRARED STUDIES OF TITANIUM DIOXIDE

### 1.5.1 PREVIOUS WORK

Infrared studies of the desorption of water from the rutile surface have been carried out by Jones and Hockey<sup>11,42,43</sup>, Jackson and Parfitt<sup>10</sup>, and Primet et al<sup>41</sup>. With some exceptions the spectra observed after particular treatments are similar, the room temperature evacuated surfaces showing bands due to surface OH species and adsorbed water molecules. On the basis of these spectra models of the rutile surface have been proposed based on some of the exposed planes on the bulk rutile crystal. These results and models are discussed in Chapter 3 together with the results, from this work, for H<sub>2</sub>O and D<sub>2</sub>O adsorption and desorption on oxidized and reduced rutile.

A summary of reagents adsorbed onto rutile and anatase is given in Tables 1.2 and 1.3. These results will be discussed in Chapters 3 to 6.

### 1.5.2 THE PRESENT WORK

The presence of hydroxyl groups, water molecules and Lewis sites on the room temperature surface of rutile has been confirmed by studies detailed in Table 1.2. The purpose of this work

TABLE 1.2

Summary of Investigations by Infrared Spectroscopy  
of Inorganic compounds adsorbed onto Titanium Dioxide

<u>Adsorbate</u>	<u>Adsorbent</u>	<u>Reference</u>
Rutile	Water	10,11,41,42,43
Anatase	Water	44,46
Rutile	Ammonia	45
Anatase	Ammonia	46,47
Anatase	Carbon Monoxide	49,50
Rutile	Carbon Dioxide	51
Anatase	Carbon Dioxide	47
Rutile	Hydrogen Chloride	11,52
Anatase	Hydrogen Chloride	53
Rutile	SO <sub>2</sub> , SOCl <sub>2</sub>	11
Anatase	Nitrogen Dioxide	54
Anatase	Carbon Tetrachloride	53
Rutile	Si,Ti,Sn Tetrachloride	55

TABLE 1.3

Summary of Investigations by Infrared Spectroscopy  
of Organic compounds adsorbed onto Titanium Dioxide

<u>Adsorbate</u>	<u>Adsorbent</u>	<u>Reference</u>
Rutile	Alcohols	56,57
Rutile	Phenol	47
Rutile	Acetic acid	58
Anatase	Acetic acid	47
Rutile	N-Hexane	58
Rutile	Benzene	58
Rutile	Diethyl Ether	58
Rutile	Acetone	58
Anatase	Trimethylamine	47
Rutile	But-1-ene	51

was to study the interaction of carbonyl and carboxylic acid groups with the surface in order to acquire further information about the nature of the surface sites.



## CHAPTER 2

### EXPERIMENTAL

#### 2.1 INTRODUCTION

##### 2.1.1 GENERAL REQUIREMENTS OF THE APPARATUS

An essential requirement for the study of surfaces is the complete absence, as far as practically possible, of any forms of contamination, either on the surface or in the apparatus<sup>19</sup>. The purity of the sample is therefore very important, particularly with respect to species which, although present in very small concentrations, are sufficient to alter the surface characteristics. These contaminating species may be introduced<sup>59</sup> during the preparation of the sample or during its storage and subsequent use. Atmospheric impurities, common to most oxides, are introduced during preparation and storage. They may usually be removed by heating in oxygen (673 K) and evacuating (673 K). Contamination of a surface is indicated by the presence of bands due to impurities or by changes in the spectra of other adsorbed species.

##### 2.1.2 THE VACUUM FRAME

Most infrared and catalytic studies are carried out with the disc in vacuo to prevent contamination by the atmosphere and to

permit dosage of gases onto the surface. Contamination by grease in the vacuum system<sup>59</sup> is prevented by the use of greaseless taps together with liquid nitrogen traps to isolate any greased taps present in the pumping system. Contamination due to leakage of air through the greaseless taps may be kept to a minimum by including as few taps as possible between the cell and pumping system, and between the cell and dosing system.

Reagents used during a previous experiment may adsorb on the walls of the apparatus and contaminate discs subsequently introduced into the cell. The vacuum frame must therefore be thoroughly evacuated after each experiment and the cell removed for cleaning. Possible contamination from reagents trapped in the pumping system may be prevented by the use of a separate pumping line ('backing line') to remove reagents. This line needs only one liquid nitrogen trap which is frequently evacuated to prevent a build-up of waste.

### 2.1.3 THE DESIGN OF AN INFRARED CELL

The basic requirement of a cell is the complete absence of materials likely to cause contamination of the solid. Other requirements vary with the conditions under which the cell is to be used and may include ease of cleaning, ease of operation and the treatment of discs at high temperature.

Two basic designs of cell are available for treating

discs to high temperatures, the disc either remaining in the infrared beam or being moved to a separate section of the cell for heating. The basic designs are modified to fit the requirements of the system in use; Buckland et al<sup>60</sup> describe one cell of each design recently used for studies of rutile and chromia.

Heat treatment of the disc in the infrared beam requires a long cell to accommodate the heater, which may be internal or external, and to prevent overheating of the cell windows, for which cooling coils are also used. The use of a long cell (approximately 80mm) may result in less light reaching the detector due to increased scattering. Replacement of discs is normally carried out by removing a section of the cell clamped to another section with an 'O' ring between to form a vacuum tight seal. This 'O' ring may cause contamination (see below and 2.2.2). The heating of a disc in the infrared beam enables reactions at elevated temperatures to be followed, although at higher temperatures the emission spectrum of the disc may also be observed.

Removal of the disc from the beam for heat treatment may cause mechanical shock and subsequent breakage of new discs, this being less likely if the disc is raised vertically<sup>60</sup> than if moved horizontally (this work). The former type of cell requires the presence of an 'O' ring seal in order to replace the disc<sup>60</sup> while the latter may be sealed by glassblowing. The absence of a heater permits the use of a short path length allowing the disc to be closer to the detector.

The requirements for a cell to be used in this work

were the complete absence of any contamination, treatment of discs up to 673 K and ease of cleaning. The cell would have to be cleaned in chromic acid after each experiment to remove organic contaminants, and consequently the windows must be easily removed and replaced and the complete cell easily detached from the vacuum frame. The cells used by Ramsbotham<sup>60</sup> and Jackson<sup>1</sup> fulfilled these criteria but subsequent work indicated that the 'O' ring in the former cell was a possible source of contamination. The cell used by Jackson has been used in all the experiments described in this section of the thesis.

Many different cell window materials<sup>5</sup> are available for use with this type of cell, sodium chloride and potassium bromide being the most common. However these are hygroscopic and calcium fluoride windows were used, these being relatively inexpensive and mechanically strong. They are opaque to infrared radiation below  $1000\text{ cm}^{-1}$ , which coincides with a strong band due to the Ti-O-Ti lattice vibrations, and do not therefore decrease the spectral range available for study.

#### 2.1.4 THE CRYOSTAT

Dosage of organic vapours (eg. acetone, acetic acid) onto reactive oxides (eg.  $\text{TiO}_2$ ,  $\text{Al}_2\text{O}_3$ ) at approximately  $10^3\text{ N m}^{-2}$  results in irreversible saturation of the surface producing

intense infrared bands which are broad and difficult to interpret<sup>47</sup>; slower rates of dosage are possible either by introducing known quantities of vapour into the cell or by reducing the vapour pressure of the liquid. The former method is difficult experimentally as very small quantities are involved and it may still result in overdosing. The latter method is preferable as the adsorption process may be monitored by recording the spectrum of the adsorbed species. Dosage may be stopped at suitable intervals to record the complete spectrum.

The vapour pressure of the liquid was reduced by lowering the liquid temperature in a cryostat<sup>61</sup>. This consisted of a bulb containing the liquid attached to the vacuum frame and surrounded by a vacuum jacket immersed in a coolant liquid (liquid nitrogen or CO<sub>2</sub>/acetone). The temperature of the liquid was controlled by a low voltage furnace surrounding the bulb and could be set at a value for the optimum rate of dosage. A disadvantage of this apparatus was the possibility of products from the surface reaction being distilled back into the cryostat.

### 2.1.5 THE INFRARED SPECTROMETER

The infrared spectrometer used was similar to those described in books on infrared spectroscopy<sup>3-6</sup>, no modifications being necessary for studies of discs. The low transmittance of discs usually required the use of an attenuator in the reference

beam and the use of wider slit programs to compensate for the subsequent loss of response.

The majority of infrared spectrometers record on chart paper with  $\text{cm}^{-1}$  as the abscissa and percent transmittance as the ordinate. The course of adsorption may sometimes be plotted by measuring the absorption of bands which are calculated from the transmittance value of the peak ( $T_1$ ) and that of the base line under the peak ( $T_2$ ). The latter is determined (Hair<sup>5</sup> P50) for a sloping base line by either drawing a tangent to the transmittance curve, assuming a linear base line, or by superimposing the original baseline onto the transmittance curve. The two transmittance values are converted to absorbance values and subtracted as follows:-

If radiation of intensity  $I_0$  is transmitted through a substance thickness  $d$ , the intensity of the emergent radiation  $I$  is given by

$$I = I_0 \exp(-\epsilon d) \text{ where } \epsilon \text{ is the extinction coefficient}$$

The absorbance  $A$  of the sample is given by:-

$$A = \epsilon d = \ln(I_0/I)$$

this is usually expressed in terms of  $\log_{10}$

$$\bar{A} = \epsilon d/2.303 = \log_{10}(I_0/I)$$

since transmittance  $T$  is given by

$$T = (I/I_0) \times 100\%$$

$$\text{and } \bar{A} = \log_{10}(100/T)$$

which assumes a base line at 100% transmittance.

If the transmittance of the peak is  $T_1$  and that of the base line directly under the peak  $T_2$  the absorbance  $\bar{A}$  of the band is given by:

$$\bar{A} = \log_{10}(100/T_1) - \log(100/T_2)$$

In order to follow the course of a reaction in detail by infrared spectroscopy it is necessary to record spectra at frequent intervals during an experiment. It is not practical, nor necessary, to present all of these spectra as many are similar and represent only intermediate stages in the absorption. The spectra presented in this thesis have been chosen to provide a complete account of the adsorption process.

Spectra may be reproduced in two forms, either superimposed on each other or with the ordinate displaced. Superimposition indicates small changes of band intensity which may not be apparent when the spectra are displaced, however it is not suitable if some bands are increasing in intensity while others are decreasing, and when narrow bands appear. In these circumstances the resultant diagram is usually confusing. Some spectra in the thesis have been presented in this form in order to compare absorbance changes directly.

The majority of spectra are presented with their ordinates displaced which does not allow the direct comparison of band intensities. To facilitate this comparison the absorbance of bands have been calculated for the majority of experiments and these are plotted against increasing adsorption as represented by the order of the spectra. The graphs have no significance other than that of a 'visual aid' for the comparison of band intensities.

### 2.1.6 THE PRETREATMENT OF RUTILE

The effect of surface chloride ions, present on rutile prepared from titanium tetrachloride, has been investigated thoroughly by Jackson<sup>1,10</sup> and is removed by alternate soxhletting and heating pretreatments. The resultant surface contains carbonate species which are removed by treatment with oxygen (673 K) and evacuation (673 K). As evacuation at this temperature causes loss of lattice oxygen a standardized cleaning procedure (2.3.1) had to be used which reduces oxygen loss to a minimum and therefore final evacuation at 673 K continued for only 15 min before cooling. The resultant surface was known as a 'standard surface' and all treatments were carried out with this surface.

The hydroxylated surface was formed by exposing the discs to saturated H<sub>2</sub>O or D<sub>2</sub>O vapour and, after heating and evacuating at beam temperature ( $\frac{1}{2}$ h), formed a 'beam temperature H<sub>2</sub>O (or D<sub>2</sub>O) surface'. Dehydroxylation by evacuation at 673 K is followed by treatment in oxygen to replace that lost by evacuation. The resultant surface is known as a '673 K H<sub>2</sub>O (or D<sub>2</sub>O) surface'.

Reduction of the standard surface was carried out by four separate doses of hydrogen (2.3.1) as H<sub>2</sub>O formed during the treatment and prevented further reduction.

Many of the treatments of rutile samples were carried out with the oxide disc at its ambient temperature in the optical



beam of the spectrometer. Throughout this thesis this temperature is designated the BT, or beam temperature. An estimate of this temperature would be that it lies between 320 and 350 K.

## 2.2 APPARATUS

### 2.2.1 THE VACUUM FRAME (Fig. 2.1)

The frame consisted of five basic units; pumping line, reagent line, mass spectrometer bulbs, cryostat and cell. The pumping line connecting the cell to the pumps contained the minimum number of taps possible to prevent contamination due to leakage through the taps during evacuation of the cell. The pumping system comprised the usual rotary oil pump and mercury diffusion pump with three liquid nitrogen traps separating them from the pumping line. The trap next to the diffusion pump was detachable, using a greased cone and trap fitted with a B29 socket, while the other two traps were sealed and prevented grease from the taps used in the pumping system from contaminating the frame. A Penning gauge connected between the detachable and sealed traps indicated pressures down to  $1.3 \times 10^{-4} \text{ N m}^{-2}$ .

All taps after the pumping system were grease-free (Rotaflo TF2/18 or Youngs POR4 and POR10) and capable of a dynamic vacuum of  $1.3 \times 10^{-4} \text{ N m}^{-2}$  but leaked slightly under static conditions. As this leakage occurred through the barrel of the tap between the glass and teflon or teflon/rubber seals the internal seal was placed to prevent leakage into the main pumping line and 'closed' spaces such as the cell, gas and liquid bulbs, and molecular sieve.

An oxygen bulb (BOC Grade X) was connected to the pumping line together with a transducer (Bell and Howell) to record the pressure. The transducer was connected to a potentiometer (Cropico P6) and calibrated ( $0-100 \text{ K N m}^{-2}$ ) with air using a mercury manometer.

All reagents, other than oxygen, were attached to the reagent line, liquids being stored in bulbs tapered to prevent cracking during freezing and thawing of the liquid. Condensable gases were stored under liquid nitrogen in a bulb fitted with a mercury manometer. Liquids were introduced either by removing a 'Rotaflo' tap and pouring in the liquid or by breaking a sealed ampule of the liquid ( $\text{CD}_3\text{COOD}$ ,  $\text{CD}_3\text{COCD}_3$ ) under vacuum (fig 2.2) after first freezing the liquid. Liquids were dried by distillation onto the molecular sieve, (4A, dried by evacuation 523 K) before transferring them to the cryostat which was connected directly to the cell via a Youngs tap (POR 4) to minimize leakage of air during the dosage of vapour.

Three 10cm diameter bulbs with cold fingers were attached via two taps (Youngs POR 4) to a line connected to the main line and were used to trap out and store samples for mass spectrum analysis.

The main and reagent lines were connected to a 'backing' line containing a sealed trap under liquid nitrogen, which was frequently evacuated to prevent a build-up of contamination.

## 2.2.2 THE CELLS

### A. Cell used by Ramsbotham<sup>60</sup>

Overnight evacuation of a dehydroxylated surface at room temperature in this cell results in the appearance of weak bands at 2960, 2925  $\text{cm}^{-1}$  and more intense bands at 1595 and 1485  $\text{cm}^{-1}$  together with partial rehydroxylation of the surface. Replacement of the neoprene 'O' ring by flat gaskets of nitrile or silicone rubber also produced contamination bands in the 3000-2800  $\text{cm}^{-1}$  and 1600-1400  $\text{cm}^{-1}$  regions, partial rehydroxylation also occurring although no leakage of air was indicated. These bands were removed by evacuation at 673 K but reappeared on further pumping at room temperature.

The insertion of a stainless steel gasket (0.32mm) between the 'O' ring and interior of the cell prevented contamination of the disc but resulted in an unsatisfactory static vacuum. The contamination was probably caused by the 'O' ring while partial rehydroxylation of the surface was due to the desorption of water from the 'O' ring.

## B. Cell used by Jackson

The cell (fig 2.3) consisted of a pyrex glass tube 40mm in diameter sealed at one end with two parallel ground glass flanges (50mm outside diameter) either side of the tube and approximately 40mm from the sealed end. The calcium fluoride windows were attached to the flanges by brick red enamel (AEI M-V No38) which, after drying at room temperature, was further dried in an oven (373 K).

The disc carriage was constructed from a flat pyrex plate (60mm x 30mm) with two holes (22mm diameter) surrounded by grooves (26mm diameter) to accommodate the discs. These were held in place by a stainless steel plate bolted to the glass holder. The carriage was supported in the cell by two pairs of glass rods (3mm diameter) at the top and bottom of the cell and moved by a magnet attracting the nail sealed in the top of the glass holder. The open end of the cell was sealed after the introduction of the discs and blown open at the end of each experiment to remove the holder and discs. A dehydroxylated surface showed no indication of contamination or leakage after remaining in the closed cell for two weeks.

Discs were heated by an external furnace controlled by a platinum resistance thermometer coupled to a relay, the temperature of the disc being measured by a chromel-alumel thermocouple in the pocket opposite the carriage holder.

After each experiment involving organic vapours the cell was detached from the frame and the windows removed by soaking the cell in acetone. The cell was then immersed in chromic acid before being washed with deionized water and dried.

### 2.2.3 THE CRYOSTAT

The construction (fig 2.4) was similar to that used by Ashmead<sup>61</sup> and differed only in minor details. A flange replaced the B55 cone and socket of the outer jacket while a circular reaction vessel used for solids was replaced by the tapered vessel. The heater voltage was set at 20V and switched by a mains-operated relay controlled by the platinum resistance thermometer. The temperature was varied by a potentiometer on the relay, and the copper-constantan thermocouple connected to a flat bed recorder (Servoscribe).

The outer vessel was evacuated via the backing line through a two way tap, which allowed air to be bled into the cryostat, and was immersed in liquid nitrogen (temperatures below 230 K) and solid CO<sub>2</sub>/acetone (230 K to 270 K). At temperatures below ~230 K the liquid (or solid) in the bulb became warmer than the upper tube and distillation occurred, solid collecting on the tube above the heater. This effect may have caused differences in the spectra of water adsorbed on rutile at apparently similar equilibrium vapour pressures, as indicated by the temperature of the ice, using the two different baths. The vapour pressures during dosage are not therefore quoted in the results except as an approximation.

#### 2.2.4 THE INFRARED SPECTROMETER

All spectra were recorded on a Perkin-Elmer 257 spectrometer (specification table 2.1)

An attenuator was placed in the reference beam to compensate for the low transmittance of the discs ( $\sim 5\%$ ) and set to give the transmittances shown in table 2.2 at particular wavenumbers. The scanning speed was slow, the gain and slit settings at particular wavenumber are shown in table 2.2 and were adjusted to give the correct response for minimum slit width and maximum gain consistent with low noise levels. The noise level is indicated in spectra 2.1 to 2.3, the decreased transmittance of the reduced sample requiring maximum slit program and maximum gain.

The beam temperature (BT) at the surface of the disc could not be measured directly but evacuation of a hydroxylated disc in the beam overnight produced a spectrum characteristic of a surface evacuated at 337 K.

The spectrometer was fitted with a readout accessory of 10mV output corresponding to full scale deflection. This was connected to a flat bed recorder (Servoscribe) set at 5mV full scale deflection enabling spectra to be enlarged. A chart speed of 30mm/min produced a trace of similar proportions to those recorded on the spectrometer.



Spectra 2.1 to 2.4 were copied direct from the chart paper and reduced in size by 40% using a Rank Xerox 7000 copier. These spectra show typical noise levels and base lines for oxidized and reduced rutile. The majority of other spectra were traced from the original recordings produced by the spectrometer or recorder and reduced in size by 10%. An accurate indication of noise levels being given in all these spectra.

Absorbances in the  $4000$  to  $2000\text{ cm}^{-1}$  region were calculated by extrapolating the linear base line on the high wavenumber side of the band while below  $2000\text{ cm}^{-1}$  the base line of the standard surface was superimposed on the spectrum. Due to changes in base line calculated absorbances may contain errors but are sufficient for comparison purposes.

### 2.2.5 OPERATION

Before a clean cell and discs were attached to the frame, the cryostat, molecular sieve, mass spectrum bulbs and main and reagent lines were thoroughly evacuated to remove traces of reagents previously adsorbed. The frame was then closed off from the pumping system which was cleared of any trapped impurities by evacuation of the traps at room temperature. The cell was attached to the frame and evacuated at room temperature through the backing line before pumping on the main line. The spectrum of rutile showed bands due to hydroxyl groups, water molecules and carbonate species. Oxygen ( $1.33 \times 10^4 \text{ N m}^{-2}$ ) was admitted into the cell and the discs heated to 673 K. The pretreatment of the discs proceeded as outlined below (2.3.1) and the cell was then closed off from the frame. If necessary the reagent was introduced into the frame as outlined in 2.2.1 and purified (2.3) before distilling approximately  $3 \text{ cm}^3$  into the cryostat. The cryostat control was set for a temperature approximately  $60^\circ$  below the melting point and the tap between the cryostat and cell opened. The progress of the adsorption was followed by recording the spectrum, on fast or medium scan, in the range containing those bands which indicated the extent of adsorption. When sufficient adsorption had occurred, the tap between the cryostat and cell was closed and the complete spectrum of the disc recorded. If no increased adsorption had occurred after one hour the temperature of the cryostat was increased. Spectra were also recorded after prolonged exposure of the disc to the vapour and after evacuation at beam temperature for one hour.

After each experiment the cell was removed for cleaning and reagent remaining in the cryostat was removed via the backing line.

## 2.3 REAGENTS

### 2.3.1 RUTILE

The rutile (code no. CL/D338) used in this work was supplied by British Titan Products (now Tioxide International) and was prepared by the hydrolysis of redistilled titanium tetrachloride before calcining at 723 K. Electron micrographs of the sample showed aggregates and crystals similar to those of a different sample described by Jackson<sup>1</sup>. The crystals were of a similar shape to those found naturally<sup>62</sup> and differed from the amorphous lumps observed in micrographs of rutile prepared from titanium sulphate.

Chloride impurities were removed by alternately soxhletting (24h) and heating in air (24h 673 K)<sup>1</sup>. This procedure was carried out four times before a final soxhlet treatment and drying (383 K 24h). The final bulk chloride content was 0.13% determined by the XRF technique. There was no evidence of significant surface chloride ion concentrations even after prolonged treatment of the disc at 673 K, the spectra of the hydroxylated surface being similar to those observed by Jackson<sup>1</sup> for low surface chloride concentrations. The possible effect of small surface chloride concentrations will be discussed later (Chapter 3).

The rutile discs were prepared by pressing ( $84 \text{ MN m}^{-2}$ ) 0.15 to 0.25g of oxide under vacuum ( $2.6 \times 10^2 \text{ N m}^{-2}$ ) in a 25.4mm diameter die. The adherence of the disc to the die

faces was prevented by pressing the powder between two discs of typing paper.

The spectrum of discs evacuated at room temperature showed a band due to surface carbonate species at  $1440\text{ cm}^{-1}$ . Evacuation at 673 K (1 h) removed this band while heating in oxygen 673 K (1 h) and cooling caused the reappearance of the band at a reduced intensity. Subsequent evacuations (673 K, 1 h) and heating in oxygen (673 K, 1 h) before cooling in oxygen reduced this band to a weak shoulder or removed it completely. The 'standard surface' was therefore prepared by alternate heating in oxygen (673 K, 1 h) and evacuating (673 K, 1 h) until on cooling in oxygen only a weak band was observed at  $1440\text{ cm}^{-1}$ . The discs were reheated (673 K, 1 h), evacuated (673 K, 1 h) and cooled to beam temperature ( $\frac{1}{4}$  h). The spectrum of the standard surface is shown in spec. 2.1.

Hydroxylated surfaces (BT,  $\text{H}_2\text{O}$ ) were produced by heating the disc with water vapour (673 K, 2 h), cooling ( $\frac{1}{2}$  h) and evacuating (BT,  $\frac{1}{2}$  h). Deuterated surfaces were similarly prepared by heating in  $\text{D}_2\text{O}$  vapour (673 K, 2 h) and evacuating (673 K, 1 h) at least twice before cooling in  $\text{D}_2\text{O}$  vapour and evacuating (BT,  $\frac{1}{2}$  h). 673 K surfaces were prepared by evacuating (673 K, 12 h), heating in oxygen ( $1.33 \times 10^4\text{ N m}^{-2}$ , 673 K, 1 h), evacuating (673 K,  $\frac{1}{4}$  h) and cooling ( $\frac{1}{4}$  h).

Surfaces were reduced by heating in hydrogen ( $1.33 \times 10^4\text{ N m}^{-2}$ , 673 K, 1 h) and evacuating (673 K, 1 h) four

times before evacuating (673 K, 12 h) and cooling to beam temperature (spec. 2.3). Dosing  $D_2O$  or  $H_2O$  onto the surface (BT,  $\frac{1}{2}$  h) and evacuation (BT,  $\frac{1}{2}$  h) formed the hydroxylated surface (spec. 2.4).

Sintered samples for use in the water adsorption and desorption experiments were prepared by heating rutile discs in air at 973 K for 13 h before sealing them in the cell. The standard surface was prepared as described above for non-sintered rutile.

Impurities: Cationic impurities do not vary appreciably with samples prepared by the same method from the same source and are of the order<sup>63</sup>:

A < 1, P = 0, K = 5, Ca = 20, V 0.02, Cr 0.1, Fe < 1

Mn < 0.02, As = 3, Sn = 50, Ba = 0.1, Pb = 0.5

Surface area =  $22\text{m}^2\text{g}^{-1}$ .

### 2.3.2 $H_2O$ and $D_2O$

$H_2O$  was triply distilled, once from alkaline potassium permanganate and twice from itself. Dissolved gases were removed by the freeze-thaw process.

$D_2O$  (Koch-light 99.7% isotopic purity) was used as supplied after degassing.

### 2.3.3 ACETONE $h_6$ AND $d_6$

Analar acetone  $h_6$  (Hopkin and Williams) was stored over dry calcium sulphate for two days prior to distillation under nitrogen from fresh  $CaSO_4$  through a column packed with glass helices. After discarding the first  $10\text{ cm}^3$  the fraction distilling between 329 K and 330 K was collected and stored under nitrogen. Gases were removed by the freeze-thaw technique and the acetone was dried over molecular sieve before transference to the cryostat.

Acetone  $d_6$  (CIBA Isotopic purity 99.5%) was used as supplied after degassing and drying as above. The mass spectrum of the vapour at room temperature showed 2.5%  $CD_3\text{COCHD}_2$  (99.6% Isotopic purity), 0.02%  $CD_3\text{COCD}_2\text{COCD}_3$  and less than 0.01% of other impurities (mass numbers 114, 134).

### 2.3.4 HEXAFLUOROACETONE

Hexafluoroacetone (Pierce Chemical Company) was used as supplied after drying over molecular sieve. No impurities were detected in the mass spectrum of the vapour.

### 2.3.5 ACETIC ACID $d_4$

Acetic acid  $d_4$  (CIBA Isotopic purity  $> 99.5$  atom%) was used as supplied after degassing. No impurities were observed in the mass spectrum of the vapour, Isotopic purity

could not be confirmed by this technique due to possible exchange of the acidic deuterium with water vapour in the apparatus.

#### 2.3.6 OXYGEN AND HYDROGEN

British Oxygen Grade X gases were used as supplied.



### 3. ADSORPTION AND DESORPTION OF WATER AND DEUTERIUM OXIDE

#### 3.1 INTRODUCTION

Several detailed infrared studies of water desorption<sup>10,11,42,44</sup> from hydroxylated rutile and water adsorption<sup>10,42</sup> onto dehydroxylated rutile propose models of the rutile surface based on the (110) surface plane<sup>10,44</sup> and on the (110), (101) and (100) surface planes<sup>42</sup>. Both results and conclusions from these studies differ and this work was undertaken to examine these differences in detail and also to study the reduced surface which, contrary to a previous report<sup>45</sup>, differs considerably from the oxidized surface.

A Summary of the experiments appears overleaf:-

	<u>Graph</u>	<u>Spectra</u>
Desorption of H <sub>2</sub> O from Oxidized Rutile		
a) Beam Temperature H <sub>2</sub> O Surface	3.1	3.1
b) Sintered Beam Temperature H <sub>2</sub> O Surface	3.2	3.2
Adsorption of H <sub>2</sub> O and D <sub>2</sub> O onto Oxidized Rutile		
a) H <sub>2</sub> O onto a 673 K H <sub>2</sub> O Surface	3.3	3.3
b) D <sub>2</sub> O onto a 673 K D <sub>2</sub> O Surface	3.4	3.4
c) H <sub>2</sub> O onto a sintered 673 K H <sub>2</sub> O Surface	3.5	3.5
Adsorption of H <sub>2</sub> O and D <sub>2</sub> O onto Reduced Rutile		
a) Reversibility of the Reduction Process	---	3.6
b) H <sub>2</sub> O onto a 673 K H <sub>2</sub> O Surface	---	3.7
c) D <sub>2</sub> O onto a 673 K D <sub>2</sub> O Surface	3.6	3.8

The spectra are presented in the appendix. Spectra 3.1 and 3.2 contain some duplicate spectra doubled in size on the flat-bed recorder and superimposed on each other to present a direct comparison of absorbances. Spectra 3.4 and 3.7 were also traced from the recorder, the former to supplement the results presented in spec. 3.3.

Graphs of absorbance changes precede the relevant spectra.

## 3.2 RESULTS

### 3.2.1 DESORPTION OF WATER FROM OXIDIZED RUTILE

#### A. Beam Temperature H<sub>2</sub>O Surface

(Spectra 3.1 and Graph 3.1)

The Spectrum of a hydroxylated rutile surface produced by exposing a standard surface to H<sub>2</sub>O vapour (BT,  $\frac{1}{2}$ h) and evacuating (BT,  $\frac{1}{2}$ h) showed bands at 3680(sh), 3655, 3610, 3520, 3420 and 1620 cm<sup>-1</sup> (spec. 3.1a). Heating this surface in H<sub>2</sub>O (673 K, 5h), cooling and evacuating (298 K, 14h) (spec. 3.1b) increased the 3420 cm<sup>-1</sup> band and decreased the 3680 cm<sup>-1</sup> shoulder, no other changes occurring. Evacuation at beam temperature ( $\frac{1}{2}$ h) (spec. 3.1c) caused a slight increase in the 3655 cm<sup>-1</sup> band and decreased the 3610, 3520 and 1620 cm<sup>-1</sup> bands.

Evacuation to 368 K (spec. 3.1d,e) increased the 3680, 3655 cm<sup>-1</sup> bands to a maximum, removed the 3610 and 3520 cm<sup>-1</sup> bands and decreased the 3420 and 1610 cm<sup>-1</sup> bands, the latter having shifted from 1620 cm<sup>-1</sup>. Further evacuation to 423 K (spec. 3.1f,g) caused broadening of the 3680 cm<sup>-1</sup> shoulder and decreased the 3655, 3420 and 1610 cm<sup>-1</sup> bands, the intensity of the 1610 cm<sup>-1</sup> band being reduced to 50% of the absorbance remaining after the 368 K evacuation. On further pumping to 481 K (spec. 3.1h-k) the 3680 cm<sup>-1</sup> shoulder decreased

to reveal a  $3700\text{ cm}^{-1}$  band while the  $3655\text{ cm}^{-1}$  band decreased to approximately 20% of its maximum value and the  $3420\text{ cm}^{-1}$  band disappeared to leave a broad  $3400\text{ cm}^{-1}$  band. The  $1610\text{ cm}^{-1}$  band decreased slightly to an intensity which remained constant until evacuation at 663 K. On evacuation to 663 K (spec. 1-p) the  $3655\text{ cm}^{-1}$  band decreased to a very weak shoulder on the  $3700\text{ cm}^{-1}$  band which also decreased, while the broad  $3400\text{ cm}^{-1}$  band flattened. Apparent absorption due to the  $1610\text{ cm}^{-1}$  band was still present after the 663 K evacuation.

#### B. Beam Temperature $\text{H}_2\text{O}$ Sintered Surface

(Spectra 3.2 and Graph 3.2)

The sintered discs were heated in water (673 K, 2h) before cooling and evacuating (BT, 1h). The spectrum of resultant surface (spec. 3.2a) was considerably different from the non-sintered rutile (spec. 3.1b), the  $3680\text{ cm}^{-1}$  shoulder was less intense while the  $3655$  and  $3420\text{ cm}^{-1}$  bands were more intense - the latter being much more sharp compared with that on the non-sintered rutile. The  $3610$  and  $3520\text{ cm}^{-1}$  bands were less intense, the former being observed only as a weak shoulder. The  $1610\text{ cm}^{-1}$  band was 30% of its value on the corresponding non-sintered surface.

Evacuation at 383 K (spec. 3.2a-c) reduced the  $3680\text{ cm}^{-1}$  band, increased the  $3655\text{ cm}^{-1}$  band to a maximum at

approximately 353 K (graph 3.2) and decreased the  $3410\text{ cm}^{-1}$  band. The  $3610$  and  $3520\text{ cm}^{-1}$  bands disappeared by evacuation at 338 K while the  $1620\text{ cm}^{-1}$  band had nearly disappeared by 383 K in contrast to that on the non-sintered surface. Further evacuation at 443 K (spec. 3.2d-f) caused little change in the  $3655\text{ cm}^{-1}$  band and  $3500\text{ cm}^{-1}$  region in contrast to the non-sintered surface. The  $3680\text{ cm}^{-1}$  shoulder decreased on raising the evacuation temperature from 398 K to 410 K and then remained relatively constant until 503 K. The  $1620\text{ cm}^{-1}$  band decreased further and disappeared after evacuation at 458 K.

On evacuation at 478 K (spec. 3.2g-i) the  $3655$  and  $3420\text{ cm}^{-1}$  bands showed sharp decreased similar to those for the corresponding bands on the non-sintered surface, the  $3420\text{ cm}^{-1}$  band disappearing to leave a broad  $3400\text{ cm}^{-1}$  shoulder much less intense than that on the non-sintered rutile. The  $3700\text{ cm}^{-1}$  band appeared after evacuation at 468 K and further evacuation to 583 K (spec. 3.2j-1) decreased the  $3655\text{ cm}^{-1}$  band to a shoulder on this band.

### 3.2.2 ADSORPTION OF H<sub>2</sub>O AND D<sub>2</sub>O ONTO OXIDIZED RUTILE

---

#### A. H<sub>2</sub>O onto a 673 K H<sub>2</sub>O surface

---

(Spectra 3.3 and Graph 3.3)

The starting surface (spec. 3.3a) showed a band at 3700 cm<sup>-1</sup> with a very weak shoulder at 3655 cm<sup>-1</sup>. Initial adsorption (spec. 3.3b-d) caused an increase in the 3700 and 3655 cm<sup>-1</sup> bands, the latter increasing more than the former. Broad bands also appeared in the 3400 and 1610 cm<sup>-1</sup> regions. Further adsorption (spec. 3.3e,f) of H<sub>2</sub>O increased the 3655 cm<sup>-1</sup> band, the 3700 cm<sup>-1</sup> band becoming a broad shoulder on the more intense 3655 cm<sup>-1</sup> band (spec. 3.3e). This shoulder narrowed and became more intense on further adsorption (spec. 3.3f) to form a shoulder at 3680 cm<sup>-1</sup>, the band at 3700 cm<sup>-1</sup> having now disappeared. The broad band at 3400 cm<sup>-1</sup> increased and a broad band formed at 1610 cm<sup>-1</sup>.

On increasing the dosage of H<sub>2</sub>O bands formed at 3610 and 3520 cm<sup>-1</sup> (spec. 3.3g) and the broad band centred on 1620 - 1610 cm<sup>-1</sup> also increased. These bands all increased with increases in H<sub>2</sub>O pressure (spec. 3.3h,j,l,n,o,q,r), the 1610 cm<sup>-1</sup> broad band shifting to 1625 cm<sup>-1</sup>. The 3655 cm<sup>-1</sup> band increased by approximately 6% (spec. 3.3h,j) in contrast to the sharp rise previous to the appearance of the 3610 and 3520 cm<sup>-1</sup> bands and decreased at higher vapour pressures of

H<sub>2</sub>O (spec. 3.3 l,n,o,q,r) shifting to 3620 cm<sup>-1</sup>. Little change occurred in the 3680 cm<sup>-1</sup> band although it became prominent at high vapour pressures (spec. 3.3 o,q,r). The 3400 cm<sup>-1</sup> broad band increased while the 3420 cm<sup>-1</sup> peak was only observed at a late stage in the adsorption (spec. 3.3 k-s).

#### Evacuation of the cell (spec. 3.3 i,k,m,p,s)

caused little change in the spectrum during earlier stages of the adsorption (compare spec. 3.3 h and i), evacuation of surfaces with greater H<sub>2</sub>O coverage decreased the 3610, 3520, 3420 and 1630 cm<sup>-1</sup> bands (spec. 3.3 k,m,p,s) and increased the 3655 cm<sup>-1</sup> band, little change was observed in the 3680 cm<sup>-1</sup> band.

Comparison of the evacuated surface spectra showed increases in the 3655 cm<sup>-1</sup> band (graph 3.3 and spec. 3.3 i,k,m,p,s) and in the 3610, 3520, 3410 and 1630 cm<sup>-1</sup> bands (spec. 3.3 i,k,m) as the adsorbed amount of H<sub>2</sub>O on the surfaces prior to evacuation increased.

#### B. D<sub>2</sub>O onto a 673 K Oxidized Surface

(Spectra 3.4 and Graph 3.4)

The adsorption of D<sub>2</sub>O onto rutile showed similar spectra to those of H<sub>2</sub>O, the bands being shifted by a factor of approximately  $\sqrt{2}$  to lower wavenumbers due to the substitution of the hydrogen atom by the heavier deuterium atom. Using the readout accessory on the spectrometer, the spectra were reproduced at twice the size of the original trace

and with the ordinate scale reversed. The spectra (3.4) showed clearly the initial stages of adsorption.

The initial dosage of  $D_2O$  (spec. 3.4 a-e) increased the  $2695\text{ cm}^{-1}$  band (corresponding to the  $3655\text{ cm}^{-1}$  band) while the original  $2720\text{ cm}^{-1}$  band became a broad shoulder on this band (spec. 3.4 d-e). The  $2680\text{-}2500\text{ cm}^{-1}$  region also increased in intensity. Further dosage of  $D_2O$  (spec. 3.4 f-i) increased the  $2690\text{ cm}^{-1}$  band while two shoulders appeared at  $2720$  and  $2710\text{ cm}^{-1}$  (corresponding to the  $3700$  and  $3680\text{ cm}^{-1}$  bands on the  $H_2O$  surface). Optical density also increased in the  $2680\text{-}2500\text{ cm}^{-1}$  region, bands appearing at  $2660$  and  $2600\text{ cm}^{-1}$  (corresponding to  $3610$  and  $3520\text{ cm}^{-1}$   $H_2O$  bands). On increased dosage of  $D_2O$  the  $2720\text{ cm}^{-1}$  band merged into the  $2710\text{ cm}^{-1}$  band while the  $2660$  and  $2610\text{ cm}^{-1}$  bands increased as observed for the adsorption of  $H_2O$ .

### C. Adsorption of $H_2O$ onto a 673 K $H_2O$ Oxidized Sintered Surface (Spectra 3.5 and Graph 3.5)

Initial adsorption of  $H_2O$  produced spectra similar to those for the non-sintered surface spec. 3.5a, corresponding to spec. 3.3g. The difference of intensities between the two samples was due to the greater density ( $0.31\text{g cm}^{-2}$  compared with  $0.39\text{g cm}^{-2}$ ) of the sintered rutile disc.

Further adsorption of  $H_2O$  (spec. 3.5 a,b,d) resulted in a decrease of the  $3680\text{ cm}^{-1}$  shoulder and increases in the



3610, 3520 and 1610  $\text{cm}^{-1}$  bands. A band appeared at 3410  $\text{cm}^{-1}$  which was sharper than on the corresponding non-sintered surface. On evacuation (spec. 3.5 c,e) of these surfaces the 3680  $\text{cm}^{-1}$  band decreased, the 3655  $\text{cm}^{-1}$  increased slightly (graph 3.5) and the 3610, 3520 and 1610  $\text{cm}^{-1}$  bands decreased to lower intensities than observed for the non-sintered rutile. The 3410  $\text{cm}^{-1}$  band decreased on evacuation.

Dosage of  $\text{H}_2\text{O}$  at higher vapour pressures (spec. 3.5 f,g,h,j) decreased the intensity of the 3680  $\text{cm}^{-1}$  band which became a separate band and also decreased the 3655  $\text{cm}^{-1}$  band shifting it to 3620  $\text{cm}^{-1}$ . The 3520, 3410 and 1610  $\text{cm}^{-1}$  bands increased while the 3610  $\text{cm}^{-1}$  band was observed only as a shoulder, in contrast to the non-sintered surface.

Evacuation of these surfaces (spec. 3.5 i,k) reduced the 3680  $\text{cm}^{-1}$  band to a constant value, increased the 3655  $\text{cm}^{-1}$  band and reduced the 3610, 3520, 3410 and 1620  $\text{cm}^{-1}$  bands to lower intensities than observed for the corresponding non-sintered surface (spec. 3.3 s).

Heating in  $\text{H}_2\text{O}$  (673 K,2h) cooling and evacuating (BT,1h) produced little change except a 25% increase in the 3410  $\text{cm}^{-1}$  band.

### 3.2.3 ADSORPTION OF H<sub>2</sub>O AND D<sub>2</sub>O ONTO REDUCED RUTILE

#### A. Reversibility of the Reduction Process

(Spec 3.6)

Reduction of discs caused a decrease in transmittance resulting in the need for maximum gain and maximum slit width between 4000 to 3000 cm<sup>-1</sup> (2.2.4). The loss of response and low signal:noise ratio prevented the accurate measurement of spectra in this region and deuterated surfaces were used in most of the experiments on BT reduced surfaces. Reduction also caused the discs to turn a blue-grey colour and increased the slope of the base line (spec. 2.3, 2.4).

Adsorption of D<sub>2</sub>O onto the surface (BT, ½h) and evacuation (BT, ½h) resulted in the formation of bands at 2720, 2695, 2535 cm<sup>-1</sup> and a broad band at 3660 cm<sup>-1</sup> (spec. 3.6a). A second dose of D<sub>2</sub>O (BT, 1½h) and evacuation (BT, ¾h) removed the 3660 cm<sup>-1</sup> band which reappeared on further dosage of D<sub>2</sub>O (298 K, 5 days) and evacuation (BT, ½h) (spec. 3.6b) together with a broad band at 1570 cm<sup>-1</sup>.

Reoxidation of the surface (O<sub>2</sub>, 1.33 x 10<sup>4</sup> N m<sup>-2</sup>, 673 K, 1h, x2) (spec. 3.6c) and dosage of D<sub>2</sub>O (BT, 4h) followed by evacuation (BT, 1h) (Spec. 3.6d) formed the usual 'beam temperature, D<sub>2</sub>O' surface. Further reduction (usual process) and evacuation (673 K, 60h) followed by treatment

with  $D_2O$  (BT,  $\frac{1}{2}$ h) and evacuation (BT,  $\frac{1}{2}$ h) resulted in a surface (spec. 3.6e) similar to that observed after the initial reduction (spec. 3.6a) except for the absence of a  $3660\text{ cm}^{-1}$  band. Heating in  $D_2O$  (673 K, 2h and 16h) (spec. 3.6 f,g) cooling and evacuation increased the  $2690$  and  $2535\text{ cm}^{-1}$  bands and also increased the broad band beneath the  $2535\text{ cm}^{-1}$  peak.

B. Adsorption of  $H_2O$  onto a 673 K  $H_2O$  Reduced Rutile Surface  
(Spec. 3.7)

As previously stated the response and signal:noise ratio are too low for the recording of accurate spectra in the  $4000 - 3000\text{ cm}^{-1}$  region, and it was not possible to study the rehydroxylation of a reduced surface using  $H_2O$ . Spec. 3.7 shows a rehydroxylated surface after evacuation (BT,  $\frac{1}{2}$ h) and indicates the quality of the spectrum in the range  $4000 - 3000\text{ cm}^{-1}$ . The intensity of the band observed at  $1620\text{ cm}^{-1}$  is 35% that of the same band on the corresponding oxidized surface. No  $1560\text{ cm}^{-1}$  band was observed.

C. Adsorption of  $D_2O$  onto a 673 K  $D_2O$  Reduced Rutile Surface  
(Spec. 3.8 and Graph 3.5)

Bands appeared at  $2720$  and  $2695\text{ cm}^{-1}$  on the initial adsorption of  $D_2O$  onto reduced rutile (spec. 3.8 a-e) and increased with dosage, the former more rapidly than the latter (in contrast to the oxidized surface) to reach a maximum by spec. 3e. The  $2710\text{ cm}^{-1}$  shoulder was not observed, while the

absorbance of the base line below  $2680\text{ cm}^{-1}$  increased.

Further adsorption of  $\text{D}_2\text{O}$  (spec. 3 f,h,i,j) decreased the  $2720\text{ cm}^{-1}$  band while the  $2695\text{ cm}^{-1}$  band continued to increase, the  $2720\text{ cm}^{-1}$  band becoming a shoulder at the higher intensities (spec. 3.8 i,j), with a possible shoulder at  $2710\text{ cm}^{-1}$  (spec. 3.8j). The  $2535\text{ cm}^{-1}$  band appeared (spec. 3.8j) together with increases in the  $2680 - 2500\text{ cm}^{-1}$  region. Evacuation of the  $\text{D}_2\text{O}$  vapour (spec. 3.8k) increased the  $2720\text{ cm}^{-1}$  band to its maximum, decreased the  $2695\text{ cm}^{-1}$  band (in contrast to the oxidized surface) and reduced the  $2680 - 2500\text{ cm}^{-1}$  band.

Adsorption of  $\text{D}_2\text{O}$  at higher vapour pressures (spec. 3.8 l,m) decreased the  $2720\text{ cm}^{-1}$  band to a shoulder on the increased  $2695\text{ cm}^{-1}$  band while bands appeared at  $2660, 2610\text{ cm}^{-1}$  and the  $2535\text{ cm}^{-1}$  band increased in intensity. Dosage of  $\text{D}_2\text{O}$  at relatively high vapour pressures (spec. 3.8 o) produced a spectrum with vapour bands present. No comparable spectra were observed for the oxidized rutile at similar vapour pressures. Evacuation of these surfaces increased the  $2720\text{ cm}^{-1}$  band to its maximum value and decreased the  $2655$  and  $2535\text{ cm}^{-1}$  bands to intensities which were greater than on the previous evacuated surface.

Evacuation of the surface at  $473\text{ K}$  (16h) (spec. 3.8 q) decreased the  $2695\text{ cm}^{-1}$  band to a weak shoulder on the  $2720\text{ cm}^{-1}$  peak which had also decreased.

### 3.2.4 SUMMARY

A Summary of bands observed is shown in Table 3.1.

Desorption of water to 368 K from non-sintered rutile first removed the 3610 and 3520  $\text{cm}^{-1}$  bands together with a decrease in the 1620  $\text{cm}^{-1}$  band. Evacuation at 473 K removed the 3420  $\text{cm}^{-1}$  band to leave a broad 3400  $\text{cm}^{-1}$  band and reduced the intensities of the 3655  $\text{cm}^{-1}$  band (by 70%) and 3680  $\text{cm}^{-1}$  shoulder which resolved to reveal a 3700  $\text{cm}^{-1}$  band. Evacuation at 663 K reduced the 3655  $\text{cm}^{-1}$  band to a shoulder on the weak 3700  $\text{cm}^{-1}$  band and removed the 3400  $\text{cm}^{-1}$  broad band. A broad band at 1600  $\text{cm}^{-1}$  was still present. Evacuation of the sintered surface was similar except the 3610, 3520, 1610  $\text{cm}^{-1}$  bands were less intense and the 1610  $\text{cm}^{-1}$  band was removed by evacuation at 358 K. Differences also occurred in the behaviour of the 3700  $\text{cm}^{-1}$  band while the 3420  $\text{cm}^{-1}$  band was more intense than for the corresponding non-sintered surface.

Initial adsorption onto oxidized rutile resulted in an increase of the 3700, 3655, broad 3400 and 1610  $\text{cm}^{-1}$  bands, the 3700  $\text{cm}^{-1}$  band merging into the 3680  $\text{cm}^{-1}$  shoulder before the appearance of the 3610 and 3520  $\text{cm}^{-1}$  bands. Higher vapour pressures increased the 3610, 3520 and 1610  $\text{cm}^{-1}$  bands, decreased the 3655  $\text{cm}^{-1}$  band and formed the 3420  $\text{cm}^{-1}$  peak. Evacuation increased the 3655  $\text{cm}^{-1}$  band and decreased the 3610, 3520, 3420 and 1610  $\text{cm}^{-1}$  bands.

Spectra recorded during the adsorption on the adsorption of  $D_2O$  onto a reduced surface differed from those recorded during similar adsorption onto the oxidized surface. The  $2720$  and  $2695\text{ cm}^{-1}$  bands increased on initial adsorption while the  $2720\text{ cm}^{-1}$  band formed a shoulder on the  $2695\text{ cm}^{-1}$  band after it had reached its maximum. Evacuation increased the  $2720\text{ cm}^{-1}$  band back to its maximum and decreased the  $2695\text{ cm}^{-1}$  band. Dosage at higher vapour pressures formed the  $2660$ ,  $2600$  and  $2535\text{ cm}^{-1}$  bands, the first two disappearing on evacuation, while the  $2535\text{ cm}^{-1}$  decreased in intensity.

### 3.3 DISCUSSION AND CONCLUSIONS

In the following discussion only bands observed on the H<sub>2</sub>O surface will be considered although the remarks apply to the equivalent bands on the deuterated surface unless stated.

#### 3.3.1 PRELIMINARY ASSIGNMENTS

Bands observed above 2000 cm<sup>-1</sup> on H<sub>2</sub>O and D<sub>2</sub>O surfaces have frequencies typical of those observed for OH and OD stretching vibrations<sup>5,6</sup> and may therefore be assigned to hydroxyl groups either directly bonded to the surface or present in water molecules. Individual groups are assigned to one of these types of hydroxyl groups by considering the spectrum of water and the results from adsorption and desorption experiments. Adsorption of compounds which interact with hydroxyl groups or other surface sites provide further information on the nature of the surface (3.3.3).

The fundamental frequencies observed for H<sub>2</sub>O and D<sub>2</sub>O are shown in Table 3.2<sup>64</sup>. The 1610 cm<sup>-1</sup> band observed on the H<sub>2</sub>O surface is assigned to the bending vibration of water molecules. The reduction of this band during evacuation to 393 K coincided with the disappearance of the 3610, 3520 cm<sup>-1</sup> bands and a reduction in the broad 3400 cm<sup>-1</sup> underlying the 3420 cm<sup>-1</sup> peak. The behaviour of the 3610, 3520 and broad

3400  $\text{cm}^{-1}$  bands is similar to that of the 1610  $\text{cm}^{-1}$  band and they may be tentatively assigned to water molecules on the rutile surface or hydroxyl groups hydrogen-bonded to water molecules. The remaining 3700, 3655 and 3420  $\text{cm}^{-1}$  bands are assigned to hydroxyl groups on the surface of rutile while the 3680  $\text{cm}^{-1}$  shoulder will not be assigned and is discussed later together with a detailed discussion of the behaviour of all the bands observed.

To account for the different types of OH groups observed and the results obtained from other infrared studies on the rutile surface (Table 1.2) a model of the surface structure must be considered.

### 3.3.2 SURFACE STRUCTURE

The structure of an oxide surface may be assumed either completely heterogeneous or formed from a number of well defined crystal planes. The infrared spectrum of a heterogeneous surface would contain broad bands due to hydroxyl groups in many different environments and is not considered for oxides which show sharp discrete bands. The latter model has been adopted to explain the observed bands in infrared spectra of silica<sup>65</sup>, alumina<sup>66</sup>, rutile<sup>10,41,44</sup>, anatase<sup>67</sup>, zinc oxide<sup>68</sup> and magnesium oxide<sup>69</sup>.



The planes assumed for the microsurface are deduced from those present on the massive crystal if the oxide crystallites are of similar structure<sup>10,41,68</sup>. Electron and x-ray diffraction studies may indicate the predominant planes exposed on other crystallites<sup>66</sup> while the requirement of a low surface energy, that is minimum loss of coordination of surface ions, also indicates the favourable surface planes<sup>69</sup>.

The nature of the hydroxyl and water species on the oxide surface is determined by considering the adsorption of water molecules onto the uncoordinated ions present in the surface. Possible division of the water molecules into hydroxyl ions and protons may lead to acidic and basic sites in the surface<sup>67</sup> onto which other water molecules may adsorb.

Peri<sup>66</sup> adopted an alternative method for the model of the surface of  $\gamma$ -alumina. All the (100) sites were initially saturated with hydroxyl groups and a 'Monte Carlo' method applied, using a computer, to determine the random elimination of OH groups to form water, assuming certain conditions. Five observed bands between 3800 and 3700  $\text{cm}^{-1}$  were assigned to five types of hydroxyl groups which differed by the number of nearest oxide neighbours (0 to 4) surrounding them.

The crystallites of rutile used in these experiments resembled the massive mineral crystals<sup>62</sup> (section 2.3.1) and the

planes exposed on the surface are assumed identical. Rutile mineral crystals are of the Zircon Type<sup>62</sup> with the (110), (100), (101) and (111) planes exposed. Table 3.3 shows the percentage occurrence of the exposed planes as determined by electron diffraction studies on a rutile crystal<sup>70</sup>.

Diagrams of the (110), (101) and (100) planes are shown in figs. 3.1-3 (redrawn from ref. 41). The (110) plane (fig. 3.1) consists of coplanar oxygen ions (fully coordinated) and titanium ions (5 coordinate) with oxygen ions (2 coordinate) above the plane bridged between two fully coordinated titanium ions. The four coplanar oxygen ions round the uncoordinated titanium ion are in the 'equatorial(e) position (Ti-O(e) = 0.1944 N m) while the vacancy is in the axial(a) position (Ti-O(a) = 0.1988 N m).

The (101) plane is shown in figure 3.2. All of the  $Ti^{4+}$  ions are five coordinate with a vacancy in the equatorial position. The (110) plane (fig. 3.3) contains 5 coordinate titanium ions with the vacancy in the axial position. The (211) and (111) planes have 3 coordinate titanium ions and a complex structure which may be seen by reference to the appropriate crystal model.

The model of the rutile surface to be used in this work is based on that shown in table 3.3 in which the (110) plane predominates while the other four planes account for 40% of the surface. The titanium and oxygen atoms are considered

as ions in the text but are drawn as though covalent bonded to indicate spatial distribution.

### 3.3.3 ADSORPTION ONTO THE RUTILE SURFACE

#### A. Infrared Studies of Water Adsorption

The effect of surface chloride adsorbed on rutile has been investigated by Jackson and Parfitt<sup>10</sup> and found to affect the infrared spectrum of the BT, H<sub>2</sub>O surface at surface concentrations higher than 147-277ppm. Above these concentrations the 3615 and 3530 cm<sup>-1</sup> bands were not observed, the 3400 cm<sup>-1</sup> was of greater intensity and split into shoulders at 3410 and 3300 cm<sup>-1</sup> due to the interaction of water molecules with the chloride ions.

Jones and Hockey<sup>11</sup> compared rutile prepared from titanium tetrachloride and treated<sup>1</sup> to remove chloride ions with rutile prepared from the isopropoxide<sup>11</sup>. They found that the former sample retained more water at beam temperature, was completely dehydroxylated by evacuation at 673 K and contained all the hydroxyl and water species on the surface, all the bands being completely exchanged by exposure to D<sub>2</sub>O at room temperature. After storing the sample in a closed pyrex tube for four months complete exchange at room temperature did not occur due to aggregation of the particles. Similar results were observed for other 'chloride' rutiles<sup>51,52</sup>. The infrared spectrum of the rutile prepared from titanium isopropoxide showed lower scattering characteristics than the 'chloride' samples, a less intense 3520 cm<sup>-1</sup> band and a sharp 3410 cm<sup>-1</sup> band. 'Chloride' samples which had been sintered also showed this sharp band.

The assignments of bands observed on  $H_2O$ , oxidized, rutile surfaces during adsorption and desorption studies<sup>10,11,42,44</sup> are shown in table 3.4. Jackson and Parfitt<sup>10</sup>, and Primet et al<sup>44</sup> considered only the predominant (110) cleavage plane while Jones and Hockey<sup>42</sup> considered the (110), (101) and (100) planes assuming these to form 98% of the surface with percentage occurrences of 60, 19, 19 respectively. These models are briefly described below while the assignments will be discussed in section 3.3.4 which details the behaviour of the bands observed in this work.

The spectra observed by Jackson and Parfitt<sup>10</sup> during the adsorption and desorption of water are similar to those observed in this work with some exceptions. The spectrum of their beam temperature surface compared with the corresponding surface in this work showed more intense 3610 and 3520  $cm^{-1}$  bands while the 3420  $cm^{-1}$  peak was obscured by a broad 3400  $cm^{-1}$  band which on evacuation to 423 K divided to produce a peak at 3420  $cm^{-1}$  with a broad shoulder at 3350  $cm^{-1}$ . The 3420  $cm^{-1}$  band did not decrease significantly until after evacuation at 573 K, contrasting with its disappearance after a 473 K evacuation in this work. The sample investigated by Jackson<sup>11</sup> appears to retain more water at room temperature and during evacuation at higher temperatures than the sample studied in this work. Another difference is the appearance of a 3690  $cm^{-1}$  band after evacuation at 473 K for 2h which disappeared on further evacuation.

The infrared spectrum of the sintered rutile surfaces are similar in both studies with the exception of the  $3690\text{ cm}^{-1}$  band observed by Jackson.

The model of the rutile surface adopted by Jackson and Parfitt<sup>10</sup> is similar to that adopted by Boehm for anatase.  $\text{H}_2\text{O}$  molecules adsorb on the uncoordinated metal ions (row A<sup>41</sup>) in the (110) plane before dividing to leave  $\text{OH}^-$  groups on the  $\text{Ti}^{4+}$  ions and protons on the two coordinate oxygen ions (row B). The  $\text{Ti}^{4+}$  ions with a vacant site (row A) carry a formal positive charge of  $2/3+$  while the oxygen ions with a vacant site (row B) carry a  $2/3-$  charge. On hydroxylation these are reduced to  $1/3-$  and  $1/3+$  respectively and the surface energy is lowered.

The hydroxyl groups formed on the cation (row A) are monodentate in attachment (terminal groups) and more basic, due to the  $1/3-$  charge, than the OH groups (row B) bidentate in attachment (bridged groups) with a  $1/3+$  charge. The terminal groups are sufficiently close (296pm) to hydrogen bond and condense by a proton tunneling mechanism at temperatures above  $473\text{ K}$ <sup>77</sup> while the bidentate nature of the bridged hydroxyl groups (296pm apart) hinders mutual condensation. The  $3700\text{ cm}^{-1}$  band was therefore assigned to the bridged hydroxyls and the  $3670\text{ cm}^{-1}$  band to the terminal hydroxyl groups. Other assignments are shown in table 3.4.

Prinet et al<sup>44</sup> consider hydroxyl groups attached to

the five coordinate titanium ions on the (110) face which are surrounded by the four equatorial oxygen ions forming a square plane of sides 253nm and 296nm. The edges of these planes are considered adjacent resulting in hydroxyl groups 253nm and 296nm apart which hydrogen bond to produce bands at 3410 and 3655  $\text{cm}^{-1}$  respectively, while the 3685  $\text{cm}^{-1}$  band is assigned to the isolated hydroxyl groups. This model appears to be incorrect as the edges of the planes are joined in one direction only on the (110) face to give row A hydroxyl 296nm apart.

Dehydroxylation-rehydroxylation cycles reduced the temperature required to remove the OH groups while after ten cycles no more specific OH groups were reformed. It was proposed that dehydroxylation initially removes hydrogen bonded OH groups to form Ti-O-Ti bridges which reform hydroxyl groups on rehydration with the possible migration of protons or hydroxyl groups. After the condensation of hydrogen bonded OH groups migration of protons or hydroxyl groups removes isolated OH groups leaving an oxygen ion attached to one  $\text{Ti}^{4+}$  ion and a five coordinate  $\text{Ti}^{4+}$  ion, capable only of coordinately bonding to  $\text{H}_2\text{O}$  molecules. Subsequent dehydroxylation-rehydroxylation cycles increase these uncoordinated metal ions consequently decreasing the number of OH groups formed on rehydroxylation.

The 'chloride free' rutile sample used by Jones and Hockey<sup>11,41,42</sup> has a  $\text{BT}, \text{H}_2\text{O}$  spectrum similar to those observed

by Jackson<sup>10</sup> and Griffiths (this work) for a sintered surface, but showed considerable differences on evacuation at elevated temperatures. The  $3680\text{ cm}^{-1}$  shoulder did not develop into a  $3700\text{ cm}^{-1}$  band but disappeared with the  $3610\text{ cm}^{-1}$  shoulder. The  $3410$  and  $3650\text{ cm}^{-1}$  bands behaved in a similar manner to those observed in this work, the former band disappearing first, but the  $3650\text{ cm}^{-1}$  band did not disappear and remained after evacuation at  $673\text{ K}$  ( $\frac{1}{2}\text{h}$ ).

Jones and Hockey<sup>41</sup> consider the initial adsorption of water onto the (110) plane to form terminal (row A) and bridged (row B) hydroxyl groups. The bidentate OH groups shift to form a monodentate attachment to the titanium ions which become five coordinate. The  $3650\text{ cm}^{-1}$  band is assigned to the row A hydroxyls while the  $3410\text{ cm}^{-1}$  band is assigned to the row B hydroxyls, the lower frequency being due to the greater unsaturation of the underlying titanium ion reducing the bond strength. All the hydroxyl groups are considered to lie with their axes perpendicular to the surface which prevents hydrogen bonding between hydrogen atoms and neighbouring oxygen atoms.

Adsorption of  $\text{H}_2\text{O}$  molecules onto the (100) and (101) planes and subsequent division would result in each titanium ion being attached to two hydroxyl groups which occupy an individual cross-sectional area of  $6-7 \times 10^{-2}\text{ N m}^2$ . As the cross-sectional area of an OH ion  $1 \times 10^{-1}\text{ N m}^2$  the  $\text{H}_2\text{O}$  molecules are considered to bond via a  $\sigma$ - bond formed using a filled orbital of the oxygen atom in the water molecule



and the empty orbital on the titanium ion.

The water molecules on the (101) plane are directed such that the hydrogen atoms do not interact with surface oxygen ions while the direction of those on the (100) plane does enable the hydrogen atoms to interact with the supra-planar oxygen ions. The two bands at 3680 and 3610  $\text{cm}^{-1}$  are assigned to the  $\nu_3$  and  $\nu_1$  vibrations of water molecules on the (101) plane and the 3550  $\text{cm}^{-1}$  to hydrogen bonded molecules on the (100) plane. The loss of water molecules from the (110) plane is not as energetically favourable as loss from the (100) plane as molecules on the former plane are in the equatorial position of the titanium ion and those on the latter are in the axial position.

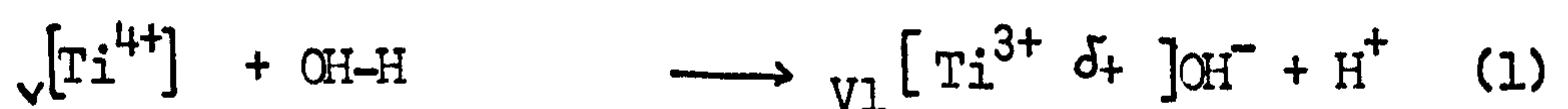
#### B. Other Studies of the Adsorption of Water onto Rutile

Munuera and Stone<sup>71</sup> have investigated the adsorption of water onto rutile and the temperature programmed desorption (TPD) of water from rutile. TPD showed two peaks at 523 K and 643 K, the former due to a strongly adsorbed form of molecular water and the latter due to dissociatively adsorbed water forming surface hydroxyl groups. Calibration of the 643 K peak indicated not more than 50% of the sites on the (110) plane were hydroxylated assuming all the surface to consist of this plane. The coverage corresponds to a 100% hydroxylation of the (110) plane assuming a 60% surface occurrence<sup>41</sup>.

Bickley and Jayanty<sup>72</sup> also observe two TPD peaks at 423 K and 643 K on a sample calcined in air at 1123 K (5h).

After repeated cycles of outgassing and baking in oxygen (1123 K) the water peaks were greatly reduced but partially restored by immersing the sample in boiling water. The first peak corresponds to 65% total water desorbed while the remaining 35% arises from the condensation of surface hydroxyl groups.

Waldsax and Jaycock<sup>73,111</sup> have reported some calculations on the surface adsorption energies of water on rutile. A map of the surface electrostatic field 0.2nm above the surface of rutile shows the most favourable adsorption site to be over the five coordinated  $Ti^{4+}$  ion. The bonding energy is  $-104 \text{ kcal mole}^{-1}$ ; the molecule being orientated with the dipole almost vertically downwards. The first dissociation energy of H-OH is  $117 \text{ kcal mole}^{-1}$ , the water molecule is assumed to dissociate (eqn.1) with the proton descending the steepest field slope to the two-coordinated oxygen (eqn.2, complete reaction).



(Roman numerals denote the coordination number of the atom).

On the basis of these calculations total hydroxylation of the (110) face is expected in contrast to the 50% hydroxylation observed<sup>71</sup>.

Waldsax and Jaycock also calculated<sup>111</sup> the effect of substituting  $Al^{3+}$  and  $Ti^{3+}$  ions into the place of the five

coordinate  $\text{Ti}^{4+}$  ion. The potential well of  $-104 \text{ kcal mole}^{-1}$  for the unsubstituted (110) face rose to  $-41 \text{ kcal mole}^{-1}$  for  $\text{Al}^{3+}$  and  $-35 \text{ kcal mole}^{-1}$  for  $\text{Ti}^{3+}$ .

Calculations carried out on water adsorption on the (100) surface show a potential well of  $-98 \text{ kcal mole}^{-1}$  to exist on the surface but with 60% of the surface having binding energies of less than  $10 \text{ kcal mole}^{-1}$ .

Morimoto et al<sup>74</sup> have investigated the water content and heats of immersion of rutile samples prepared from titanium sulphate and suitably treated to remove surface impurities. The samples studied were: unsintered rutile (RI), rutile heated in air (1073 K, 4h) and exposed to saturated water vapour for five days (RT)(RII), and the unsintered sample immersed in hot water (353 K, 3 days) and dried (383 K, 10h)(RIII). The water content (expressed as  $\text{OH}^{\circ}/\text{A}^2$ ) was determined after outgassing temperatures of 373-1273 K and found to decrease in the order RIII > RI > RII at any given temperature. Sample RIII began to sinter at 873 K  $200^{\circ}$  lower than RII possibly due to condensation dehydration of hydroxyl groups from the facing surfaces of contacting particles<sup>75</sup>. Heats of immersion were found to have a maximum at 673 K in the order RIII > RI > RII identical to the order of water content. These results support those observed in this work that show the sintered surface adsorbs less water than the unsintered surface.

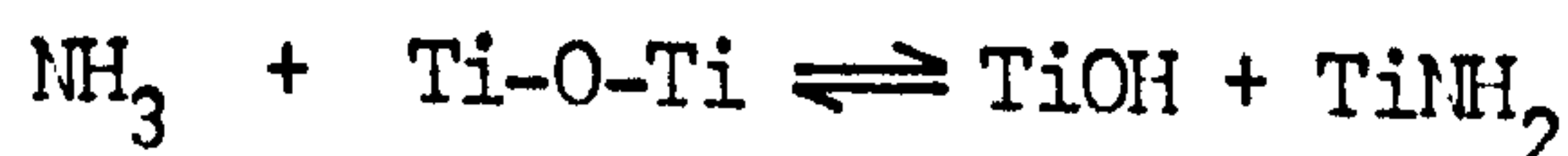
Day et al<sup>85</sup> have recently studied water adsorption onto rutile using an electrobalance. The adsorption isotherm shows two 'knees' at relative pressures of 0.03 and 0.22, the latter corresponding to monolayer coverage. The quantity of water adsorbed at the second 'knee' on a surface outgassed at 393 K corresponds to that required for a close packed monolayer. The water molecules desorbed below 393 K are removed from the monolayer while those removed above 393 K are coordinately bound to the surface. 1.4 molecules  $\text{N m}^{-2}$  of  $\text{H}_2\text{O}$  were removed from 373 to 473 K and 1.7 molecules  $\text{N m}^{-2}$  from 473 K to 673 K while the total quantity of  $\text{H}_2\text{O}$  desorbed was half that observed by Jones and Hockey<sup>42</sup> who assume that hydrogen-bonded water was removed by overnight evacuation at 298 K.

### C. Lewis and Brønsted Acid Sites on Rutile

The existence of sites on metal oxides which exhibit Lewis and Brønsted acidity is well documented<sup>5,6</sup>. The reactions of the acidic and basic OH groups on  $\text{TiO}_2$  with various acids and bases have been investigated<sup>67</sup> while the acidity of surface hydroxyl groups on several oxides (not  $\text{TiO}_2$ ) has also been determined<sup>76</sup>. Ammonia has been used extensively<sup>5,6</sup> to study the acidic nature of oxide surfaces as it may act as a Brønsted base, to form ammonium ions, or coordinate to Lewis acid sites, each of these forms having a characteristic

spectrum. Pyridine<sup>5,6</sup> has also been used as it shows characteristic spectra dependant on its action as a Lewis base, a Brønsted base (to form the pyridinium ion) or as a compound capable of hydrogen bonding to the hydroxyl groups.

Parfitt et al<sup>45</sup> have studied the adsorption of ammonia onto rutile and observed four N-H stretching bands between  $3400\text{ cm}^{-1}$  and  $3200\text{ cm}^{-1}$  which were assigned to ammonia molecules coordinated to two Lewis sites. The disappearance of the  $3700\text{ cm}^{-1}$  band on adsorption and reappearance on evacuation of the sample indicate hydrogen bonding to the hydroxyl group assigned to this band while an increase in the  $3660\text{ cm}^{-1}$  hydroxyl band after evacuation of excess ammonia is assumed to indicate the reaction



No bands due to  $\text{NH}_4^+$  were observed after dosage onto wet or dry surfaces or after admission of  $\text{H}_2\text{O}$  vapour to a surface pretreated with ammonia indicating that no Brønsted sites were present on the surface. Adsorption of ammonia onto a surface pretreated with hydrogen chloride did produce ammonium ions.

Jones and Hockey<sup>11</sup> adsorbed pyridine onto rutile and observed bands due to pyridine molecules bonded to Lewis sites, bands due to pyridinium ions or hydrogen-bonded molecules were not observed. The bands at  $3650$  and  $3410\text{ cm}^{-1}$  were unaffected by the adsorption of pyridine while the  $3680$ ,  $3610$ ,  $3550$  and  $1600\text{ cm}^{-1}$  bands decreased indicating that pyridine adsorbed by displacing coordinately bonded water.

Parfitt et al<sup>48</sup> observed a series of bands on the adsorption of pyridine onto rutile which were interpreted as adsorption onto one type of Lewis site. Two other bands were assigned to pyridine molecules weakly adsorbed onto the second type of Lewis site<sup>45</sup>. No bands due to pyridinium ions were observed on dry and wet surfaces but were observed on surfaces pretreated with hydrogen chloride, and tin tetrachloride<sup>55</sup>.

Prinet et al<sup>47</sup> observed bands due to the  $\text{NH}^+$  group after adsorbing trimethylamine onto anatase evacuated at 473 K and concluded that some OH groups on this surface show Brønsted acidity.

Parfitt et al<sup>52</sup> investigated the adsorption of hydrogen chloride onto "wet" and "dry" rutile surfaces. Initial dosage of HCl onto the dry surface increased the  $3660 \text{ cm}^{-1}$  hydroxyl band, shifted the  $3700 \text{ cm}^{-1}$  band to a shoulder and increased the  $3400$  and  $1600 \text{ cm}^{-1}$  bands indicating the formation of water. Further adsorption decreased the  $3690 \text{ cm}^{-1}$  band due to reaction while the  $3660 \text{ cm}^{-1}$  band decreased slightly indicating the former to be more reactive.  $3360$  and  $1565 \text{ cm}^{-1}$  bands were observed at high partial pressures of HCl which were assigned to the species  $\text{Ti}^{4+}(\text{H}_2\text{O})\text{Cl}^-$ . Dosage of HCl onto a "wet" surface removed the  $3690 \text{ cm}^{-1}$  shoulder and the  $3660 \text{ cm}^{-1}$  band, which reappeared at lower intensity on evacuation indicating a hydrogen-bonding interaction.

Jones and Hockey<sup>11</sup> investigated the reactions of HCl, SOCl<sub>2</sub> and SO<sub>2</sub> with the groups on a beam temperature surface. Initial adsorption of HCl onto a BT H<sub>2</sub>O surface with a spectrum indicating less coordinated water than observed by Parfitt et al<sup>52</sup> replaced all the bands except the 3655 and 3410 cm<sup>-1</sup> by a broad 3400 cm<sup>-1</sup> band. Further adsorption removed the 3680 cm<sup>-1</sup> band before the 3655 cm<sup>-1</sup> band, increased the 3400 cm<sup>-1</sup> band alongside the 3410 cm<sup>-1</sup> band and produced a band at 1565 cm<sup>-1</sup>. Evacuation at 473 K increased the 3655 cm<sup>-1</sup> band and removed the 3400 cm<sup>-1</sup> band to leave a very weak 3410 cm<sup>-1</sup> absorption, which indicated the effect of surface chloride in reducing the 3410 cm<sup>-1</sup> band and decreasing the dehydroxylation temperature.

Thionyl chloride reacted readily at room temperature with the hydroxyl groups on rutile in contrast to the slow reaction with silica hydroxyls and indicated the former to be appreciably ionic in nature. The reaction of the rutile surface with sulphur dioxide was similar to that with hydrogen chloride, the 3680 cm<sup>-1</sup> band being removed and the 3655 cm<sup>-1</sup> band decreasing. No broad bands were observed at 3400 and 1565 cm<sup>-1</sup> and the 3550 band did not disappear but increased in intensity.

#### D. Conclusions

Broad conclusions may be drawn from the above work.

- i) Two hydroxyl groups exist on the beam temperature rutile surface, probably on the (110) plane. They may be hydrogen-bonded.
- ii) Two Lewis sites exist on the surface, one stronger than the other. These may be related to the two types of  $\text{Ti}^{3+}$  ions observed by e.s.r. spectroscopy<sup>27,28</sup>.
- iii) No Brønsted sites exist on the surface.
- iv) Sintering affects the beam temperature surface, increasing and sharpening the  $3410 \text{ cm}^{-1}$  band.
- v) The presence of surface chloride affects the properties of the rutile surface.

The behaviour and assignment of the individual bands is now considered. The adsorption and desorption processes on the surfaces studied is considered in 3.5.



### 3.4 BEHAVIOUR OF OBSERVED BANDS

#### 3.4.1 3700 cm<sup>-1</sup> BAND

This band is hidden on the BT, H<sub>2</sub>O, oxidized unsintered surface (spec. 3.3) and does not appear until evacuation at 423 K - 455 K (spec. 3.1 g,h). On evacuation at higher temperatures it does not decrease as rapidly as the 3655 and 3410 cm<sup>-1</sup> bands and remains on a surface evacuated at 663 K (13h) together with a weak 3660 cm<sup>-1</sup> shoulder and residual absorption at 1600 cm<sup>-1</sup>. Behaviour on the sintered surface (spec. 3.2) is similar although it is less intense and does not show a regular decrease.

This band is present on 673 K H<sub>2</sub>O and D<sub>2</sub>O oxidized surfaces before dosage of H<sub>2</sub>O and D<sub>2</sub>O respectively. Dosage of H<sub>2</sub>O (spec. 3.3) and D<sub>2</sub>O (spec. 3.4) appear to increase the intensity of this band which may, in part, be due to increases in the adjacent 3680 and 3655 cm<sup>-1</sup> bands. The intensity of the band reaches a maximum absorbance (specs. 3.3f, 3.4h) just before merging into the 3680 cm<sup>-1</sup> shoulder. The rate of increase of the 3655 cm<sup>-1</sup> band decreases considerably near this maximum (graphs 3.3 and 3.4). Dosage of H<sub>2</sub>O onto the sintered surface produces results similar to those observed for the 3700 cm<sup>-1</sup> on the unsintered sample.

Dosage of  $D_2O$  on a 673 K reduced surface (spec. 3.8) produces a band at  $2720\text{ cm}^{-1}$  which behaves differently from that observed on a  $D_2O$  oxidized surface and the equivalent  $3700\text{ cm}^{-1}$  on an  $H_2O$  oxidized surface. On initial dosage the  $2720\text{ cm}^{-1}$  band increases more rapidly (graph 3.6) than the  $2695\text{ cm}^{-1}$  band and reaches a maximum (spec. 3.8e) while the latter is less intense. At higher vapour pressures it decreases in intensity, forming a shoulder on the  $2695\text{ cm}^{-1}$  band which increases in intensity. On evac the  $2720\text{ cm}^{-1}$  band increases to its maximum value to become a discrete band while the  $2695\text{ cm}^{-1}$  band decreases.

Jones and Hockey<sup>11,41,42</sup> do not observe this band while Jackson and Parfitt<sup>10</sup> assign it to the bidentate hydroxyl group and Primet et al<sup>42</sup> to an isolated hydroxyl group of the five-coordinate titanium ion on the (110) plane. Of the terminal and bridged hydroxyls the latter is the more acidic and would have a lower frequency than the former<sup>76</sup>; the  $3700\text{ cm}^{-1}$  band is not therefore assigned to bridged hydroxyl groups.

The  $3700\text{ cm}^{-1}$  band is the most thermally stable and highest frequency band observed on the rutile surface. Bands of this type on other oxides are usually assigned to isolated hydroxyl groups<sup>5,6,68,69</sup> which is the assignment adopted here, the five-coordinate  $Ti^{4+}$  ions (row A) on the predominant (110) plane<sup>70</sup> being the probable sites<sup>73</sup>. The  $3700\text{ cm}^{-1}$  band is therefore assigned to isolated terminal

(row A) hydroxyl groups. Other studies<sup>10,41</sup> assign the  $3655\text{ cm}^{-1}$  band to this group.

#### 3.4.2 $3680\text{ cm}^{-1}$ BAND

On the BT,  $\text{H}_2\text{O}$  oxidized sintered and unsintered surfaces this band is present as a shoulder on the  $3655\text{ cm}^{-1}$  band. On evacuation of the unsintered rutile it increases with the  $3655\text{ cm}^{-1}$  band (graph 3.1) before decreasing and revealing the  $3700\text{ cm}^{-1}$  band (spec. 3.1h) while on the sintered surface it does not increase and reveals the  $3700\text{ cm}^{-1}$  at a lower intensity than on the unsintered surface.

On initial dosage of  $\text{H}_2\text{O}$  (spec. 3.3) and  $\text{D}_2\text{O}$  (spec. 3.4) onto oxidized rutile it is observed as a shoulder between the  $3700$  and  $3655\text{ cm}^{-1}$  bands (or deuterium equivalents) and increases with the  $3655\text{ cm}^{-1}$  band eventually obscuring the  $3700\text{ cm}^{-1}$  band. Dosage of water at higher pressures does not increase the intensity of this band but it becomes predominant due to the decrease and shift of the  $3655\text{ cm}^{-1}$  band. The  $3680\text{ cm}^{-1}$  shoulder is not observed on dosage of  $\text{D}_2\text{O}$  onto reduced rutile except in the presence of high relative vapour pressures. It disappears on evacuation with the decrease of the  $3655\text{ cm}^{-1}$  band and the disappearance of the  $3610$  and  $3520\text{ cm}^{-1}$  bands.

Jackson and Parfitt<sup>10</sup> observed a band at  $3690\text{ cm}^{-1}$  between the  $3700$  and  $3670\text{ cm}^{-1}$  bands on unsintered and sintered

rutile samples evacuated at 473 K (2h, unsintered) and 373 K (10h, sintered) respectively and also during the exchange of OH groups with deuterium at 473 K and 573 K<sup>51</sup>. This band was assigned to bridged (row B) hydroxyl groups hydrogen-bonded to terminal groups. Jones and Hockey<sup>11</sup> observed the 3680 cm<sup>-1</sup> band as a shoulder on the 3650 cm<sup>-1</sup> band and noted that it disappeared with the 3610 cm<sup>-1</sup> band, assigning it to the  $\nu_3$  vibration of molecular water on the (101) face. Neither of these assignments is acceptable in the present work as the 3700 cm<sup>-1</sup> band is not assigned to the bridged hydroxyls and the 3680 cm<sup>-1</sup> and 3610 cm<sup>-1</sup> bands do not disappear together.

The 3680 cm<sup>-1</sup> band is difficult to assign, it is not predominant and the behaviour is influenced by the presence of the 3700 and 3655 cm<sup>-1</sup> bands. It does not reveal the 3700 cm<sup>-1</sup> band until after evacuation above 423 K and is therefore caused by hydroxyl groups or strongly bonded water as possibly indicated by the 3400 cm<sup>-1</sup> band. The 3680 and 3400 cm<sup>-1</sup> bands shows similar behaviour, both being observed on initial adsorption of H<sub>2</sub>O onto oxidized rutile but the equivalent deuterated bands are not observed on the reduced surface until high relative D<sub>2</sub>O pressures. The 3680 cm<sup>-1</sup> band does not increase with the 3400 cm<sup>-1</sup> band at high vapour pressures of H<sub>2</sub>O on oxidized surfaces. The 2680 cm<sup>-1</sup> band is assigned to isolated hydroxyl groups (3700 cm<sup>-1</sup>) which are perturbed by a weak interaction with water molecules adsorbed onto other sites on the surface.

### 3.4.3 THE 3655 $\text{cm}^{-1}$ BAND

This is the most predominant band in the spectrum of the hydroxylated beam temperature oxidized surface. It increases on evacuation at 373 K before decreasing rapidly during evacuation of the unsintered surface at 483 K (graph 3.1). Evacuation of the sintered surface rapidly decreases the intensity of this band in the temperature range 453-473 K (graph 3.2). Further evacuation decreases the band to a weak shoulder on the 3700  $\text{cm}^{-1}$  band. The 3655  $\text{cm}^{-1}$  band behaves in a similar manner to the 3410  $\text{cm}^{-1}$  band.

Initial dosage of  $\text{H}_2\text{O}$  onto an oxidized surface causes a rapid increase in the intensity of this band which may also increase on evacuation. The rapid increase slows after the 3700  $\text{cm}^{-1}$  band merges in the 3680  $\text{cm}^{-1}$  shoulder and as the 3610 and 3520  $\text{cm}^{-1}$  bands appear. Further dosage of water does not appear to change the intensity of the 3655  $\text{cm}^{-1}$  band until the 3520 and 3610  $\text{cm}^{-1}$  bands are equal to those observed on the evacuated beam temperature surface. Increasing dosage of  $\text{H}_2\text{O}$  then decreases the 3655  $\text{cm}^{-1}$  band, shifting it to 3620  $\text{cm}^{-1}$  at high concentrations, while evacuation increases the intensity over that observed on the previous evacuated surface. No corresponding increase is observed in the intensity of the 1610  $\text{cm}^{-1}$  band on the evacuated surface confirming the initial assignment that this band is due to hydroxyl groups. It is also probable that these hydroxyl groups are formed continuously on  $\text{H}_2\text{O}$  adsorption and that the intensity of the 3655  $\text{cm}^{-1}$  band

is decreased by hydrogen-bonding of water molecules to these groups (3.4.4), the majority of this water being removed by evacuation with a resultant increase in the  $3655\text{ cm}^{-1}$  band.

This band continually increases with dosage of  $\text{D}_2\text{O}$  onto the reduced surface (spec. 3.8) and decreases on evacuation to an intensity greater than that observed on the previous evacuated surface. The behaviour on the reduced surface is therefore considerably different from the corresponding band on the oxidized surface which is not decreased by evacuation.

The removal of the hydroxyl groups assigned to the  $3655\text{ cm}^{-1}$  band on evacuation at 453–473 K (oxidized rutile) and beam temperature (reduced rutile) indicates that they are not isolated hydroxyl groups (usually removed  $\sim 470\text{ K}$ ) but hydrogen-bonded terminal (row A) hydroxyl groups which may be removed by proton tunnelling<sup>77</sup>. The hydrogen-bonding shift ( $45\text{ cm}^{-1}$ ) may be compared with correlations of O...O distance and hydrogen-bond wavenumber or shift obtained for other compounds<sup>78,79</sup>. No exact comparisons may be made as the slope of the graph, O...O distance against wavenumber of hydrogenic species, is steep in the range  $3700\text{--}3400\text{ cm}^{-1}$  and small variations in the O...O distance cause large changes in the frequency. A further limitation is the assumption that the O--H...O bond is linear which might not be true for hydrogen bonding on the rutile surface. Using the results of Nakamoto et al<sup>79</sup> the  $3655\text{ cm}^{-1}$  band implies an O...O distance

of 310pm compared to .296pm for Ti-O bonds perpendicular to the (110) plane.

Glensier and Hartert<sup>80</sup> studied the wavenumber shifts of OH groups in metal hydroxides and correlated the hydrogen-bonding energy and O...O distance with the wavenumber of the shifted hydroxyl band. Jackson (ref. 1 page 195) used this information to calculate the wavenumber of hydroxide bands with shifts equal to those he observed for the rutile bands. The O...O distances and hydrogen-bond energies were then calculated. Table 3.5 shows the results after applying this technique to bands observed in this work. The use of these results from metal hydroxides may not be entirely valid but they indicate a shift of approximately  $45 \text{ cm}^{-1}$  may result from hydrogen-bonding between hydroxyl groups where the oxygen-oxygen distance is 296 Å m.

Evacuation of water vapour from oxidized or reduced rutile increases the intensity of  $3655 \text{ cm}^{-1}$  compared with that of the previous evacuated surface indicating that the hydroxyl groups are formed by a slow reaction. This reaction will be considered in detail later together with a discussion of the behaviour of the band on the reduced surface.

#### 3.4.4 THE $3610$ AND $3520 \text{ cm}^{-1}$ BANDS

These bands, which are more intense on the unsintered BT surface than the sintered, are removed by evacuation to 368 K

together with a decrease in the 3420 and 1620  $\text{cm}^{-1}$  bands and an increase in the 3655  $\text{cm}^{-1}$  band. Dosage of  $\text{H}_2\text{O}$  onto a 673 K oxidized surface does not produce these bands until the later stages of adsorption when their appearance coincides with a slowing of the rate of increase of the 3655  $\text{cm}^{-1}$  band. Further dosage increases the 3610, 3520, 3420 and 1620  $\text{cm}^{-1}$  bands and decreases the 3655  $\text{cm}^{-1}$  band. The 3610 and 3520  $\text{cm}^{-1}$  bands are not observed on the reduced surface except at high relative vapour pressures when they are much less intense than on the equivalent oxidized surface, and are completely removed by evacuation.

Jackson and Parfitt<sup>10</sup> interpreted the bands as either an interaction of water with various OH species or the effect on the OH stretching frequency of physisorbed water. Jones and Hockey<sup>41</sup> assign the 3610  $\text{cm}^{-1}$  band to the  $\nu_1$  vibration of water on the (101) face and the 3550  $\text{cm}^{-1}$  band to hydrogen-bonded water coordinated to titanium ions in the (100) face. This model assumes 38% of the rutile to be formed of the (100) and (110) faces, 60% being formed of the (110) face, while electron diffraction studies<sup>70</sup> of a single crystal show only 15% of the rutile surface to be covered by these faces, 60% by the (110) and the remaining 25% formed from the (211) and (111) faces. The assignments may be correct but adsorption on to the (211) and (111) faces must be considered.



The 3610 and 3520  $\text{cm}^{-1}$  bands are tentatively assigned to water molecules adsorbed on the surface or hydroxyl groups hydrogen-bonded to water molecules. The absence of these bands on the reduced surface indicates that the water molecules are not adsorbed directly onto hydroxyl groups, as these are present on the reduced surface, but are coordinately bonded to the rutile surface and may be hydrogen-bonded to hydroxyl groups on the (110) plane. The increase of the 3655  $\text{cm}^{-1}$  band with the decrease of the 3610, 3520 and 3410  $\text{cm}^{-1}$  bands during evacuation to 373 K, and the decrease of this band during dosage of  $\text{H}_2\text{O}$  when the 3610, 3520, 3410  $\text{cm}^{-1}$  bands increase imply that one of the bands is due to the perturbed 3655  $\text{cm}^{-1}$  band while the other might be due to the coordinately bound water.

#### 3.4.5 THE 3420 $\text{cm}^{-1}$ BAND

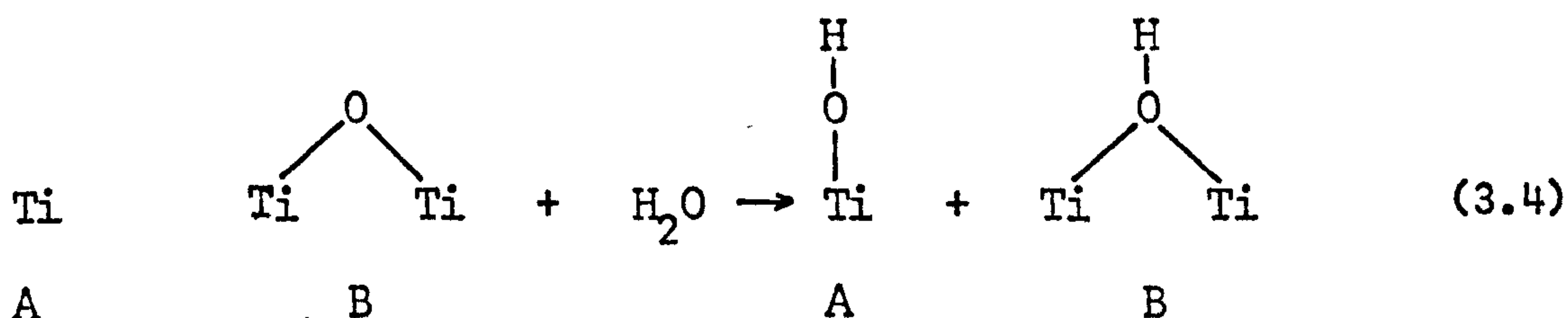
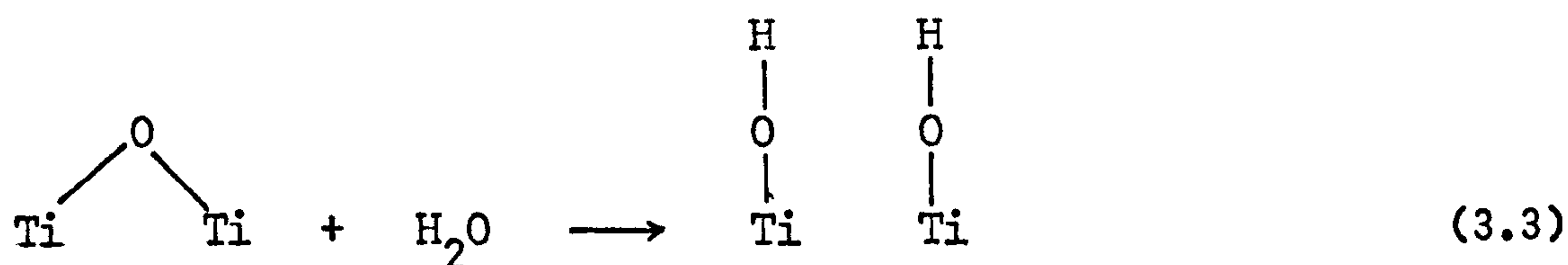
Heating a beam temperature oxidized unsintered surface in  $\text{H}_2\text{O}$  (673 K, 5h) increased the intensity of this band (spec. 3.1 b) and decreased the 3680  $\text{cm}^{-1}$  shoulder, no other changes occurring. Evacuation from 373 K to 473 K rapidly removed this peak (graph 3.1) to leave a broad band at 3400  $\text{cm}^{-1}$ . This band behaved similarly on the sintered surface (at 3410  $\text{cm}^{-1}$ ) but was more sharp and intense than on the oxidized surface and disappeared to leave a 3400  $\text{cm}^{-1}$  of lower intensity. On both surfaces the 3420  $\text{cm}^{-1}$  band decreased at a slightly faster rate than the 3655  $\text{cm}^{-1}$  band.

Dosage of  $\text{H}_2\text{O}$  onto oxidized sintered and unsintered rutile did not produce this band until the  $3610$  and  $3520 \text{ cm}^{-1}$  bands had developed. The graphs (3.3 and 3.5) of absorbance changes do not indicate the formation of this band but show a steady increase in intensity throughout the adsorption process possibly due to the underlying  $3400 \text{ cm}^{-1}$  band which also reduces the intensity of the  $3420 \text{ cm}^{-1}$  band on the evacuation of  $\text{H}_2\text{O}$ . Heating the sintered surface in  $\text{H}_2\text{O}$  increased the  $3420 \text{ cm}^{-1}$  band (spec. 3 k,1).

Dosage onto a  $\text{D}_2\text{O}$  surface produced the  $3420 \text{ cm}^{-1}$  band only at high relative vapour pressures while evacuation decreased the intensity, but to a value greater than that on the previous evacuated surface (graph 3.6).

Jackson and Parfitt<sup>11</sup> assign the band to terminal groups shifted  $250 \text{ cm}^{-1}$  by hydrogen-bonding. This shift implies a band half-width of  $200 \text{ cm}^{-1}$ <sup>81</sup> which is not observed for the sharp band on the sintered surface. Jones and Hockey<sup>41</sup> assign the band to row B hydroxyls which are monodentate above the  $\text{Ti}^{4+}$  ions.

The division of  $\text{H}_2\text{O}$  molecules on the surface may occur either by breaking a bridged oxygen (eq<sup>n</sup> 3.3) or by forming hydroxyl groups on rows A and B<sup>10,41,73</sup> (eq<sup>n</sup> 3.4)



The first reaction (equation 3.3) is unfavourable where the bridged oxygen is in row B, as loss of coordination occurs, but is favourable if the two titanium ions are in row A, the bridging oxygen being previously formed by the condensation of two hydrogen-bonded hydroxyl groups. Equation 3.4 shows the formation of a bridged hydroxyl group which, being more acidic than the row A terminal hydroxyls, would vibrate at a lower frequency. The  $3420 \text{ cm}^{-1}$  band has been assigned to hydroxyl groups, it is not hydrogen-bonded and the low frequency indicates it to be more acidic than the terminal hydroxyls. The  $3420 \text{ cm}^{-1}$  band is therefore assigned to row B bridged hydroxyls. These groups do not realign to monodentate ligands<sup>41</sup> as loss of coordination of the  $\text{Ti}^{4+}$  occurs. The dehydration process involving these groups is considered in 3.5. No hydrogen bonding occurs between the terminal and bridged hydroxyl groups as the O...O distance is too great (325pm), and between bridged groups (296pm apart) as the O-H bonds are parallel.

The  $3420\text{ cm}^{-1}$  band increases slowly even in the presence of excess water vapour which is removed by pumping at beam temperature. The  $3655\text{ cm}^{-1}$  band also increases slowly after the appearance of the  $3420\text{ cm}^{-1}$  peak indicating that  $\text{H}_2\text{O}$  molecules are now dividing to produce  $\text{OH}^\ominus$  ions on the row A titanium ions with protons on the row B oxygen ions<sup>73</sup>. The dissociation of the  $\text{H}_2\text{O}$  molecules is a slow reaction due probably to the distance between rows A and B which prevents interaction of water hydrogen atoms with row B oxygen ions.

The shape and intensity of the  $3420\text{ cm}^{-1}$  band varies with the pretreatment and source of the sample. In the spectra of rutile prepared from  $\text{TiCl}_4$  which was calcined in air (973 K) the band is broad (ref. 10 and this work) while in the spectra of rutile prepared from the isopropoxide the band is sharp and intense. The spectra of 'chloride' rutile discs after sintering show a sharp intense  $3420\text{ cm}^{-1}$  band similar to that on the 'isopropoxide' rutile which was sintered during its preparation. The sintering process may affect the shape of the  $3420\text{ cm}^{-1}$  band directly, by altering the surface structure, or indirectly by removing surface chloride which is known to affect the  $3420\text{ cm}^{-1}$  band at high concentrations<sup>1,51</sup>.

The intensity of the  $3420\text{ cm}^{-1}$  band may also be increased by heating the disc in  $\text{H}_2\text{O}$  vapour (673 K) which may result in loss of chloride ions as hydrogen chloride or may cause sintering by condensing hydroxyl groups from the facing

surfaces of contacting particles<sup>75</sup>. It is probable that the  $3420\text{ cm}^{-1}$  band is broadened by surface chloride on a rutile that has been pretreated<sup>1</sup>, however care must be exercised when drawing conclusions from differences between sintered and unsintered samples as changes in surface structure may occur.

#### 3.4.6 THE $3400\text{ cm}^{-1}$ BAND

This broad band remained after the removal of the  $3420\text{ cm}^{-1}$  band by evacuation to 473 K and also appeared during the initial stages of  $\text{H}_2\text{O}$  adsorption, continuing to increase during further adsorption. Evacuation (BT) decreased the band together with the  $3420\text{ cm}^{-1}$  peak. The  $3400\text{ cm}^{-1}$  band was less intense on the sintered and reduced surfaces and not observed by Jones and Hockey<sup>11</sup> while Jackson and Parfitt<sup>10</sup> recorded a broad  $3400\text{ cm}^{-1}$  band splitting into shoulders at  $3420\text{ cm}^{-1}$  and  $3350\text{ cm}^{-1}$ . The latter peak was assigned to strongly physisorbed water in micropores or associated with surface chloride species. The  $3400\text{ cm}^{-1}$  band has been tentatively assigned to molecular water adsorbed on the rutile surface or hydroxyl groups hydrogen-bonding to water on the surface. 60% of the rutile surface consists of the (110) plane while the remaining 40% is formed from the (211), (111), (101) and (100) planes on which water molecules may adsorb. Those adsorbed on the three-coordinate titanium ions on the (111) and (211) planes (total surface occupancy 25%) are able to bond with the hydrogen atoms directed towards surface oxygen ions to form hydrogen-bonds.

Water molecules on the (100) plane which has some high energy sites<sup>111</sup> are similarly directed<sup>41</sup> while those on the (101) plane may be directed with the hydrogen atoms away from the surface oxide ions<sup>41</sup>, which assumes the lone-pair of electrons bonding to the empty titanium ion orbital to be in the plane of the atoms. However the oxygen atom is  $sp^3$  hybridized<sup>83</sup> and the angle between the lone-pair and HOH plane will be approximately  $110^\circ$  which may result in the hydrogen atoms hydrogen-bonding to the surface oxygen ions and to other water molecules on the surface. The infrared spectrum of water molecules adsorbed on the (111), (211), (101), (100) planes will show broad bands due to hydrogen bonding and it is to these that the  $3400\text{ cm}^{-1}$  band is assigned.

At high relative vapour pressures of water, molecules physisorbed on those coordinately bonded to the surface increase the intensity of this band. The presence of this band after evacuation at 473 K indicates some water molecules to be strongly adsorbed on the (111) and (211) planes<sup>70</sup> (table 3.3) containing ions of low coordination.

The lower intensity of the  $3400\text{ cm}^{-1}$  band on the sintered surface compared to that on the unsintered surface may be due to a decrease in the surface occupancy on the higher index planes, (211) and (111), which would decrease in area during sintering due to the degree of unsaturation of the surface ions. The lower intensity may also be caused by loss of chloride ions onto which water molecules strongly adsorb<sup>1,10,51</sup>.

### 3.4.7 1625 - 1600 cm<sup>-1</sup> BAND

This band has been assigned to the  $\nu_2$  bending vibration of water molecules. On evacuation at elevated temperatures it decreases and shifts from 1630 to 1600 cm<sup>-1</sup> due to a change from trimeric to monomeric water species<sup>89</sup>. It does not appear to be completely removed from the non-sintered oxidized surface though this may be due to a change in the base line. The intensity of the band on the sintered surface is approximately 35% lower than that on the unsintered surface and disappears on evacuation to 358 K.

Initial adsorption of H<sub>2</sub>O onto sintered and unsintered rutile formed this band which increased during dosage and decreased to a constant value after high relative vapour pressures. Dosage of H<sub>2</sub>O onto reduced rutile at high vapour pressures and evacuation reduced this band to approximately 35% of the corresponding oxide surface intensity.

### 3.4.8 1570 cm<sup>-1</sup> BAND

This band has only been observed after exposing a reduced disc to D<sub>2</sub>O for 5 days. It has also been observed by Parkyns<sup>46</sup> on 'oxygen deficient' anatase and was assigned to water molecules coordinated to Ti<sup>3+</sup> ions.

### 3.4.9 SUMMARY

A summary of the assignments of bands observed in this work is included in table 3.1.

The 3700, 3680, 3655 and 3420  $\text{cm}^{-1}$  bands are assigned to groups on the predominant (110) plane, which is the only face on which water may divide and produce one OH group (terminal or bridged) for each titanium ion. Division of water on the other faces would result in at least two hydroxyls per titanium ion which is not possible<sup>41</sup>; consequently molecular water coordinately bonds to these planes.

The existence of two types of Lewis sites<sup>65</sup> and  $\text{Ti}^{3+}$  ions<sup>27,28</sup> in the surface is not explained by this model which has many different sites on the exposed planes. These sites will be discussed in chapter 7.

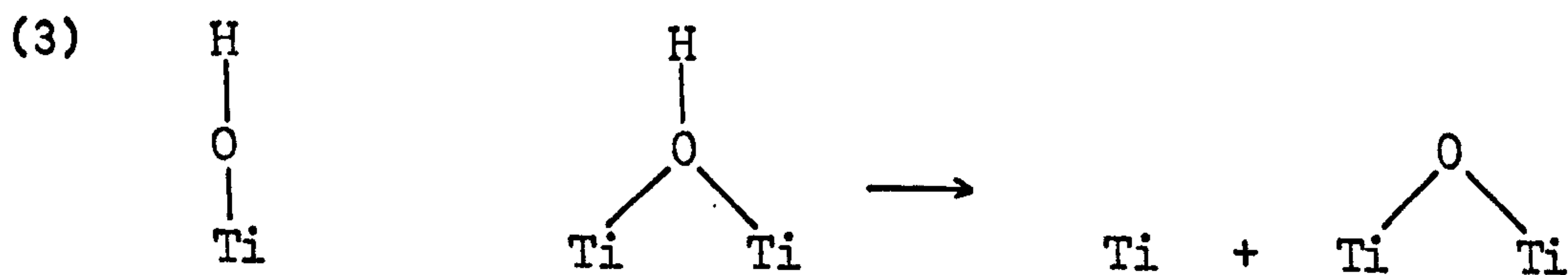
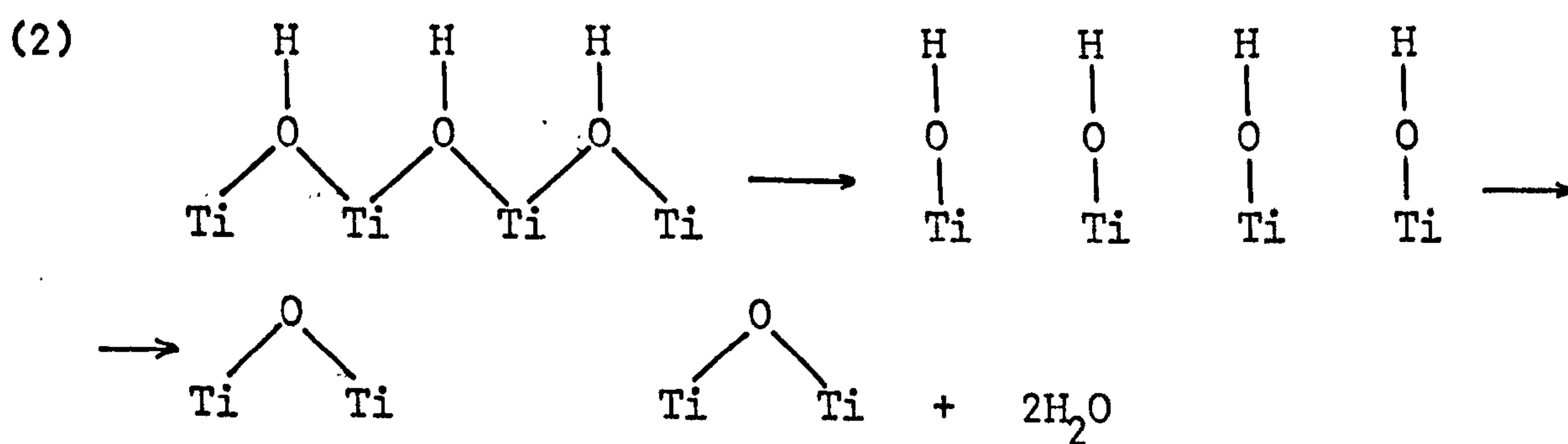
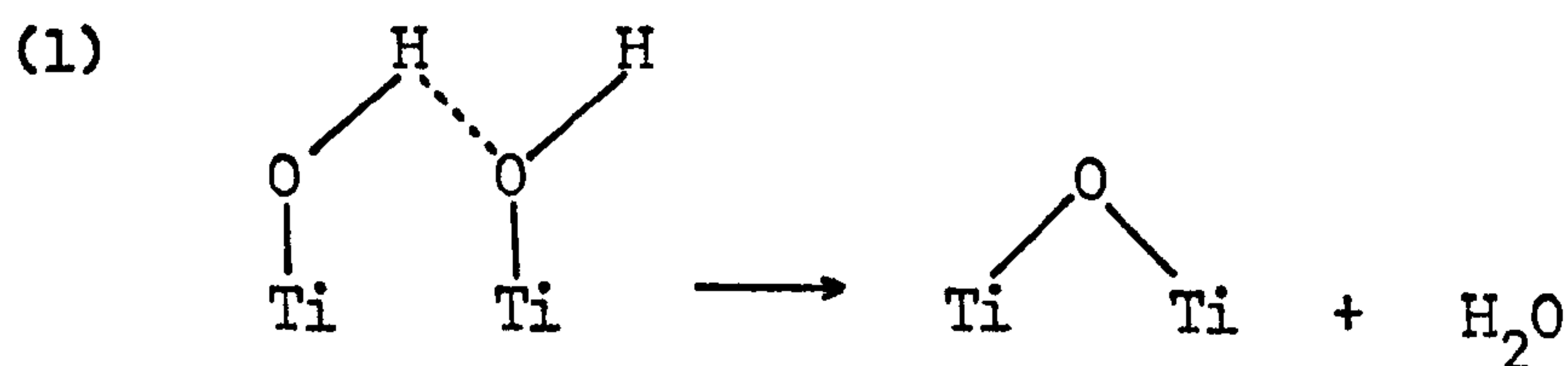
The reactions occurring during adsorption and desorption of water may now be deduced by reconsidering the results in conjunction with the above assignments.



3.4.10 REACTIONS OCCURRING ON THE ADSORPTION AND DESORPTION OF WATER

A. Oxidized Rutile

Evacuation at 370 K removes the water hydrogen bonded to the surface hydroxyl groups resulting in an increase in intensity of the hydrogen-bonded hydroxyl ( $3655\text{ cm}^{-1}$ ) band. Further heating removes the terminal and bridging hydroxyl groups, the band resulting from the latter disappears first. The removal of these hydroxyl groups may occur by several mechanisms



Mechanism (1) involving terminal hydroxyl groups is expected to be the most favourable as the hydroxyl groups are at their closest. However the disappearance of the bridged hydroxyl groups indicates that mechanism (2), proposed by Hockey<sup>41</sup>, is as favourable. Mechanism (3) between a terminal and bridged hydroxyl group predominates at higher temperatures when the surface concentration of hydroxyl groups on the surface is relatively low.

There is an apparent excess of hydroxyl groups over hydrogen ions after evacuation at about 500 K as shown by the presence of the terminal hydroxyl bands ( $3700, 3655 \text{ cm}^{-1}$ ) without the bridged hydroxyl ( $3420 \text{ cm}^{-1}$ ) (spec. 3.11). The hydrogen ions corresponding to the terminal hydroxyl groups may be attached to oxygen atoms in surface defects resulting in a band in the  $3400 \text{ cm}^{-1}$  region coinciding with the broad band due to strongly held water molecules.

Initial adsorption of water onto the oxidized surface produces hydrogen-bonded terminal hydroxyl groups ( $3655 \text{ cm}^{-1}$ ) suggesting that the reverse of mechanism (1) is predominant. This mechanism requires the presence of oxygen ions bridging two terminal titanium ions which would not be an unstable structure as the unsaturated coordination of the titanium ions is partially satisfied. Che et al<sup>29</sup> also postulate the formation of weakly coordinated oxygen ions ( $\text{O}^{2-}$ ) in considering the formation of radical anions.

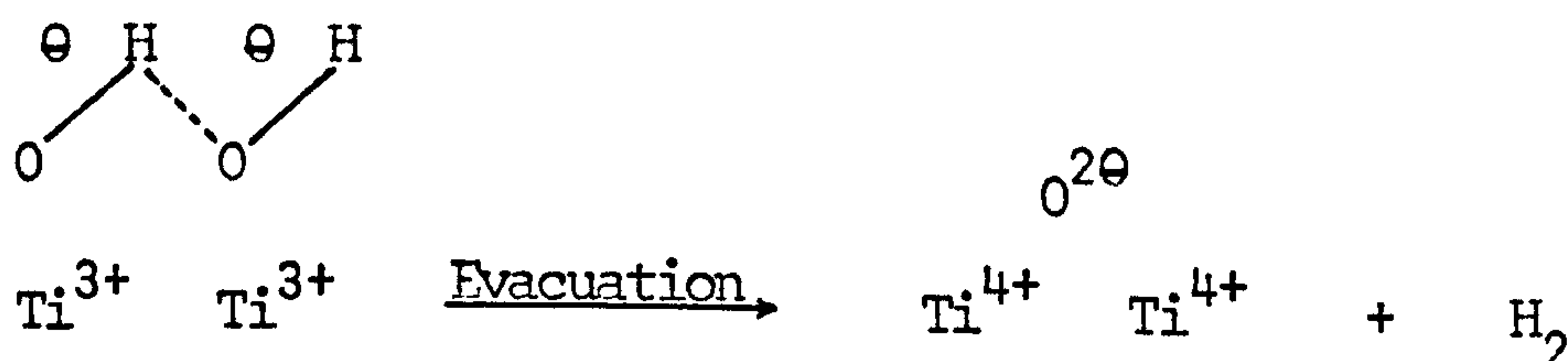
During the later stages of adsorption mechanism the appearance of the  $3420\text{ cm}^{-1}$  band indicates mechanism (2) also occurs. The increase in intensity in the  $3400\text{ cm}^{-1}$  region at the same time shows that water molecules are adsorbing on the (100), (101), (111) and (211) planes. Further adsorption of water results in water molecules forming the  $3610$  and  $3520\text{ cm}^{-1}$  and also physically adsorbing to surface hydroxyl groups.

### B. The Reduced Surface

The calculations made by Jaycock and Walsax<sup>111</sup> indicate that the binding energy of  $\text{Ti}^{3+}$  ions is lower than that of  $\text{Ti}^{4+}$  ions (37 compared with  $104\text{ k cal mol}^{-1}$ ). As a result the surface concentration of water molecules will be lower on the reduced than on the oxidized surfaces. This is shown by the absence of the  $3610$  and  $3520\text{ cm}^{-1}$  bands on the evacuated reduced surface and the reduced intensity of the  $3400\text{ cm}^{-1}$  band.

The reduction of the rutile surface will also remove the bridged oxygen ion, which results from the condensation of two terminal hydrogen-bonded groups, from between the two titanium ions. Consequently the formation of the  $3655\text{ cm}^{-1}$  band is not as rapid on the reduced surface as the oxidized surface, the  $3700\text{ cm}^{-1}$  band being formed on initial adsorption (spec. 3.8).

The reduction in intensity of the  $3655\text{ cm}^{-1}$  terminal hydroxyl band on evacuation, which does not occur on oxidized rutile during the initial stages of adsorption, may be explained by the following mechanism:



The oxygen ions will then migrate to an oxygen deficient site or react with a molecule of water to form stable terminal hydroxyl groups. These increase on the evacuated surface after each dose of water onto the reduced surface (spec. 3.8).

## CHAPTER 4

4. ADSORPTION OF ACETONE AND HEXADEUTEROACETONE4.1 INTRODUCTION

Several infrared studies of the adsorption of acetone on silica<sup>85,86</sup>, alumina<sup>85,87,88,89</sup>, nickel oxide<sup>90,91,92,93,112</sup>, and rutile<sup>85</sup> have been reported. The bands observed are generally assigned to Lewis acid complexes or carboxylate species although Winde<sup>89</sup>, investigating acetone adsorbed on alumina using Raman spectroscopy, has recently assigned some of the observed bands in his and other studies to mesityl oxide. Mesityl Oxide, with isophorone and mesitylene, is produced on heating rutile in acetone vapour above 373 K<sup>94,95,96</sup>.

The infrared studies of acetone adsorption onto rutile<sup>85</sup> show intense bands due to the relatively high vapour pressures dosed onto the surface. The spectra presented in this chapter show the species produced by slow dosage of acetone onto oxidized and reduced rutile. The experiments are summarized below.

SpectraAdsorption of acetone and acetone  $d_6$  onto oxidized rutile

Acetone $d_6$ onto a 673 K $H_2O$ surface	4.1
Acetone $h_6$ onto a 673 K $D_2O$ surface	4.2
Acetone $d_6$ onto a BT $D_2O$ surface	4.3
Acetone $h_6$ onto a BT $D_2O$ surface	4.4
Acetone $h_6$ onto a 373 K $D_2O$ surface	4.5

Adsorption of acetone  $d_6$  onto reduced rutile

Acetone $d_6$ onto a 673 K $D_2O$ surface	4.6
Acetone $d_6$ onto a BT $D_2O$ surface	4.7

## 4.2 RESULTS

### 4.2.1 ADSORPTION OF ACETONE AND ACETONE $d_6$ ONTO OXIDIZED RUTILE

#### A. Acetone $d_6$ onto a 673 K $H_2O$ surface (spec. 4.1)

The spectrum of the 673 K  $H_2O$  surface (spec. 4.1a) showed a band at  $3700\text{ cm}^{-1}$  with a weak shoulder at  $3655\text{ cm}^{-1}$ . Initial doses of acetone (spec. 4.1 b-e) decreased the  $3700\text{ cm}^{-1}$  band to a broad  $3700\text{--}3600\text{ cm}^{-1}$  band which remained unchanged during further treatment, while a band appeared at  $2700\text{ cm}^{-1}$ , with a  $2725\text{ cm}^{-1}$  shoulder, and  $2660\text{--}2400\text{ cm}^{-1}$ . Bands arising from C-D stretching appeared at  $2225$ ,  $2120$ ,  $2060\text{ cm}^{-1}$ . Two broad bands, becoming more intense and narrowing with increasing acetone adsorption, were observed at  $1670\text{ cm}^{-1}$ , shoulder at  $1645\text{ cm}^{-1}$ , and  $1580\text{ cm}^{-1}$ . The  $1670\text{ cm}^{-1}$  band reached a maximum optical density of 0.155 (spec. 4.1 e).

Further dosing of acetone (spec. 4.1 f) removed the  $2700\text{ cm}^{-1}$  band and decreased the  $1670\text{ cm}^{-1}$  band while the shoulder at  $1645\text{ cm}^{-1}$  increased to a band. The  $1580\text{ cm}^{-1}$  band increased to a maximum (0.357) and bands appeared at  $1510$ ,  $1470$  and  $1425\text{ cm}^{-1}$ , evacuation of acetone causing an increase in these (spec. 4.1 g). Further dosage at this pressure (approximately  $0.3\text{ N m}^{-2}$ ) did not alter the infrared spectrum and an equilibrium was assumed between the surface and the vapour.

Increasing the equilibrium pressure (spec. 4.1 h,j) resulted in an increase and broadening of the C-D bands, possibly due to a shoulder at  $2210\text{ cm}^{-1}$ , and a decrease of the  $1670\text{ cm}^{-1}$  band. Evacuation of the 'equilibrium' surface (spec. 4.1 i,k) decreased the C-D,  $1645$  and  $1590\text{ cm}^{-1}$  bands, increased the  $1510\text{ cm}^{-1}$  band and caused the appearance of a band at  $1540\text{ cm}^{-1}$ .

#### B. Adsorption of Acetone $d_6$ on a 673 K $D_2O$ Oxidized Surface

(Spec. 4.2)

The results are similar to the previous experiment (spec. 4.1) with some differences. The O-D band at  $2720\text{ cm}^{-1}$  present on the starting surface disappeared while the corresponding O-H band at  $3700\text{ cm}^{-1}$  on the 673 K  $H_2O$  surface did not disappear completely. The separation of the C-H bands at  $2970$ ,  $2930$  and  $2880\text{ cm}^{-1}$  was less than that of the C-D bands. Bands corresponding to the  $1670$ ,  $1645$ ,  $1580$  and  $1510\text{ cm}^{-1}$  bands observed during the adsorption of acetone  $d_6$  (spec. 4.1) appeared at  $1685$ ,  $1660$ ,  $1595$  and  $1530\text{ cm}^{-1}$ . No band corresponding to the  $1540\text{ cm}^{-1}$  band (spec. 4.1 i) was observed. The maximum optical densities of the  $1670$  and  $1580\text{ cm}^{-1}$  bands were less than the corresponding absorbances for acetone  $d_6$  (87% and 79% respectively). Bands not appearing on the adsorption of acetone  $d_6$  were observed at  $1465$ ,  $1380$ ,  $1360$  and  $1345\text{ cm}^{-1}$ .



Exposing the disc to  $D_2O$  vapour (298 K, 15h) and evacuating (BT, 1h) (spec. 4.2 p) produced a broad band in the 2700-2400  $cm^{-1}$  region with peaks at 2680, 2655, 2600 and 2520  $cm^{-1}$  and increased the intensity of the 1550 - 1400  $cm^{-1}$  region with peaks at 1490, 1445 and 1430  $cm^{-1}$ . No surface species were removed by  $D_2O$  adsorption except those causing the 1680  $cm^{-1}$  band, which decreased.

C. Adsorption of acetone  $d_6$  onto a BT,  $D_2O$  Oxidized Surface  
(Spec. 4.3)

Initial adsorption of acetone  $d_6$  (spec. 4.3 b,c) caused the appearance of the 1670 and 1580  $cm^{-1}$  bands, the latter being less intense, in contrast to the spectrum of the equivalent 673 K surfaces in which the two bands were of equal intensity. All the bands in the O-D stretching region decreased slightly (less than 10%) except the 2535  $cm^{-1}$  band.

Further adsorption (spec. 4.1 d-h) decreased the 2710, 2695, 2660 and 2600  $cm^{-1}$  bands, the 2710  $cm^{-1}$  shoulder decreasing more rapidly than the 2695  $cm^{-1}$  band until it disappeared (spec. 4.3 e), while the 2660 and 2600  $cm^{-1}$  bands remained until spec. 4.3 f. The C-D stretching bands appeared with the 1580  $cm^{-1}$  band. The 1670  $cm^{-1}$  band increased to a maximum (0.22 spec. 4.3 e) before decreasing in intensity, the 1580  $cm^{-1}$  band increased and bands appeared at 1645, 1535, 1510 and 1425  $cm^{-1}$ . Further increases in acetone  $d_6$  pressure

decreased the 2695 and 1670  $\text{cm}^{-1}$  bands, the former reaching a minimum (0.046 o.d. spec. 4.3 l) and shifting to 2670  $\text{cm}^{-1}$ ; the 2535  $\text{cm}^{-1}$  band was unaffected. The 2225  $\text{cm}^{-1}$  band increased and broadened due to the appearance of a 2210  $\text{cm}^{-1}$  band while the 1580  $\text{cm}^{-1}$  band increased to a maximum (0.336 spec. 4.3 k). The 1535, 1510, and 1425  $\text{cm}^{-1}$  bands increased to spec. 4.1 j, further dosage of acetone  $d_6$  decreased them and increased the 1580  $\text{cm}^{-1}$  band, while evacuation decreased the 1580  $\text{cm}^{-1}$  band and increased the 1535, 1510 and 1425  $\text{cm}^{-1}$  bands.

D. Adsorption of Acetone  $h_6$  onto a BT,  $D_2O$  Oxidized Surface  
(Spec. 4.4)

On initial dosage of acetone a band appeared at 3655  $\text{cm}^{-1}$  with a 3680  $\text{cm}^{-1}$  shoulder, followed by bands at 3610, 3520, 3420  $\text{cm}^{-1}$  (spec. 4.4 a-d). The intensity of the OD and  $D_2O$  bands decreased while the 1685  $\text{cm}^{-1}$  band increased, only a weak 1595  $\text{cm}^{-1}$  band was observed. Further adsorption (spec. 4.4 e-j) increased the bands in the 4000 - 3000  $\text{cm}^{-1}$  region and decreased those in the 2750 - 2500  $\text{cm}^{-1}$  region until the OD and  $D_2O$  bands had disappeared with the exception of a broad 2500  $\text{cm}^{-1}$  band. The OH and  $H_2O$  bands did not correspond to the initial  $D_2O$  spectrum indicating that some displacement of groups had occurred. Adsorption of acetone at higher pressures did not remove the exchanged OH and  $H_2O$  bands.

The behaviour of bands below  $2000\text{ cm}^{-1}$  was similar to that observed for acetone  $d_6$  onto the beam temperature  $D_2O$  surface (spec. 4.3), the  $1535$  and  $1510\text{ cm}^{-1}$  bands being observed as a broad  $1545\text{ cm}^{-1}$  band with a  $1510\text{ cm}^{-1}$  shoulder. Spec. 4.4 k,l,m,n, show the changes in band intensities on adsorbing acetone onto an evacuated surface. The  $1685\text{ cm}^{-1}$  band initially increased while the broad  $1510\text{-}1550\text{ cm}^{-1}$  band decreased (spec. 4.4 l). The  $1685\text{ cm}^{-1}$  band then decreased and the  $1660$  and  $1595\text{ cm}^{-1}$  bands increased (spec. 4.4 m) until the intensity of the  $1685\text{ cm}^{-1}$  band was similar to the initial value after 25 mins (spec. 4.4 n).

E. Adsorption of Acetone  $h_6$  onto a 373 K  $D_2O$  Oxidized Surface  
(Spec. 4.5)

The results are similar to those observed during the adsorption of acetone onto a beam temperature  $D_2O$  surface (spec. 4.4).  $3655$  and  $3420\text{ cm}^{-1}$  bands appeared on initial adsorption of acetone (spec. 4.5 b-e) the former reaching a maximum (0.078 spec. 4.5 e) before decreasing with increasing acetone pressure. The  $1685\text{ cm}^{-1}$  reached a maximum absorbance (0.166 spec. 4.5 e) appearing with the  $1595\text{ cm}^{-1}$  band, in contrast to adsorption on the BT surface.

#### 4.2.2 ADSORPTION OF ACETONE $d_6$ ONTO REDUCED RUTILE

---

##### A. Acetone $d_6$ onto a 673 K, $H_2O$ Surface

---

On the initial adsorption of acetone  $d_6$  (spec. 4.6 a-e) bands appeared at 2720, 2210, 2110, 2050, 1670 and 1425  $cm^{-1}$  with a broad 1580-1470  $cm^{-1}$  band showing peaks at 1575, 1530 and 1480  $cm^{-1}$ . The 1670  $cm^{-1}$  band reached a maximum (spec. 4.6 d) which was lower than that on the corresponding oxidized surface. The 1580  $cm^{-1}$  band was not observed as a discrete band but as part of the broad band with the 1530 and 1480  $cm^{-1}$  peaks. The 1645  $cm^{-1}$  band was not observed.

Further adsorption of acetone  $d_6$  (spec. 4.6 f-h) removed the 2720  $cm^{-1}$  band, decreased the 1670  $cm^{-1}$  band and increased the 2210, 2110, 2050, 1480 and 1425  $cm^{-1}$  bands while a shoulder appeared at 1325  $cm^{-1}$ .

##### B. Adsorption of Acetone $d_6$ onto a BT, $D_2O$ Reduced Surface

---

(Spec. 4.7)

Initial adsorption of acetone  $d_6$  onto the reduced surface (spec. 4.7 a-d) was similar to that onto the oxidized surface, the 1670  $cm^{-1}$  band appearing before the broad band centred on 1550  $cm^{-1}$  while slight decreases ( $\sim 12\%$ ) were observed in the hydroxyl bands. No C-D bands were observed.

Further adsorption (spec. 4.7 e-h) decreased the 2720 and 2695  $\text{cm}^{-1}$  bands, the former disappearing (spec. 4.7 h) while the intensity of the 2535  $\text{cm}^{-1}$  band remained unchanged. A band appeared at 2210  $\text{cm}^{-1}$  followed by bands at 2110 and 2050  $\text{cm}^{-1}$ , the 1670  $\text{cm}^{-1}$  band decreased and the broad 1550  $\text{cm}^{-1}$  absorption increased, no discrete 1580  $\text{cm}^{-1}$  band was observed until spec. 4.5 h. The shoulder at 1425  $\text{cm}^{-1}$  increased together with a band which appeared (spec. 4.7 g) at 1475  $\text{cm}^{-1}$ .

Dosage of acetone  $\text{d}_6$  at higher pressures decreased the 2695  $\text{cm}^{-1}$  band to a minimum (spec. 4.7 i) and shifted it to 2670  $\text{cm}^{-1}$ , and increased the 2210  $\text{cm}^{-1}$  band. The 1670 and 1580  $\text{cm}^{-1}$  bands were merged into a broad shoulder on the 1480  $\text{cm}^{-1}$  band which increased with the 1425  $\text{cm}^{-1}$  band.

Evacuation of the acetone  $\text{d}_6$  decreased the hydroxyl bands, the 2210  $\text{cm}^{-1}$  C-D band and the 1580  $\text{cm}^{-1}$  band. The 1480  $\text{cm}^{-1}$  band did not change in intensity while the 1425  $\text{cm}^{-1}$  band increased.

#### 4.2.3 SUMMARY OF BANDS OBSERVED

Table 4.1 summarises those bands observed below 2000  $\text{cm}^{-1}$  in this work.

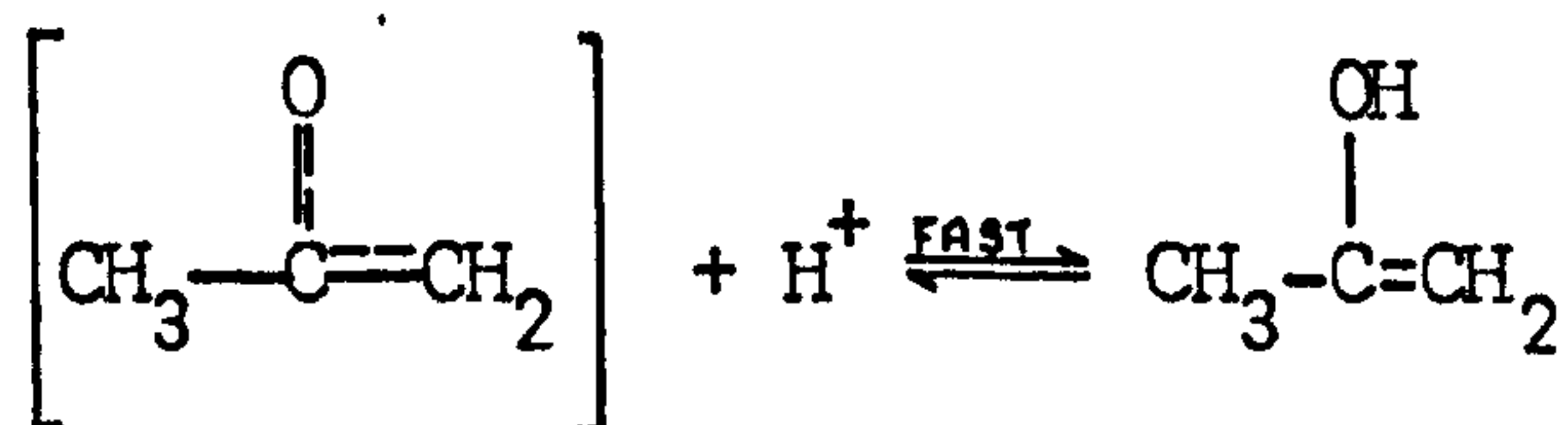
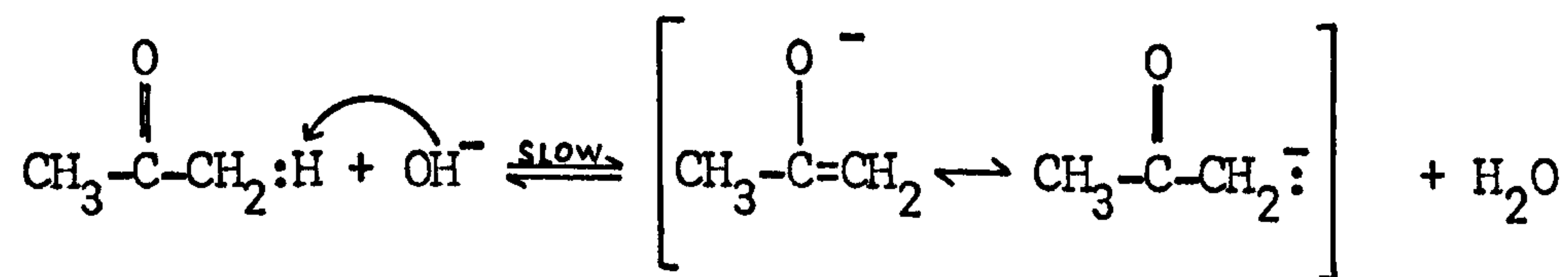
### 4.3 DISCUSSION AND CONCLUSIONS

#### 4.3.1 PROPERTIES OF ACETONE

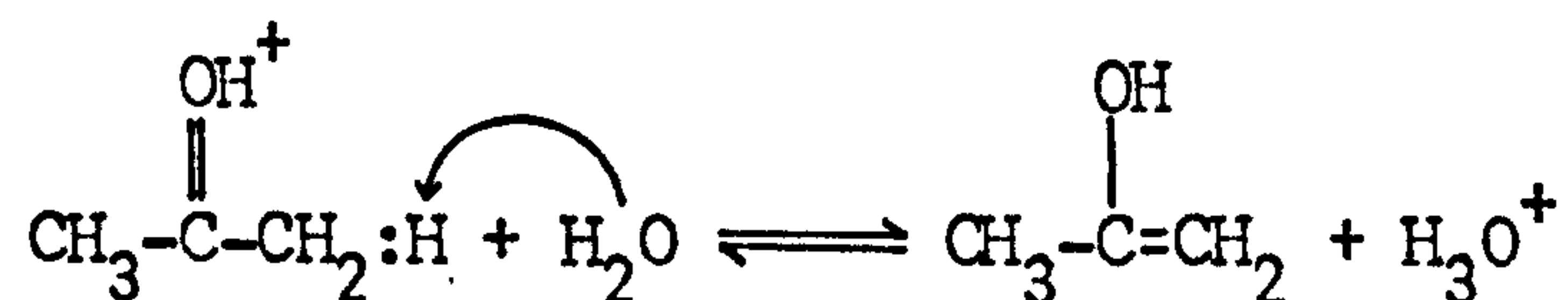
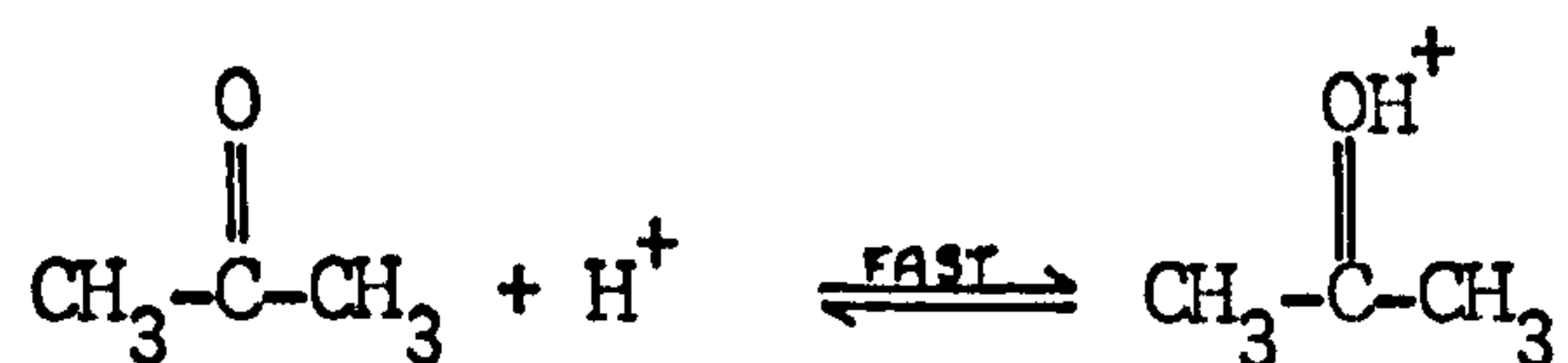
##### A. Enolization<sup>97,98</sup>

The enol form of acetone,  $\text{CH}_3\text{C}(\text{OH})=\text{CH}_2$ , may be formed by an acid or base catalysed reaction.

Base catalysed reaction:



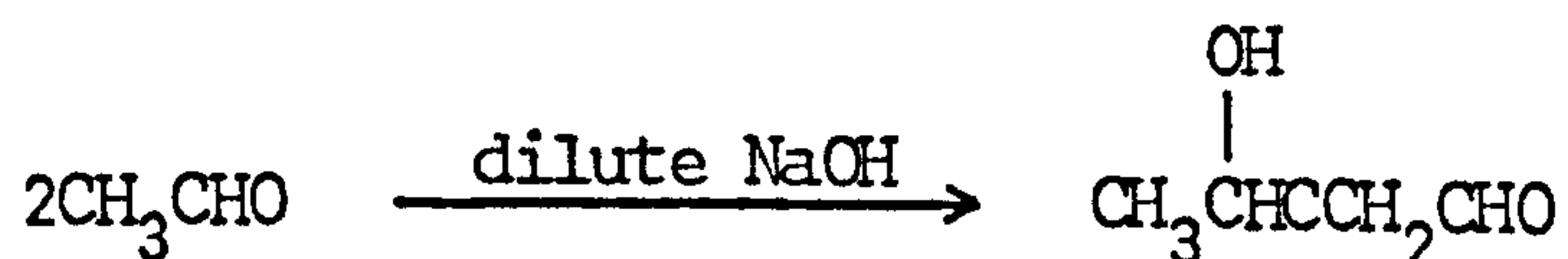
Acid catalysed reaction:



The acid catalysed reaction differs from the base catalysed in that the enol is formed directly and not subsequently to the formation of the enolate anion.

## B. Aldol Condensation

Acetaldehyde, in the presence of sodium hydroxide, or hydrochloric acid, undergoes condensation to form  $\beta$ -hydroxybutraldehyde (acetaldol).

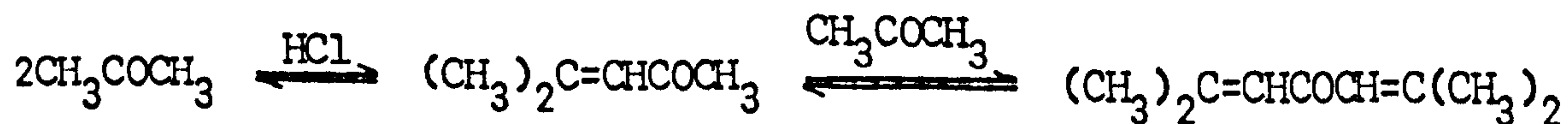


Acetone undergoes a similar reaction in the presence of barium hydroxide to form diacetone alcohol.

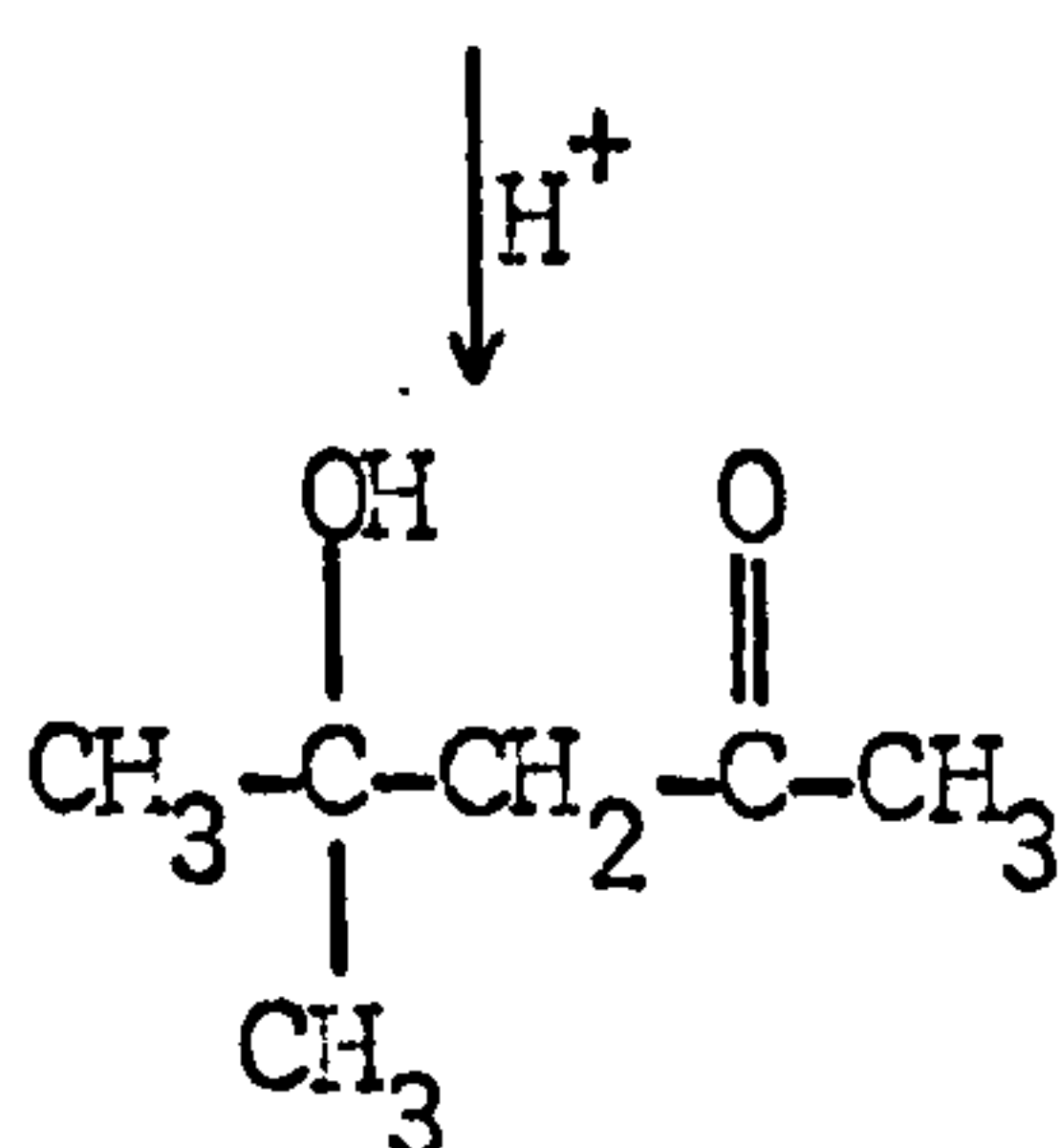
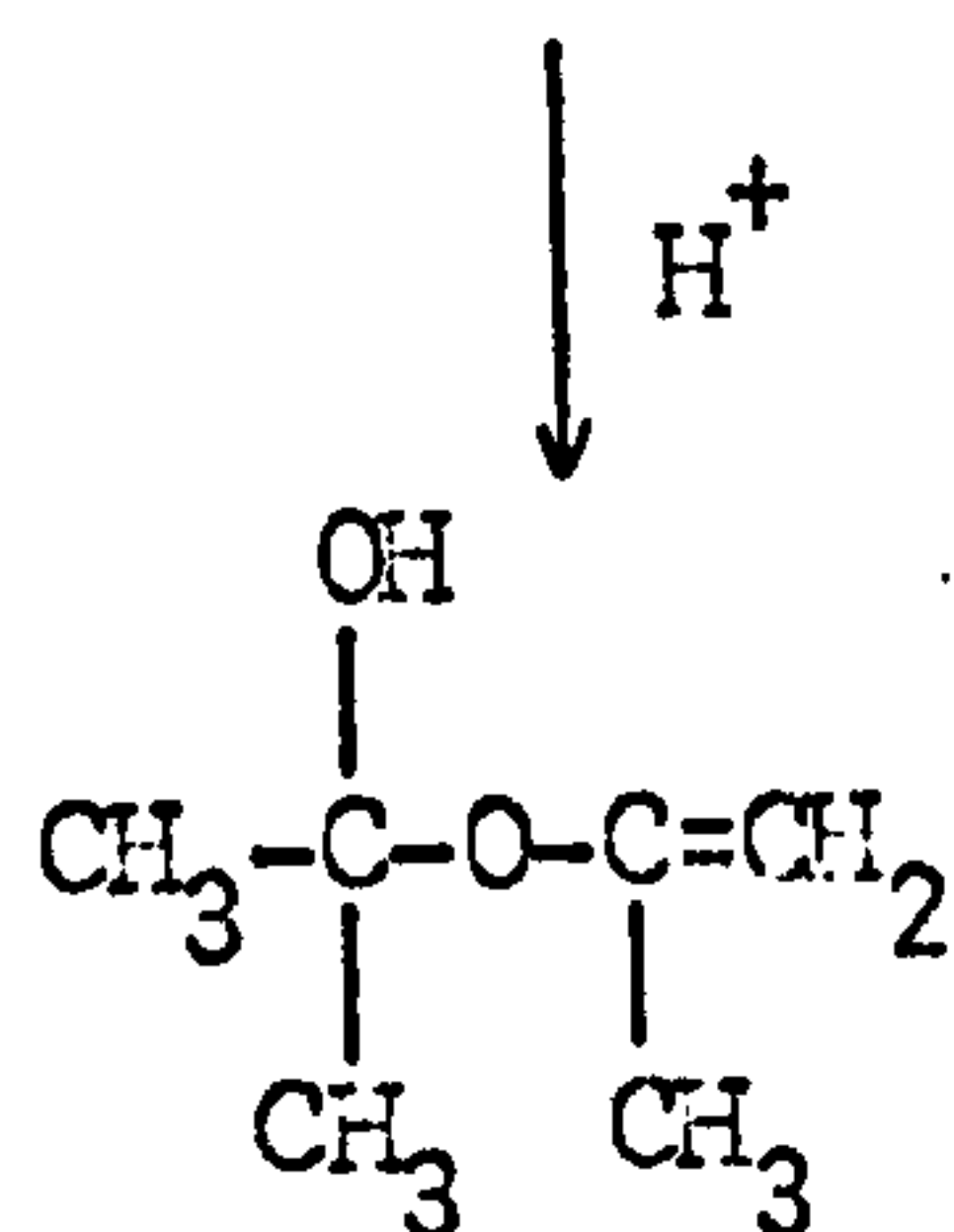
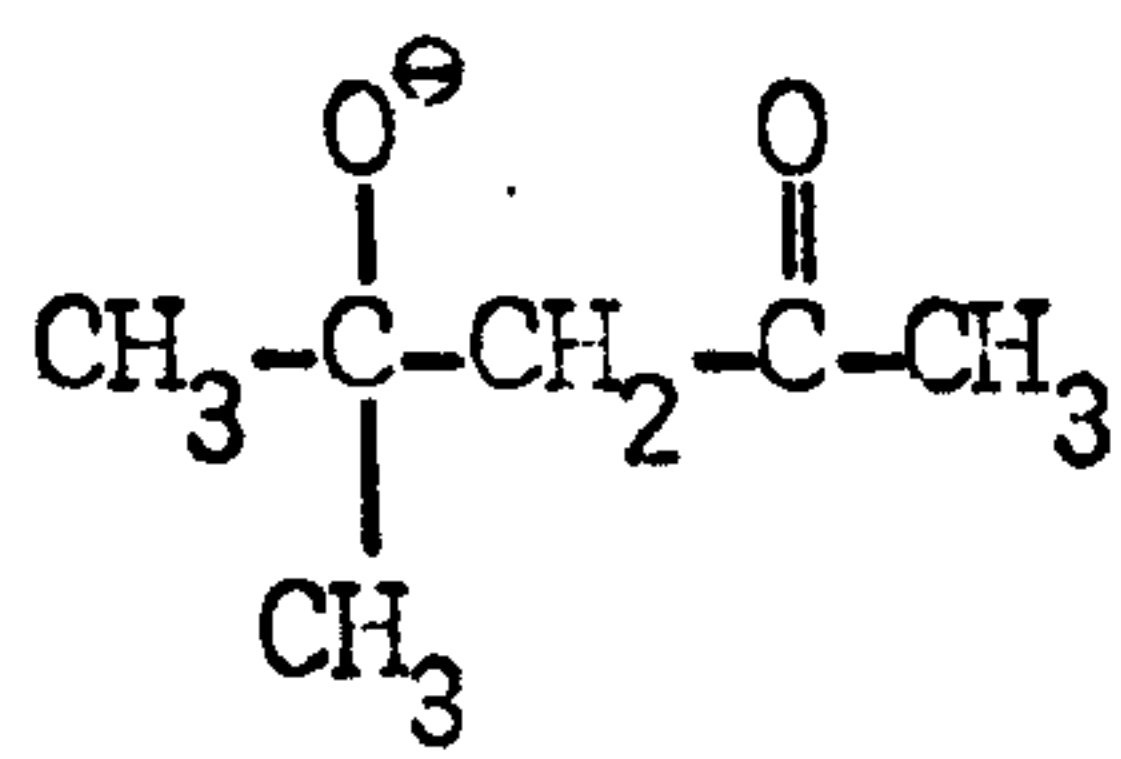
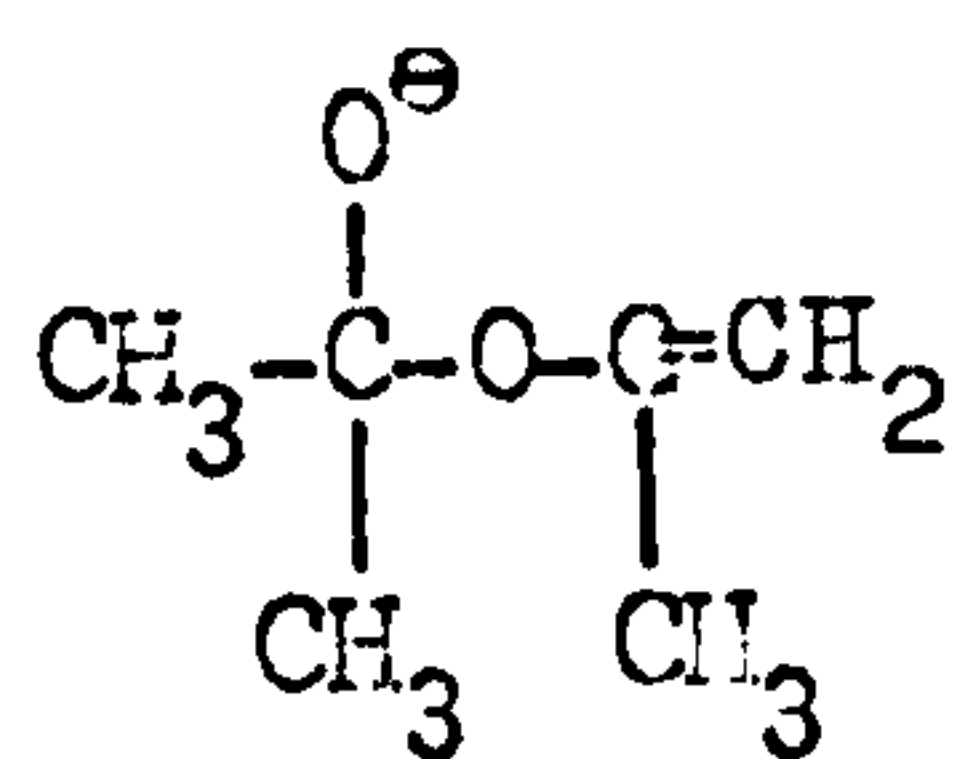
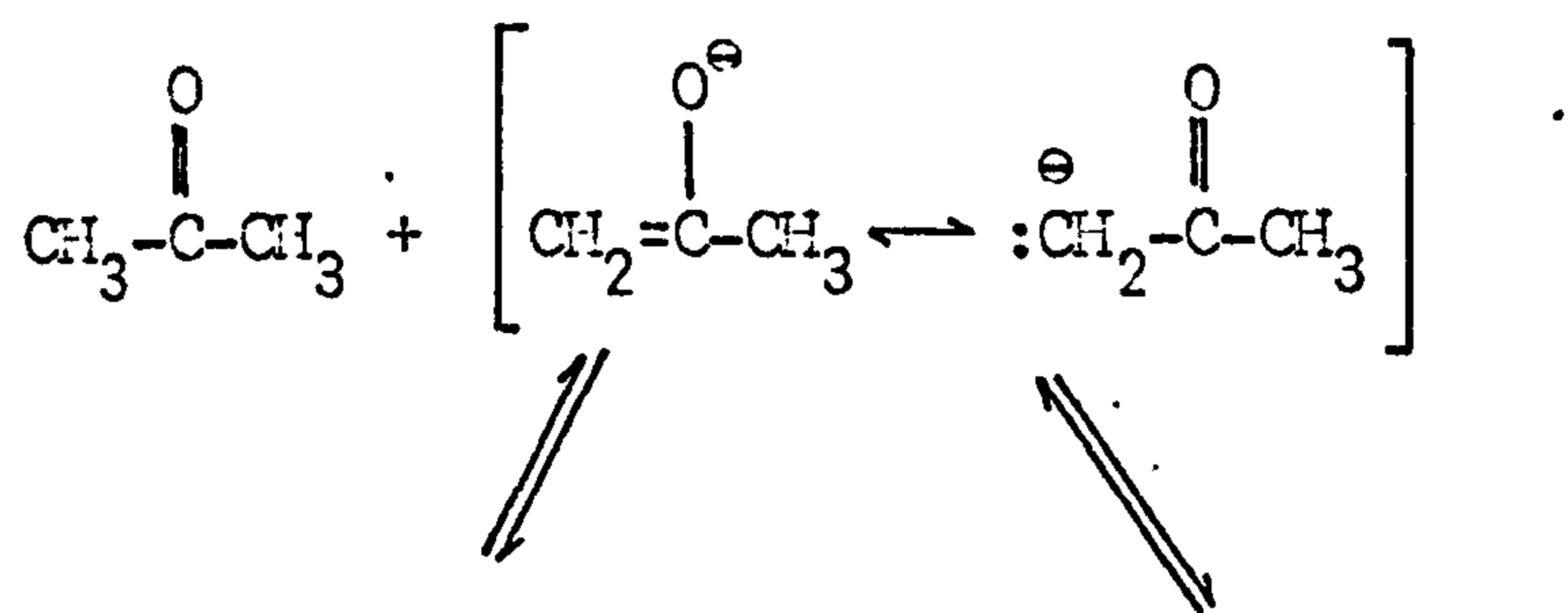


The equilibrium lies almost entirely to the left but the yield may be increased by boiling in a Soxhlet with barium hydroxide in the thimble.

Acetone in the presence of hydrochloric acid yields mesityl oxide and phorone.

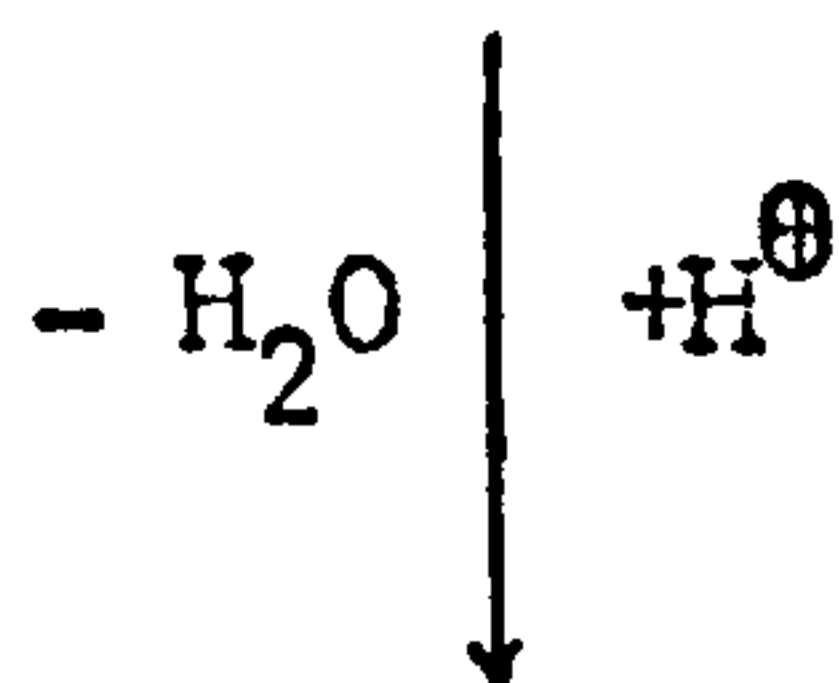


These reactions occur via the enolate anion.

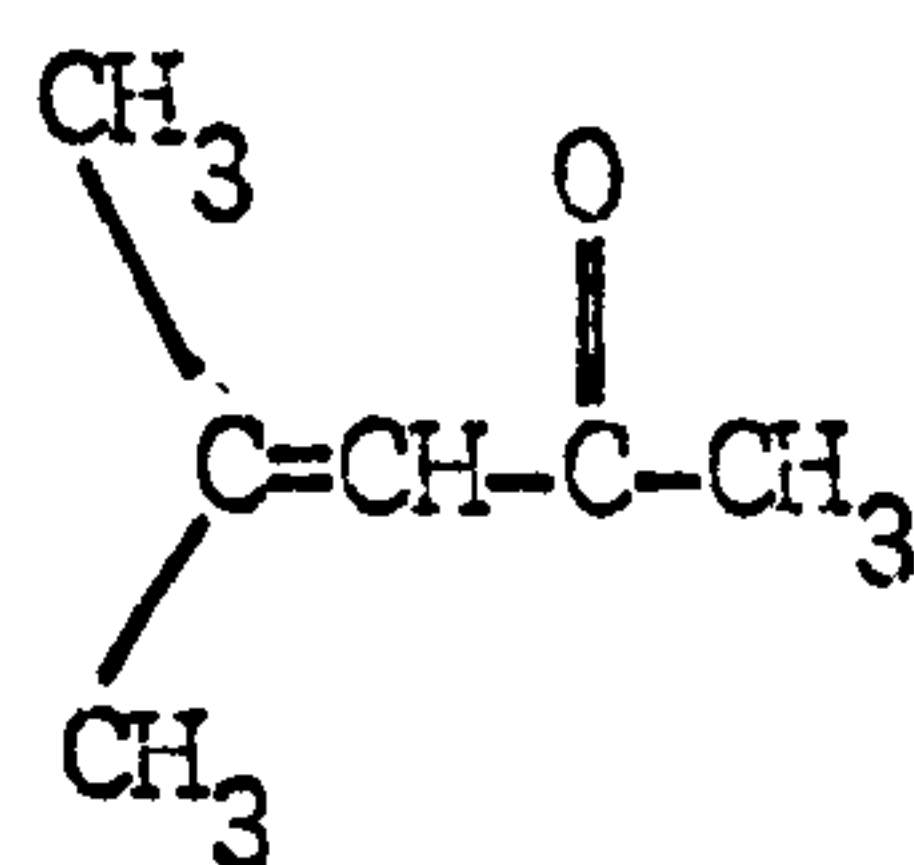


(1)

(2)



The formation of (1) is not thermodynamically favourable<sup>97</sup>.



mesityl oxide



### C. Other Reactions

Reduction of acetone forms isopropanol; oxidation is difficult and results in fracture of the molecule to form a mixture of acids containing fewer carbon atoms than the original molecule.

Acetone and other ketones may form complexes with Lewis acids including  $\text{TiCl}_4$ <sup>99,100</sup>,  $\text{HfCl}_4$ <sup>101</sup>,  $\text{Zr Cl}_4$ <sup>101</sup>,  $\text{SnCl}_4$ <sup>102</sup>, and  $\text{BF}_3$ <sup>103</sup>. Bands assigned to the C=O stretch of acetone in these complexes (table 4.2) are shifted approximately  $50 \text{ cm}^{-1}$  lower than the CO stretch in liquid acetone<sup>104</sup>.

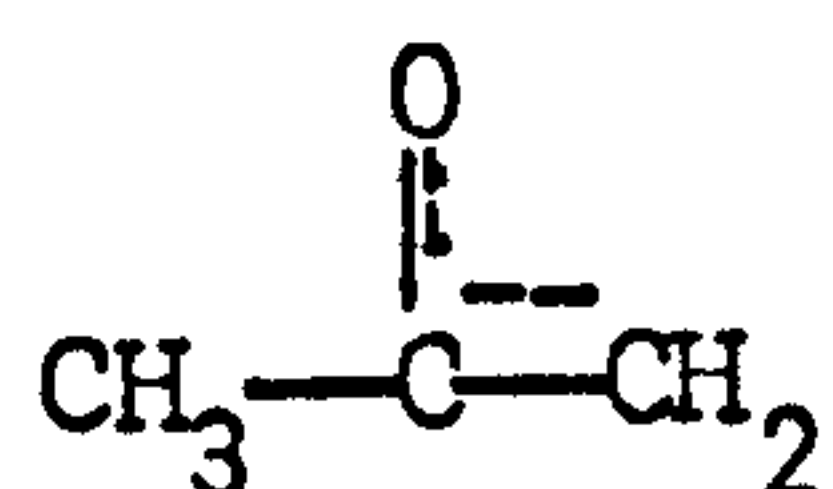
#### 4.3.2 ADSORPTION OF ACETONE ONTO OXIDES

Infrared studies of acetone adsorption on silica<sup>85,86</sup> show hydrogen-bonding of the carbonyl group to surface hydroxyls when acetone vapour ( $6.6 \times 10^2 \text{ N m}^{-2}$ ) is present<sup>85</sup>. Evacuation (298 K) removes most of the adsorbed acetone which is completely removed after evacuation to 373 K to leave a silica surface showing a slight increase in the intensity of the hydroxyl band<sup>85</sup>.

Spectra of acetone adsorbed on rutile and alumina at room temperature contain bands in the  $1700\text{--}1550 \text{ cm}^{-1}$  region (table 4.3) which Winde<sup>89</sup> assigns to adsorbed mesityl oxide.

Those bands observed by Kiselev and Uvarov<sup>85</sup> are assigned to acetone molecules adsorbed on surface hydroxyl groups and Lewis sites. Evacuation of the oxides to 383 K removes the hydrogen-bonded molecules<sup>85</sup> while evacuation to 523 K forms carboxylate species<sup>85</sup>.

Acetone adsorbed on magnesium and nickel oxides<sup>112</sup> also produces bands in the 1700 to 1550  $\text{cm}^{-1}$  region. The bands have been assigned to coordinately bound acetone and to acetone bound dissociatively as an enolate complex:-

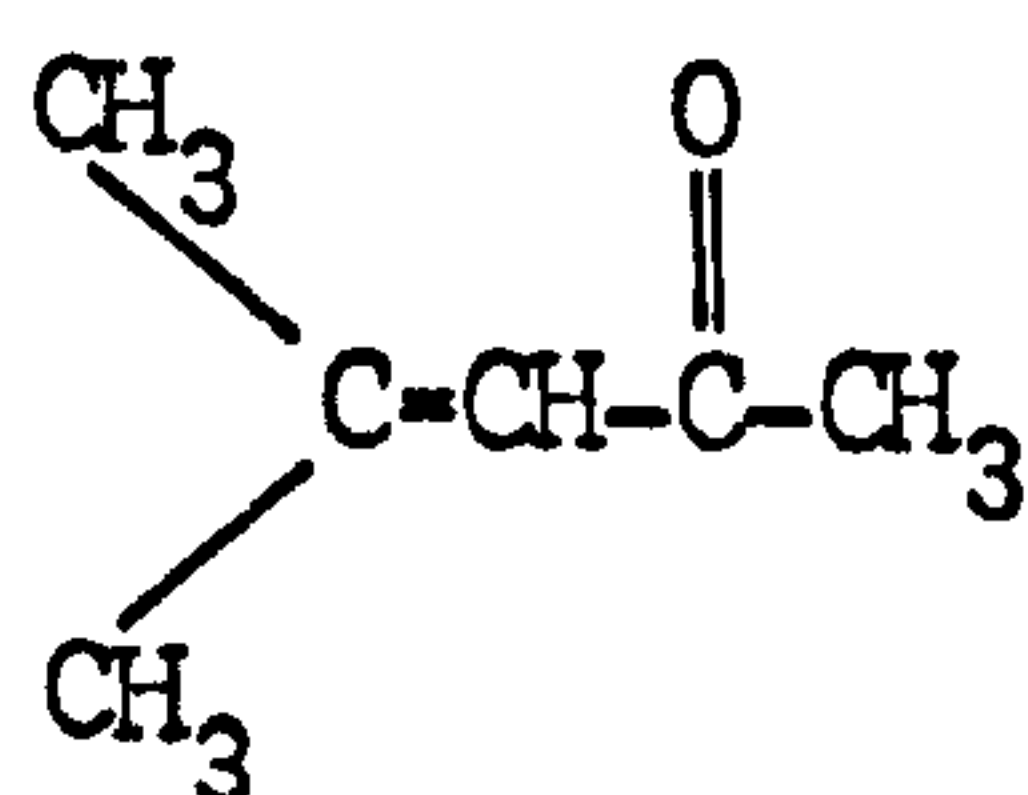


Carboxylate ions are also observed after high temperature (>423 K) treatment of alcohols, aldehydes and carboxylic acids adsorbed on rutile and alumina. The bands assigned to these ions are shown in table 4.4 together with bands for the acetate ion. The highest wavenumber band (1590  $\text{cm}^{-1}$  for alumina 1555  $\text{cm}^{-1}$  for Rutile) is assigned to the antisymmetric carbonyl stretch and the lowest to the symmetric methyl deformation while there is disagreement as to the assignment of the two intermediate bands. Primet<sup>47</sup> assigns the bands by comparing them with the assignments for the acetate ion bands<sup>106</sup> and concludes that the 1450  $\text{cm}^{-1}$  band, the higher of the intermediate frequency bands, is caused by antisymmetric methyl deformation. Greenler<sup>105</sup> shows this band

shifts only  $13\text{ cm}^{-1}$  on deuteration of the acetate species while the  $1390\text{ cm}^{-1}$  band disappears.

Kadushin et al<sup>90,91</sup> observed bands at 1640, 1570, 1515, 1450, 1415, 1390 and  $1360\text{ cm}^{-1}$  in the spectrum of acetone adsorbed on nickel oxide. The  $1570\text{ cm}^{-1}$  and one component of the  $1640\text{ cm}^{-1}$  band are assigned to water coordinately bonded to the surface while the other component of the  $1640\text{ cm}^{-1}$  band is assigned to the C=O vibration in the molecular complex of acetone with the surface of NiO. The  $1515\text{ cm}^{-1}$  band is tentatively assigned to the valence vibration of either C=O or C=C bonds of the enolate complex of acetone.

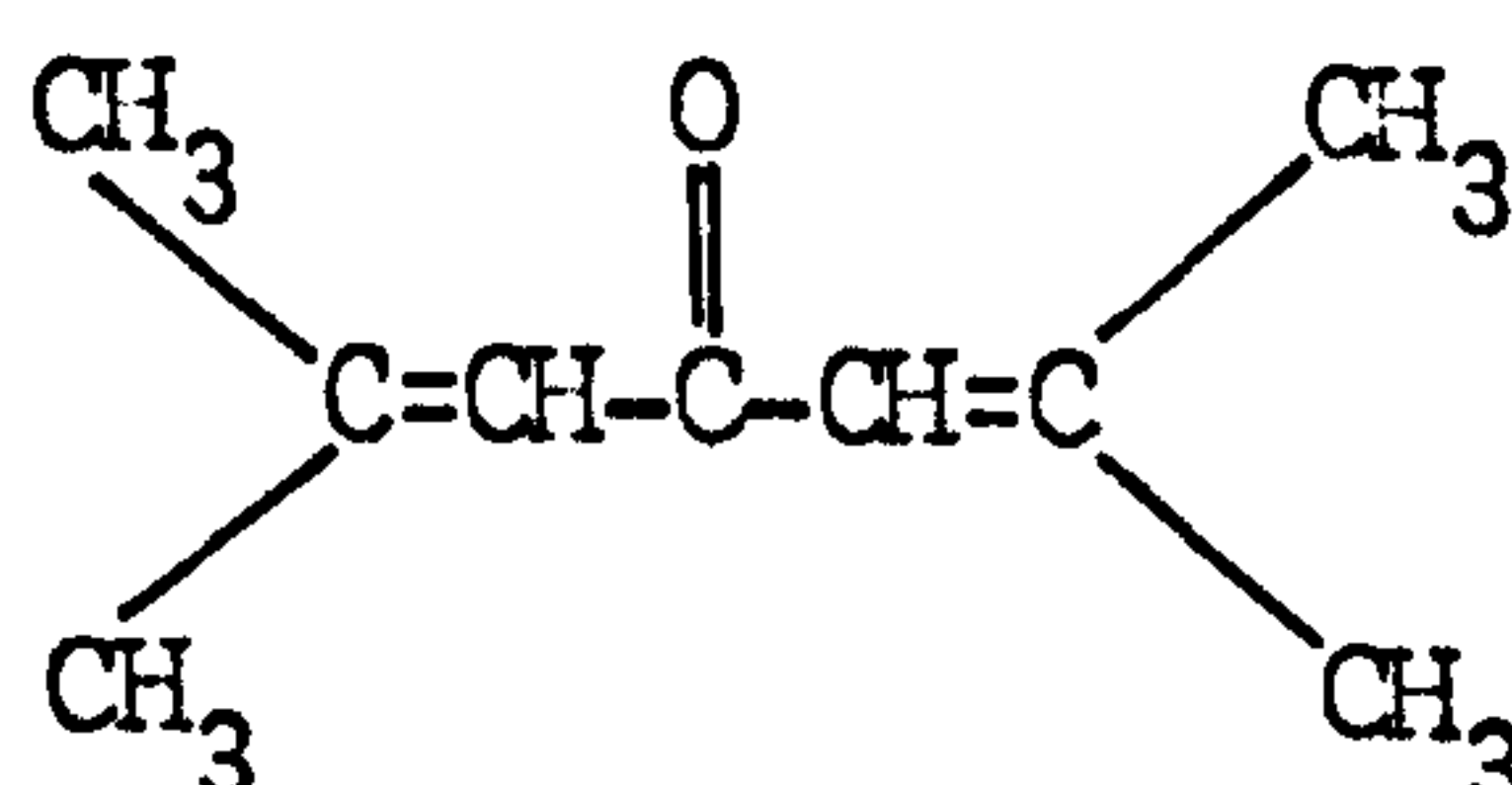
Heating rutile in the presence of acetone vapour yields<sup>94,95,96</sup> mesityl oxide (I) phorone (II) isophorone (III) and mesitylene (IV)



(I)

mesityl oxide

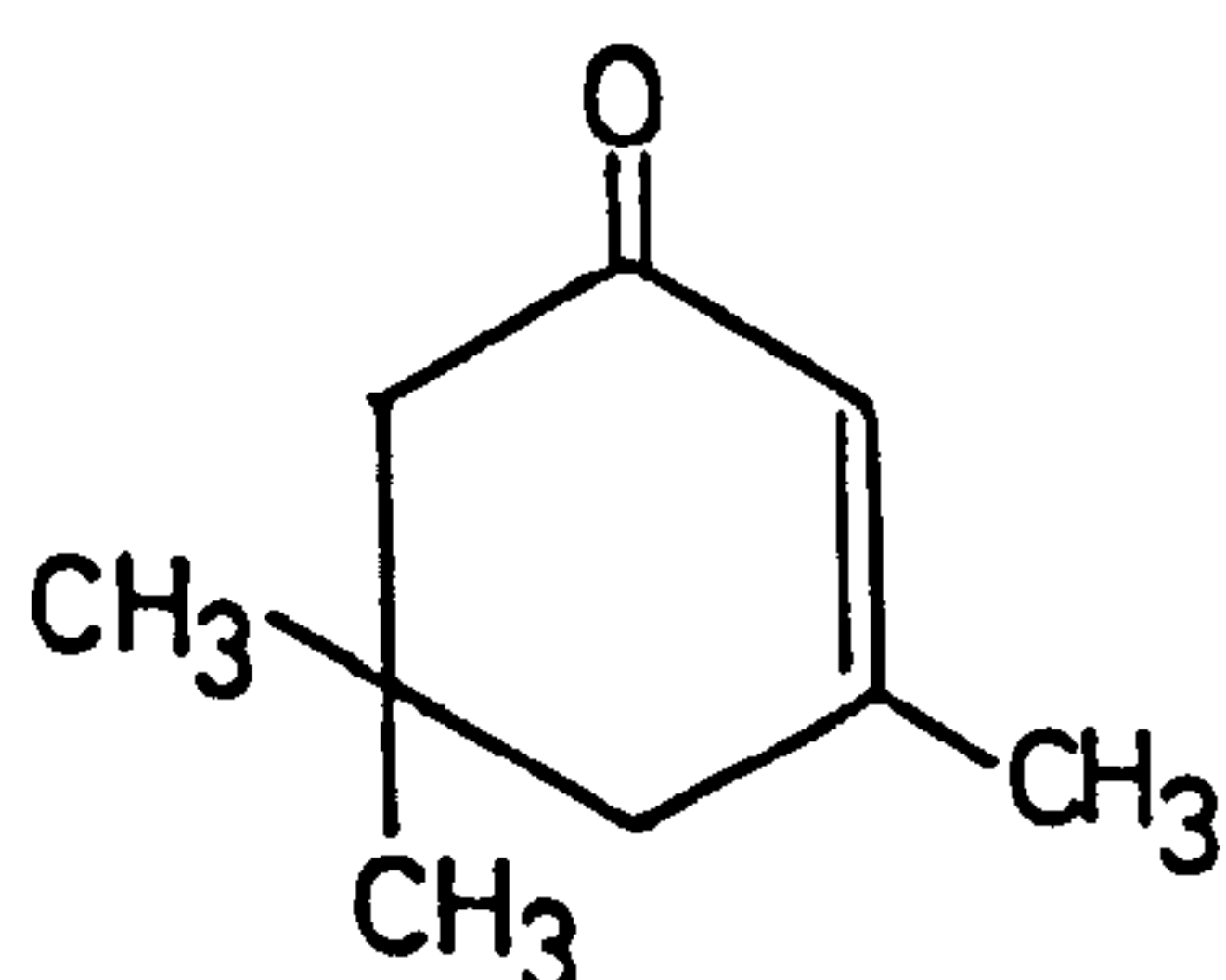
4-methyl-3-penten-2-one



(II)

phorone

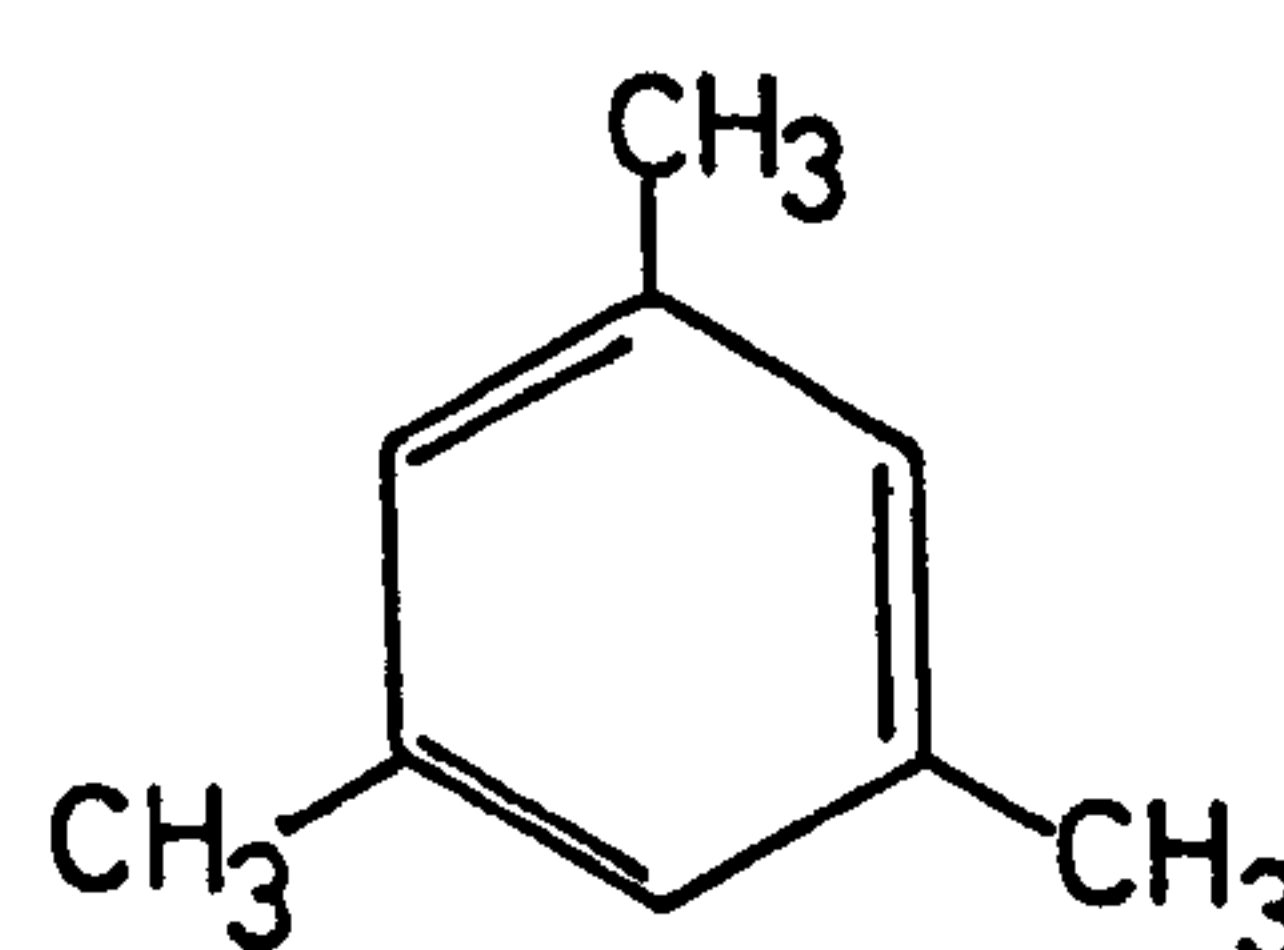
2:6-Dimethyl-2:5-heptadien-4-one



(III)

isophorone

3:5:5-Trimethyl-2-cyclohexenone



(IV)

mesitylene

1:3:5-trimethylbenzene

Mesityl oxide and mesitylene have been adsorbed on rutile, the former (spec. 4.8) showing bands at 2970, 2940, 2910, 1660, 1595, 1445, 1380, 1368  $\text{cm}^{-1}$  which are not removed on evacuation, and a band at 1550  $\text{cm}^{-1}$  which appears on standing (8h) the disc at BT in the evacuated cell. Mesitylene shows bands at 3100, 2930, 2860, 2575, 1610  $\text{cm}^{-1}$  with a broad band at 1480-1440  $\text{cm}^{-1}$  which resolves to two bands at 1480 and 1440  $\text{cm}^{-1}$ . Evacuation removes the adsorbed species.

### 4.3.3 BEHAVIOUR OF BANDS

#### A. Hydroxyl Bands

##### i) 3700 $\text{cm}^{-1}$ Isolated hydroxyl

Initial adsorption of acetone  $d_6$  onto a 673 K  $\text{H}_2\text{O}$  surface (spec. 4.1) reduces this band while OD bands appear at 2720, 2695 and 2520  $\text{cm}^{-1}$ . These increase until the 3700  $\text{cm}^{-1}$  band is decreased to a broad absorption (spec. 4.1 e) and the 2720  $\text{cm}^{-1}$  band becomes a shoulder on the more intense 2695  $\text{cm}^{-1}$  band unlike the equivalent OH bands on the initial surface. Further adsorption (spec. 4.1 f) removes the 2720 and 2695  $\text{cm}^{-1}$  bands while the broad 2520  $\text{cm}^{-1}$  band remains.

Similar results are observed on adsorbing acetone  $h_6$  onto a 673 K  $\text{D}_2\text{O}$  surface, the 3700  $\text{cm}^{-1}$  band appears together with a 3655  $\text{cm}^{-1}$  shoulder which becomes the more

intense band (spec. 4.2 f) as the  $2720\text{ cm}^{-1}$  band disappears. Unlike the  $3700\text{ cm}^{-1}$  band on the initial  $\text{H}_2\text{O}$  surface the  $2720\text{ cm}^{-1}$  band is not completely removed. The  $3655$  and  $3700\text{ cm}^{-1}$  bands are also removed on further adsorption.

The isolated hydroxyl group readily exchanges the hydrogen atom for a deuterium atom from the acetone  $\text{d}_6$  molecule before being removed completely. The appearance of a band due to hydrogen-bonded hydroxyl groups ( $3655/2695\text{ cm}^{-1}$ ) which becomes more intense than the isolated hydroxyl band may be due to the partial removal of the latter by acetone or the formation of hydrogen-bonded hydroxyls.

Adsorption of acetone  $\text{d}_6$  onto  $\text{D}_2\text{O}$  oxidized and reduced surfaces (spec. 4.3 and 4.7) removed the  $2720$  and  $2710\text{ cm}^{-1}$  bands completely while the  $2690\text{ cm}^{-1}$  decreased more slowly and was not completely removed.

#### ii) $3680\text{ cm}^{-1}$ band

This band is present on the BT  $\text{D}_2\text{O}$  and  $\text{H}_2\text{O}$  surfaces (spec. 4.3 and 4.4) and on the  $373\text{ K}$   $\text{D}_2\text{O}$  surface (spec. 4.5). It is the first hydroxyl band to disappear on all three surfaces. It is not observed during exchange of the OD groups on the  $373\text{ K}$   $\text{D}_2\text{O}$  surface by acetone  $\text{h}_6$  (spec. 4.5) and is very weak on the BT  $\text{D}_2\text{O}$  surface (spec. 4.4) after similar treatment due to removal by the acetone molecule.

The removal of the  $2710\text{ cm}^{-1}$  band, with the  $2720\text{ cm}^{-1}$  band on the appearance of the  $1645$  and  $1580\text{ cm}^{-1}$  bands (spec. 4.3 a-e) indicates that the species producing these bands removes the isolated hydroxyl groups.

The high thermal stability and high reactivity of the isolated terminal hydroxyl groups, also observed during reactions of pyridine<sup>11</sup>, HCl<sup>11</sup> and SO<sub>2</sub><sup>11</sup> with the BT surface, may be explained by their position on sites probably surrounded by defects which prevent hydrogen bonding to other hydroxyl groups and permits the unhindered approach of adsorbing molecules.

### iii) $3655\text{ cm}^{-1}$ band-H-bonded Hydroxyl Groups

The behaviour of this band on the 673 K surfaces (spec. 4.1 and 4.2) is similar to that of the  $3700\text{ cm}^{-1}$  band but is observed as a shoulder in the spectrum of the initial surfaces and a peak more intense than the  $3700$  (or  $2720$ )  $\text{cm}^{-1}$  band after exchange has occurred. Initial adsorption of acetone h<sub>6</sub> onto a BT D<sub>2</sub>O surface (spec. 4.4 a-c) results in the appearance of the  $1670$  and  $3655\text{ cm}^{-1}$  bands indicating the species absorbing at  $1670\text{ cm}^{-1}$  to cause initial exchange of the OD deuterium atoms. Further adsorption (spec. 4.4 d-h) increases the intensity of bands at  $3655$ ,  $3610$ ,  $3520$ ,  $3420\text{ cm}^{-1}$  which are not removed at higher acetone vapour pressures; broadening of these bands indicates hydrogen bonding. The exchanged bands are of lower intensity than the original bands, which disappear, with

the exception of a broad  $2520\text{ cm}^{-1}$  band, indicating that hydroxyl and water species not undergoing exchange reactions are removed.

Initial adsorption (spec. 4.3 a-c) of acetone  $d_6$  on to the  $D_2O$  BT surface increases the  $1675\text{ cm}^{-1}$  band but does not decrease the  $2695\text{ cm}^{-1}$  band while further adsorption (spec. 4.4 d-n) increases the  $1580\text{ cm}^{-1}$  band and decreases the  $2695\text{ cm}^{-1}$  band to a minimum. A plot of absorbance  $2695\text{ cm}^{-1}$  band against absorbance  $1580\text{ cm}^{-1}$  is an approximate straight line. The  $2695\text{ cm}^{-1}$  band is not completely removed indicating that the terminal hydroxyl groups remain on the surface, probably those which have undergone exchange reactions with the species absorbing at  $1670\text{ cm}^{-1}$ . During the adsorption of acetone no shift is observed in the position of the initial  $3655$  or  $2695\text{ cm}^{-1}$  bands indicating that no hydrogen bonding between acetone molecules and hydroxyl groups occurs.

Adsorption of acetone  $d_6$  onto a BT  $D_2O$  reduced surface (spec. 4.7) removes the  $2695\text{ cm}^{-1}$  band to leave a broad  $2670\text{ cm}^{-1}$  band. (spec. 4.4 k,l).

#### iv) $3610, 3520\text{ cm}^{-1}$ bands

The decrease in intensity of these bands on the initial adsorption of acetone  $d_6$  onto a BT,  $D_2O$  surface (spec. 4.3 a-d) might be caused by heating of the disc by the beam or displacement of coordinated water by the acetone  $d_6$  species absorbing at  $1670\text{ cm}^{-1}$ . The bands are not removed on initial adsorption (spec. 4.4 a-d) of acetone  $h_6$  onto a BT,  $D_2O$  surface, which increases

the  $1670\text{ cm}^{-1}$  band, but decrease due to exchange of the deuterium atoms, bands appearing at  $3610$  and  $3520\text{ cm}^{-1}$ . Further adsorption decreases and removes these bands with the  $2695\text{ cm}^{-1}$  band (spec. 4.4 g,h) and increases the  $1645$ ,  $1580\text{ cm}^{-1}$  bands. Water molecules are not displaced by the species absorbing at  $1670\text{ cm}^{-1}$  but are removed by the species absorbing at  $1645$  and  $1580\text{ cm}^{-1}$ . Munuera and Stone report that adsorbed water is not displaced by acetone vapour.

#### v) $3420\text{ cm}^{-1}$ Bridged Hydroxyl Group

This band is decreased by 20% of the original intensity during the adsorption of acetone  $d_6$  onto the BT,  $D_2O$  surface at relatively low vapour pressures (spec. 4.3 a-h). Further adsorption increases the band intensity, by approximately 10-20%, while evacuation reduces it to its minimum value. Adsorption of acetone  $h_6$  onto a BT,  $D_2O$  surface (spec. 4.4) exchanges the deuterium atoms, a band appearing at  $3420\text{ cm}^{-1}$ , and decreases the original  $2535\text{ cm}^{-1}$  band to a broad band at  $2520\text{ cm}^{-1}$ . The  $2535\text{ cm}^{-1}$  band on the 373 K  $D_2O$  surface (spec. 4.5) shows similar behaviour. On the 373 K and BT  $D_2O$  surfaces the  $3420\text{ cm}^{-1}$  OH band produced by exchange is not removed after exposing the surface to high vapour pressures, while the original  $2535\text{ cm}^{-1}$  band disappears after the  $2695\text{ cm}^{-1}$  terminal hydroxyl band.

The  $2535\text{ cm}^{-1}$  bridged hydroxyl band is increased in intensity during adsorption of acetone  $d_6$  onto the reduced surface while on evacuation the intensity is reduced to the original



value. The increase in intensity may be due to an increase in a broad band beneath the  $2535\text{ cm}^{-1}$  band (spec. 4.7 i-1).

The behaviour of this band is different from that of the  $2695$  and  $2720\text{ cm}^{-1}$  bands assigned to the terminal hydroxyl groups in that although bridged hydroxyl groups may undergo exchange reactions no reactions with acetone molecules occur which remove the groups.

#### vi) $3400\text{ cm}^{-1}$ band Coordinated Water Molecules

The band is observed on the BT  $\text{H}_2\text{O}$ ,  $\text{D}_2\text{O}$  and  $373\text{ K}$   $\text{D}_2\text{O}$  surfaces and shows behaviour similar to that of the  $2535\text{ cm}^{-1}$  band on the adsorption of acetone. The coordinated  $\text{D}_2\text{O}$  molecules are capable of exchange reactions with the acetone but are not displaced by acetone molecules.

#### vii) Summary of Behaviour of the Hydroxyl and Water Bands

##### 1. Hydrogen-bonding

Hydrogen-bonding between acetone and OH/OD groups did not occur at low acetone coverages as no shift of bands was observed and no acetone molecules were removed by evacuating the disc.

##### 2. Exchange reactions

- a) All OH/OD bands initially present were capable of exchange; those formed by exchange reactions with BT and

373 K surfaces were not removed at high acetone vapour pressures while those bands not exchanged, with the exception of a broad  $2520\text{ cm}^{-1}$  were removed by acetone adsorption.

b) The species absorbing at  $1685/1670\text{ cm}^{-1}$  were able to exchange hydrogen or deuterium atoms.

c) The species absorbing at  $1660/1645$  and  $1595/1580\text{ cm}^{-1}$  removed those terminal hydroxyl groups which had not undergone an exchange reaction.

### 3. Removal of bands

a) The isolated terminal hydroxyl groups ( $3700/3720\text{ cm}^{-1}$ ) and those weakly hydrogen-bonded ( $3680/2710\text{ cm}^{-1}$ ) are more reactive than the row A hydrogen-bonded hydroxyl groups ( $3655/2695\text{ cm}^{-1}$ ).

b) The  $3610/2660$  and  $3520/2600\text{ cm}^{-1}$  bands due to water molecules are removed by the species causing the  $1660/1645$  and  $1595/1580\text{ cm}^{-1}$  bands. The  $3400/2520\text{ cm}^{-1}$  band is not affected by these species.

c) The species causing the  $1685/1670\text{ cm}^{-1}$  bands does not remove any bands except by exchange.

## B. CH/CD Bands

Bands due to CH and CD stretching vibrations appear in the 3000-2800 and 2300-2000  $\text{cm}^{-1}$  ranges respectively. The relative positions and band intensities of the CH and CD bands differ, the 2970 and 2930  $\text{cm}^{-1}$  bands are 40  $\text{cm}^{-1}$  apart and of similar intensity while the corresponding CD bands, 2225 and 2120  $\text{cm}^{-1}$ , are 105  $\text{cm}^{-1}$  apart, the former being more intense than the latter. The relative intensities of the CH bands also differ with the surface pretreatment, on the 673 K  $\text{D}_2\text{O}$  surface (spec. 4.2) the 2970  $\text{cm}^{-1}$  band is more intense than the 2930  $\text{cm}^{-1}$ , while on the BT,  $\text{D}_2\text{O}$  (spec. 4.4) and 373 K  $\text{D}_2\text{O}$  surfaces (spec. 4.5) the 2930  $\text{cm}^{-1}$  is more intense than the 2970  $\text{cm}^{-1}$ .

The CH and CD bands appear during the initial adsorption of acetone onto 673 K and 373 K surfaces, while on the BT surfaces they appear with the 1660/1645 and 1595/1580  $\text{cm}^{-1}$  bands. A plot, intensity of 2225  $\text{cm}^{-1}$  band against intensity of 1580  $\text{cm}^{-1}$ , is a straight line passing through the origin indicating that the two bands arise from the same adsorbed species.

The 2970/2225  $\text{cm}^{-1}$  band broadens when the 1550-1510  $\text{cm}^{-1}$  region begins to increase in intensity (specs. 4.1 h, 4.2 h, 4.3 h) due to the appearance of bands at 2260 and 2210  $\text{cm}^{-1}$ . The 2210  $\text{cm}^{-1}$  band becomes more intense than the 2225  $\text{cm}^{-1}$  band as the intensity of the 1510  $\text{cm}^{-1}$  band increases (spec. 4.3 m-p). This band is also observed as the most intense C-D band appearing on reduced surfaces (spec. 4.6 and 4.7) together with an intense

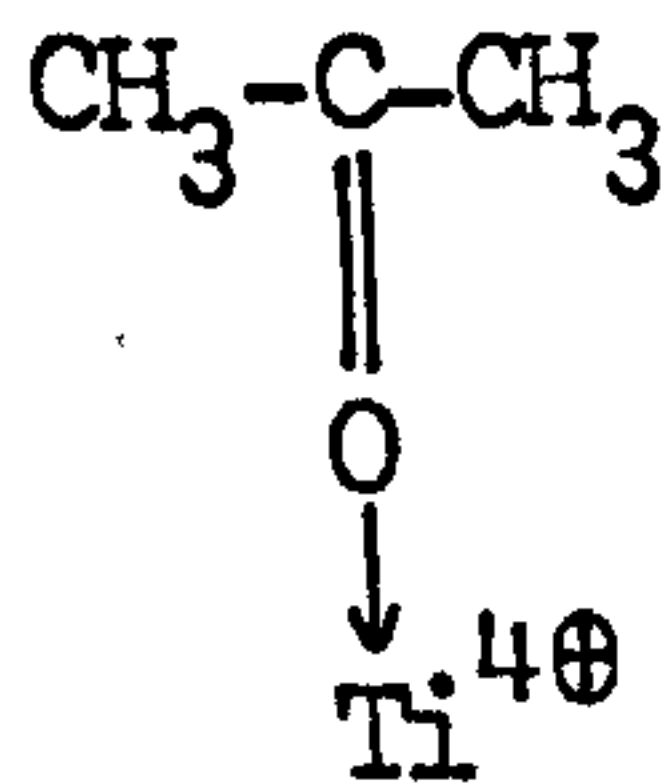
1480  $\text{cm}^{-1}$  band. The 2210  $\text{cm}^{-1}$ , 1510 and 1480  $\text{cm}^{-1}$  bands arise from the same species.

The CD, CH bands will be assigned after considering the assignment of the bands below 2000  $\text{cm}^{-1}$ .

C. 1685/1670  $\text{cm}^{-1}$  band

The appearance of this band on a hydroxylated surface coincides only with exchange of the OH or OD groups, no water molecules or hydroxyl groups are perturbed or removed and the band is not removed on evacuation of the rutile. The band does not therefore arise from acetone hydrogen-bonded to OH groups.

The wavelength of this band is about 30  $\text{cm}^{-1}$  less than the C=O group vibration in acetone liquid and is typical of the wavelength of the C=O group in Lewis acid complexes of acetone (table 4.2). The band is therefore assigned to acetone Lewis bonded to a surface titanium ion.



The relatively low shift of the C=O frequency, 30  $\text{cm}^{-1}$  as opposed to at least 50  $\text{cm}^{-1}$  in other complexes and the continued presence of water molecules bonded to the surface indicate that the acetone molecules bond to the weak sites from which water molecules have been removed by evacuation.

The acetone molecules are able to exchange with about 25% of all of the water and hydroxyl groups indicating that weak sites exist on all surface planes.

No CD or CH bands were observed on the appearance of this band on the hydroxylated surface showing the surface concentration was low. On the reduced surface the maximum intensity reached by this band was lower than on the oxidized surface probably because of the higher surface concentration of  $Ti^{3+}$  ions which would not readily form a Lewis complex as they have one electron in the previously empty d-orbital.

D. 1660/1645  $cm^{-1}$  band

The behaviour of this band is similar to that of the 1595/1580  $cm^{-1}$  band and the intensity varies linearly with that of the other band. It is probable that they are due to the same species and the assignment of these bands is considered below.

E. 1595/1580  $cm^{-1}$  band

On 373 K and 673 K oxidized surfaces these appear with the 1685/1670  $cm^{-1}$  bands as broad bands which narrow at the apex during the subsequent increase in intensity. On a BT surface the band does not appear until the 1685/1670  $cm^{-1}$  band is near its maximum which indicates water molecules removed at 373 K hinder the formation of these species. The species

remove terminal (row A) hydroxyl groups but do not react with the bridged (row B) hydroxyls. The formation of the species is however independent of the terminal hydroxyl groups as the maximum intensity of the band does not vary with the surface hydroxylation.

The adsorption of mesityl oxide onto rutile produces similar bands to the 1660 and 1595  $\text{cm}^{-1}$  bands (spec. 4.8) as well as a 1440  $\text{cm}^{-1}$  band. It is therefore considered that both of these bands are due to mesityl oxide adsorbed onto rutile. The 1660  $\text{cm}^{-1}$  band is the C=O vibration where the oxygen is Lewis bonded to a titanium ion while the 1595  $\text{cm}^{-1}$  band is the C=C vibration.

The existence of two surface sites of differing Lewis acidity has been demonstrated by other workers (3.3.3) and the 1685  $\text{cm}^{-1}$  band results from adsorption of acetone on the weaker of the two sites. The hydroxyl groups and water molecules on a BT hydroxylated surface occupy the stronger sites and the appearance of the 1660 and 1585  $\text{cm}^{-1}$  bands after the 1685  $\text{cm}^{-1}$  on this surface, together with the removal of the terminal OH bands with the increase in the two bands, indicates that mesityl oxide is formed on the stronger sites. The mesityl oxide molecule may be formed by the reaction between an acetone molecule adsorbed on the stronger site with one in the gas phase or one adsorbed on an adjacent site. Spec. 4.4 k-n shows that when acetone is dosed on after evacuation the 1685  $\text{cm}^{-1}$  is the first band to be

produced, the 1660 and 1595  $\text{cm}^{-1}$  bands forming more slowly. Thus some mesityl oxide is formed by a reaction between acetone molecules on strong and weak sites.

Hydroxyl groups resulting from exchange reactions with the Lewis bonded acetone are not removed on the formation of mesityl oxide probably because of steric hindrance from the neighbouring acetone molecule. The terminal OD groups remaining on the BT  $\text{D}_2\text{O}$  surface after acetone  $\text{d}_6$  adsorption (spec. 4.3 p) have therefore taken part in an exchange reaction with the deuterium atoms in the acetone, or mesityl oxide, molecules. Spectra 4.4 and 4.5 show that although the 2535  $\text{cm}^{-1}$  bridged hydroxyl band may be completely exchanged it reappears as the hydrogenated equivalent band but is not as sharp. This broadening of the bridged hydroxyl band does not occur in the all-deuterium system.

The mesityl oxide formed is not removed by evacuation, although the band intensities do decrease after relatively high vapour pressures of acetone, and this is considered below. Mesityl oxide in carbon tetrachloride shows bands due to C=O at 1715 and 1690  $\text{cm}^{-1}$  and to C=C at 1620  $\text{cm}^{-1}$ . On rutile the C=O bands are observed at 1665  $\text{cm}^{-1}$  and the C=C at 1595  $\text{cm}^{-1}$ . After prolonged exposure to the rutile surface bands are observed at 1540 and 1440  $\text{cm}^{-1}$  similar to those observed after acetone adsorption at high pressures.

### F. Bands in the region below $1550\text{ cm}^{-1}$

On the oxidized surface bands appear in this region after the acetone and mesityl oxide bands and increase in intensity after the mesityl oxide bands have reached maximum intensity. The bands decrease in intensity when the rutile is exposed to acetone and increase on evacuation. The reaction which produces the molecules absorbing below  $1550\text{ cm}^{-1}$  is therefore favoured by the removal of the acetone and mesityl oxide.

The bands occurring below  $1550\text{ cm}^{-1}$  are shown in table 4.1. The  $1540\text{ cm}^{-1}$  band appears on the adsorption of both acetone and deuterioacetone but is prominent only on adsorption of the former whereas the  $1510\text{ cm}^{-1}$  band which also appears on all the oxidized surfaces is only prominent after the adsorption of deuterioacetone. The  $1540\text{ cm}^{-1}$  and  $1510\text{ cm}^{-1}$  bands are considered to arise from the same surface species, the  $1540\text{ cm}^{-1}$  band being due to the hydrogenated isomer and the latter to the deuterated. The  $1510\text{ cm}^{-1}$  band formed as a weak shoulder on the  $1540\text{ cm}^{-1}$  band on surfaces dosed with acetone  $h_6$  probably results from the exchange reaction occurring on these surfaces since all surfaces had OD or  $D_2O$  groups on them (spec. 4.2, 4.4, 4.5). The appearance of a  $1540\text{ cm}^{-1}$  band, which has been assigned to a hydrogenated species, in an all deuterium system cannot be explained by exchange.

The  $1480\text{ cm}^{-1}$  band which appears on the reduced surface after the adsorption of acetone is considered to be due to the same species as the other bands in this region and is



discussed in the following chapter describing the adsorption of acetic acid.

The weak  $1465\text{ cm}^{-1}$  band is observed on spectra 4.1, 4.2, 4.4 and 4.5 and is probably due to C-H vibrations.

The  $1440\text{ cm}^{-1}$  band is observed in the spectrum of mesityl oxide adsorbed on rutile but varies in intensity with the  $1540\text{ cm}^{-1}$  band which is not assigned to mesityl oxide. Similarly the corresponding deuterium species absorbs at  $1425\text{ cm}^{-1}$ , this band varying with the  $1510\text{ cm}^{-1}$  band. The  $1440\text{ cm}^{-1}$  mesityl oxide band is weaker than the  $1595\text{ cm}^{-1}$  band and is not observed before the  $1440\text{ cm}^{-1}$  band associated with the  $1540\text{ cm}^{-1}$  band appears.

The predominant bands in the region are the  $1540$  and  $1440\text{ cm}^{-1}$  bands formed by adsorption of acetone  $h_6$  or the  $1510$  and  $1425\text{ cm}^{-1}$  bands on the adsorption of acetone  $d_6$ . These bands are of similar wavelength to those observed for acetates<sup>113-116</sup> and bands observed in this region on oxide surfaces have been assigned to acetate species (table 4.4). The bands are therefore assigned to the asymmetric and symmetric vibrations of the acetate group.

The bands due to CH and CD vibrations at  $2970$ ,  $2930$ ,  $2880\text{ cm}^{-1}$  and  $2225$ ,  $2120$ ,  $2060\text{ cm}^{-1}$  respectively are assigned to the mesityl oxide CH and CD vibrations since their intensity varies with the C=O and C=C mesityl oxide bands. The shoulders

observed at 2955 and 2210  $\text{cm}^{-1}$  on the principal peak vary in intensity with the acetate bands, and result from the methyl hydrogen, or deuterium, atom vibrations.

#### G. Summary

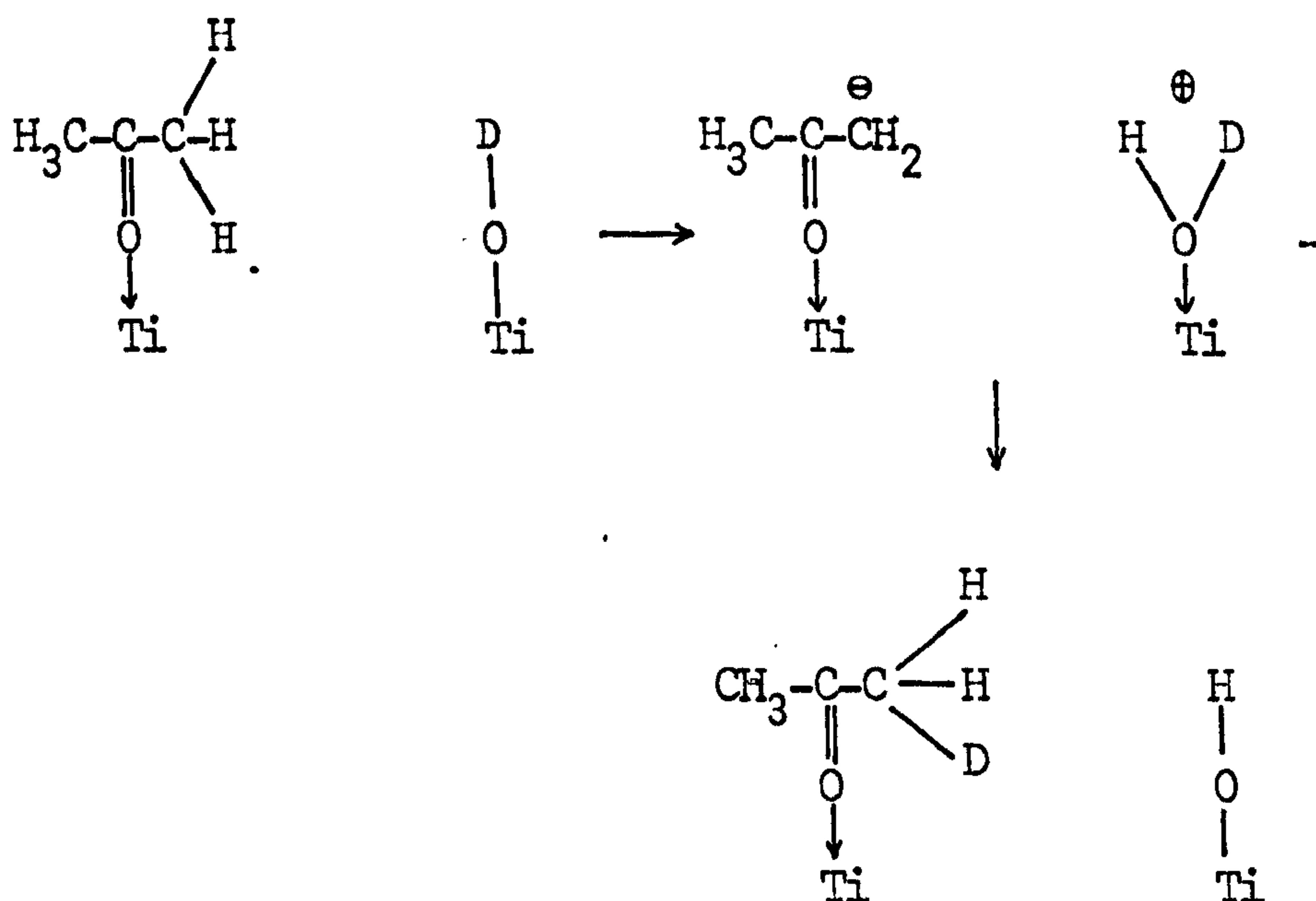
A summary of bands observed below 2000  $\text{cm}^{-1}$  and their assignments is given in table 4.5.

#### 4.3.4 SURFACE REACTIONS

##### A. Adsorption acetone onto BT hydroxylated oxidized surface

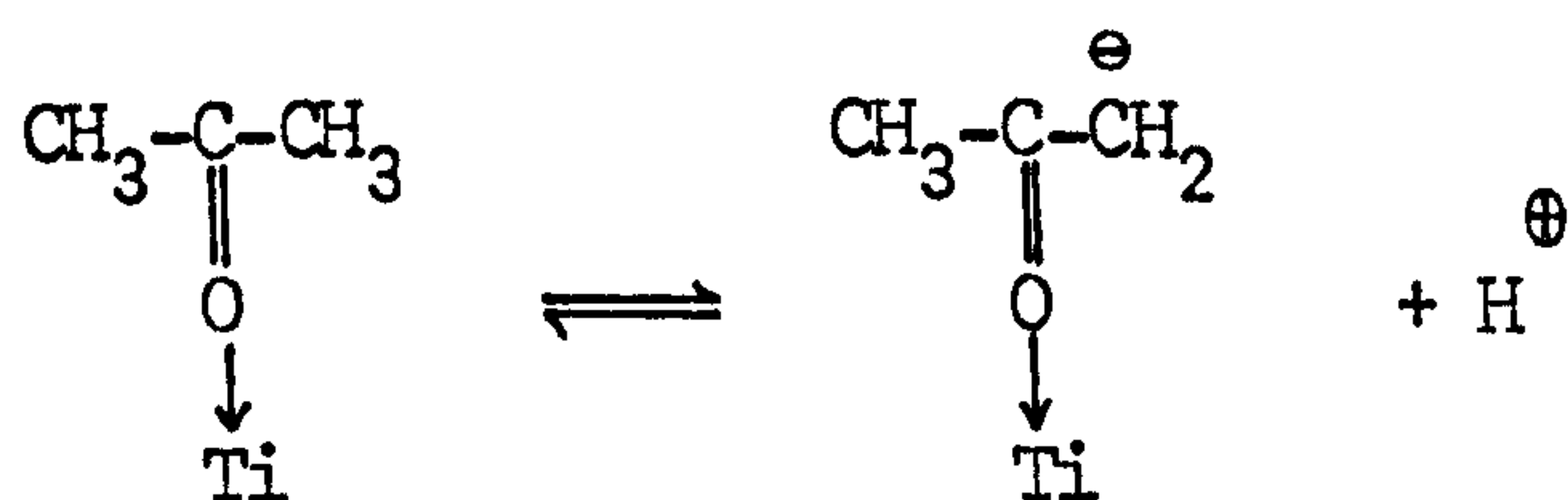
Exposure of a hydroxylated rutile surface to low vapour pressures of acetone result in the formation of the  $1680\text{ cm}^{-1}$  band indicating the acetone molecules are bonding via the lone pair electrons on the oxygen atom to titanium ions. No water molecules are displaced by the formation of this complex indicating the titanium ions to be weak sites from which water molecules may be removed by evacuation at beam temperature.

The surface acetone exchanges with surrounding hydroxyl and water molecules by the following mechanism<sup>95</sup> which is identical to the first stage of base catalysed enolization (section 4.3.1).

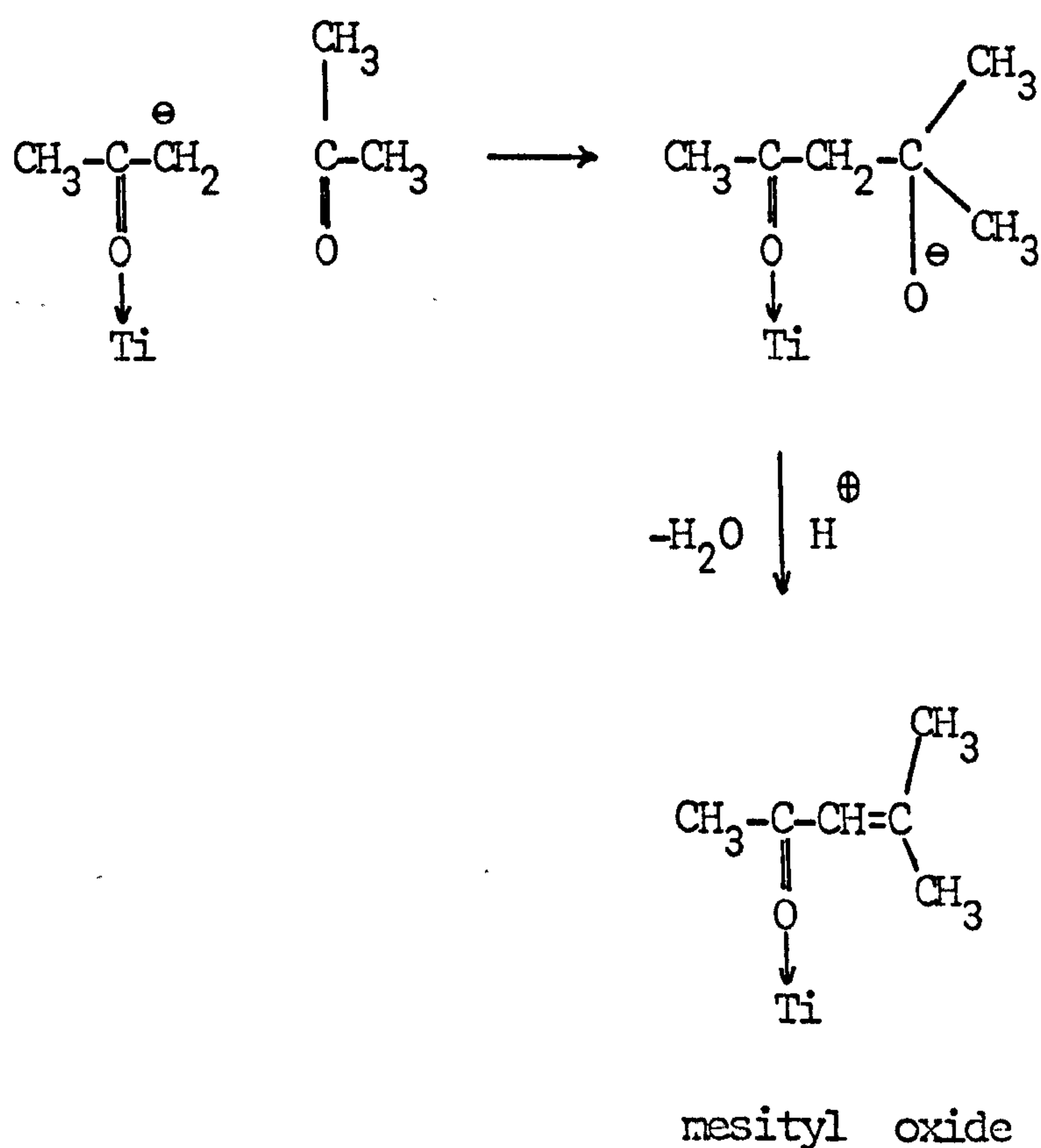


Spectra show that this reaction occurs with all hydroxyl and water groups on the surface.

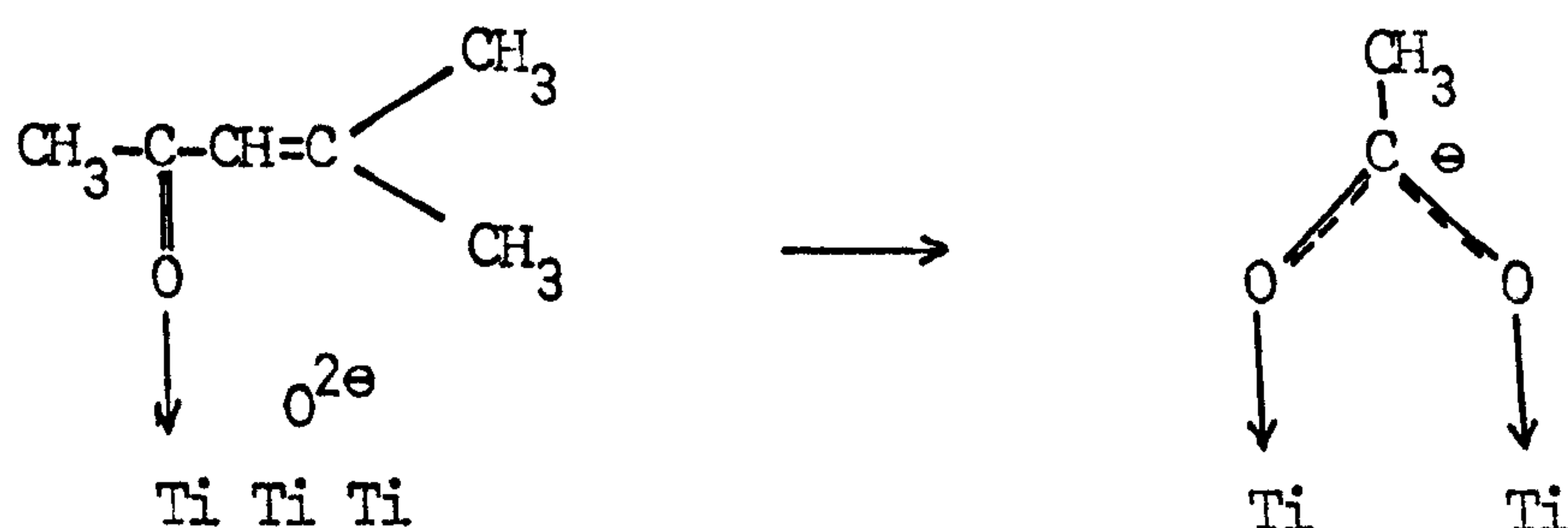
The second stage of the adsorption process occurs when the  $1680\text{ cm}^{-1}$  band has reached a maximum intensity indicating all the weaker sites to be occupied by acetone molecules. As previously considered (4.3.3e) mesityl oxide is formed on the stronger sites, the initial step in the reaction after the saturation of the weaker sites being the removal of water and the formation of a Lewis complex. The attraction of the lone pair electrons by the titanium ion will be stronger in this complex than in the complex on the weaker site thus making the loss of a hydrogen ion more favourable.



Normally the reverse reaction would occur before the carbanion had time to react at room temperature<sup>95</sup>. However the higher temperature (approx. 330 K) of the conditions and greater stability of the carbanion would make reaction with another acetone molecule possible.



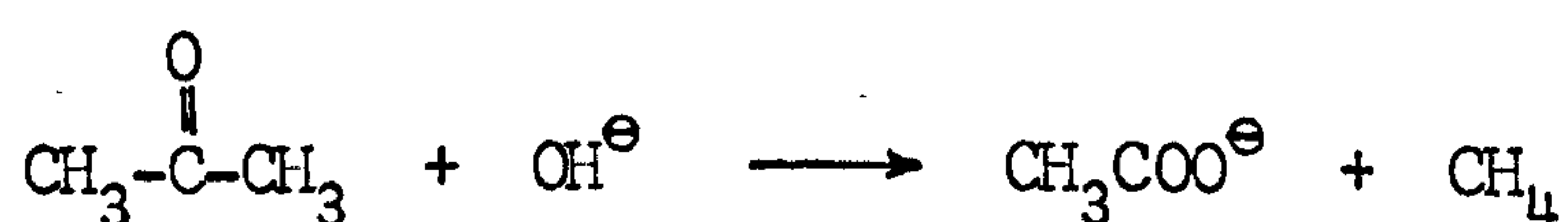
The third stage of adsorption is the formation of surface acetate species as shown by the appearance of the 1540, 1440  $\text{cm}^{-1}$  bands. The reaction which forms these species is not obvious but may arise from the increased electron density at the rutile surface due to the Lewis-bonded acetone, and mesityl oxide. This increased electron density may permit an  $\text{O}^{2e}$  ion resulting from the elimination of OH groups, either in the pretreatment process or on the adsorption of acetone, to react with a mesityl oxide or acetone molecule.



This reaction produces the fragment  $\text{CH}=\text{C} \begin{array}{l} \diagup \text{CH}_3 \\ \diagdown \text{CH}_3 \end{array}$

which might react with the water molecules produced in the reaction forming mesityl oxide to produce tertiary butyl alcohol.

Fink<sup>87</sup> proposes a reaction of acetone with alumina surface OH groups to form acetate species:-



While this reaction may occur on the rutile surface the decrease of mesityl oxide bands on the formation of the acetate bands indicates that the reaction involving the oxygen ion predominates.

Acetone thus reacts with the hydroxylated surface in three stages:-

- Stage I - the formation of a Lewis acid complex
- Stage II - the formation of mesityl oxide
- Stage III - the formation of acetate species

Each stage commences when the previous stage is almost complete.

Stages I and II are unaffected by evacuation of the surface, no change in band intensities are observed. The plotting of isotherms (band intensity against acetone pressure) was not possible because the band intensities continued to increase even

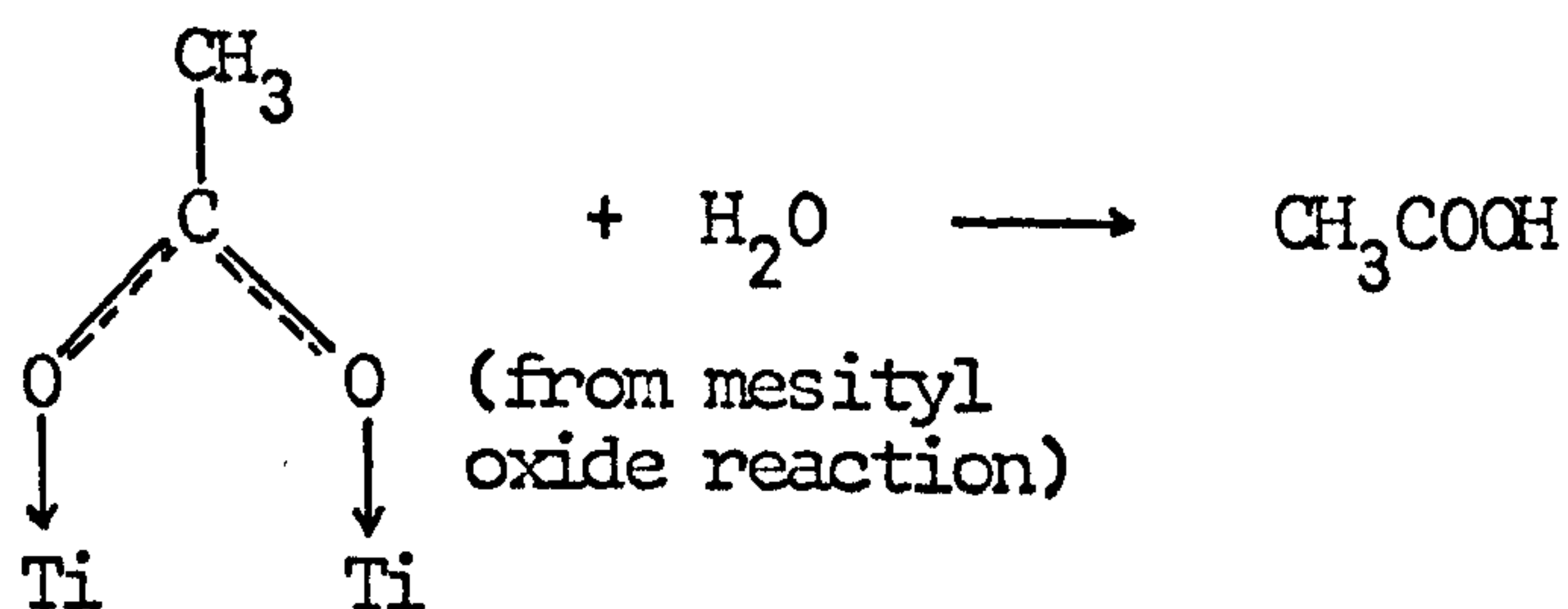
at very low vapour pressures (less than  $0.1 \text{ N m}^{-2}$ ) indicating the formation of the Lewis complex and mesityl oxide to be irreversible.

Above approximately  $0.3 \text{ N m}^{-2}$  the intensity of mesityl oxide bands did not continue to increase with each dose of acetone at the same pressure but varied with the acetone pressure, indicating the surface to be in equilibrium with the vapour. The formation of this 'equilibrium surface' coincided with the maximum intensity of the mesityl oxide bands on the evacuated surface. Above the equilibrium pressure the intensity of these bands increased and on evacuation decreased to this 'maximum' intensity.

The three stages of adsorption are related above the equilibrium pressure as shown in spec. 4.4 the equilibrium having been reached by spec. 4.4 i. Spec 4.4 k-n show that on initial adsorption Lewis acid complexes are formed (increase in  $1685 \text{ cm}^{-1}$  band) which react with acetone molecules on strong sites to form mesityl oxide causing a decrease in the  $1685 \text{ cm}^{-1}$  band and an increase in the  $1660$  and  $1595 \text{ cm}^{-1}$  bands. A slight decrease occurs in the  $1550 \text{ cm}^{-1}$  acetate bands.

Evacuation of this surface (spec. 4.4 p) decreases the surface mesityl oxide and increases the surface acetate indicating the decomposition of the mesityl oxide. The mechanism for this reaction is probably similar to that shown above for the formation of the acetate species, the removal of

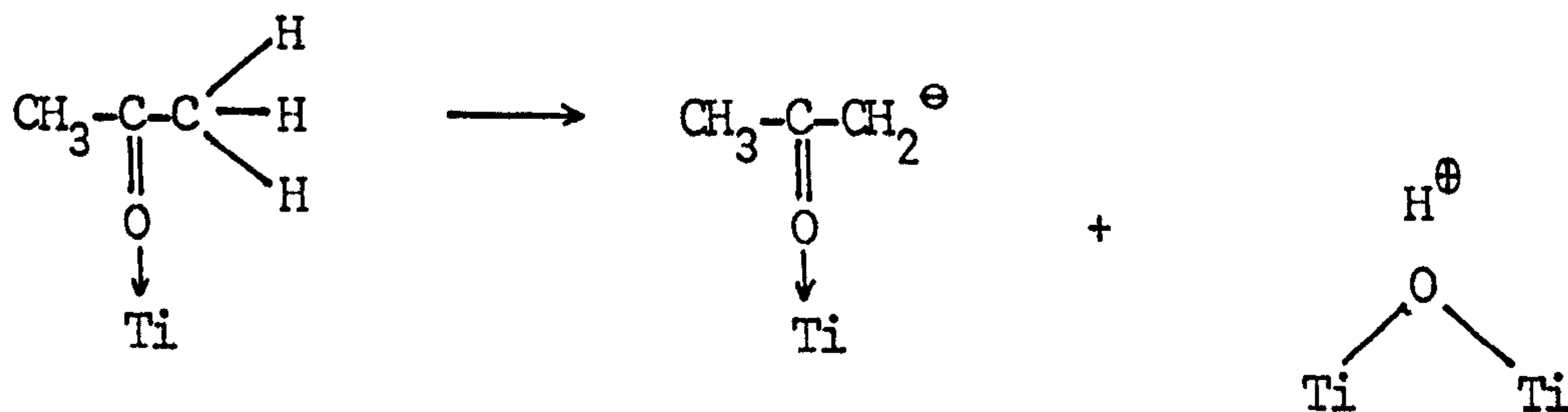
t-butyl alcohol by evacuation moving the reaction equilibrium to the right. Subsequent dosage of acetone increases the surface mesityl oxide and decreases the acetate concentration possibly by the formation of acetic acid which passes into the vapour phase.



#### B. Adsorption acetone onto 373 K and 673 K oxidized rutile

The reactions are similar to those on the BT hydroxylated surface except that stages I and II occur concurrently indicating the hindrance of stage II by Lewis bonded water.

The reaction to form mesityl oxide is similar to that shown in 4.3.4.a except that the hydrogen ion from the carbanion combines with a bridged hydroxyl.





### C. Adsorption of acetone onto a reduced surface

The surface reactions of acetone adsorbed onto reduced rutile are similar to those observed on oxidized rutile with the exception that bands due to acetate species occur with the mesityl oxide bands and not after them as observed on the rutile surface. The earlier formation of acetate species results from the increase surface electron density which discourages the formation of the Lewis bonded species and encourages the formation of acetate groups which remove electron density.

The formation of the acetate groups might be by the mechanism involving bridged oxygen ions resulting from the condensation of two terminal hydroxyl groups. Evidence from the adsorption of water (section 3.4.10 b) indicates that these are removed by reduction and the oxygen ion may therefore be from the row B bridged oxygen ions.

## CHAPTER 5

ADSORPTION OF DEUTEROACETIC ACID5.1 INTRODUCTION

Results from the adsorption of acetic acid onto oxides have already been considered in section 4.3.2 (table 4.4) and the bands observed assigned to surface acetate species. In this work acetic acid was adsorbed onto rutile at much lower pressures than used by these other workers.

The experiments carried out and reported below were:-

	<u>Spectra</u>
Adsorption onto an oxidized 673 K D <sub>2</sub> O surface	5.1
Adsorption onto an oxidized BT D <sub>2</sub> O surface	5.2
Adsorption onto a reduced 673 K D <sub>2</sub> O surface	5.3
Desorption from an oxidized 673 K D <sub>2</sub> O surface	5.4

## 5.2 RESULTS

### 5.2.1 ADSORPTION ONTO AN OXIDIZED 673 K SURFACE

Initial adsorption of acetic acid onto the rutile surface (spec. 5.1 a-g) produced OD bands at 2695, 2660, 2610 and 2535  $\text{cm}^{-1}$ . Bands at 1670, 1480 and 1440  $\text{cm}^{-1}$  were also produced together with a broad band at 1580  $\text{cm}^{-1}$  (spec. 5.1 d).

Further adsorption (spec. 5.1 h,j) decreased the 2695  $\text{cm}^{-1}$  band and increased the 2660, 2610 and 2535  $\text{cm}^{-1}$  band. The 1670  $\text{cm}^{-1}$  decreased, the 1480 and 1440  $\text{cm}^{-1}$  bands increased, and bands appeared at 1365 and 1320  $\text{cm}^{-1}$ . The 1480 band was broad indicating that other bands may be present in the 1600 to 1500  $\text{cm}^{-1}$  region.

Evacuation of the above surfaces (spec. 5.1 i,k) reduced bands in the 2660 to 2500  $\text{cm}^{-1}$  region and the 1670  $\text{cm}^{-1}$  band. Other bands were not affected.

Adsorption of acetic acid at higher pressures (spec. 5.1 l,n,o) removed the 2690 and 2660  $\text{cm}^{-1}$  bands, increased absorbance in the 2500 to 2200  $\text{cm}^{-1}$  region with weak bands appearing at 2295 and 2110  $\text{cm}^{-1}$ . A series of bands appeared in the 1800 to 1600  $\text{cm}^{-1}$  region at 1785, 1765, 1730, 1720, 1695 and 1650  $\text{cm}^{-1}$ . No changes were observed in the

1480 and 1440  $\text{cm}^{-1}$  bands which had reached zero transmittance in intensity, and a shoulder at 1340  $\text{cm}^{-1}$  appeared on the 1365  $\text{cm}^{-1}$  band.

Evacuation after the above adsorptions (spec. 5.1 m,p) removed the bands at 2295 and 2110  $\text{cm}^{-1}$  and those in the region 1600-1600  $\text{cm}^{-1}$ . Bands remaining in the OD region after the final evacuation (spec. 5.1 p) were at 2630, 2600 and 2540  $\text{cm}^{-1}$ . Evacuation caused little change in the region below 1500  $\text{cm}^{-1}$ .

#### 5.2.2 ADSORPTION OF ACETIC ACID ONTO A BT SURFACE

Initial adsorption of acetic acid onto the hydroxylated surface (spec. 5.2a) caused a decrease in the 2710 and 2690  $\text{cm}^{-1}$  bands and increases in the 2660, 2610 and 2535  $\text{cm}^{-1}$  bands (spec. 5.2 b,d). Intense bands appeared at 1485 and 1440  $\text{cm}^{-1}$  with a weaker band at 1365  $\text{cm}^{-1}$ . The 1485  $\text{cm}^{-1}$  band was broad indicating that other bands might be adjacent in the 1600-1500  $\text{cm}^{-1}$  region.

Evacuation of these surfaces (spec. 5.2 c,e) increased the 2710 and 2690  $\text{cm}^{-1}$  bands, but not to their original intensity, and decreased the 2660, 2610 and 2535  $\text{cm}^{-1}$  bands. The bands below 2000  $\text{cm}^{-1}$  were relatively unaffected by evacuation.

Further adsorption (spec. 5.2 f,g,i) continued to decrease the 2710 and 2690  $\text{cm}^{-1}$  bands and increase the 2660, 2610 and 2535  $\text{cm}^{-1}$  bands which were decreased on evacuation (spec. 5.2 h,j) to below their intensities on the starting

surface (spec. 5.2 a). Below  $2000\text{ cm}^{-1}$  no increase was observed in the  $1480$  and  $1440\text{ cm}^{-1}$  bands, which have reached zero transmittance, but the former band broadened on increased adsorption and was not affected by evacuation. Bands also appeared at  $1340$  and  $1320\text{ cm}^{-1}$ .

Bands appearing in the  $1750$  to  $1600\text{ cm}^{-1}$  region (spec. 5.2 f,g,i) were removed by evacuation (spec. 5.2 h,j) to leave a shoulder at  $1630\text{ cm}^{-1}$ .

Adsorption of  $\text{D}_2\text{O}$  and subsequent evacuation at beam temperature (spec. 5.2 k) increased intensity in the  $2700$  to  $2500\text{ cm}^{-1}$  region and formed two shoulders at  $2640$  and  $2620\text{ cm}^{-1}$ .

### 5.2.3 ADSORPTION OF ACETIC ACID ONTO A 673 K REDUCED SURFACE

Initial adsorption of acetic acid onto the reduced surface (spec. 5.3 a-f) produced weak OD bands at  $2720$  and  $2690\text{ cm}^{-1}$ . Bands produced below  $2000\text{ cm}^{-1}$  were similar to those on the oxidized surfaces except the weak  $1630\text{ cm}^{-1}$  is observed before the bands in the  $1750$ - $1600\text{ cm}^{-1}$  region appeared and the  $1480$  and  $1440\text{ cm}^{-1}$  bands did not reach zero transmittance. The  $1480\text{ cm}^{-1}$  band was also broad on this surface indicating other bands to be present. Evacuation (spec. 5.3 g) decreased the OD bands while the bands below  $2000\text{ cm}^{-1}$  were unaffected.

Increased adsorption produced bands in the  $1800$ - $1600\text{ cm}^{-1}$  range at  $1785$ ,  $1765$ ,  $1725$ ,  $1695$  and  $1630\text{ cm}^{-1}$  which were different in appearance from those observed in this region for the oxidized surface. All of these bands were removed on

evacuation (spec. 5.3 k) with the exception of a weak  $1725\text{ cm}^{-1}$  band and the  $1630\text{ cm}^{-1}$  band.

#### 5.2.4 DESORPTION OF ACETIC ACID AT ELEVATED TEMPERATURES

A clean rutile surface was dosed with acetone vapour at room temperature and evacuated at beam temperature to produce the surface shown in spec. 5.4 a. This differed from spectra produced by slow dosage (spec. 5.1 o) in that no bands were observed below  $1400\text{ cm}^{-1}$ .

Evacuation at 463 K for  $1\frac{1}{2}$ h (spec. 5.4 b) removed the OD bands and produced bands at  $1630$ ,  $1365$  and  $1325\text{ cm}^{-1}$ . Further evacuation at 523 K removed the  $1630\text{ cm}^{-1}$  band and decreased the broad  $1480$  and  $1440\text{ cm}^{-1}$  bands which were resolved by increasing the attenuation to four bands at  $1540$ ,  $1515$ ,  $1480$  and  $1440\text{ cm}^{-1}$ . The  $1365\text{ cm}^{-1}$  band decreased in intensity with this treatment, the  $1325\text{ cm}^{-1}$  band disappeared while a band appeared at  $1340\text{ cm}^{-1}$ . The bands below  $1400\text{ cm}^{-1}$  were removed by evacuation to 616 K and the  $1515$ ,  $1480$  and  $1440\text{ cm}^{-1}$  bands considerably reduced. The  $1540\text{ cm}^{-1}$  band was visible as a shoulder on the  $1515\text{ cm}^{-1}$  band.

Mass spectrum analysis of the compounds removed from the surface by evacuation shows many bands which are mainly due to acetic acid fragments. However, fragments due to a condensation product were observed at  $m/e$  132, 114 and 98 and are considered later.

## 5.3 DISCUSSION AND CONCLUSIONS

### 5.3.1 PROPERTIES OF ACETIC ACID

The properties of acetic acid relevant to the present studies are considered below.

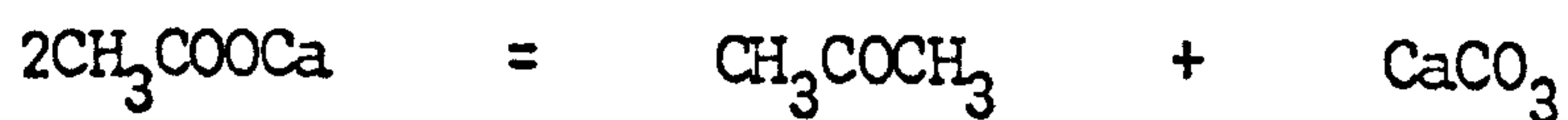
#### A. Decarboxylation

Acetic acid may be decarboxylated by heating the salt with soda lime



#### B. Formation of ketones

Acetone may be produced by the heating of calcium acetate



#### C. Oxidation

Acetic acid is strongly resistant to oxidation but prolonged heating with an oxidising agent produces carbon dioxide and water.

### 5.3.2 ADSORPTION OF CARBOXYLIC ACIDS ONTO OXIDES

Infrared bands observed on the adsorption of acetic onto oxide surfaces are shown in table 5.1. The bands observed by Primet<sup>47</sup> and Kiselev<sup>85</sup> were very intense and were resolved by heating. In their study of acetic acid adsorbed on alumina in carbon tetrachloride Hayashi et al<sup>118</sup> observed two groups of two bands which were assigned to acetate species on two different sites.

Low et al<sup>117</sup> studied the adsorption of a series of  $C_nH_{2n}O$  molecules on a magnesium oxide surface. They do not detail fully the bands observed on the adsorption of acetic acid and evacuation at 298 K but the spectra presented permit the approximate band positions to be determined. The  $1530\text{ cm}^{-1}$  band is a slight shoulder on the  $1550\text{ cm}^{-1}$  band and since the spectrum is similar to that of acetic acid on alumina<sup>118</sup> the 1560, 1530, 1440, 1410 bands have been interpreted here as two types of surface acetate species.

Heating the above surface in the closed cell at 873 K for 10 minutes completely changed the spectrum to give bands at 1640, 1460, 1360 and  $1300\text{ cm}^{-1}$  which were assigned to bidentate (1640 and  $1300\text{ cm}^{-1}$ ) and unidentate (1460 and  $1360\text{ cm}^{-1}$ ) carbonate species.

Munuera<sup>119</sup> studied the mechanism of formic acid dehydration on titanium dioxide using temperature programmed desorption and infrared spectroscopy. He concluded that two



types of mechanism were involved, one between 423 K and 523 K involving a protonated formic acid molecule and the other, between 623 K and 723 K, involved a formate ion. The results might however have been affected by surface silica impurities, indicated by the strong stable  $3725\text{ cm}^{-1}$  band.

### 5.3.3 ASSIGNMENT OF OBSERVED BANDS

#### A. Bands in the $4000\text{--}2000\text{ cm}^{-1}$ region

Adsorption of acetic acid onto a dry surface produces all the bands observed on the adsorption of  $\text{D}_2\text{O}$  onto a 673 K oxidised surface. The relative intensity of the basic hydroxyl bands ( $2710, 2690\text{ cm}^{-1}$ ) to the other bands ( $2660, 2610, 2535\text{ cm}^{-1}$ ) is, however, much less than observed on the adsorption of water. This might be due to reactions involving acetic acid and the basic hydroxyl groups or a blockage of the basic hydroxyl sites by Lewis bonded acetic acid.

Adsorption of acetic acid onto a BT  $\text{D}_2\text{O}$  surface also produces water molecules as shown by increases in the 2610 and broad underlying  $2500\text{ cm}^{-1}$  band. This increase in intensity is removed on evacuation indicating the water molecules to be only weakly adsorbed. The basic hydroxyl groups are removed on the adsorption of acetic acid (spec. 3.3 a,c,e,h,j recorded enlarged), the decrease mainly occurring in the later stages of adsorption indicating that the reaction occurs only at high surface coverage of acetic acid. Similarly the removal of the basic hydroxyl groups formed on the 673 K surface occurs only at higher coverages.

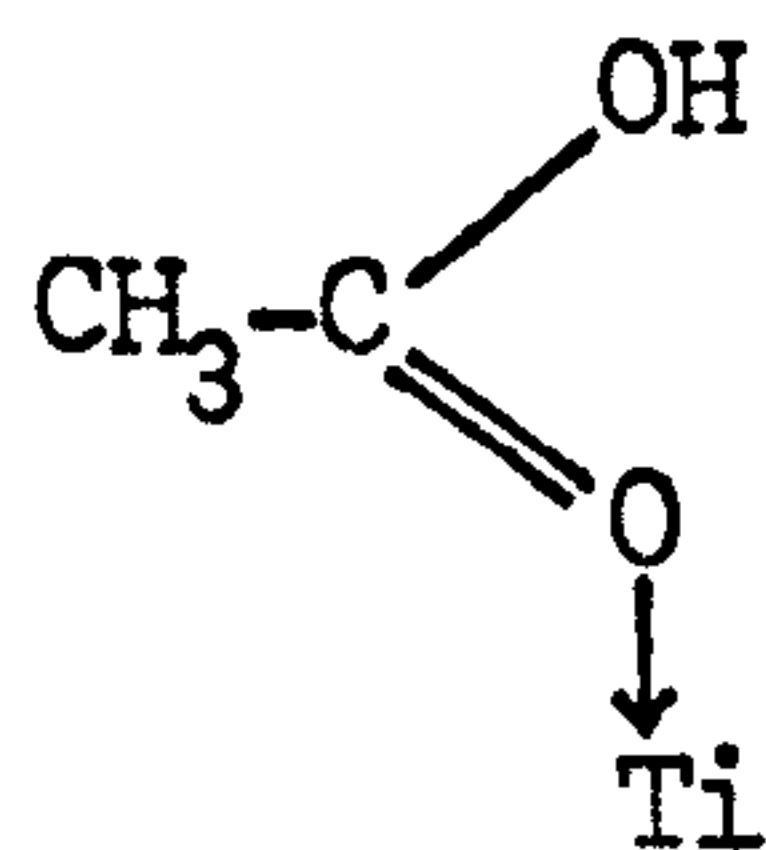
Acetic acid adsorbed onto the reduced surface only produces weak hydroxyl bands which disappear on further dosage.

No bands are observed due to C-D vibrations which indicates either that the species causing the intense 1480 and 1440  $\text{cm}^{-1}$  bands contain no C-D bands or the absorbance of these vibrations is much less than that of the C=O bands which cause the 1480 and 1440  $\text{cm}^{-1}$  bands.

The reasons for the formation of water on the adsorption of acetic acid are considered below.

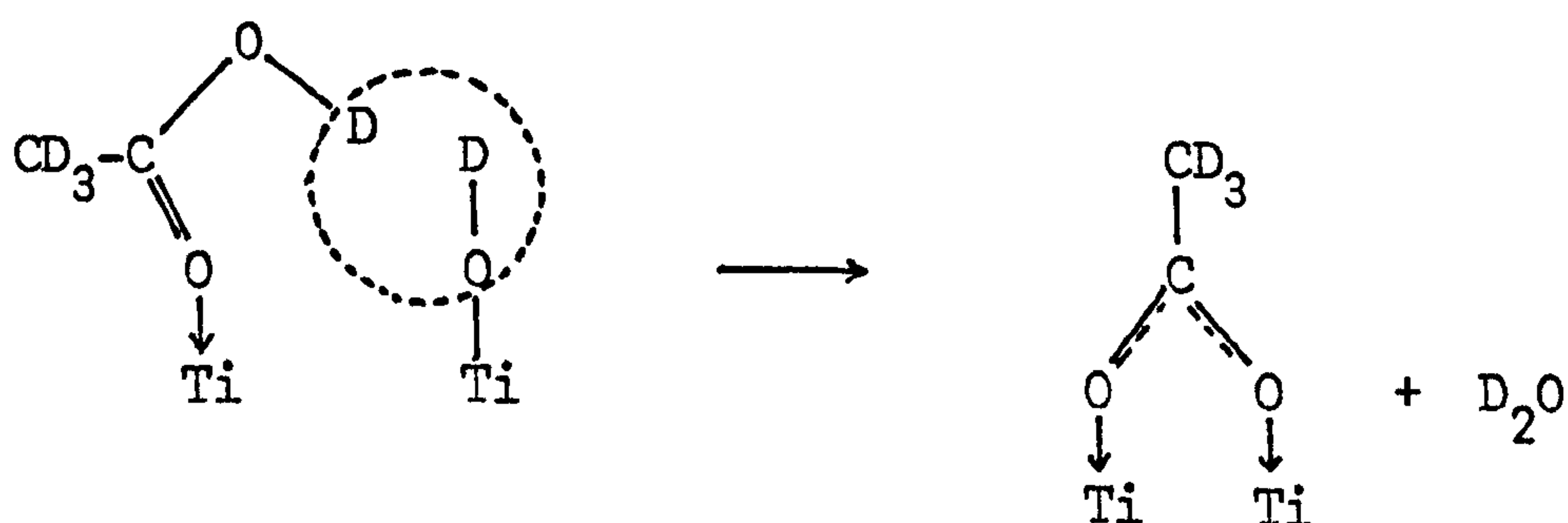
#### B. Bands in the 2000-1000 $\text{cm}^{-1}$ region

Initial adsorption onto the 673 K surface produces a 1670  $\text{cm}^{-1}$  band which is a similar wavelength to those acetone bands assigned to Lewis bonded C=O groups. The band therefore results from acetic acid molecules Lewis bonding to the surface:-



This band does not appear on the BT  $\text{D}_2\text{O}$  surface in contrast to the results from the adsorption of acetone which show the Lewis bonded species to be formed before the molecules react. On the adsorption of acetic acid onto the hydroxylated

surface either the water and hydroxyl molecules prevent the formation of the Lewis complex or react immediately with it. The latter explanation is probable since water or hydroxyl molecules did not prevent the formation of the acetone Lewis complexes. The reaction of the acetic acid complex is as follows:-



This reaction accounts for the removal of the basic OD groups, the formation of water and the appearance of the 1480 and 1440  $\text{cm}^{-1}$  bands which are considered below. The removal of the 1670  $\text{cm}^{-1}$  band on the 673 K surface at higher acetic acid pressures (spec. 5.1 g-j) results from this reaction which also keeps the basic hydroxyl bands (2710, 2695  $\text{cm}^{-1}$ ) at a lower intensity, in comparison with the 2353  $\text{cm}^{-1}$  acidic hydroxyl band, than is observed on the normal adsorption of water.

The intense 1480 and 1440  $\text{cm}^{-1}$  bands are resolved by heating to 1540, 1515, 1480 and 1440  $\text{cm}^{-1}$ . These bands are assigned to acetate species, produced by the above reaction, adsorbed onto the two types of Lewis sites. The 1540 and 1480  $\text{cm}^{-1}$  bands result from acetate species adsorbed onto the weaker sites and the 1515 and 1440  $\text{cm}^{-1}$  from acetate species on

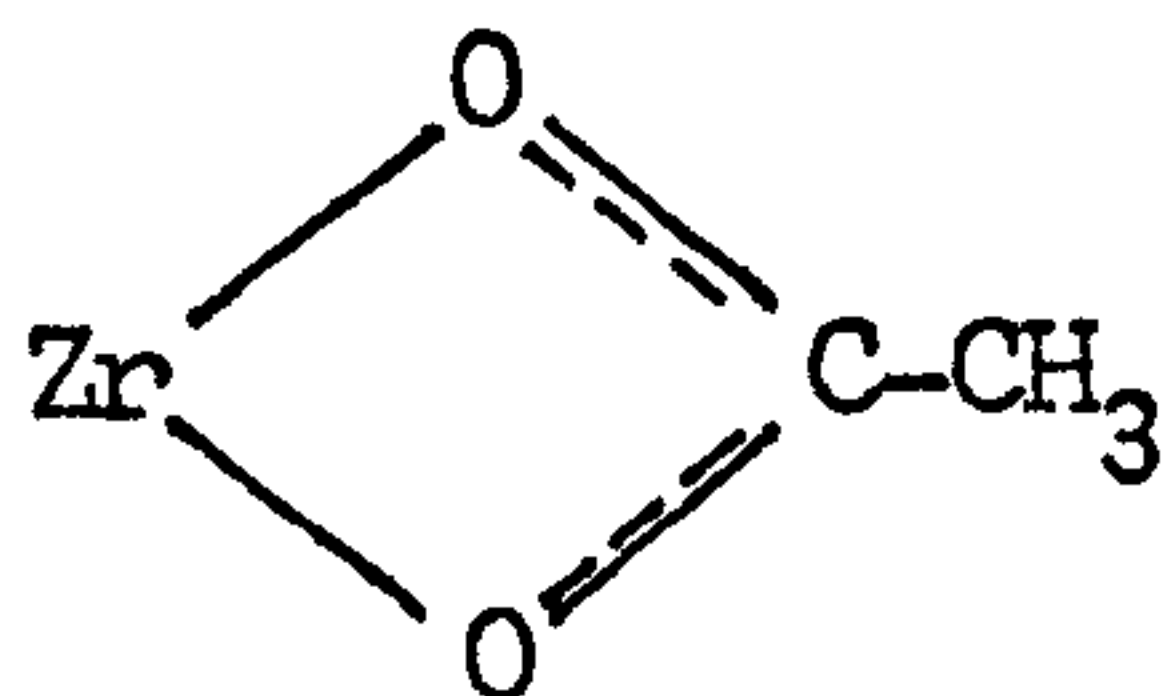
the stronger sites, the lower wavenumber band being due to the symmetric O=C=O stretch.

These bands assigned to acetate species resulting from the adsorption of acetone onto oxidized rutile occur, at 1540, 1440  $\text{cm}^{-1}$  (hydrogenated) and 1510, 1425  $\text{cm}^{-1}$  (deuterated). Comparison of these with the bands formed on acetic acid adsorption indicate that the acetate molecules are formed on the stronger sites. It is on these sites that the mesityl oxide is adsorbed which is oxidized to surface acetate species.

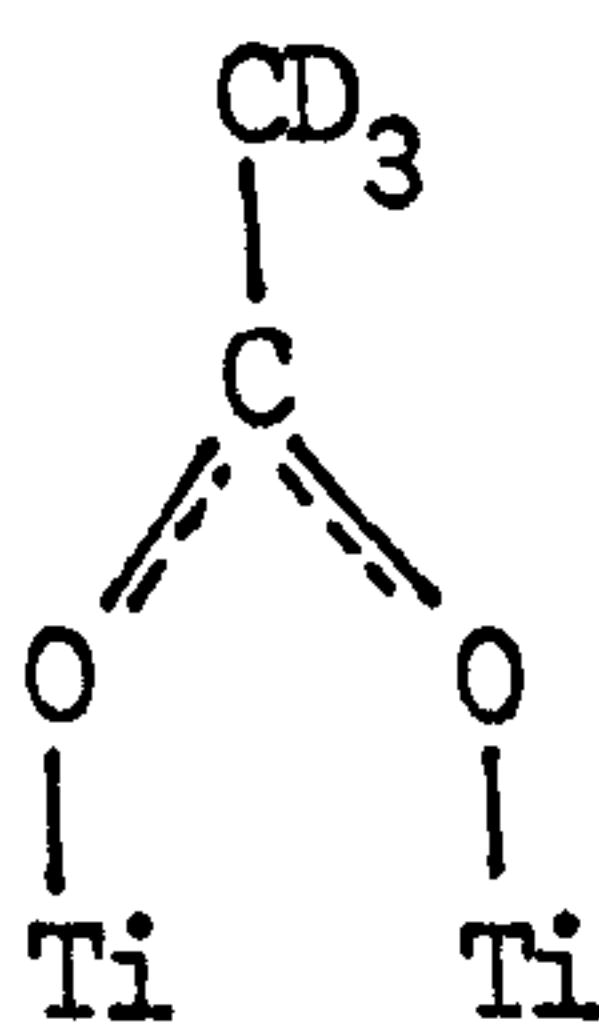
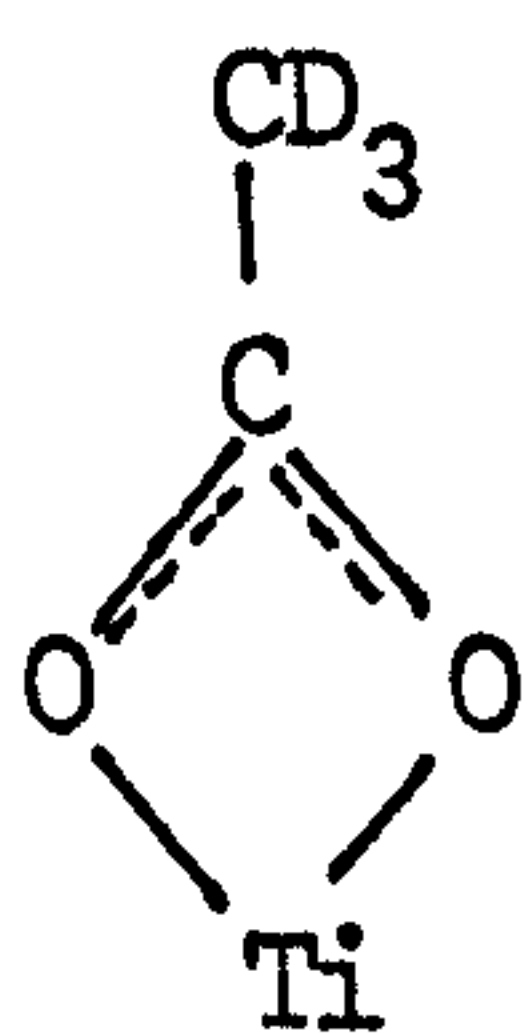
Acetone adsorbed onto the reduced surface produces bands similar to those formed on the adsorption of acetic acid onto both oxidized and reduced surfaces. Acetate species are therefore considered to be adsorbed on both strong and weak sites on the reduced surface whereas on the oxidized surface only the stronger sites are occupied by acetate ions. This difference may result in part from fewer weaker sites being occupied by the Lewis bonded complex, since the higher electron density at the surface will make this type of bonding unfavourable. It is also possible that the reduction process increases the number of weaker sites by increasing the surface concentration of  $\text{Ti}^{3\oplus}$  ions which reduce the surface bonding energy<sup>111</sup>.

The average separation of the acetate bands is 140  $\text{cm}^{-1}$  114,115,116 whereas the separation observed in this work is 60 and 75  $\text{cm}^{-1}$  for acetate species on the weak and strong sites respectively. Separations as low as 100  $\text{cm}^{-1}$  are

observed for  $\text{Zn}(\text{ac})_2 \cdot 2\text{H}_2\text{O}$ , and  $\text{Cd}(\text{ac})_2$ , the former having a bidentate structure<sup>113</sup>.



Grigor'ev<sup>115</sup> proposes that the separation of the two bands decreases with the O-C-O angle which may indicate that the O-C-O angle of the surface acetate species is near  $110^\circ$  the angle in  $\text{Zn}(\text{ac})_2 \cdot 2\text{H}_2\text{O}$ . The low separation does indicate that the C-O bands are similar to those in the acetate ion and that both oxygen ions are therefore involved in bonding either in a bidentate or bridged structure.



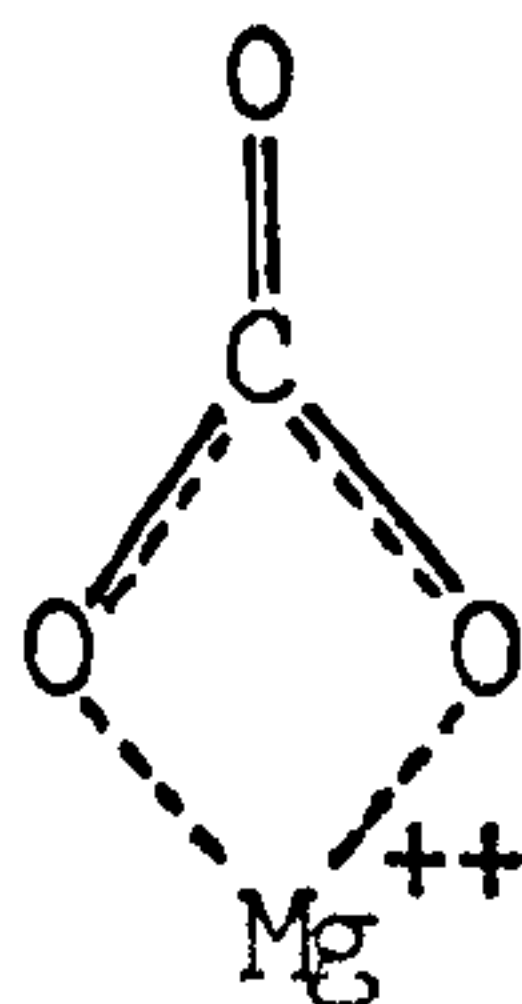
Edwards and Hayward<sup>116</sup> however, consider that the band separation is not a reliable indication of the mode of coordination of the acetate groups to the metal.

No bands due to C-D vibrations are observed in the spectra even at relatively high surface concentrations of acetate ions due to the low intensity of these vibrations in

comparison with the C=O vibrations. The absence of any C-D vibrations is not taken as evidence that the 1480 and 1440  $\text{cm}^{-1}$  bands are due to a carbonate type species since temperatures in excess of beam temperature are required to form these. Bands assigned to carbonate species have been observed<sup>117</sup> after exposing magnesium oxide to acetic acid at 298 K, degassing, and heating at 773 K for 10 minutes in a closed cell. These bands were observed at 1640, 1460, 1360 and 1300  $\text{cm}^{-1}$  and did not resemble those produced after evacuation of the acetic acid at 298 K which were similar to those observed in this work.

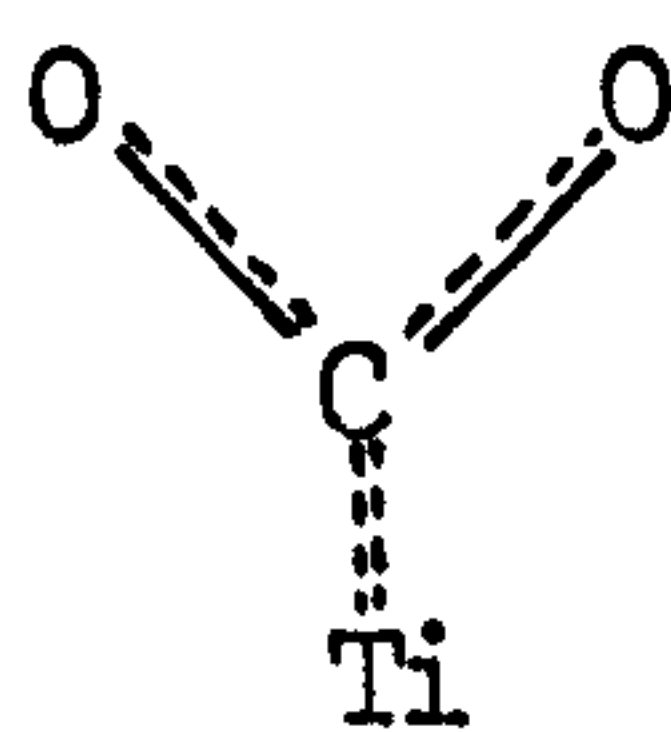
Bands were observed at 1785, 1765, 1730, 1695, 1650  $\text{cm}^{-1}$  (spec. 5.1 o) after adsorption of acetic acid onto oxidized rutile at high vapour pressures and were removed by evacuation. The 1785, 1765 and 1730  $\text{cm}^{-1}$  are bands due to acetic acid vapour while the other bands result from acetic acid physically adsorbed on the rutile surface. These bands are not observed on the adsorption of acetic acid onto the reduced surface at high vapour pressures indicating that molecules are not physically adsorbed in high concentrations on this type of surface. These results are similar to those observed when the reduced surface was exposed to water vapour at high pressure, a much lower surface concentration of physically adsorbed molecules was observed in comparison with the oxidized surface.

The  $1630\text{ cm}^{-1}$  band appears on the BT oxidized surface after exposure to high vapour pressures of acetic acid (spec. 5.2k,j) and on the reduced surface at lower vapour pressures (spec. 5.3d). This band has been assigned<sup>117,120</sup> to the C=O stretch in the bidentate carbonate species:-



The corresponding asymmetric stretch is the  $1340\text{ cm}^{-1}$  band which appears as a shoulder on the  $1365\text{ cm}^{-1}$  band.

The  $1365\text{ cm}^{-1}$  band, which is present before the appearance of the  $1630\text{ cm}^{-1}$  band (spec. 5.2 i) is probably due to the symmetric stretch of a unidentate carbonate species,

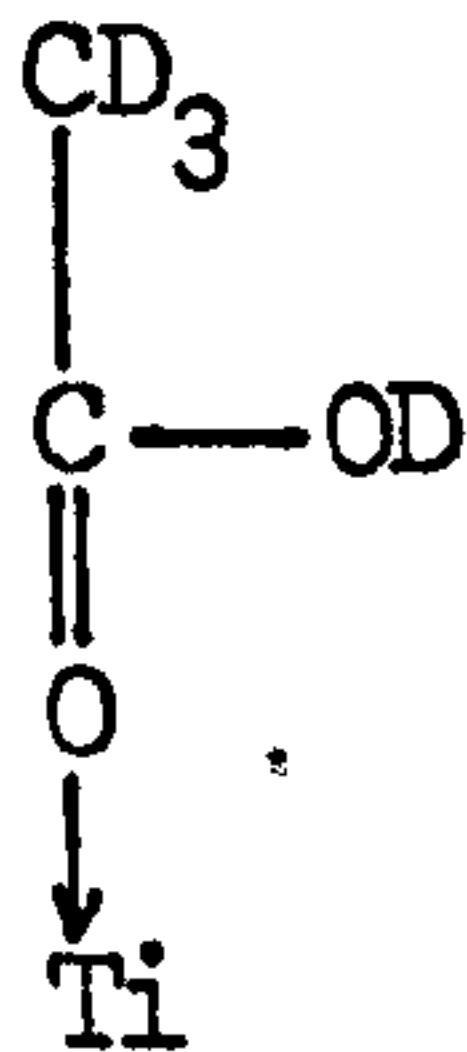


the antisymmetric stretch coinciding with the more intense  $1480\text{ cm}^{-1}$  acetate band.

Assignment of bands observed below  $2000\text{ cm}^{-1}$  is shown in table 5.2.

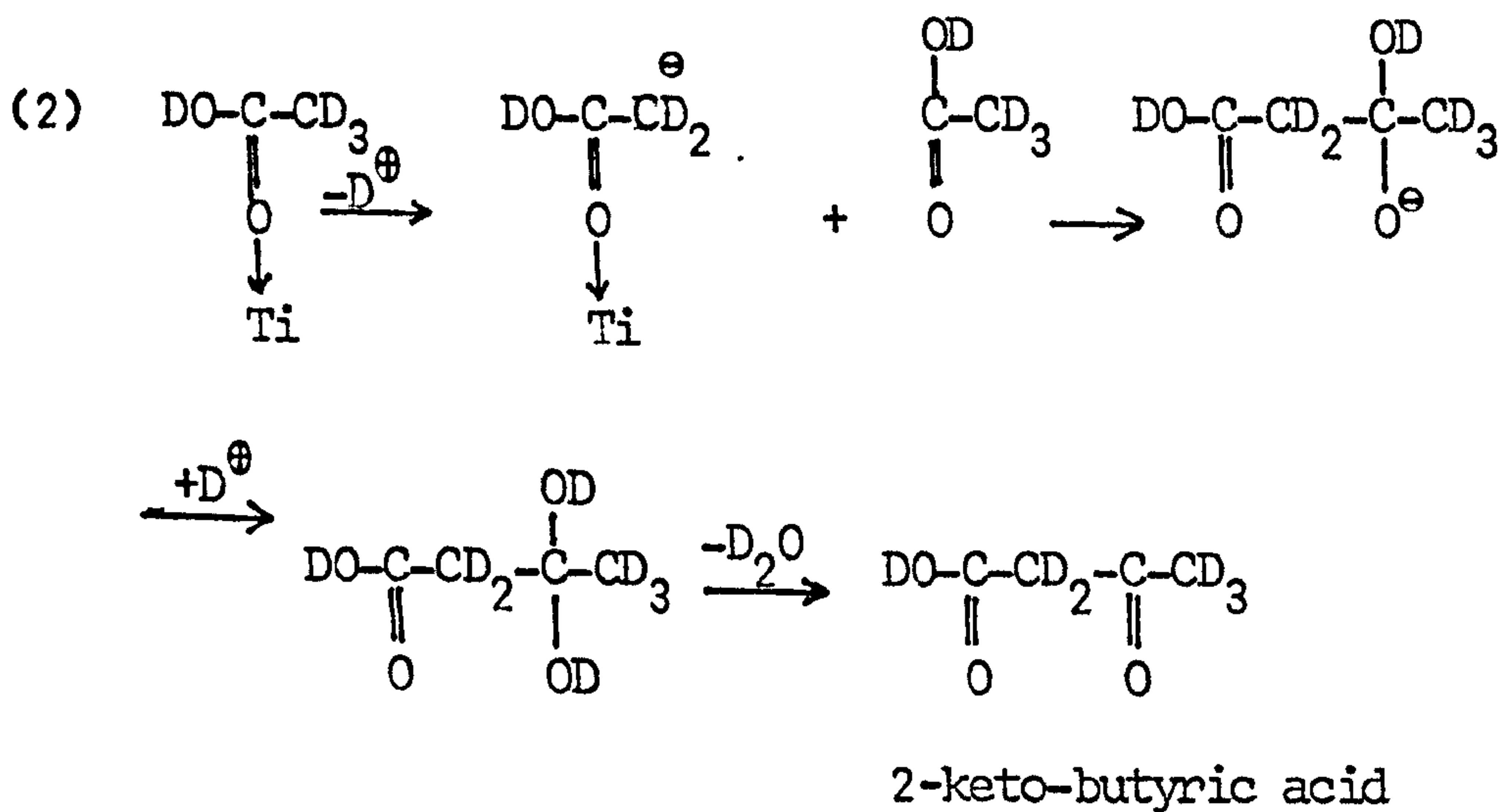
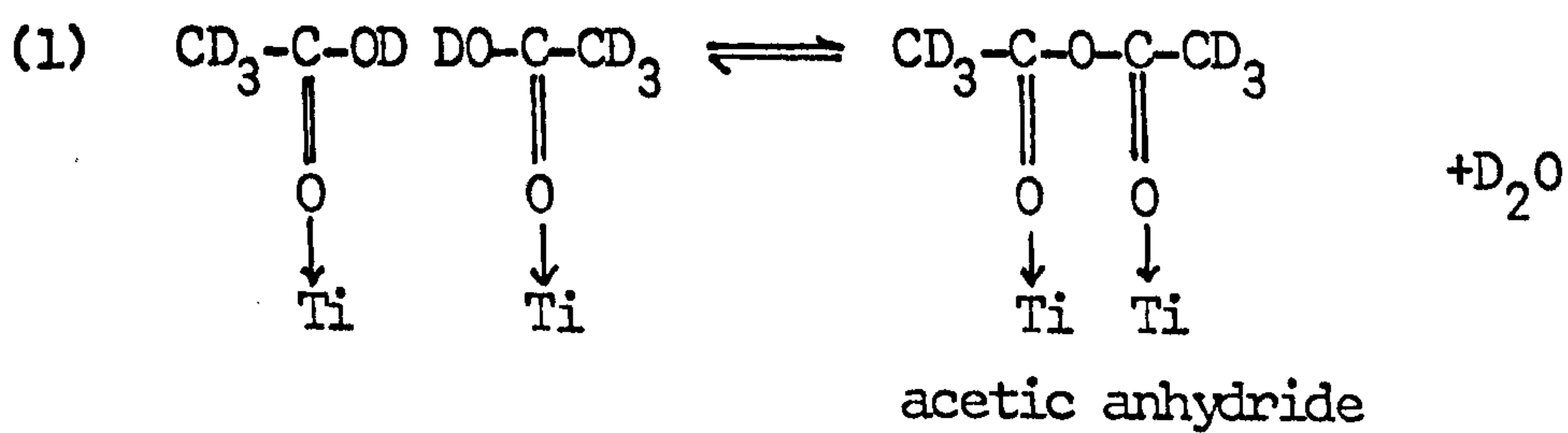
### 5.3.4 SURFACE REACTIONS

Initial adsorption of acetic acid  $d_4$  onto rutile produces the Lewis acid complex on the 673 K oxidized surface only.



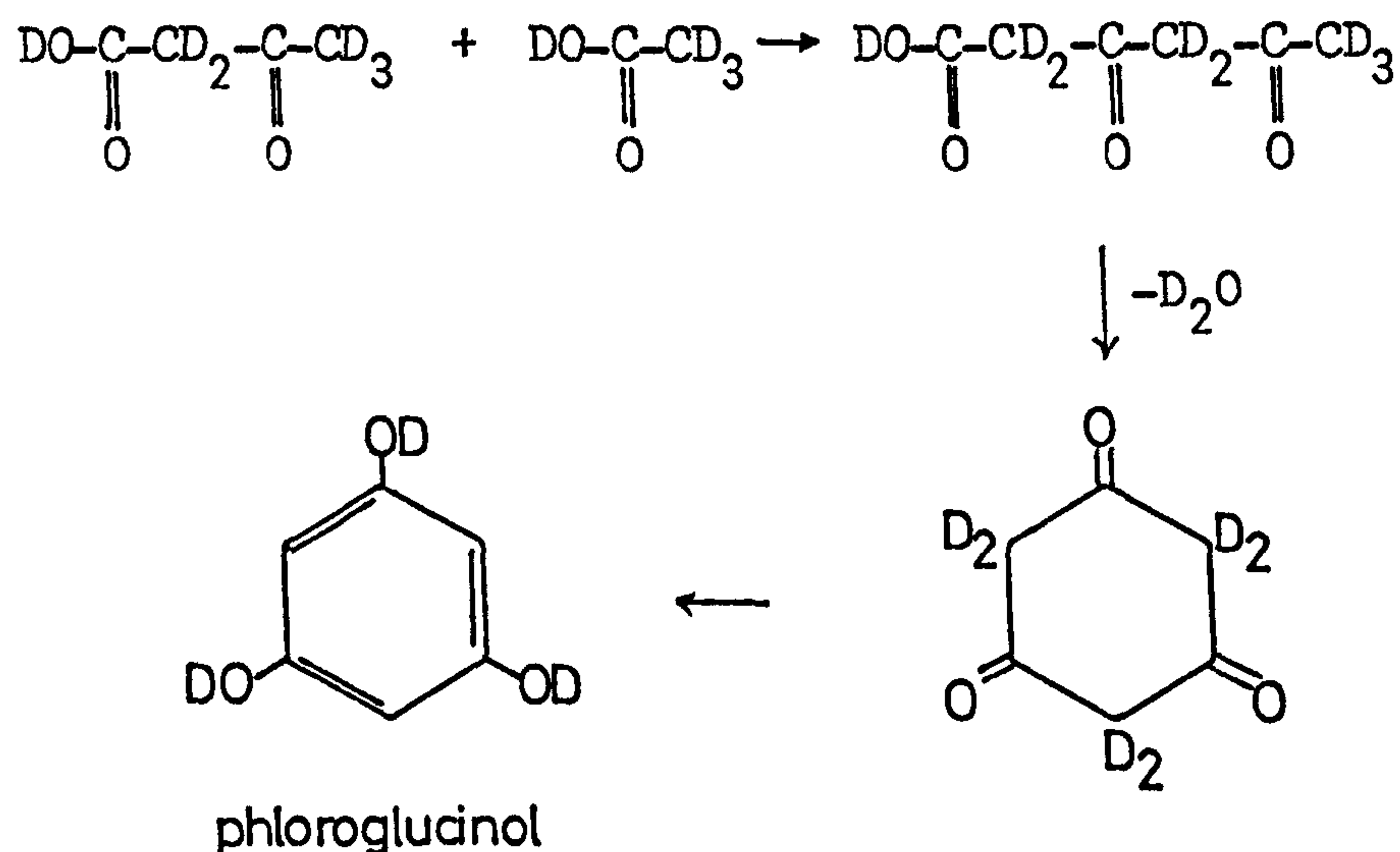
The reason for the absence of this complex on the other surfaces has been considered.

Water molecules and acetate species are formed on all surfaces during the initial stages of adsorption. The formation of water may occur via two mechanisms.





The reaction of this product with another acetic acid molecule may produce deuterated phloroglucanol

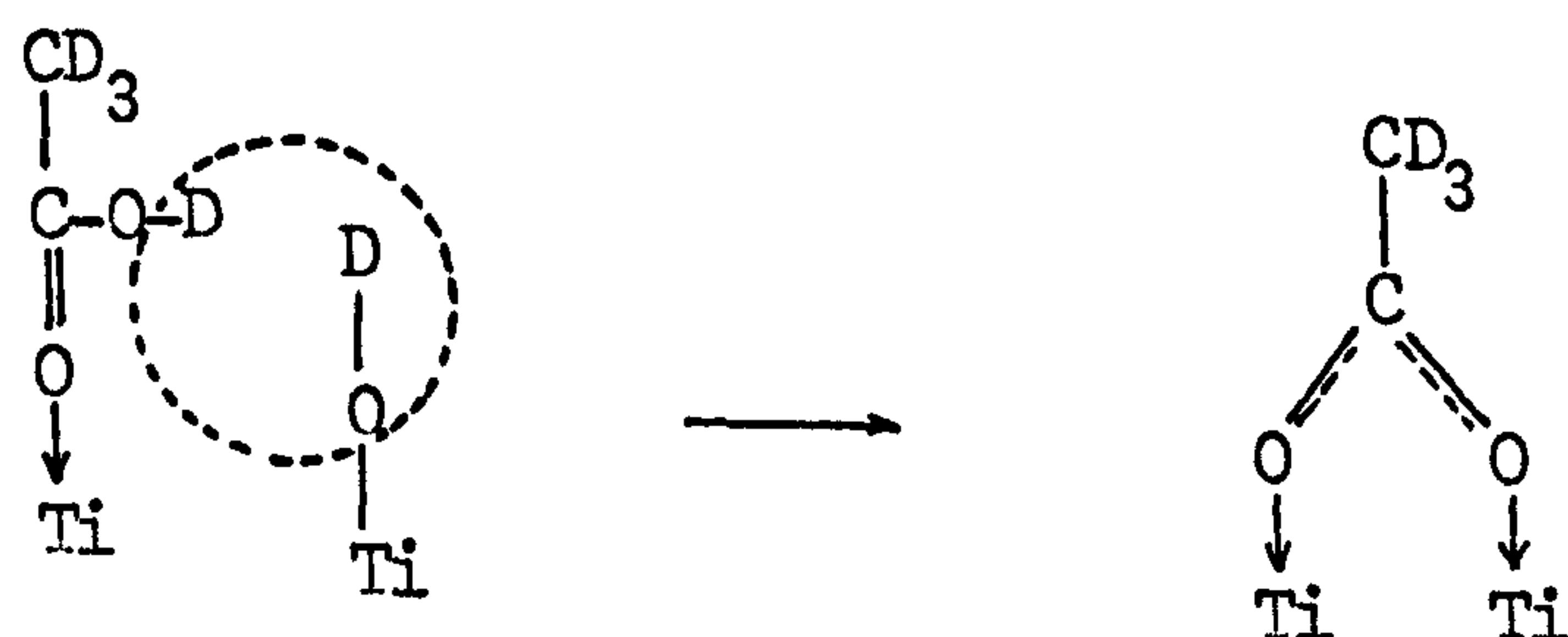


Reaction (1) which forms acetic anhydride is the simpler mechanism and is a reaction observed when acetic acid is passed over a suitable catalyst at 870 K. The spectra of anhydrides contain two bands due to C=O stretching in the region 1850-1740 cm<sup>-1</sup> and the absence of any bands above 1630 cm<sup>-1</sup> indicates that no anhydride is present on the surface.

Mechanism (2) is more complex and is similar to the mechanism proposed for the formation of mesityl oxide (4.3.4) from acetone both reactions involving a carbanion attacking the carbon atom attached to the oxygen atom. The mechanism is supported by the observation of mass peaks at 132, 114 and 98 in the mass spectrum of the vapour after contact with the heated rutile surface. The absence of phloroglucinol bands

from any spectra may be explained by the absence of any groups capable of strong bonding with the surface. Alcohol and unsaturated groups bond with the surface at the saturated vapour pressure of the adsorbate<sup>56,87</sup> but it is possible no adsorption will take place at the much lower pressures at which the phloroglucinol is formed.

The presence of water molecules on the rutile surface results in the formation of acetate species from the reaction of acetic acid molecules with the basic hydroxyl groups as previously considered.



## CHAPTER 6

ADSORPTION OF HEXAFLUOROACETONE  
ONTO OXIDIZED AND REDUCED RUTILE6.1 INTRODUCTION6.1.1 AIM

The existence of the two types of Lewis sites on the rutile surface has been shown in this and other studies (section 3.3.3 c), although the nature and strength of these sites has not clearly been established. Lapport<sup>132</sup> suggested that the shift in carbonyl stretching ( $\Delta\nu_{\text{CO}}/\text{cm}^{-1}$ ) of a carbonyl group forming a Lewis acid complex with a metal halide could be used as a measure of the Lewis acidity of the halide. Cook<sup>133</sup> extended this work and specified five criteria (reproduced in ref. 134) for the ligand to fulfill in order that Lewis acidity may be estimated.

Hair and Chapman<sup>134</sup> applied these criteria to the study of Lewis acid sites on alumina-containing surfaces using hexachloroacetone in place of the usual carbonyl compounds such as acetone or benzaldehyde, which are oxidized by alumina. Spectra were recorded for  $\gamma$ -alumina and two types of silica-alumina cracking catalysts by suspending the solid in a fluorolube oil after exposure to hexachloroacetone vapour at temperatures up to 770 K. The results showed that there was a wide distribution range of sites of varying Lewis acidity, the strength of sites on the alumina and alumina-silica surfaces being of a similar strength.

Hexafluoroacetone was used as the Lewis base in this work as the high boiling point of hexachloroacetone (477 K) made it unsuitable for manipulation under vacuum.

### 6.1.2 EXPERIMENTS

The following series of experiments was carried out to determine the interaction of hexafluoroacetone with the rutile surface

	<u>Spectra</u>
Adsorption of hexafluoroacetone onto a	
673 K D <sub>2</sub> O oxidized surface	6.1
BT D <sub>2</sub> O oxidized surface	6.2
673 K D <sub>2</sub> O reduced surface	6.3
BT D <sub>2</sub> O reduced surface	6.4

Owing to the nature of the adsorption, treatment of the rutile disc was more extensive than in the work involving water, acetone and acetic acid adsorption. Each experiment consisted of several stages generally in the following order:-

- a) Adsorption of hexafluoroacetone
- b) Desorption at elevated temperatures
- c) Adsorption of D<sub>2</sub>O
- d) Desorption of D<sub>2</sub>O at elevated temperatures

Full details of the treatments are given in the legend preceding each series of spectra.

## 6.2 RESULTS

### 6.2.1 ADSORPTION OF HEXAFLUOROACETONE ONTO A 673 K D<sub>2</sub>O SURFACE

Initial adsorption of vapour onto the disc (spec. 6.1b,c,d) produced bands at 1810, 1640, 1615, 1580, 1480, 1440, 1330 cm<sup>-1</sup> with a broad series of bands centred at 1200 cm<sup>-1</sup>.

Evacuation at 423 K (spec. 6.1 e) removed the bands at 1810 and 1330 cm<sup>-1</sup> due to hexafluoroacetone vapour (spec. 6.5) and increased the 1615 and 1580 cm<sup>-1</sup> bands while a weak 1670 cm<sup>-1</sup> band became apparent. Further evacuation at higher temperatures (spec. 6.1 f-h) removed all the bands except for a weak band at 1365 cm<sup>-1</sup> and a shoulder at 1235 cm<sup>-1</sup>. The 1580 and 1480 cm<sup>-1</sup> band increased on heating at temperatures up to 473 K (spec. 6.1 f) and decreased on heating at higher temperatures.

Exposure of the disc to D<sub>2</sub>O vapour (BT, 2½h) and evacuation (BT, ½h) produced a broad 2740 to 2400 cm<sup>-1</sup> band with peaks at 2700 and 2520 cm<sup>-1</sup> (spec. 6.1 i). A weak band also appeared at 1595 cm<sup>-1</sup>. Evacuation of this surface (spec. 6.1 j) increased and shifted the 1595 cm<sup>-1</sup> band to 1580 cm<sup>-1</sup> and produced bands at 1480 and 1200 cm<sup>-1</sup>.

Further exposure of the disc to D<sub>2</sub>O vapour at 473 K (spec. 6.1 k) produced bands in the OD region at 2760, 2720 cm<sup>-1</sup> with a broad band 2700-2400 cm<sup>-1</sup>. The 1580 cm<sup>-1</sup> band was shifted to 1600 cm<sup>-1</sup> and a broad band appeared in the range 1500-1200 cm<sup>-1</sup>, the 1480 cm<sup>-1</sup> band was observed as a shoulder on this band.

### 6.2.2 ADSORPTION OF HEXAFLUOROACETONE ONTO A BT, D<sub>2</sub>O OXIDIZED SURFACE

Initial adsorption onto the starting surface (spec. 6.2a) produced no bands in the 1800-1400  $\text{cm}^{-1}$  region (spec. 6.2 b), in contrast to adsorption onto the 673 K surface, but increased bands in the 2680 to 2560  $\text{cm}^{-1}$  region. Evacuation (spec. 6.2 c) only decreased all bands in the 2680 to 2450  $\text{cm}^{-1}$  region and did not restore the original spectrum (spec. 6.2 a).

Further adsorption (spec. 6.2 d-e) decreased the band at 2695  $\text{cm}^{-1}$  due to hydrogen-bonded hydroxyl groups while a 2680  $\text{cm}^{-1}$  band increased in intensity. Bands also appeared at 2640, 2460, 1810 and 1600  $\text{cm}^{-1}$ , while the 2535  $\text{cm}^{-1}$  band decreased slightly.

On evacuation at beam temperature a spectrum similar to 6.2c was recorded. Evacuation at 373 K (12h) (spec. 6.2 f) produced a spectrum in the 2700-2400  $\text{cm}^{-1}$  region similar to a standard BT D<sub>2</sub>O surface evacuated at this temperature. The 1600  $\text{cm}^{-1}$  band increased, shifting to 1580  $\text{cm}^{-1}$ , and a band appeared at 1480  $\text{cm}^{-1}$ .

Spectra 6.2 g-o show spectra recorded after exposing the disc to increasing pressures of vapour and then evacuating at a series of elevated temperatures (details in legend to spec. 6.2). Adsorption of the vapour increased bands which formed at 2680, 2610, 2460  $\text{cm}^{-1}$ , decreased the 2695 and 2535  $\text{cm}^{-1}$  bands and increased the 1580 and 1480  $\text{cm}^{-1}$  bands. Evacuation of vapour at

elevated temperatures restored the 2700-2400  $\text{cm}^{-1}$  region to the spectra of normal  $\text{D}_2\text{O}$  surfaces after treatment at these temperatures, increased the 1580 and 1480  $\text{cm}^{-1}$  bands and produced a shoulder at 1615  $\text{cm}^{-1}$ .

Evacuation at 543 K without readsorption of vapour (spec. 6.2 p-v) removed all the bands, except a broad band at 2530  $\text{cm}^{-1}$ .

Exposure of the disc to  $\text{D}_2\text{O}$  vapour (BT,  $\frac{3}{4}$ h) and evacuation (BT,  $1\frac{1}{2}$ h) (spec. 6.2 w) produced a spectrum similar to spec. 6.1 i, which was similarly formed by adsorption of  $\text{D}_2\text{O}$  onto a surface previously exposed to hexafluoroacetone and evacuated at 543 K. Subsequent evacuation (spec. 6.2 x) did not form bands at 1580 and 1480  $\text{cm}^{-1}$  as occurred in the previous experiment. These bands were only formed after readsorption of hexafluoroacetone vapour (spec. 6.2 y) and evacuation at 453 K. Evacuation of the  $\text{D}_2\text{O}$  (spec. 6.2 x) reduced the broad OD bands to weak bands at 2695, 2680 and 2535  $\text{cm}^{-1}$ . Subsequent exposure to hexafluoroacetone vapour removed the 2695  $\text{cm}^{-1}$  band (spec. 6.2 y).

Re-exposure of the disc to  $\text{D}_2\text{O}$  vapour (spec. 6.2 a ) produced an OD spectrum similar to spec. 6.2w and shifted the 1580  $\text{cm}^{-1}$  band to 1600  $\text{cm}^{-1}$ . On evacuation of this surface (453 K, 2h) a band appeared at 2740  $\text{cm}^{-1}$  and the broad 2700 to 2400  $\text{cm}^{-1}$  band was reduced in intensity.

### 6.2.3 ADSORPTION OF HEXAFLUOROACETONE ONTO A 673 K D<sub>2</sub>O REDUCED SURFACE

---

Exposure of the initial surface (spec. 6.3a) to increasing pressures of vapour (spec. 6.3 b-f) produced bands at 1810, 1770, 1740, 1710, 1660, 1570, 1480, 1390, 1340 cm<sup>-1</sup>. Evacuation (BT) removed the bands at 1810 and 1340 cm<sup>-1</sup> due to the vapour phase while adsorption of D<sub>2</sub>O and evacuation (BT, 1h) (spec. 6.2 g) removed the 1660 cm<sup>-1</sup> band, considerably decreased the 1740 and 1710 cm<sup>-1</sup> bands and shifted the 1570 cm<sup>-1</sup> band to 1580 cm<sup>-1</sup>.

Further evacuation at 473 K, 18h, (spec. 6.2 h) removed the 1740, 1710 cm<sup>-1</sup> bands, increased and shifted the 1580 cm<sup>-1</sup> band to 1570 cm<sup>-1</sup>, increased the 1480 cm<sup>-1</sup> band and formed a band at 1430 cm<sup>-1</sup>. Evacuation at 573 K, ½h (spec. 6.2i) removed all bands except two at 1460 and 1430 cm<sup>-1</sup>.

Adsorption of hexafluoroacetone (spec. 6.2j) and evacuation (spec. 6.2k) produced additional bands at 1660 and 1580 cm<sup>-1</sup>. Exposure of this surface to D<sub>2</sub>O at 473 K, 16h and evacuation (BT, ½h) (spec. 6.3 l) formed OD bands at 2750, 2710 cm<sup>-1</sup> and a broad band centred on 2530 cm<sup>-1</sup>, increased the 1580 and 1430 cm<sup>-1</sup> bands and produced bands at 1520 and 1480 cm<sup>-1</sup>.



#### 6.2.4 ADSORPTION OF HEXAFLUOROACETONE ONTO A BT, D<sub>2</sub>O REDUCED SURFACE

Exposure of the initial surface (spec. 6.4 a) to increasing vapour pressures (spec. 6.4 b-e) removed the 2710 cm<sup>-1</sup> band and increased the 2695 cm<sup>-1</sup> band (spec. 6.4 b) before decreasing this band and increasing a 2680 cm<sup>-1</sup> band which appeared (spec. 6.4 c). Bands due to O-D stretching appeared at 2610 and 2460 cm<sup>-1</sup> and bands at 1810, 1770, 1730, 1580, 1520 and 1480 cm<sup>-1</sup> were also formed.

Evacuation at BT (spec. 6.4 f) removed the 1810 and weak 1520 cm<sup>-1</sup> bands while dosage of D<sub>2</sub>O, BT and evacuation (spec. 6.4 g) removed the 1770, 1730 cm<sup>-1</sup> bands and decreased the 1515 cm<sup>-1</sup> band. Evacuation at 588 K removed all the remaining bands and formed two at 1460 and 1430 cm<sup>-1</sup>. These bands increased with a second dose of D<sub>2</sub>O at 473 K (spec. 6.4 i) together with weak bands at 2740, 2710, 2650 and 2520 cm<sup>-1</sup>.

Adsorption of hexafluoroacetone (spec. 6.4 j) increased the intensity of the OD region to a broad band and resulted in the appearance and slow increase of a 1580 cm<sup>-1</sup> band. Heating the disc in the vapour at 473 K increased the 1580 and 1480 cm<sup>-1</sup> bands while the broad OD band decreased to give bands at 2710, 2680, 2600 and 2530 cm<sup>-1</sup>.

### 6.3 DISCUSSION AND CONCLUSIONS

#### 6.3.1 PROPERTIES OF HEXAFLUOROACETONE AND DERIVATIVES

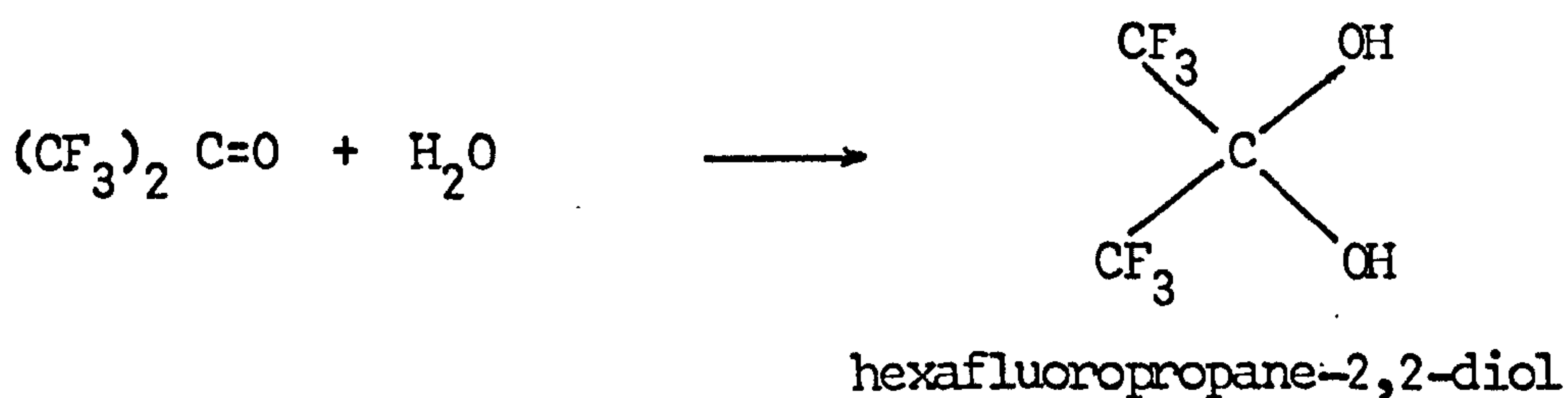
Krespan and Middleton<sup>135</sup> have reviewed the properties of hexafluoroacetone and those relevant to this work are considered below.

##### A. General Properties

Hexafluoroacetone has a boiling point of 246 K and is thermally stable to 573 K. The spectrum of the vapour (spec. 6.5) shows bands at 1810  $\text{cm}^{-1}$  (C=O stretch)<sup>136</sup> and 1340, 1274, 1250, 1220  $\text{cm}^{-1}$  (asymmetric  $\text{CF}_3$  stretches)<sup>136</sup> in the region recorded in this work.

##### B. Reaction with hydroxyl groups

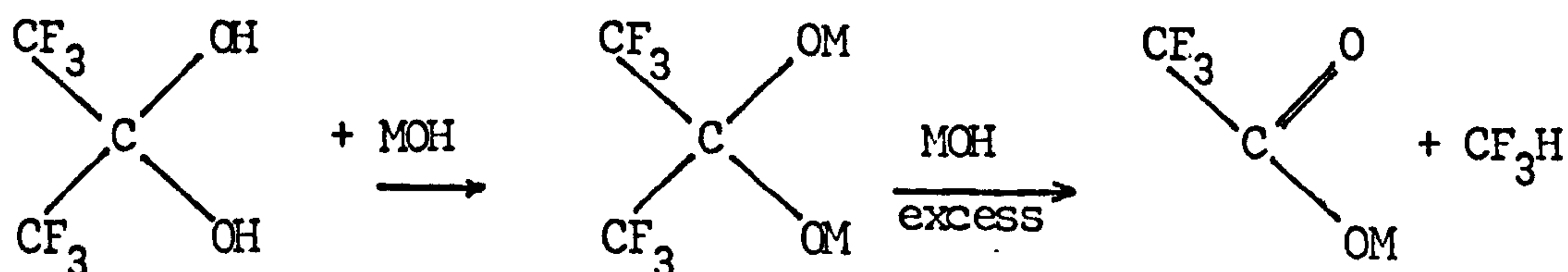
Hexafluoroacetone will react with one equivalent of water to form a fluorinated gem-diol (mpt 322 K).



The gem-diol is very acidic ( $\text{pK}_a$  6.58)<sup>137</sup> and salts may be formed either by reaction with a base or by addition of a base directly to hexafluoroacetone.

### C. Properties of gem-diols

Studies carried out on the alkali metal salts<sup>138, 139</sup> show them to be stable in solution after the addition of one equivalent of base but to decompose on the addition of excess base to the related carboxylate, and in most cases a haloform.



All of the mono alkali metal salts (except lithium) decomposed at 373 K to produce metal trifluoroacetate, metal fluoride, fluoroform, hexafluoroacetone and perfluoropropane-2,2-diol.

### 6.3.2 BEHAVIOUR OF BANDS

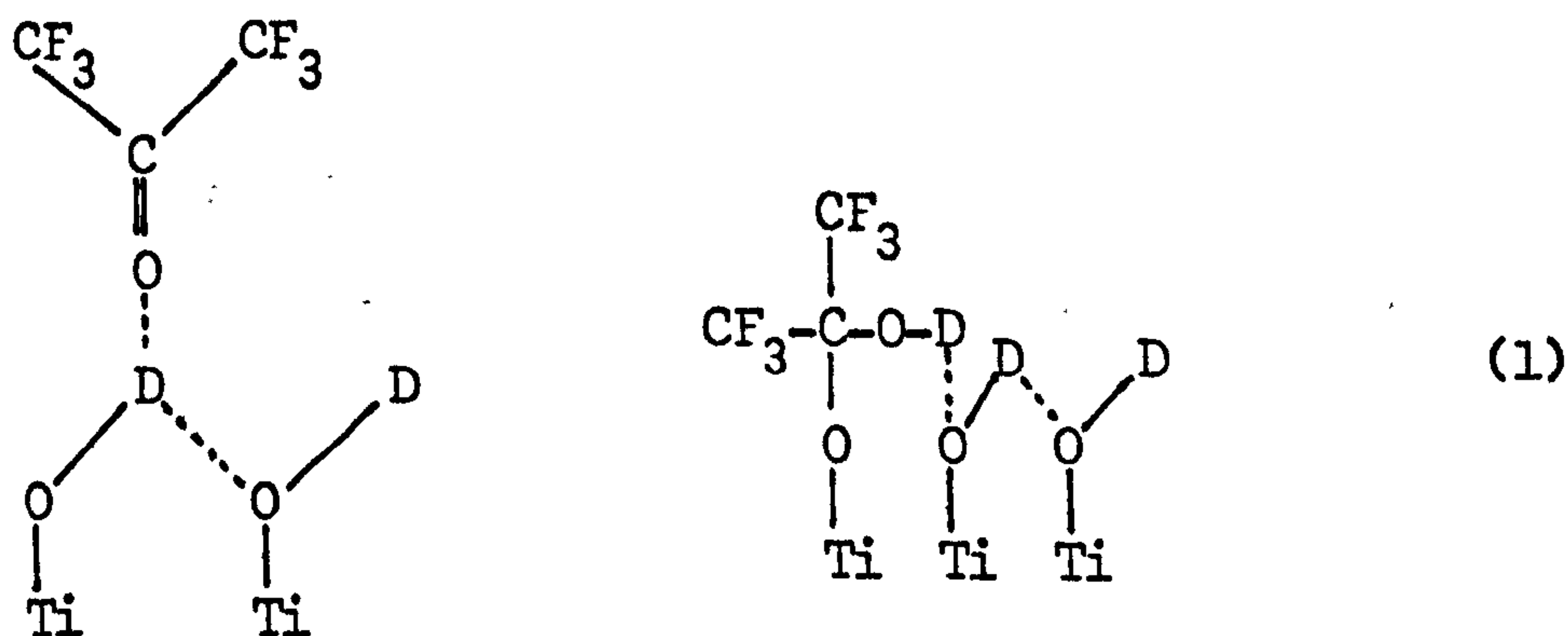
#### A. Bands in the 4000-2000cm<sup>-1</sup> region

Bands not due to surface groups existing on a standard BT, D<sub>2</sub>O surface (spec. 6.2 a) occur at 2680, 2610 and 2460 cm<sup>-1</sup> when hexafluoroacetone is adsorbed onto a surface with OD groups present, and at 2740 cm<sup>-1</sup> when rutile is heated in D<sub>2</sub>O vapour after treatment with hexafluoroacetone.

Initial adsorption of hexafluoroacetone (spec. 6.2) results in a change to the O-D spectrum while bands due to the carbonyl group Lewis bonding to the surface are not observed. These observations are in complete contrast to the adsorption of acetone onto the same surface which only Lewis bonds in the initial stages.

The appearance of the 2680, 2610 and 2460  $\text{cm}^{-1}$  bands coincides with the reduction in a 2695  $\text{cm}^{-1}$  band. Removal of the adsorbed species does not occur with evacuation at BT but removal after evacuation at 373 K restores the intensity of the 2695  $\text{cm}^{-1}$  band.

The three bands may be assigned by considering the reactions which might occur when hexafluoroacetone is adsorbed. The reaction with the terminal hydroxyl groups is as follows:



Further reaction to form a bidentate salt would result in the loss of two hydroxyl groups as a water molecule, which is not observed.

The salts  $(\text{CF}_3)_2\text{C}(\text{OH})\text{Li}\cdot 1.5\text{H}_2\text{O}$  and  $(\text{CF}_3)_2\text{C}(\text{OH})\text{Na}\cdot \text{H}_2\text{O}$  show two bands in the OH region<sup>138</sup> at approximately 3650 and 3400  $\text{cm}^{-1}$  (deuteroequivalents 2690 and 2500  $\text{cm}^{-1}$ ). The 3650  $\text{cm}^{-1}$  may be assigned to the hydroxyl band while the 3400  $\text{cm}^{-1}$  band is due to the water of crystallization.

Comparison of these results with those observed indicates that the 2610  $\text{cm}^{-1}$  band is due to the hydroxyl group in

the gem-diol salt hydrogen-bonded to a terminal group. This interaction also shifts the  $2695\text{ cm}^{-1}$  band of the terminal hydroxyl group to  $2680\text{ cm}^{-1}$ .

The  $2460\text{ cm}^{-1}$  band together with the increase in the underlying  $2500\text{ cm}^{-1}$  due to water on the (100) and (101) planes is due to a hydrogen-bonding interaction with the hexafluoroacetone. The nature of this interaction is not clear from the spectra observed but may involve the reversible formation of a gem-diol which hydrogen-bonds to other water molecules. Such a molecule would have to be strongly bonded in order to remain on the surface after evacuation at BT and it is possible that some other form of bonding may also be present.

The  $2740\text{ cm}^{-1}$  represents an OD group of higher frequency than has previously been observed on the rutile surface. It is unlikely to be a hydroxyl band directly bonded to surface titanium atoms but results from a reaction of  $\text{D}_2\text{O}$  with surface species formed on the adsorption of hexafluoroacetone and subsequent heat treatments.

#### B. Bands below $2000\text{ cm}^{-1}$ (table 6.1)

A series of weak bands are observed on both hydroxylated and dehydroxylated reduced rutile at  $1770$  and  $1730\text{ cm}^{-1}$  and on dehydroxylated rutile at  $1710$  and  $1660\text{ cm}^{-1}$ . The bands are not removed by evacuation at BT but are removed or significantly reduced by the adsorption of  $\text{D}_2\text{O}$  (spec. 6.3 g, 6.4 g) and are in the wavenumber range occupied by C=O stretching vibrations. It

is probable that these bands result from Lewis bonding interactions with the surface. The bands are not observed on the oxidized surface and the sites probably result from defects formed during reduction.

The two bands at 1670 and 1640  $\text{cm}^{-1}$  observed during the adsorption of hexafluoroacetone onto the 673 K oxidized surface are shifted 130 and 160  $\text{cm}^{-1}$  from the C=O vapour band, indicating that the sites are relatively strong.

The bands at 1580 and 1480  $\text{cm}^{-1}$  are observed on all surfaces together with a 1615  $\text{cm}^{-1}$  shoulder on the oxidized surfaces. The 1580  $\text{cm}^{-1}$  band shifts in the presence of water to 1600  $\text{cm}^{-1}$ . The bands are produced by the initial adsorption of hexafluoroacetone on all surfaces except the BF, D<sub>2</sub>O oxidized when they appear after the removal of some surface water molecules by evacuation at 373 K. Evacuation at 540 K removes the bands which may be regenerated by adsorbing D<sub>2</sub>O onto the disc and evacuating at elevated temperatures (spec. 6.1 j) though readsorption of hexafluoroacetone is usually necessary (spec. 6.2 z, 6.3 j, 6.4 j).

The 1580 and 1480  $\text{cm}^{-1}$  bands are typical of carboxylate groups and are assigned to trifluoroacetate species on the surface. Comparison of the bands with those observed<sup>140</sup> for  $\text{TiO}(\text{OCOCF}_3)_2$  at 1630 and 1470  $\text{cm}^{-1}$  supports this assignment. The nature of the decomposition of this species is discussed in section 6.3.3. The

1615  $\text{cm}^{-1}$  may be due to trifluoroacetate species on weaker sites than those forming the 1580  $\text{cm}^{-1}$  band. The band is not however observed on the reduced surface although it might be hidden under the 1580  $\text{cm}^{-1}$  band which is broader on this surface.

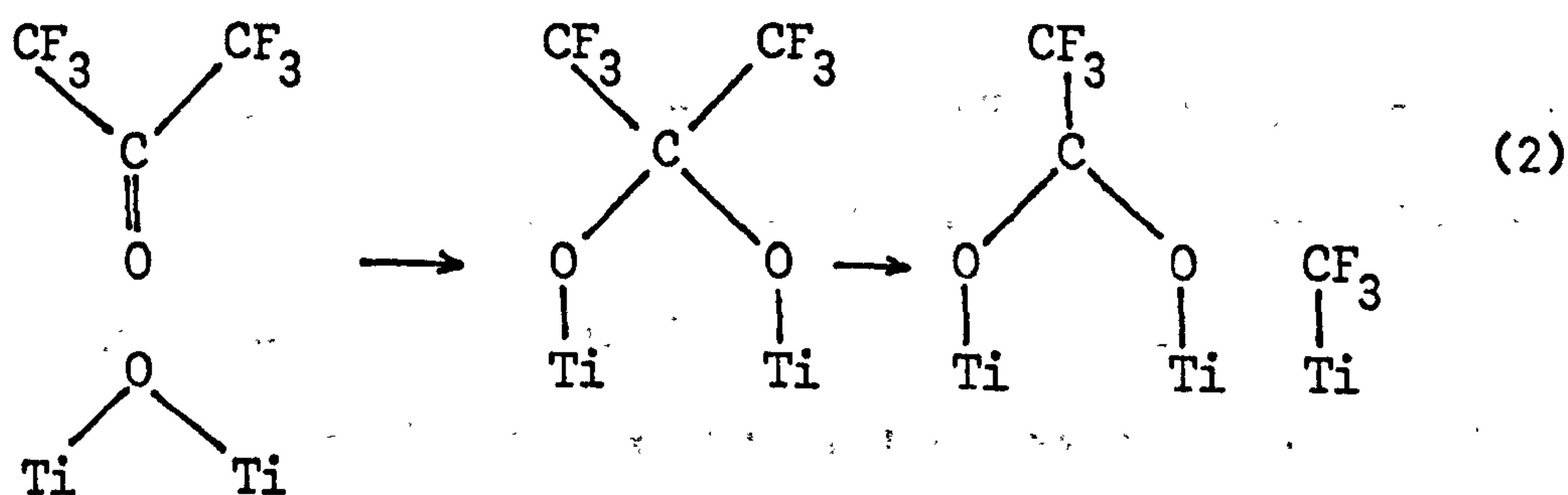
Bands are observed on the reduced surface at 1460 and 1430  $\text{cm}^{-1}$  after removal of the trifluoroacetate species by evacuation at high temperatures. The bands are not intense and are due to carbonate groups formed on the decomposition of the trifluoroacetate groups.

Intense bands below 1300  $\text{cm}^{-1}$  are observed on the surface due to C-F vibrations but their behaviour is not easily determined due to the low transmittance in this region.

A summary of band assignments is shown in table 6.2.

### 6.3.3 SURFACE REACTIONS

Adsorption of hexafluoroacetone onto the 673 K oxidized surface results in the formation of trifluoroacetate species which may be formed by reaction of hexafluoroacetone with the oxygen ions, resulting from condensation of row A hydroxyl groups.



The trifluoroacetate species decomposes above 470 K to produce a surface with few sites for the formation of hydroxyl groups (spec. 6.1 i, 6.2 w, 6.4 i) indicating that decomposition products occupy some surface sites. The decomposition<sup>140</sup> of  $\text{TiO}(\text{OOCF}_3)_2$  occurs at 540 K to give  $\text{COF}_2$ ,  $\text{CF}_3\text{COF}$ ,  $\text{CO}_2$ ,  $\text{CO}$ ,  $\text{TiO}_2$  and  $\text{TiF}_4$  and it is probable that surface species such as  $\text{Ti-F}$ ,  $\text{Ti-O-CF}_3$  and  $\text{Ti-CF}_3$  are produced from the surface trifluoroacetate.

Adsorption of water and subsequent heating causes condensation of some of these groups, and reactions with  $\text{D}_2\text{O}$ , to reform the surface trifluoroacetate species and a species with an O-D band at  $2740 \text{ cm}^{-1}$  (spec. 6.1 k).

Adsorption onto both oxidized and reduced 673 K surfaces results in bands between  $1800$  and  $1640 \text{ cm}^{-1}$  (table 6.1).

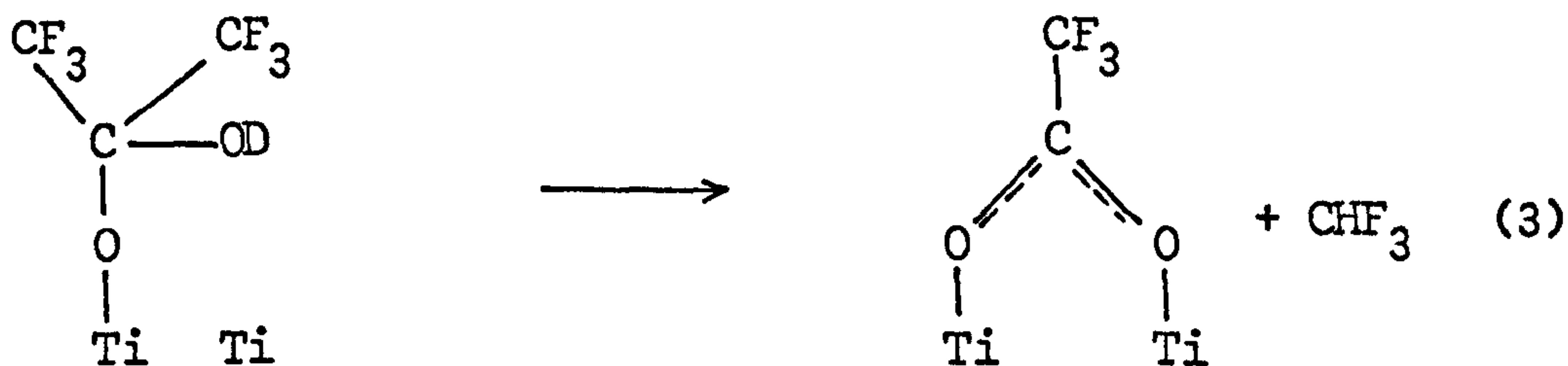


The bands are not strong and have been assigned to Lewis bonding of the C=O group in hexafluoroacetone, the number of bands observed indicates that the surface contains more types of Lewis sites than the two ('strong' and 'weak') found in this and other work. It is probable that these sites might arise from a small number of defects, or that steric hindrance causes several different interactions with the same weak or strong sites.

Reactions on the surface of 673 K reduced rutile are similar to those on the oxidized surface with the exception of the bands formed at 1460 and 1430  $\text{cm}^{-1}$  (spec. 6.3 i) which result from carbonate species formed during the decomposition of the trifluoroacetate species.

The adsorption of hexafluoroacetone onto the hydroxylated surface differs considerably from that of acetone onto the same surface. Acetone Lewis-bonds to the weak sites and removes water from the stronger sites. Hexafluoroacetone does not bond to the weaker Lewis sites, either because it is a weaker base or is sterically hindered, nor is it able to remove water molecules.

The monodentate salt of the gem-diol is formed on adsorption of hexafluoroacetone onto the hydroxylated surface (equation 1) and rearranges to form the trifluoroacetate if an adjacent site is available. Such a site may be created by removal of water or hydroxyl molecules on heating.



Other reactions on the hydroxylated oxidized surface are similar to those on the dehydroxylated surfaces.

Adsorption of hexafluoroacetone onto the hydroxylated (BT) reduced surface removes the  $2710 \text{ cm}^{-1}$  isolated hydroxyl band and increases the  $2695 \text{ cm}^{-1}$  band. In contrast to the oxidized surface, bands due to the formation of trifluoroacetate species were also observed. The removal of the isolated OD group occurs by equation (1) to form the monodentate salt of the gem-diol which cannot hydrogen bond as no adjacent hydroxyl groups are near. The hydroxyl group thus remains free and results in a band at  $2695 \text{ cm}^{-1}$  coinciding with the row A hydroxyl band.

Absence of water molecules on the reduced surface allows the formation of the trifluoroacetate species by mechanism (2) or (3).

## CHAPTER 7

SUMMARY7.1 EXPERIMENTAL PROCEDURES

The basic techniques used in this work are similar to those used by many other workers to record the infrared spectra of vapours or gases adsorbed onto solid surfaces. No attempt has previously been made to adsorb at very low vapour pressures compounds which, if dosed on at room temperature vapour pressure, react to form intense bands. The use of a cryostat in this work to dose on highly reactive compounds at very low pressures has enabled the surface reactions to be closely followed by infrared spectroscopy.

Interpretation of the infrared spectra produced has in some cases been difficult and would have been aided by the use of other techniques such as mass spectroscopy. This was used in certain circumstances but was not generally suitable due to the difficulty of trapping out the small quantities of reaction products.

## 7.2 THE RUTILE SURFACE

Results obtained in the study of water adsorption and desorption onto rutile were mainly interpreted in terms of the surface planes, while results from the adsorption of acetone, acetic acid and hexafluoroacetone were interpreted in terms of 'strong' and 'weak' Lewis sites on the rutile surface. Some reconciliation of the two approaches was proposed in the discussion of acetone results where it was stated that acetone Lewis bonded to 'weak' sites from which water molecules could be removed by evacuation at beam temperature. Water molecules and hydroxyl groups occupied all the 'strong' sites on which acetone reacted to form mesityl oxide. 'Weak' and 'strong' sites were found to exist on all planes.

It has been proposed<sup>2</sup> that the two types of site arise from the two bond lengths (axial and equatorial) around the titanium ion, the shorter (equatorial) position being the stronger site. This is not considered acceptable as the acetone results indicate that the row A terminal hydroxyl groups, which are in the axial position, are on 'strong' sites.

The 'weak' sites correspond to those sites onto which a neutral reversible form of water is adsorbed resulting in a decrease of work function but not changing the conductivity (section 1.4.2 and ref. 30). The strong site is presumably responsible for the charged reversible form accompanied by a decrease in the work function and an increase in the conductivity<sup>30</sup>.

The neutral reversible form of water may be those water molecules producing the 3610 and 3520  $\text{cm}^{-1}$  bands which are completely removed by evacuation to 373 K, while the charged reversible form of adsorbed water may produce the 3400  $\text{cm}^{-1}$  band which is not removed completely even after evacuation at 673 K.

It is probable that the two types of sites arise from the electrical properties of the surface and the weak sites may be associated with  $\text{Ti}^{3+}$  ions which have been calculated<sup>111</sup> to have a lower binding energy than corresponding  $\text{Ti}^{4+}$  ions. The increase of  $\text{Ti}^{3+}$  sites occurring on the reduction of rutile therefore increases the number of weak sites and consequently decreases the surface concentration of water at beam temperature. The reduction process however only increases the concentration of  $\text{Ti}^{3+}$  ions from 0.3% to 1.0% (ref. 20 and section 1.2) of which only 40% are on the surface<sup>17</sup>. It is probable therefore that other surface electrical effects act to decrease the amount of water adsorbed on the reduced surface.

### 7.3 FURTHER WORK

Considerable information has been gained about the nature of sites on the rutile surface in this work but as indicated above further study of the Lewis sites is required.

Further information about the sites might be obtained by infrared study of the adsorption of stronger bases than hexafluoroacetone. However, the importance of the surface electrical properties indicates that studies should be made of the work function and conductivity of oxidized and reduced samples during the adsorption of Lewis bases.

## CHAPTER 8

A TECHNIQUE FOR THE STUDY OF THE SOLID/LIQUID  
INTERFACE USING INFRARED SPECTROSCOPY

8.1 INTRODUCTION8.1.1 AIM OF THIS WORK

Infrared spectroscopy has been widely used, as indicated in the previous chapters, to study the adsorption of a vapour or gas onto the surface of a solid. The main advantage of the technique is experimental simplicity. There are, however, certain disadvantages:-

- a) It may not be used for the adsorption of solids of low vapour pressure (e.g. fatty acids).
- b) The weight of vapour adsorbed may not easily be determined.
- c) Results from the study of a vapour/solid interface cannot be applied to a liquid/solid interface for the same adsorbent due to the effect of the solvent in the latter case. Thus results from the study of acetone vapour adsorbed onto rutile may differ from those of acetone in hexane adsorbed onto rutile.

The aim of these experiments was to develop a technique for the study of the solid/liquid interface using infrared spectroscopy. The experimental details are included in section 8.2.

### 8.1.2 OTHER STUDIES OF THE SOLID/LIQUID INTERFACE USING INFRARED SPECTROSCOPY

The following four techniques have been used to study the solid/liquid interface:-

- a) Reflectance spectra of evaporated metal or metal sulphides.
- b) Adsorption onto a powder from solution. Powder removed, dried and infrared recorded by pressing it into a self-supporting, or potassium bromide disc, or supporting it in a nujol mull<sup>57</sup>.
- c) Adsorption onto a powder from solution and transfer of the dispersion to an infrared cell<sup>118,121-123</sup>.
- d) Adsorption from solution onto a self-supporting disc, all treatments being carried out in a cell attached to a vacuum frame<sup>124-128</sup>.

Technique (a) is limited in application and in technique (b) the drying and subsequent pressing may result in changes to the adsorbate-adsorbent interaction. Results from the adsorption of acetic acid on alumina<sup>118</sup> using technique (c) have been discussed (section 5.3) but it is not a suitable method if atmospheric contamination is to be avoided.

Hasegawa and Low<sup>124-126</sup> developed a cell using technique (d) and found the main problems of the technique to be bubbles forming in the liquid due to inadequate degassing, and infrared



bands of the solvent. These bands obscured part of the spectral region under investigation and lowered the instrument response, but could be removed by using a matched cell in the reference beam, although this distorted some bands if compensation was not precise<sup>124</sup>. In later work<sup>125</sup> a crystal wedge was used in the reference cell to ensure precise compensation.

Using this cell Hasegawa and Low were able to record the spectrum resulting from the adsorption of aniline onto silica<sup>124</sup>, stearic acid onto zinc oxide<sup>125</sup>, silica<sup>126</sup>, and alumina<sup>126</sup>, and of decanoic acid onto magnesia<sup>126</sup>. The solvent in each case being carbon tetrachloride.

Results from the adsorption of stearic acid onto zinc oxide<sup>125</sup> and alumina<sup>126</sup> showed the formation of surface stearates. In addition a series of bands due to the disturbed 'wagging' of methylene groups in the hydrocarbon chains were observed. Comparison of these bands with those observed for some stearates indicated that at relatively high surface coverage the chains of surface carboxylate were tilted by about  $60^\circ$ . This band progression observed for stearates on zinc oxide was not observed for alumina indicating the stearate chains to be randomly orientated.

Decanoic acid was adsorbed onto magnesia<sup>126</sup> from solution and from the gas phase. Comparison of the results showed that although surface reactions to form carboxylates were similar there were considerable differences in the arrangement of the molecules at the surface. In the liquid system the orientation of

the surface carboxylate was regular and the dimers formed at high surface coverage arranged in a similar way to those in solid decanoic acid. The carboxylates and dimers resulting from adsorption of decanoic acid from the gas phase were, however, randomly orientated.

The study of the solid/liquid interface using infrared spectroscopy not only provides a method of studying the adsorption of high boiling point compounds but may also provide information about any regular orientation of surface molecules which does not occur on adsorption from the gas phase, possibly due to an absence of the polarizing effect of the solvent<sup>126</sup>.

### 8.1.3 INITIAL EXPERIMENTS

The first apparatus was designed and built to record the spectrum of rutile powder immersed in a solution of an organic adsorbate in carbon tetrachloride. The rutile powder was treated and poured into the cell under vacuum to prevent contamination by the atmosphere and the solution then added. As the path length of the cell necessary for the introduction of the rutile powder between the windows resulted in a very high optical density over the whole infrared range, it was decided to use pressed discs.

Rutile was replaced by silica in the experiments because of the reaction with carbon tetrachloride<sup>49</sup>. Other solvents could not be used because of their high optical density.

## 8.2 EXPERIMENTAL

### 8.2.1 DESIGN OF THE CELL

The basic requirements of a cell suitable for the recording of solid-liquid interface spectra are:-

- (1) Low path length due to the high optical density of some solvents<sup>124</sup>.
- (2) Attachment to a system in which the solid can be treated at temperatures up to 670 K in vacuo.
- (3) Absence of rubber seals or other possible contaminants.
- (4) Entry and exit tubes to allow the admission of solution into the cell and its subsequent removal.

The first two of the above requirements are the most important and difficult to fulfill since they are mutually exclusive. That is the disc must be treated at high temperatures out of the cell and then lowered between the windows, an operation not possible with a path length comparable with the thickness of the disc. A cell in which the path length could be increased to admit the disc and then closed to decrease the path length to a distance comparable with the thickness of the disc was therefore designed (fig. 8.1)

The cell as originally built had two o-rings in grooves round the variable window which screwed into the fixed part of the cell, the o-rings forming a seal between the variable window and inside of the cell body.

This design was not successful because the o-ring seal failed to hold a suitable vacuum and the turning motion of the variable window when screwed up cracked the disc. The screw threads were subsequently replaced by bolts which screwed into the main body of the cell. The failure of the o-ring seals prevented the lowering of the disc into the cell under vacuum and an alternative procedure was devised whereby the variable window holder would be bolted up to the cell base via a teflon flange to form a vacuum tight seal when the disc was under treatment or in the cell. Increasing the path length in order to lower the disc into the cell would break this seal and allow air to leak in. This was to be prevented by filling the apparatus with dry oxygen or nitrogen at above atmospheric pressure. After lowering the disc into the cell the variable window could then be bolted back onto the cell body to restore the seal.

The disc holder may also limit the minimum cell path length possible. Hasagawa and Low<sup>125</sup> used stepped windows and a holder which fitted outside them to overcome this problem. However it was decided in this work to press a thin platinum wire into the disc and attach this to the lowering mechanism. In later work<sup>127</sup> a platinum wire holder was used.

The cell, as described in detail in section 8.2.2, differs from that in reference 127 due to subsequent modifications made. These were the replacement of the magnetic lifting system by a modified grease-free tap and the use of a thicker teflon seal which increased the path length and allowed the disc to pass into the

cell without breaking the seal. The increase of path length did not affect the spectra recorded as the carbon tetrachloride bands were not in the frequency range studied<sup>127</sup>.

The advantages of the cell used in this work over that used by Hasegawa and Low<sup>124-126</sup> are its ease of operation, lower path length (in the original cell) and the movement of liquids under a pressure of inert gas which prevented bubbles forming<sup>124</sup>. The use of a reference cell in this work was not considered necessary due to the narrow path length of the cell and difficulty in obtaining an exact compensation.

#### 8.2.2 DESCRIPTION OF CELL (fig. 8.1)

The lower section of the cell consisted of a brass ring into which a calcium fluoride window (5cm diameter) was fixed with araldite. A tube at the bottom of the cell connected to the vacuum frame was used for draining liquids from the cell and as a vacuum or gas line. Discs entered the optical section of the cell via a flat tube (2.5 x 0.5 cm) through which passed two brass tubes, attached to the vacuum frame (fig. 8.2) via metal to glass seals, one being used for evacuation of the cell and the other as an inlet for liquids.

The other calcium fluoride window was fixed with araldite onto a brass ring and bolted to the cell base via a teflon seal between a knife edge and opposing groove (the bolts are only shown in the front view, which is of the cell without the variable

window). The vacuum attainable with this arrangement was  $10^{-2}$  N m<sup>-2</sup> and the path length 0.7mm.

The lifting system (fig. 8.3) was similar to that used by Hasegawa and Low<sup>124</sup> and consisted of a 4cm diameter tube, 35cm high, onto which was attached an inverted 'U' of 1cm diameter glass 30cm high. Two soft iron weights sealed in glass, one in each arm of the 'U', were connected by a nylon thread. A thin pyrex rod was hooked onto the weight passing into the wide tube, to which the silica disc was attached using 2cm of platinum wire. The disc was raised or lowered using magnets to move the weights. The modified grease-free tap used later<sup>127</sup> had the disadvantage of possible leakage through the barrel but was more smooth in its operation than the system used here.

The disc was heated at the middle of the tube, opposite a thermocouple pocket, by a surrounding furnace. Asbestos card (not shown in the diagram) was fitted round the tube at each end of the furnace to prevent a through draught of hot air.

The wide tube of the lifting mechanism was sealed to a thick glass flange clamped, via an o-ring, to a circular brass plate on top of the flat tube of the cell. The disc was guided into the flat tube by a stainless steel funnel.

Admission of gas to the lifting mechanism was via a Rotaflo tap connected, via a polythene tube, to the gas line (fig. 8.2) on the frame. The gas left through one of the vacuum

lines attached to the cell base, thus allowing treatment of the disc in a flow of gas.

### 8.2.3 VACUUM FRAME

The diagram of the system (fig. 8.3) is mainly self-explanatory. The pumping system was that used for the solid vapour experiments and has been described (2.2.1). All taps were grease-free (as described 2.2.1) and could be removed in order to add liquids into the storage vessels. Liquids were transferred from the storage vessels by condensing the vapour in a burette using cotton wool, soaked in liquid nitrogen, wrapped round the burette.

A gas bleed, consisting of a thin glass tube (diameter 1mm) immersed under 1cm of mercury, was attached to the frame to allow gas to flow out at 1cm pressure ( $1.33 \times 10^2 \text{ k N m}^{-2}$ ) above atmospheric.

### 8.2.4 REAGENTS

#### A. Silica

Sample used was Aerosil 200 (ref S41/542834) from Bush, Beach and Segner Bayley Limited. Details of pressing and treatment in the cell are given in 8.2.6.

### B. Carbon Tetrachloride

Spectroscopic grade, dried and stored on the vacuum frame over calcium chloride. Degassed by freeze-thaw method.

### C. Ether

A.R grade, dried over molecular sieve.

### D. Oxygen, Nitrogen

From gas cylinders, passed through molecular sieve previously dried at 520 K under vacuum.

## 8.2.5 SPECTROMETER

Results were recorded on the Perkin-Elmer 257 previously described. Due to the higher transmittance of the silica discs, compared with rutile, which became transparent in carbon tetrachloride the slit width was 1 with a gain setting to give the noise levels shown in the spectra (spec. 8.1).

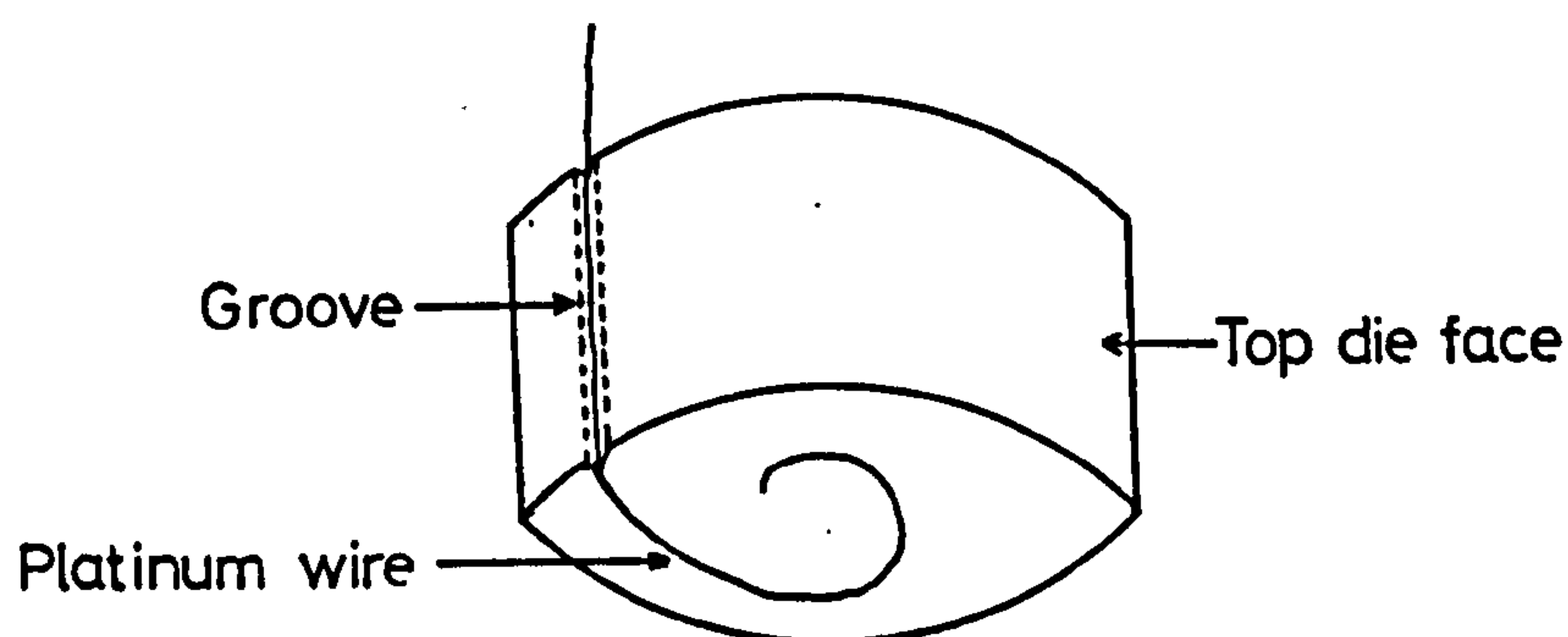
## 8.2.6 OPERATION

### A. Pressing of the silica disc

0.2g of silica were weighed, tipped onto the bottom die face and spread to an even thickness. Approximately 2.5cm of



thin platinum wire was placed in a groove engraved in the top die face and bent so that 1cm lay along the bottom surface of the die (see below).



The top die was then placed on the silica powder and pressed to  $74 \text{ MN m}^{-2}$  (5 tons/sq.in), the pressure being released immediately to prevent the disc sticking to the die faces. The die faces were removed after attaching a short length of thick platinum wire to that pressed in the disc and the disc suspended in the lifting system as described. The lifting system was then clamped to the cell.

### B. Treatment of the disc

The disc was raised to the centre of the furnace and with the adjustable cell window screwed up to the teflon seal the cell and frame were evacuated to  $10^{-2} \text{ N m}^{-2}$ . Oxygen was passed

rapidly through the molecular sieve and out of the adjacent manometer before shutting off the pumping line and other parts of the system from the cell and main line. Oxygen was then bled slowly into the cell using the tap on the lifting system ensuring, by use of the manometer, that pressures in the molecular sieve and cylinder valves remained above atmospheric. When the cell and main line were full of oxygen the rate of flow was decreased, the manometer shut off and the gas allowed to flow through the cell and lifting system into the main line and out of the gas bleed previously described.

After treatment of the silica disc in the flow of oxygen (673 K, 2h) the cell and main line were evacuated and the disc allowed to cool. Nitrogen was then introduced into the cell, as described for oxygen, except that the gas flowed through the bottom cell exit and out of the gas bleed at the initial high flow rate. The bolts holding the adjustable window were unscrewed by 2mm and the window pulled out to allow the disc to be lowered onto the cell. The window was bolted up against the teflon seal, the upper gas exit from the cell to the main line was opened and the exit at the bottom of the cell closed.

Nitrogen was admitted to the rest of the vacuum frame after transferring solute and solvent to the burettes. After recording the spectrum of the disc in nitrogen and immersed in solvent, the required volumes of solute and solvent were run into the mixing tube and agitated using a piece of soft iron sealed in glass and moved by a magnet. This system did not permit an accurate determination due to the small quantities involved and it

was subsequently modified<sup>141</sup>. The solution was run into the cell after mixing.

The presence of a flow of nitrogen above atmospheric pressure not only prevented the contamination of the discs by the neoprene o-ring but prevented the formation of bubbles in the liquid as observed by Hasegawa and Low<sup>124</sup>.

After recording the spectrum of the disc immersed in the solution the gas flow was shut off and the liquid removed via the bottom exit and backing line. The disc was then thoroughly evacuated before re-admitting nitrogen and a solution of increased concentration.

### 8.3 RESULTS AND DISCUSSION

The spectrum of the initial surface (spec. 8.1a) showed bands at 3740 and 3680  $\text{cm}^{-1}$  due to isolated and hydrogen-bonded hydroxyl groups respectively<sup>5</sup>.

Immersion of the disc in carbon tetrachloride (spec. 8.1b) increased the transmittance of the disc and shifted the 3740  $\text{cm}^{-1}$  band to 3680  $\text{cm}^{-1}$ . The path length of the cell was determined as 0.7mm by placing a variable path length cell containing carbon tetrachloride in the reference beam in order to precisely remove the solvent bands.

Increasing concentrations of diethyl ether (spec. 8.1c-e) shifted the isolated hydroxyl group to 3230  $\text{cm}^{-1}$  with a resultant decrease in intensity of the 3680  $\text{cm}^{-1}$  band. The shift ( $\Delta\nu_{\text{OH}}$ ) of 460  $\text{cm}^{-1}$  is in close agreement with observations from the gas phase adsorption of ether which give shifts of 450<sup>58</sup>, 460<sup>129</sup>, 500<sup>130</sup> and 450<sup>131</sup>  $\text{cm}^{-1}$ .

Bands due to the adsorption of ether were also observed at 2980, 2960, 2880  $\text{cm}^{-1}$ , due to C-H stretching vibrations and at 1490, 1445, 1415 and 1385  $\text{cm}^{-1}$ . These bands below 1500  $\text{cm}^{-1}$  were partially obscured by silica bands.

Removal of the liquid from the cell and subsequent evacuation (spec. 8.1 f-h) decreased the 3230  $\text{cm}^{-1}$  band and increased the 3740  $\text{cm}^{-1}$  isolated OH group. The 3680  $\text{cm}^{-1}$  band

remained relatively constant. The final surface (spec. 8.1 i) was similar to the initial surface (spec. 8.1a).

The results obtained from the adsorption of ether showed that the cell was suitable for the study of the solid/liquid interface using infrared spectroscopy and further studies have now been carried out using it<sup>127,128</sup>.

## 8.4 FURTHER WORK

### 8.4.1 DISC IMMERSED IN A LIQUID

Marshall and Rochester<sup>141,142</sup> modified the design of the original cell together with the surrounding system and were able to measure the spectra of adsorbed species and the weights of solute adsorbed, both as a function of solute concentration.

The basic problem of bands due to the solvent still remains. While it is not serious with carbon tetrachloride, which has few bands in the  $4000-1000\text{ cm}^{-1}$  region, it becomes a problem with other organic solvents most of which have much higher optical densities. Solvent bands may be eliminated by using a cell in the reference beam of identical path length but instrument response may be poor<sup>124</sup>.

Solvent bands may also be removed by running off the solution in the cell until only the bottom of the disc remains in contact with the liquid, the intention being that the whole disc remains in equilibrium with the solution by capillary action. The disadvantage of this method is that any equilibrium between the solute and surface may be changed by removal of the solution. There is also the possibility that the heat of the infrared beam may evaporate the solute and solvent making constant temperature recordings difficult and disturbing any surface equilibria.

The lowest path length attainable is of necessity equal to the thickness of the disc. Since with this path length the disc cannot be lowered between the windows, one window must be adjustable, preferably while maintaining a vacuum in the system.

The design of the cell described in this work has been modified (fig. 8.4) to allow the adjustable window to move up to the disc and reduce the path length to the thickness of the disc. The modifications are as follows:-

- (1) A flexible seal has been introduced in the adjustable window flange between that part to which the window is attached and the ring bolted to the main body via a teflon seal. The flexible seal is of metal and could consist either of a concertina metal tube of the type used in some glass-metal joints (A in fig. 8.4) or of two thin stainless steel rings bonded together on the outer edge with araldite and to either part of the adjustable window on the inner edge (B in fig. 8.4).
- (2) The two circular 5cm calcium fluoride windows are replaced by two 2.5 x 1.3 cm windows of the same material. The use of rectangular windows allows a disc holder to be used which passes outside the windows. These are not therefore recessed into the cell base as in the original cell and are attached with araldite over 2.0 x 0.6 cm holes in the cell body and adjustable flange. The circular design of the cell has been retained since it may easily be machined on a lathe. The proposed cell would be constructed from stainless steel.

- (3) The teflon seal in the main cell has been replaced by a copper o-ring clamped between a knife-edge and groove. This type of seal has been used in a later cell with good results<sup>141</sup>, since a higher vacuum is attainable without danger of contamination.
- (4) A cell holder must be used for rutile as the disc cracks if any attempt is made to press a wire in it or pass wire or quartz through it. A suitable cell holder (fig. 8.5) would be two 3mm glass rods about 5cm long, joined at the top with a 3mm rod and curved in at the bottom. The disc would be held between the two rods in a groove. The cell is designed with a U-shaped groove for the holder and also to ensure the disc rests against the fixed window. This allows movement of the adjustable window without disturbing the disc.
- (5) The rubber o-ring at the junction between the cell base and lifting system has been replaced by a metal seal which reduces the risk of contamination. The glass flange at the bottom of the lifting system has been replaced by metal and a metal-glass seal used to attach the glass tube of the lift.  
  
The cell as described would be used in conjunction with the liquid system used by K Marshall in his work<sup>142</sup>.



#### 8.4.2 POWDER IMMERSSED IN A LIQUID

In previous work it was found difficult to fill a narrow path length cell with powder. The variable path length solid-liquid cell could be used for powders using the same procedure as for discs. The cell windows would be separated while the powder was introduced (see below) and then pressed lightly together to remove the 'dead space' between the solid particles. A trial and error method would be required to determine the path length for filling, sufficient to give a suitable path length for recording of spectra. In addition the cell could be filled with or without solvent present, or with a slurry.

The proposed cell is shown in figure 8.6 (front view is with the adjustable window removed) and modifications to the above cell (fig. 8.5) necessary for the recording of powder-liquid spectra are as follows:-

- (1) All 'dead' space in the cell, for example for the disc holder, can be eliminated.
- (2) The liquid exit tube at the bottom of the cell must be plugged with a filter to prevent solid passing out of the tube (not shown in figure).
- (3) The lifting system used for discs must be replaced by a system capable of treating powder and introducing it into the cell under vacuum. A system which was successfully used for treating powders is shown in fig. 8.7

The solid is heated in glass trucks mounted on short lengths of glass tubes through which passes a long glass tube, mounted in a wide bore tube sealed at both ends. The trucks are balanced by nails sealed into glass either side of each truck and are moved, and tipped, using a magnet. Powder is introduced into the trucks by removing the barrel of a Rotaflo tap and inserting a long funnel. The tap may also be used to admit gas into the system.

The powder treatment 'train' is attached to the cell by a wide bore glass tube with a metal flange and metal o-ring as considered in the disc system. The cell would have a circular tube forming a funnel (not shown) unlike the disc system which has a flat tube to the optical part of the cell.

This system can be used to treat all solids under a pressure of inert gas but powders such as silica may not be evacuated as they pass into the rest of the vacuum system. The powders may be tipped directly into the cell, or tipped into the liquid in a separate vessel, agitated using a mechanical stirrer or ultrasonic bath, and the resultant slurry run into the cell.

APPENDIX I

TABLES

TABLE 2.1

Specification for the Perkin-Elmer 257

Infrared Spectrometer

Abscissa	Range	4000-625 $\text{cm}^{-1}$ grating change 2000 $\text{cm}^{-1}$
	Accuracy	$\pm 5 \text{ cm}^{-1}$ at 3000 $\text{cm}^{-1}$ $\pm 2.5 \text{ cm}^{-1}$ at 1750 $\text{cm}^{-1}$
	Repeatability	3 $\text{cm}^{-1}$ at 3000 $\text{cm}^{-1}$ 1.5 $\text{cm}^{-1}$ at 1750 $\text{cm}^{-1}$
Ordinate	Range	0 to 100% linear in transmittance
	Accuracy	$\pm 1\%$ of full scale
	Repeatability	4000 to 2000 $\text{cm}^{-1}$ within $\frac{1}{2}\%$ full scale
Resolution	slit program 6	4 $\text{cm}^{-1}$ at 3000 $\text{cm}^{-1}$ 2 $\text{cm}^{-1}$ at 1000 $\text{cm}^{-1}$
Scan speed	slow	100 $\text{cm}^{-1}/\text{min}$ 4000-2000 $\text{cm}^{-1}$ 50 $\text{cm}^{-1}/\text{min}$ 2000-625 $\text{cm}^{-1}$

TABLE 2.2

Spectrometer settings for Rutile

Wavenumber $\text{cm}^{-1}$	<u>OXIDIZED</u>					<u>REDUCED</u>						
	Initial Transmittance	Slit Program	Gain	Response <sup>a</sup>	Initial <sup>b</sup> Trans.	Slit Program	Gain	Response	Initial <sup>b</sup> Trans.	Slit Program	Gain	Response
4000	60	7	9.8	C	40	7	15	B	40	7	15	B
3500	50	6	9.8	C	40	7	15	P	40	7	15	P
3000	60	5	9.8	C	40	7	9.5	C&P	40	7	9.5	C&P
2500	60	5	9.8	C	50	7	9.5	C	50	7	9.5	C
2000	80	5	7.5	C	60 or 70	7	7.5	C	60 or 70	7	7.5	C

a. C = Correct    B = Bad    P = Poor

b. Varied with sample

TABLE 3.1

ASSIGNMENT OF BANDS OBSERVED ON THE  
OXIDIZED RUTILE SURFACE

Bands ( $\text{cm}^{-1}$ )		Assignment
OH	OD	
3700	2720	Isolated terminal hydroxyls on (110) plane
3680	2710	Terminal hydroxyls perturbed by water molecules
3655	2695	H-bonded terminal hydroxyls on (110) plane
3610	2660	} Surface hydroxyl groups H-bonded to molecular water or water molecules coordinately bonded to surface (110)
3520	2600	
3420	2535	Bridged hydroxyl groups on (110) plane
3400	2500	Water molecules on (101), (100), (111), (211) planes
1620	-	$\nu_2$ bending vibration of $\text{H}_2\text{O}$ molecules

TABLE 3.2

FUNDAMENTAL BANDS OF H<sub>2</sub>O AND D<sub>2</sub>O<sup>64</sup> (cm<sup>-1</sup>)

Mode	H <sub>2</sub> O		D <sub>2</sub> O	
	Vapour	Liquid	Vapour	Liquid
V <sub>3</sub> Antisymmetric	3757	3400	2788	2500
V <sub>1</sub> Symmetric	3653	3280	2767	2389
V <sub>2</sub> Bending	1595	1645	1178	1220

TABLE 3.3

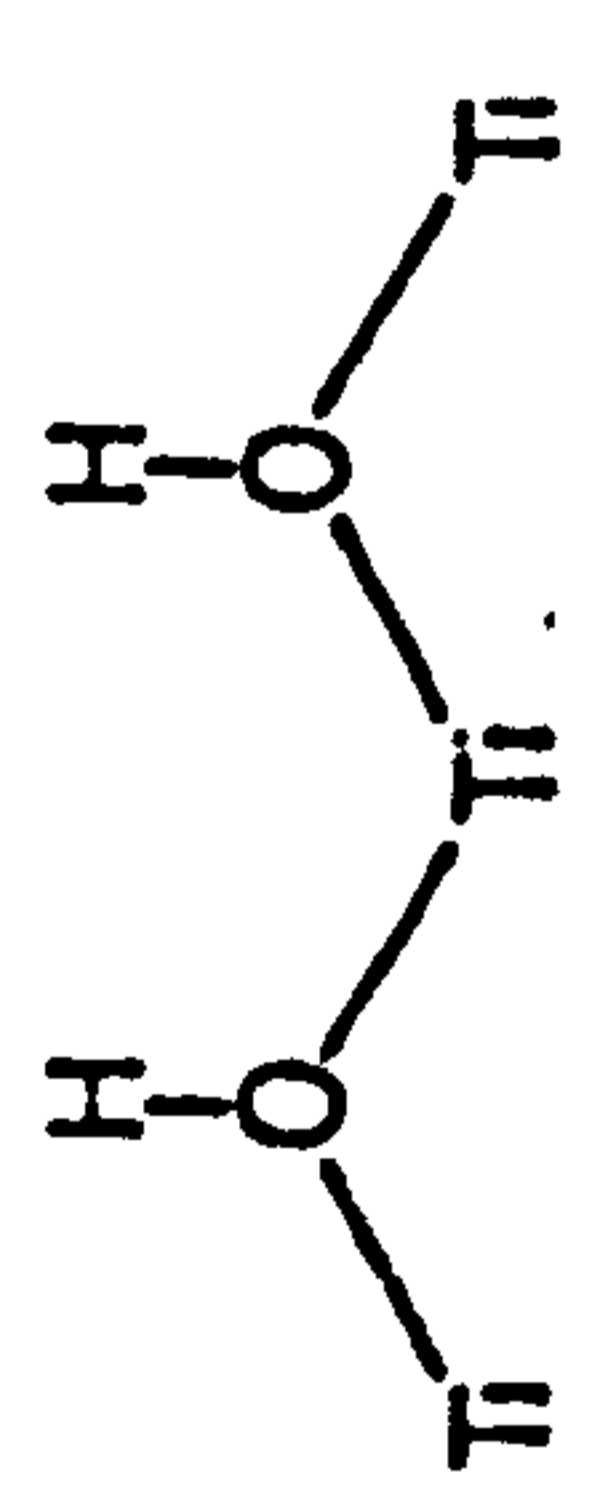
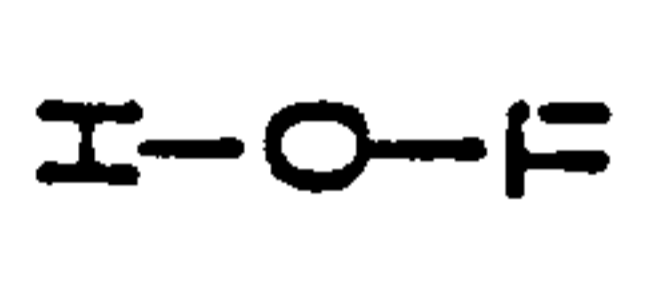
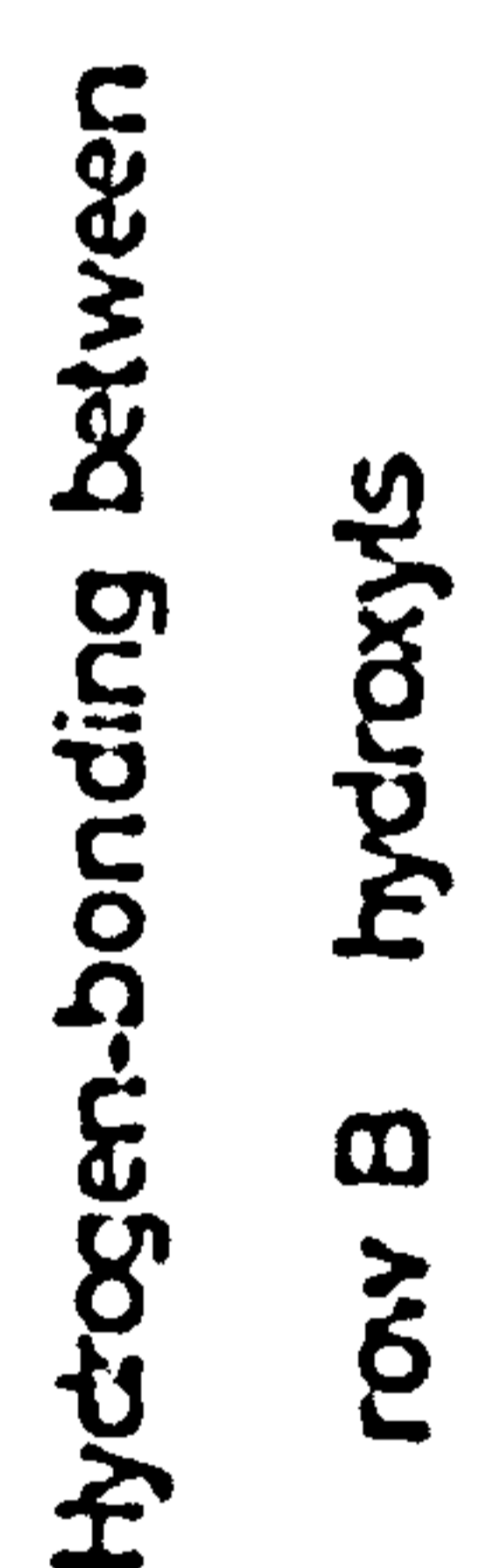
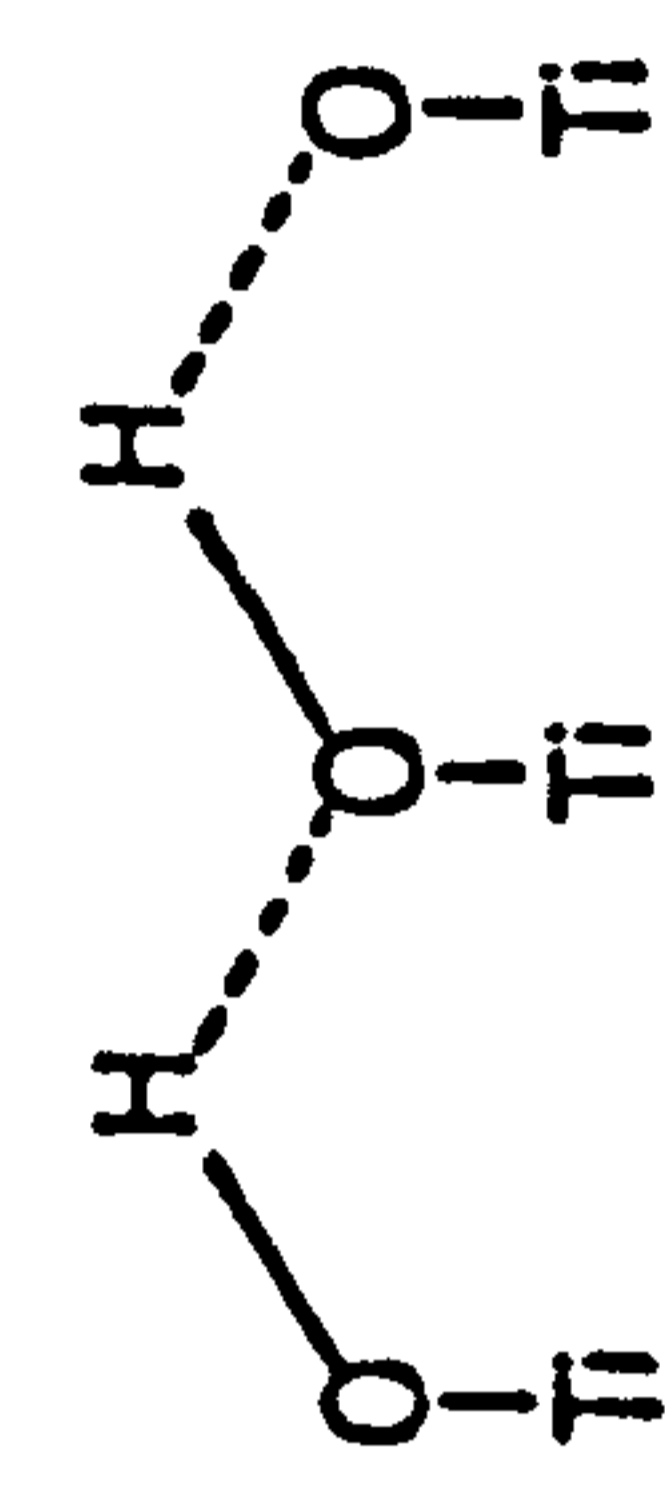
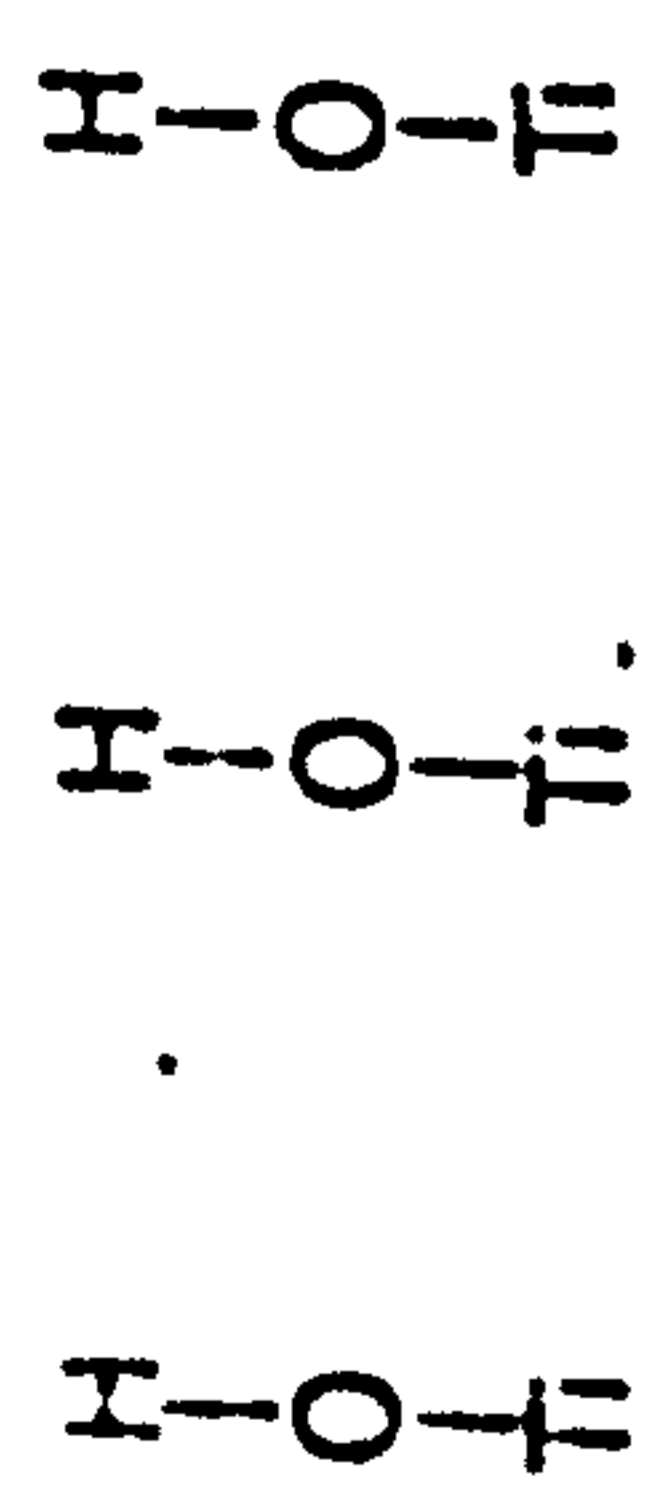
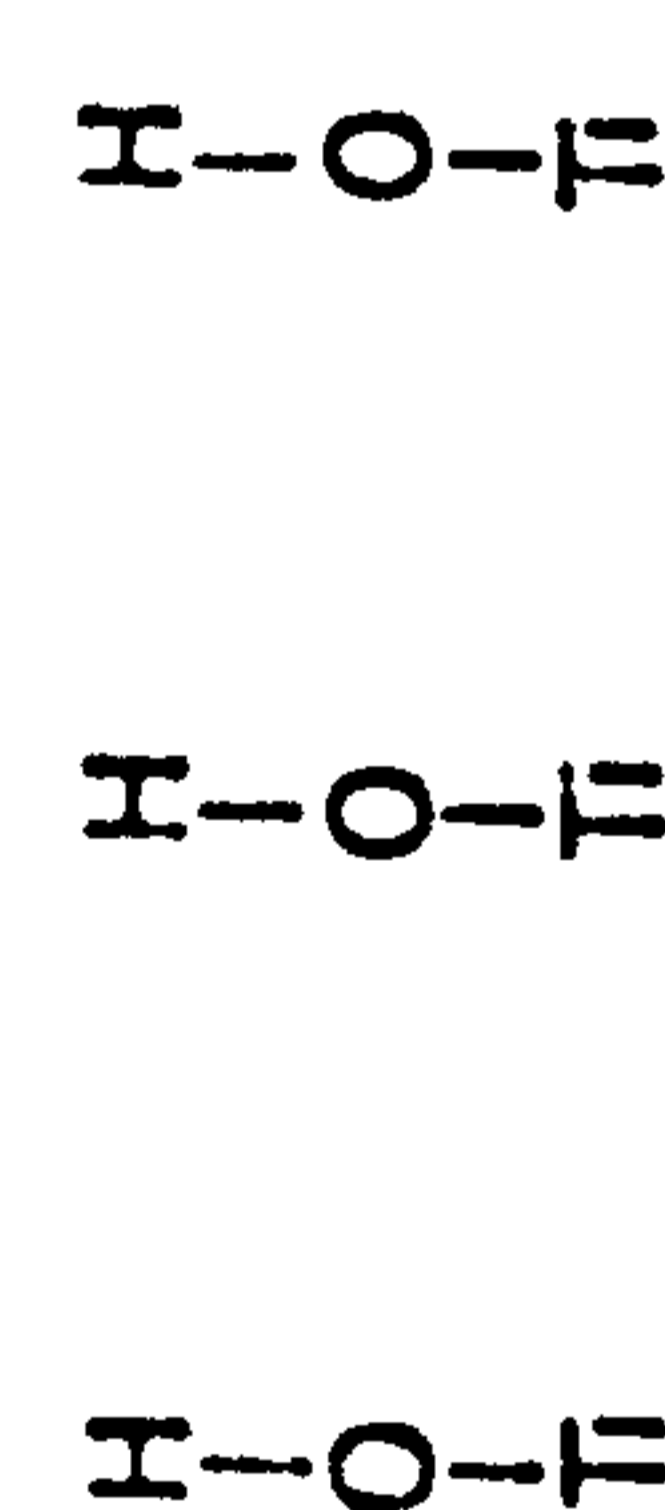
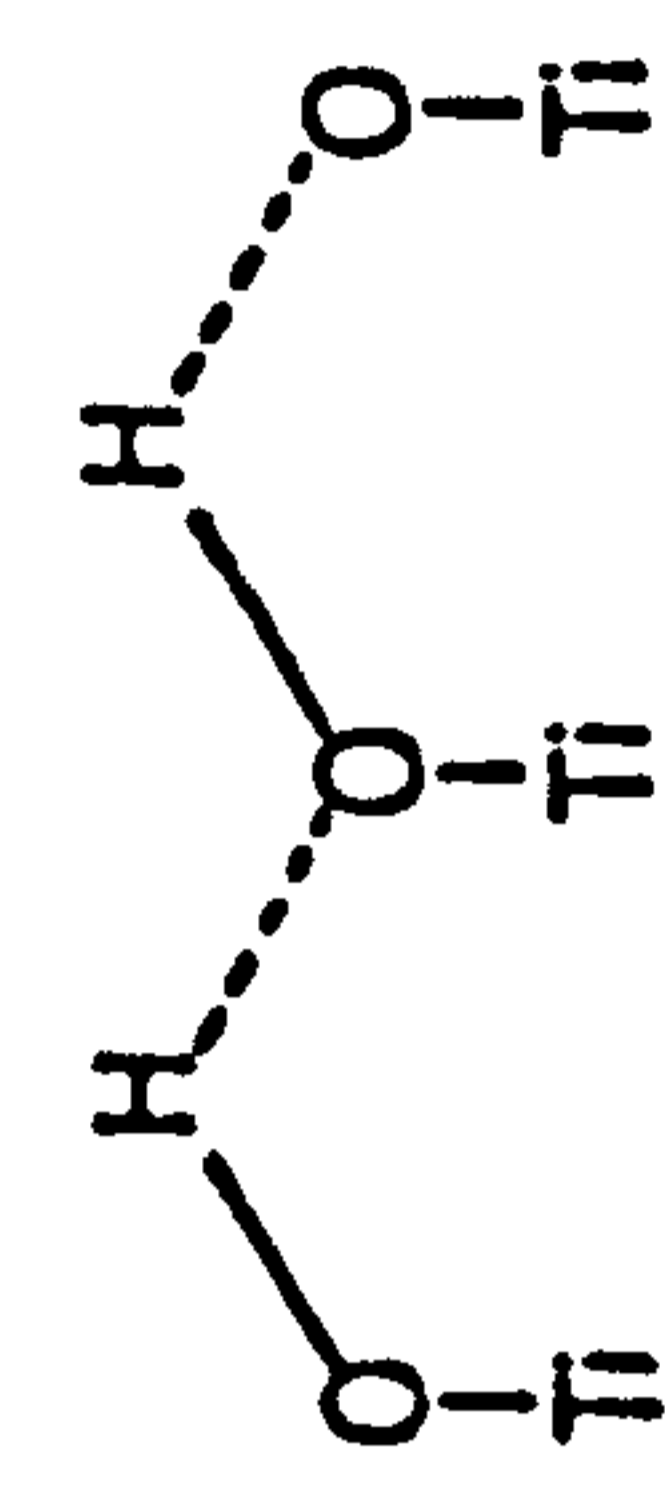
OCCURRENCE OF PLANES EXPOSED ON A RUTILE CRYSTAL

Plane Exposed	Occurrence (%)	Coordination of Surface Ions	
		Ti	O
110	60	5,6	2
100 and 010	5	5	2
101 and 011	10	5	2
111	10	3	2
211	15	3	2

TABLE 3.4

BANDS OBSERVED ON THE RUTILE SURFACE  
IN OTHER STUDIES AND THEIR ASSIGNMENTS



Bands (cm <sup>-1</sup> )	P Jones and J A Hockey <sup>41,42</sup>	P Jackson <sup>1,10</sup>	J Ramsbotham <sup>2</sup>	M Primet et al <sup>49</sup>
3700	not observed	<u>Row B bridged hydroxyls</u> 	<u>Isolated terminal hydroxyl</u> 	Isolated OH group (observed 3685 cm <sup>-1</sup> )
3680	ν <sub>3</sub> vibration water on (101) face	Hydrogen-bonding between row B hydroxyls 	Perturbed isolated hydroxyl groups 	not observed
3655	<u>Row A hydroxyls</u>  (observed 3650 cm <sup>-1</sup> )	<u>Row A (terminal) hydroxyls</u>  (observed 3570 cm <sup>-1</sup> )	<u>Row A hydroxyls H-bonded</u> 	Hydrogen-bonded OH groups on adjacent equatorial oxygen ions 296 pm apart

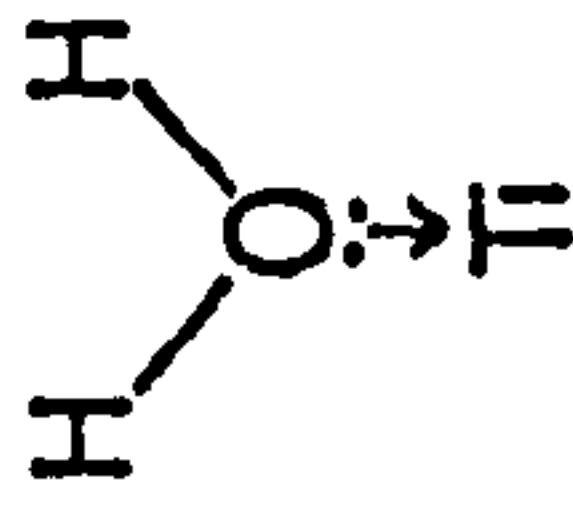
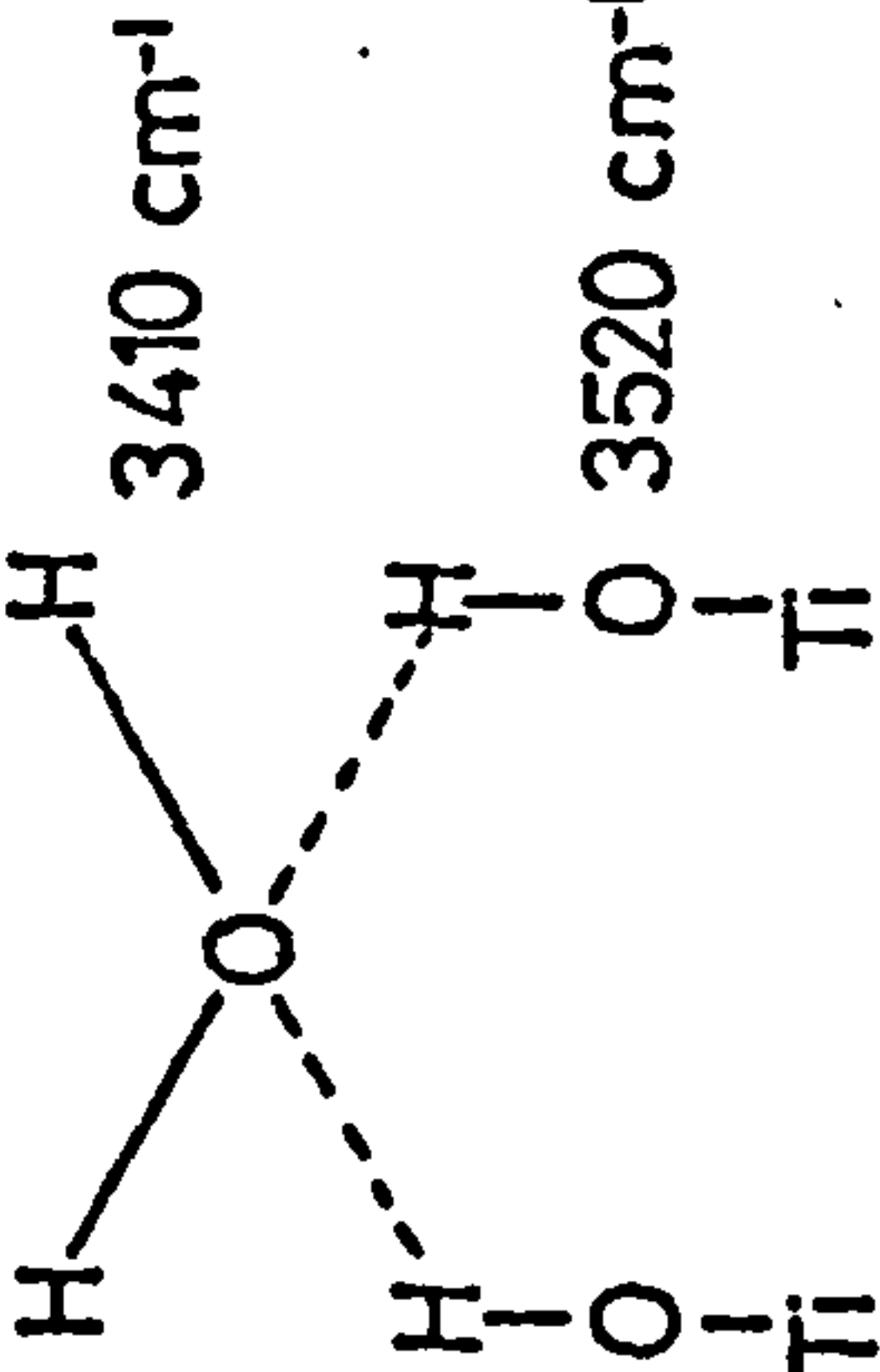
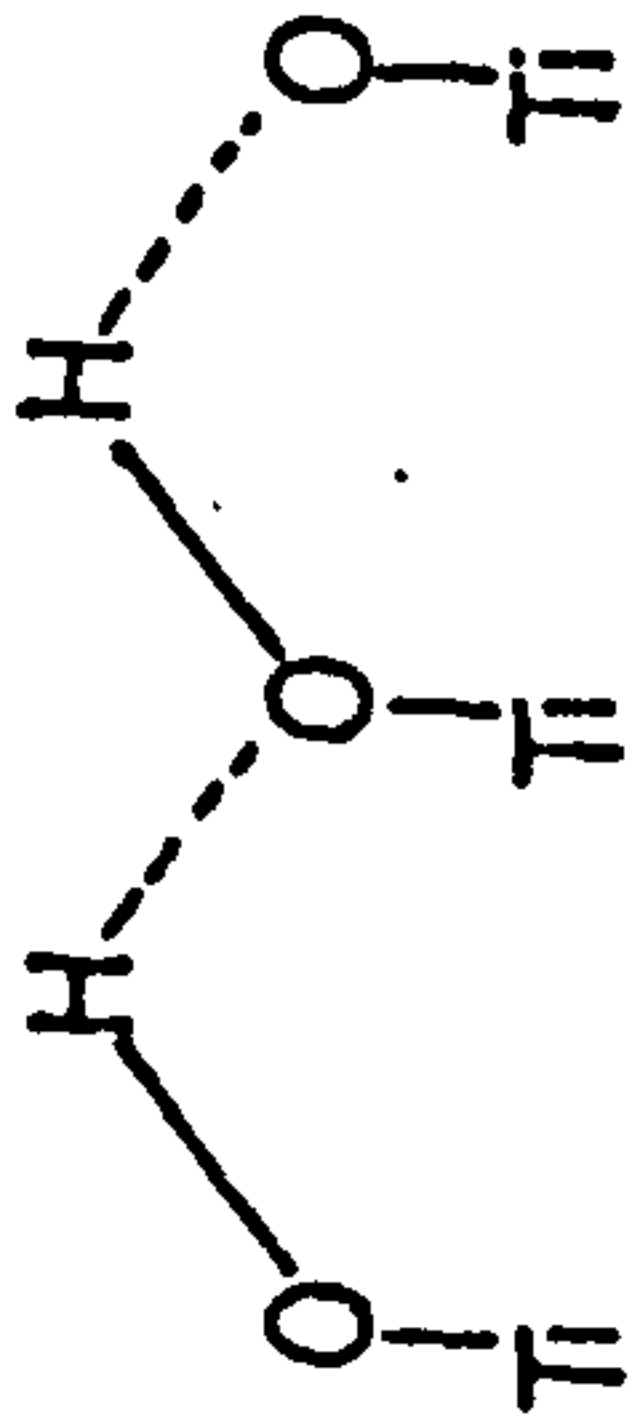
3610	$\gamma_1$ vibration water on (101) face	(observed 3615 $\text{cm}^{-1}$ ) mixture interaction of water with various OH groups	<u>Coordinated water</u>  (observed 3620 $\text{cm}^{-1}$ )	not assigned
3520	fundamental OH stretching vibration water on (100) face (observed 3550 $\text{cm}^{-1}$ )	or effect OH species on physisorbed water (observed 3530 $\text{cm}^{-1}$ )	Terminal hydroxyls hydrogen-bonded to water  Hydrogen-bonded water molecules (observed 3410 $\text{cm}^{-1}$ )	not assigned
3420	Row B hydroxyls (observed 3410 $\text{cm}^{-1}$ )	H-bonded row A hydroxyls 	Hydrogen-bonded OH groups on adjacent equatorial oxygens 253pm apart (observed 3410 $\text{cm}^{-1}$ )	not assigned
3400	not observed	strongly physisorbed water (observed 3350 $\text{cm}^{-1}$ )	water adsorbed in surface defects and pores (observed 3350 $\text{cm}^{-1}$ )	not assigned

TABLE 3.5

CALCULATED O...O DISTANCES FOR HYDROGEN-BONDED  
HYDROXYL GROUPS ON THE RUTILE SURFACE

Hydrogen-bond Wavenumber	Shift from 3700 cm <sup>-1</sup>	O...O Distance (pm)
3680	20	304 ± 5
3655	45	298 ± 5
3610	90	292 ± 5
3520	180	272 ± 5

O...O distances calculated from ref. 1 using figs. 5.1b and 2.1a as described on page 190 of reference

TABLE 4.1

BANDS OBSERVED BELOW 2000  $\text{cm}^{-1}$  AFTER ADSORPTION

OF ACETONE  $h_6$  OR  $d_6$  ONTO A RUTILE SURFACE

SURFACE ADSORBATE	<u>OXIDIZED</u>				<u>REDUCED</u>	
	673 K	BT	373 K	673 K	BT	
$H_2O$ $d_6$	$D_2O$ $h_6$	$D_2O$ $d_6$	$D_2O$ $h_6$	$D_2O$ $h_6$	$D_2O$ $d_6$	$D_2O$ $d_6$
	1685	1685	1685	1685	1670	1670
	1670	1670	1660	1660	1670	1670
	1645	1645	1595	1595	1645	1645
	1580	1580	1540	1540	1580	1580
	1540	1540	1510	1510	1540	1540
	1510	1510	1465	1465	1510?	1510
	1465	1465	1440	1440	1480	1480
	1425	1425	1380	1380	1425	1425
			1360	1360		
			1345	1345		

TABLE 4.2

THE POSITIONS OF INFRARED BANDS DUE TO CARBONYL  
STRETCHING VIBRATIONS OF LEWIS ACID COMPLEXES  
CONTAINING ACETONE

Compound	Wavenumber $\text{cm}^{-1}$	Shift $\text{cm}^{-1}$	Reference
Acetone liquid	1715	-	This work
$\text{TiCl}_4$ .acetone	1665	50	99
$\text{HfCl}_4$ .2acetone	1660	55	101
	1630	85	
$\text{ZrCl}_4$ .2acetone	1661	54	101
	1631	84	
$\text{SnCl}_4$	1650	65	102
$\text{BF}_3$ .acetone	1640	75	103

TABLE 4.3

SPECTRA OF ACETONE ADSORBED ON METAL OXIDES --  
BANDS OBSERVED IN THE 1700-1580  $\text{cm}^{-1}$  REGION

OXIDE	BANDS ( $\text{cm}^{-1}$ )			REFERENCE
Alumina	1692	1625	1600	85
	1700	1635	1590	87
	1685-1703	1612-1629	1559-1579	89
Rutile	1689		1600	85
	1685	1660	1595	This work
Magnesium Oxide	1700	1650	1610	112
Nickel Oxide	-	-	1580	112
Compare:				
Mesityl Oxide				
adsorbed onto		1660	1595	Spec. 4.8
rutile				



TABLE 4.5

ASSIGNMENT OF BANDS BELOW 2000  $\text{cm}^{-1}$  FORMED  
ON THE ADSORPTION OF ACETONE  $\text{h}_6$  AND  $\text{d}_6$  ONTO  
OXIDIZED AND REDUCED RUTILE SURFACES

Band ( $\text{cm}^{-1}$ )		Assignment
Hydrog.	Deut.	
1685	1670	C=O stretch in acetone $\text{h}_6$ Lewis bonded to a $\text{Ti}^{4+}$ ion
1660	1645	C=O stretch in mesityl oxide adsorbed onto the rutile surface
1595	1580	C=C stretch in mesityl oxide adsorbed onto the rutile surface
1540	1510	O=C=O asymmetric stretch in acetate species
	1480	Acetate species (to be assigned - chapter 5)
1465		Asymmetric methyl deformation
1440		C-H in mesityl oxide
1440	1425	Symmetric O=C=O in acetate species
1380		C-H vibrations in mesityl oxide
1360		



TABLE 5.1

BANDS OBSERVED ON THE ADSORPTION OF ACETIC  
ACID ONTO OXIDE SURFACES

Oxide	Titania		Alumina		MgO	Ions		Assignment
Treatment	473 K	423K	523 K	liquid	298 K	H	D	
Reference	47	85 <sup>a</sup>	85 <sup>a</sup>	118 <sup>c</sup>	117 <sup>b</sup>	106	106	
			1750					Adsorbed acid molecules
		1715	1715	1700				
		1625						Not assigned
	1555	1545	1585	1590 1560	1560 1530	1556	1545	C=O
	1450	1460	1470			1456	1031	C-H
	1410			1465 1420	1440 1410	1413	1406	C=O
	1340	1315	1335		1320	1344	1085	C-H
		1285		1285				Physically ads.

a) Bands not generally assigned

b) Details of all observed bands are not given in the text and were obtained from the spectra presented (fig. 4 of paper)

c) The alumina was immersed in a solution of the acid in CCl<sub>4</sub>

TABLE 5.2

ASSIGNMENT OF BANDS BELOW 2000 cm<sup>-1</sup> OBSERVED DURING  
THE ADSORPTION OF DEUTEROACETIC ACID ONTO RUTILE

Surface Treatment			Assignment
Oxidized		Reduced	
673 K	298 K	673 K	
1785		1785	Acetic acid vapour
1765		1765	
1725		1725	
1695	1695	1695	Physically adsorbed acetic acid
1670	1670		Lewis bonded acetic acid molecules
1650	1650		Physically adsorbed acetic acid
1630	1630	1630	C=O stretch in bidentate carbonate
1540	1540	1540	acetate ion on weak site
1515	1515	1515	acetate ion on strong site
1480	1480	1480	acetate ion on weak site
1440	1440	1440	acetate ion on strong site
1365	1365	1365	symmetric stretch unidentate carbonate
1340	1340	1340	asymmetric stretch bidentate carbonate
1320	1320	1320	

TABLE 6.1

BANDS OBSERVED IN THE RANGE 2000-1300  $\text{cm}^{-1}$   
AFTER THE ADSORPTION OF HEXAFLUOROACETONE  
ONTO A RUTILE SURFACE

OXIDIZED		REDUCED	
673	BT	673	BT
1810	1810	1810	1810
		1770	1770
		1740	1730
		1710	
1670		1660	
1640			
1615	1615		
1580	1580	1580	1580
1480	1480	1480	1480
		1460	1460
		1430	1430

TABLE 6.2

ASSIGNMENT OF BANDS OBSERVED DURING THE  
ADSORPTION OF HEXAFLUOROACETONE ONTO RUTILE

Band (cm <sup>-1</sup> )	Assignment
1810	$\nu$ C=O in hexafluoroacetone vapour
1770	$\nu$ C=O in hexafluoroacetone Lewis bonded to surface sites
1740	
1710	
1670	
1640	
1615	O=C=O asymmetric stretch in trifluoroacetate species adsorbed on surface
1580	
1480	O=C=O symmetric stretch in trifluoroacetate species
1460	Surface carbonate species
1430	

APPENDIX II

FIGURES

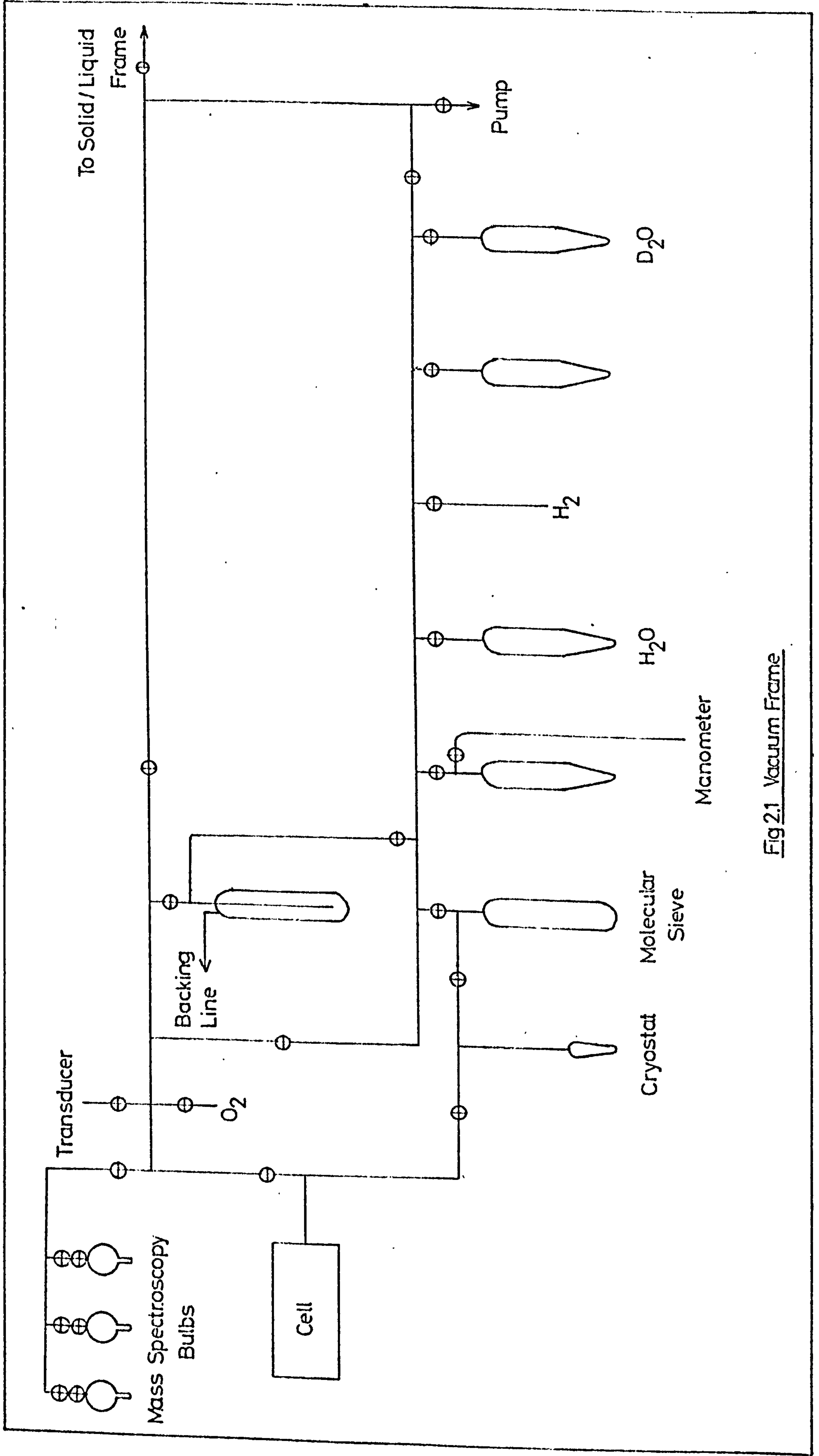


Fig 2.1 Vacuum Frame

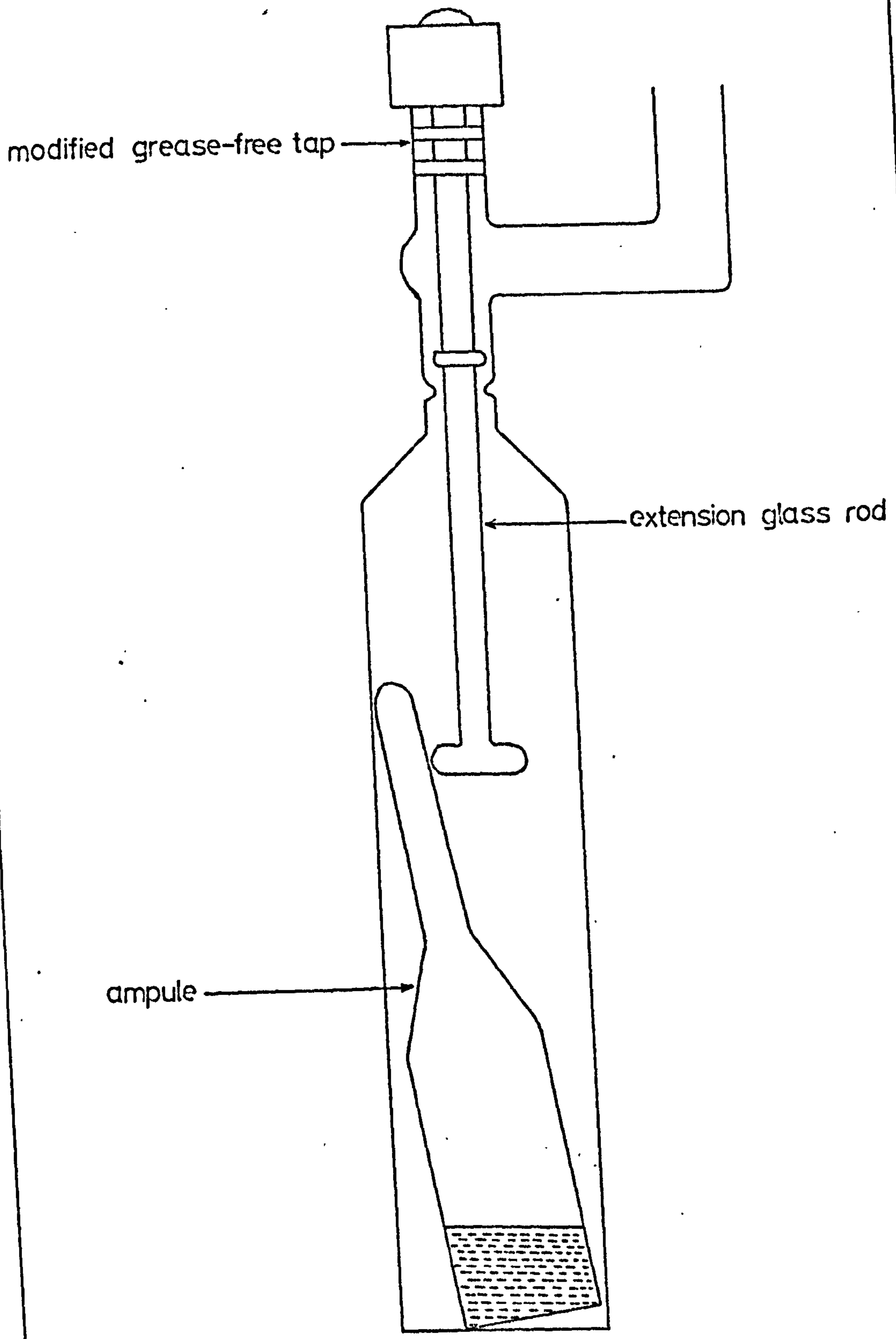


Fig 2.2 Ampule Breaker

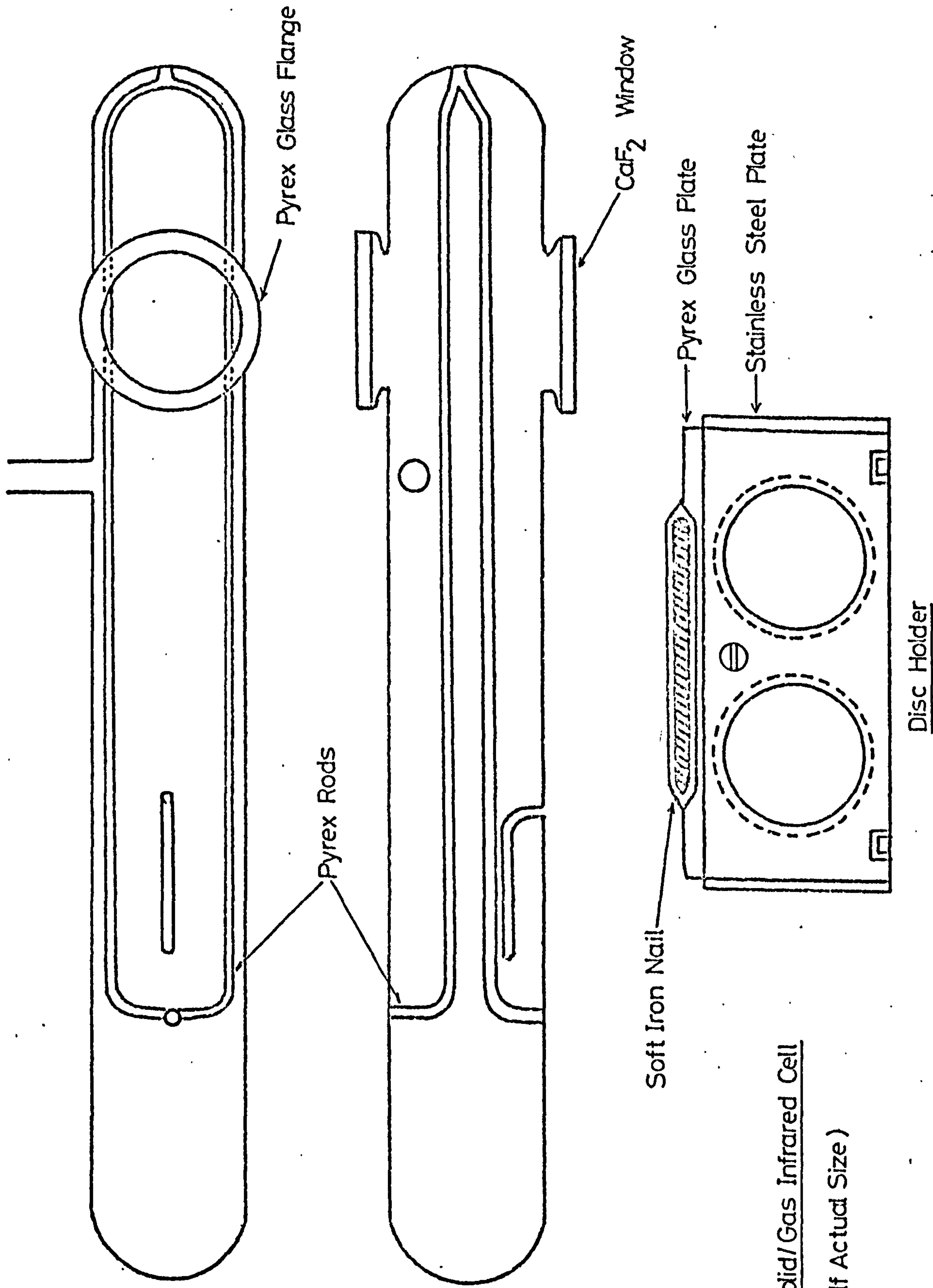


Fig 2.3 Solid/Gas Infrared Cell  
 (Half Actual Size)



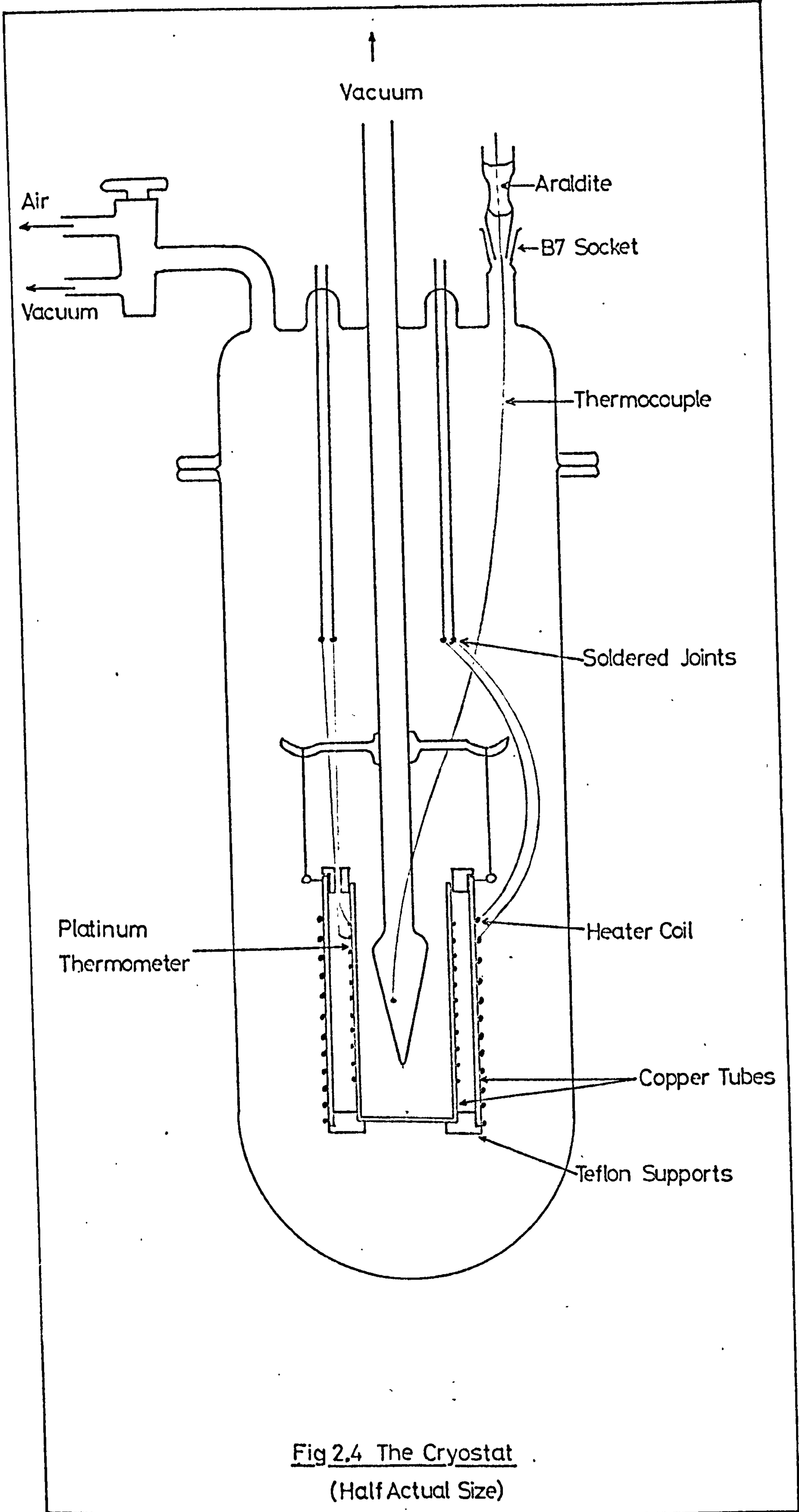
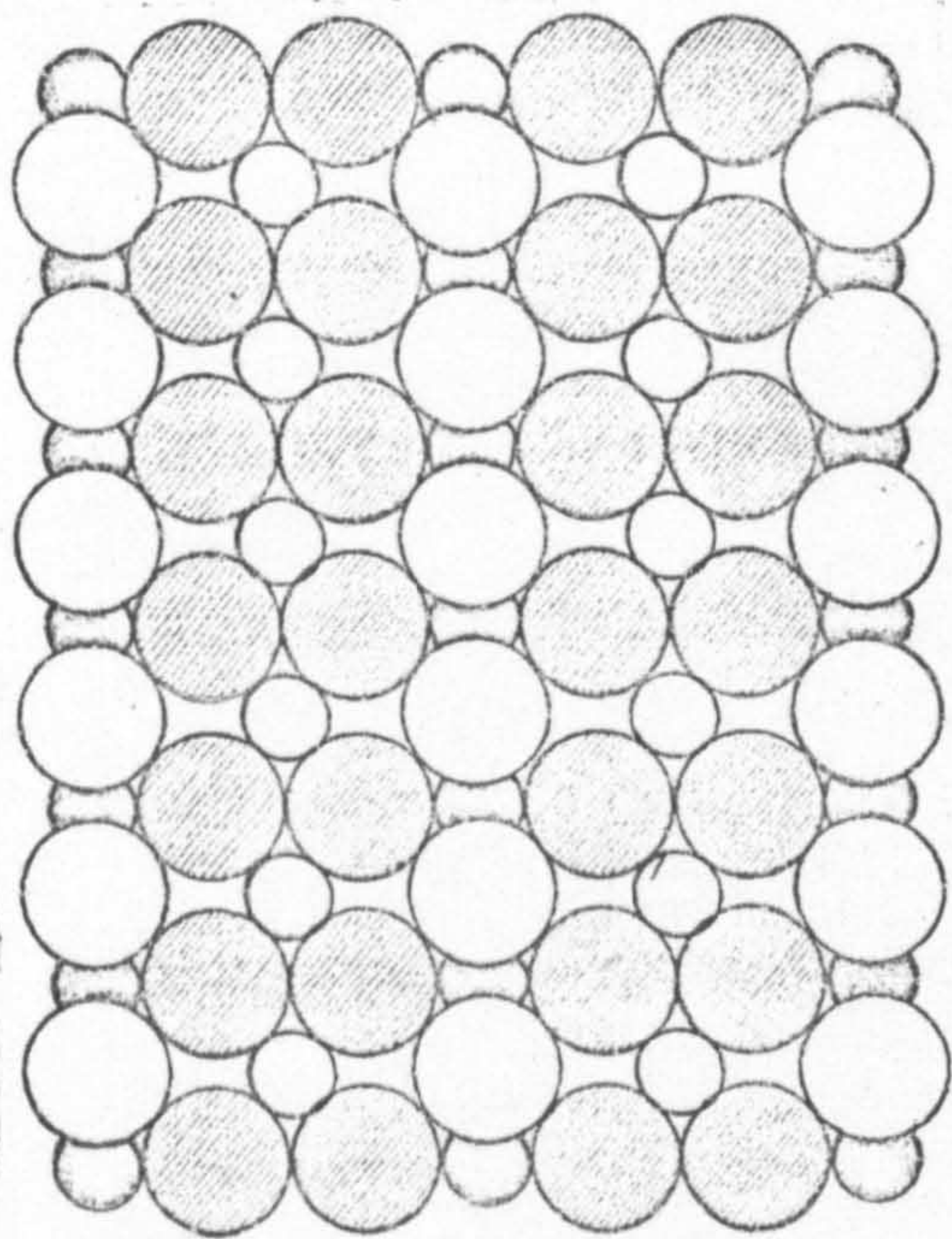

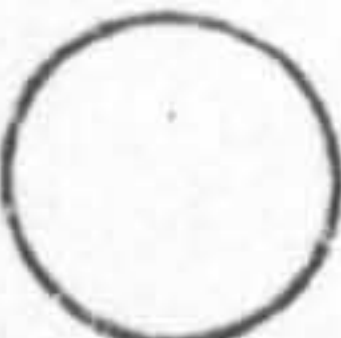
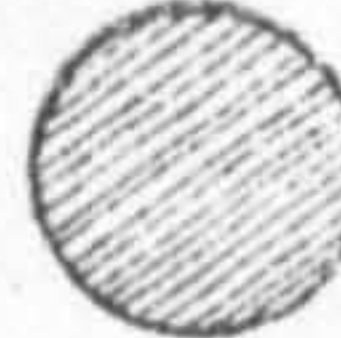


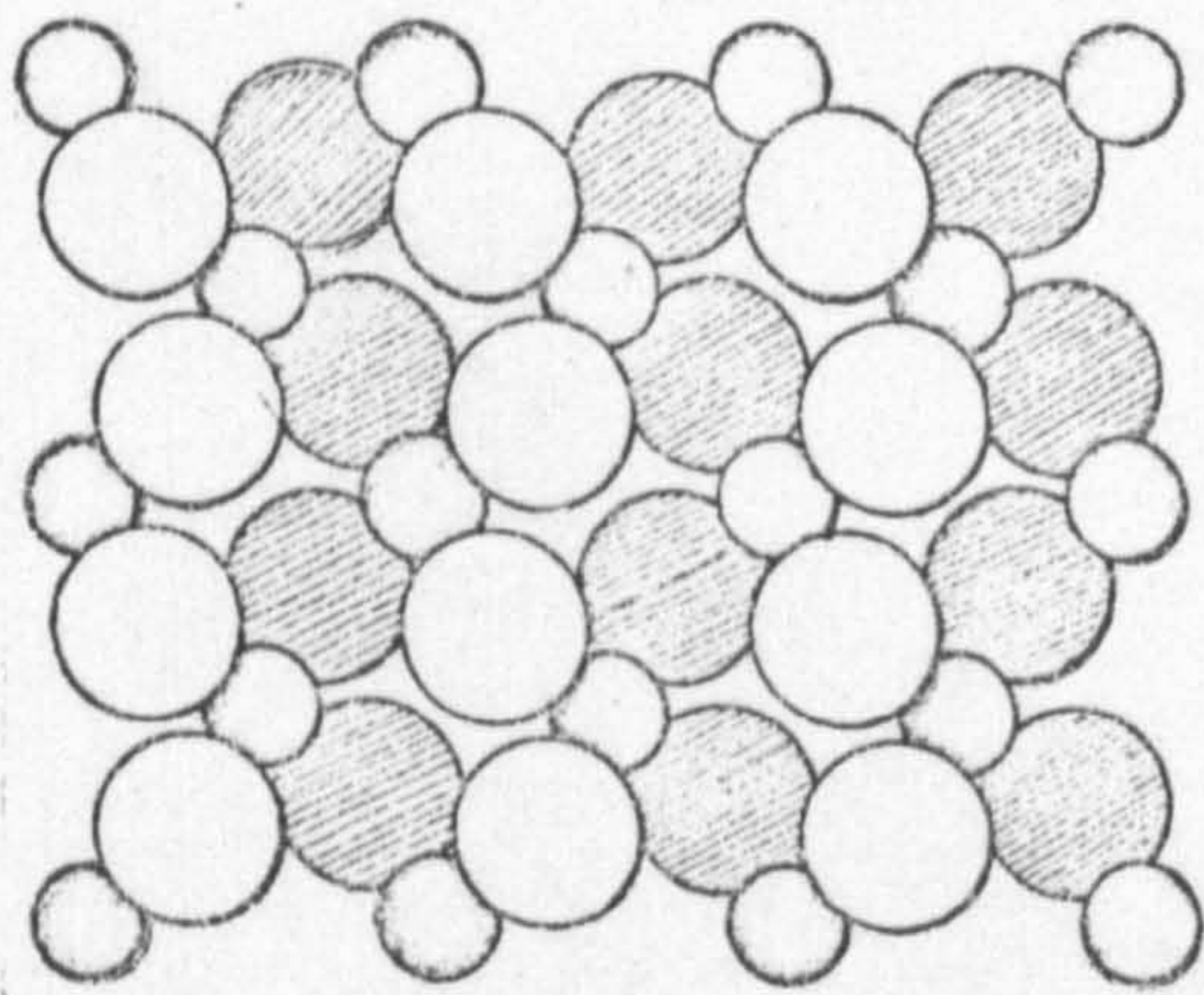
Fig 2.4 The Cryostat  
(Half Actual Size)



(110)

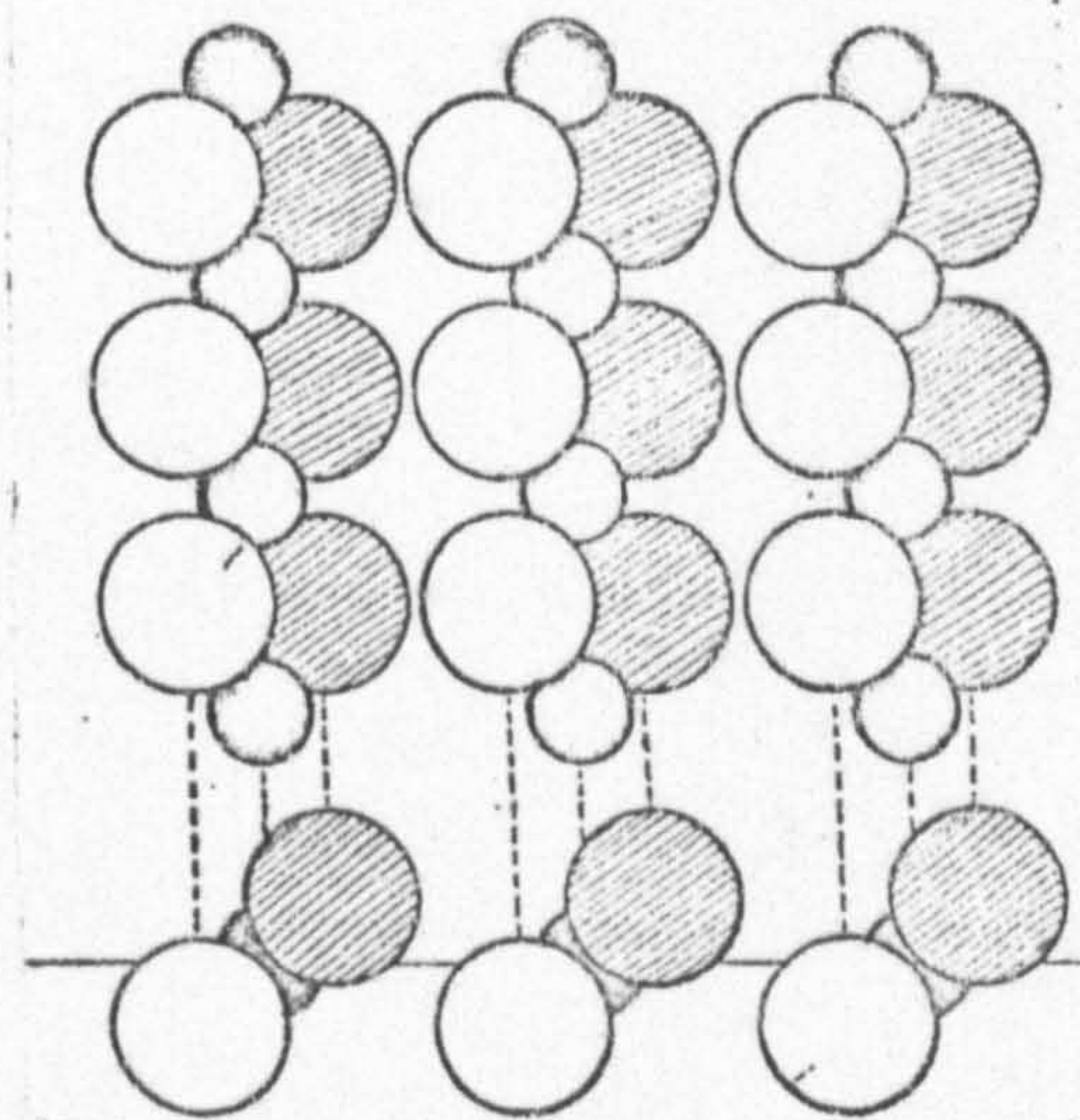
31

-  Ti ions
-  O ions above plane of Ti ions
-  O ions on, or below, plane of Ti ions



(101)

32



(100)

33

Fig 3 The Cleavage Planes of Rutile

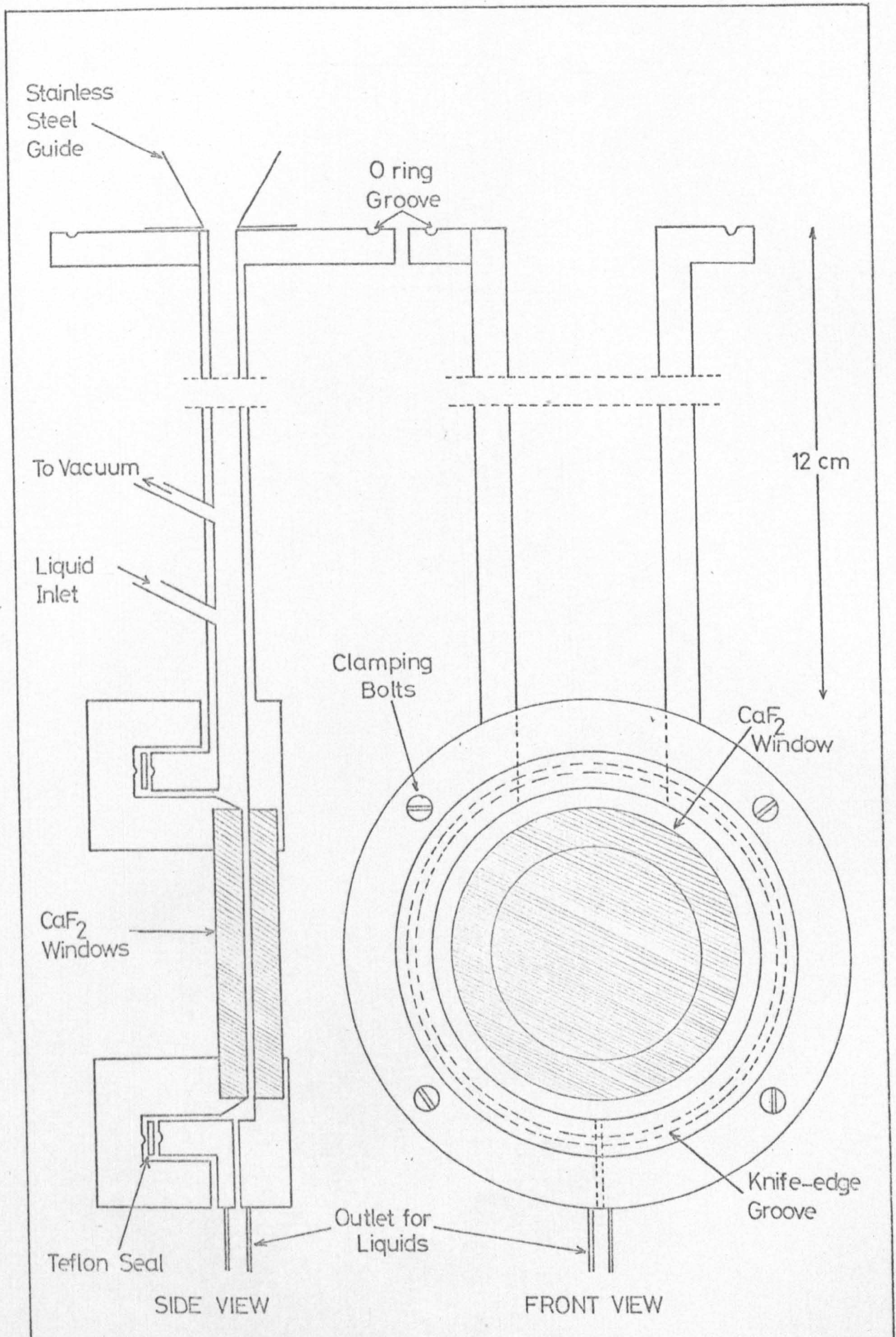


Fig 8.1 The Solid/Liquid Infrared Cell  
(Actual Size)

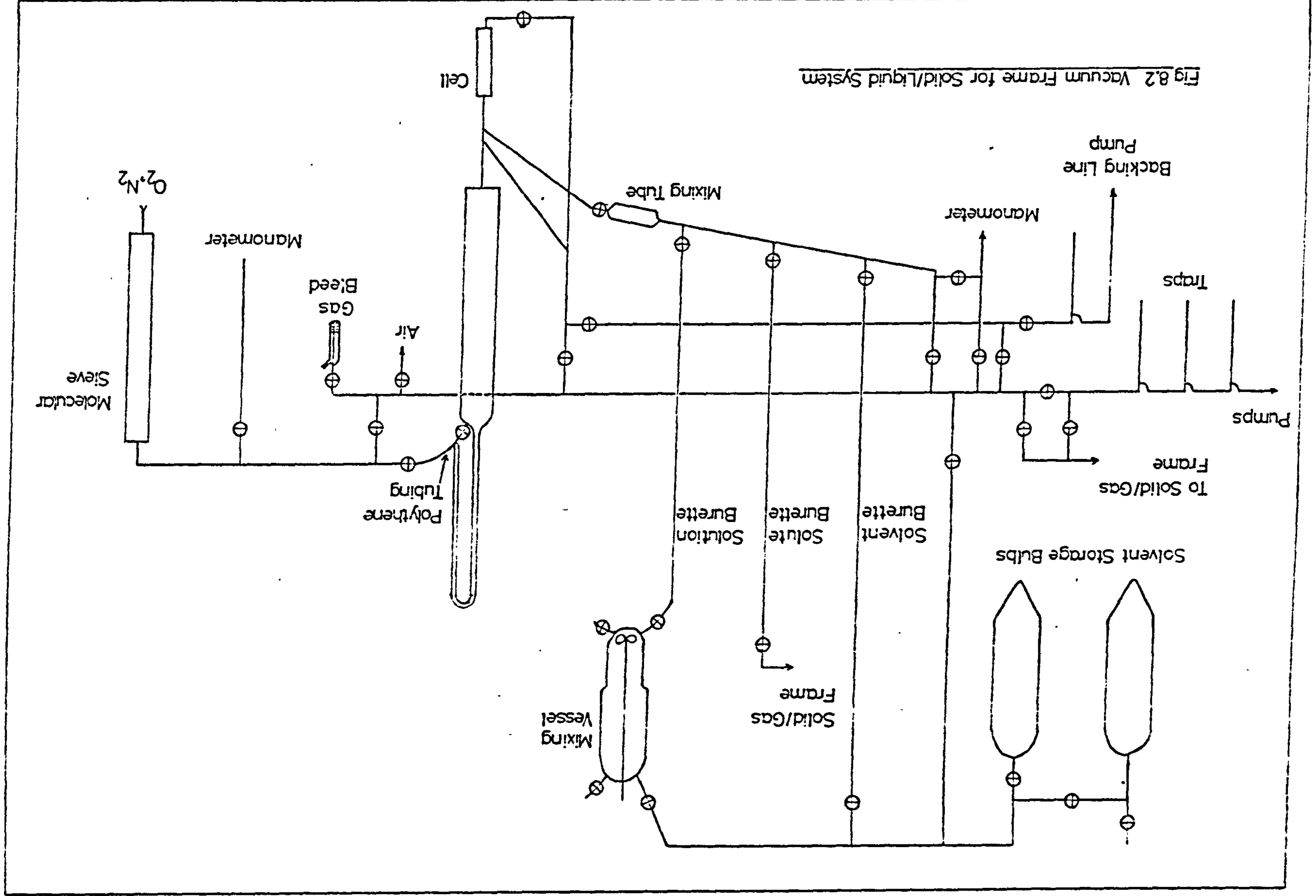


Fig 8.2 Vacuum Frame for Solid/Liquid System

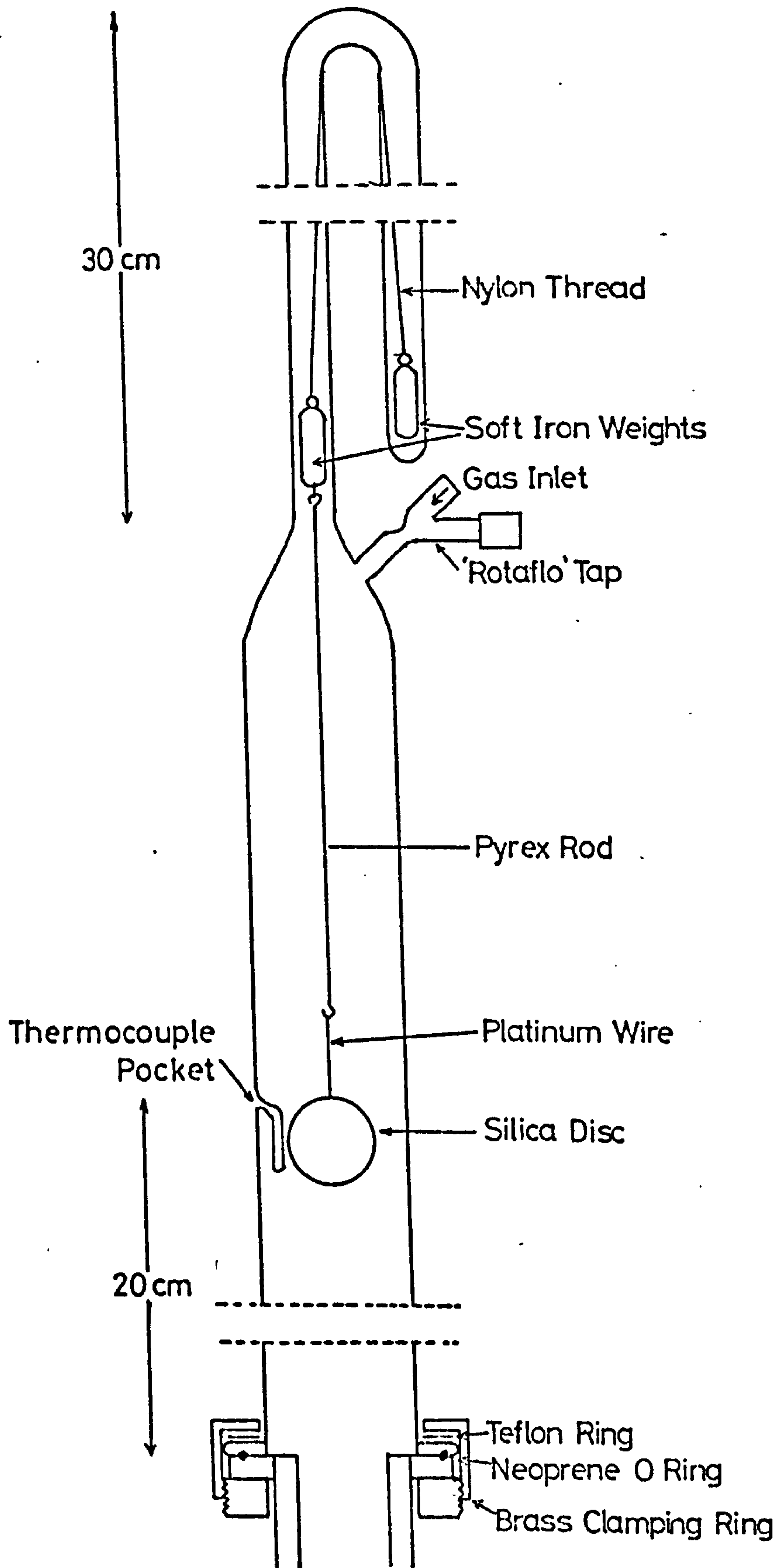


Fig 8.3 Disc Lifting System  
(Half Actual Size)

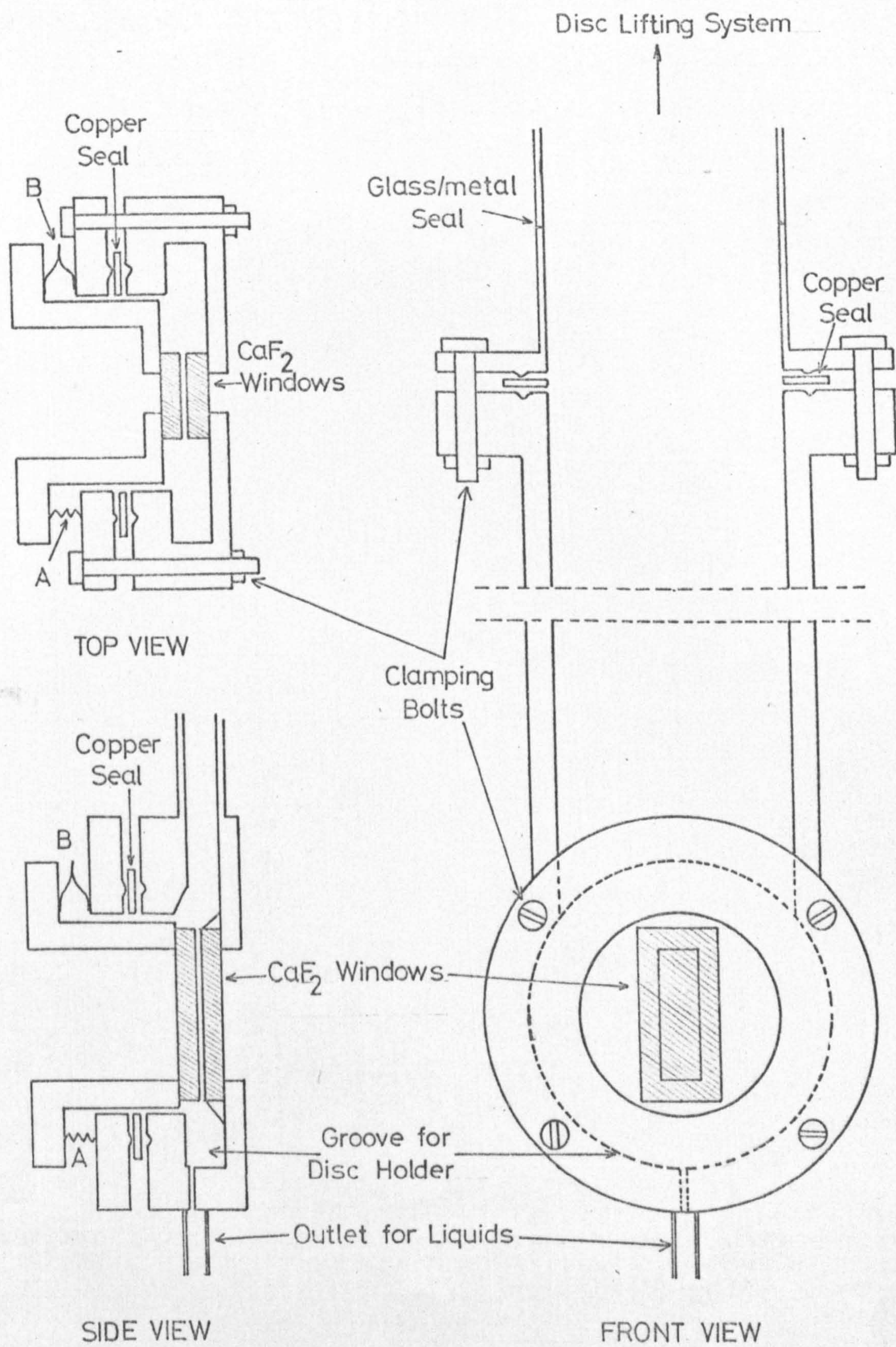


Fig 8.4 Proposed Variable Path Length Cell for use with Discs

(Actual Size)

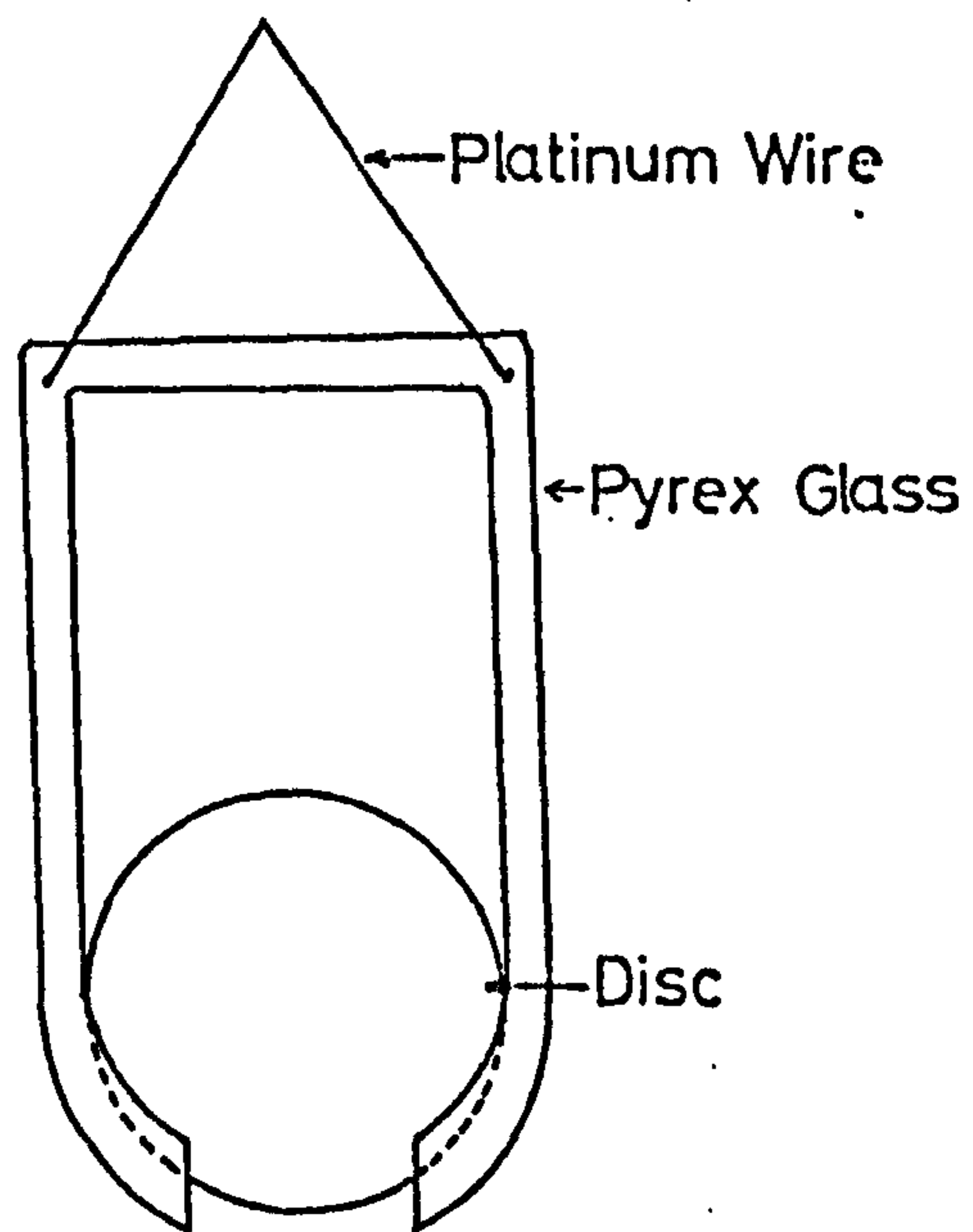


Fig 8.5 Proposed Disc Holder

(Actual size)

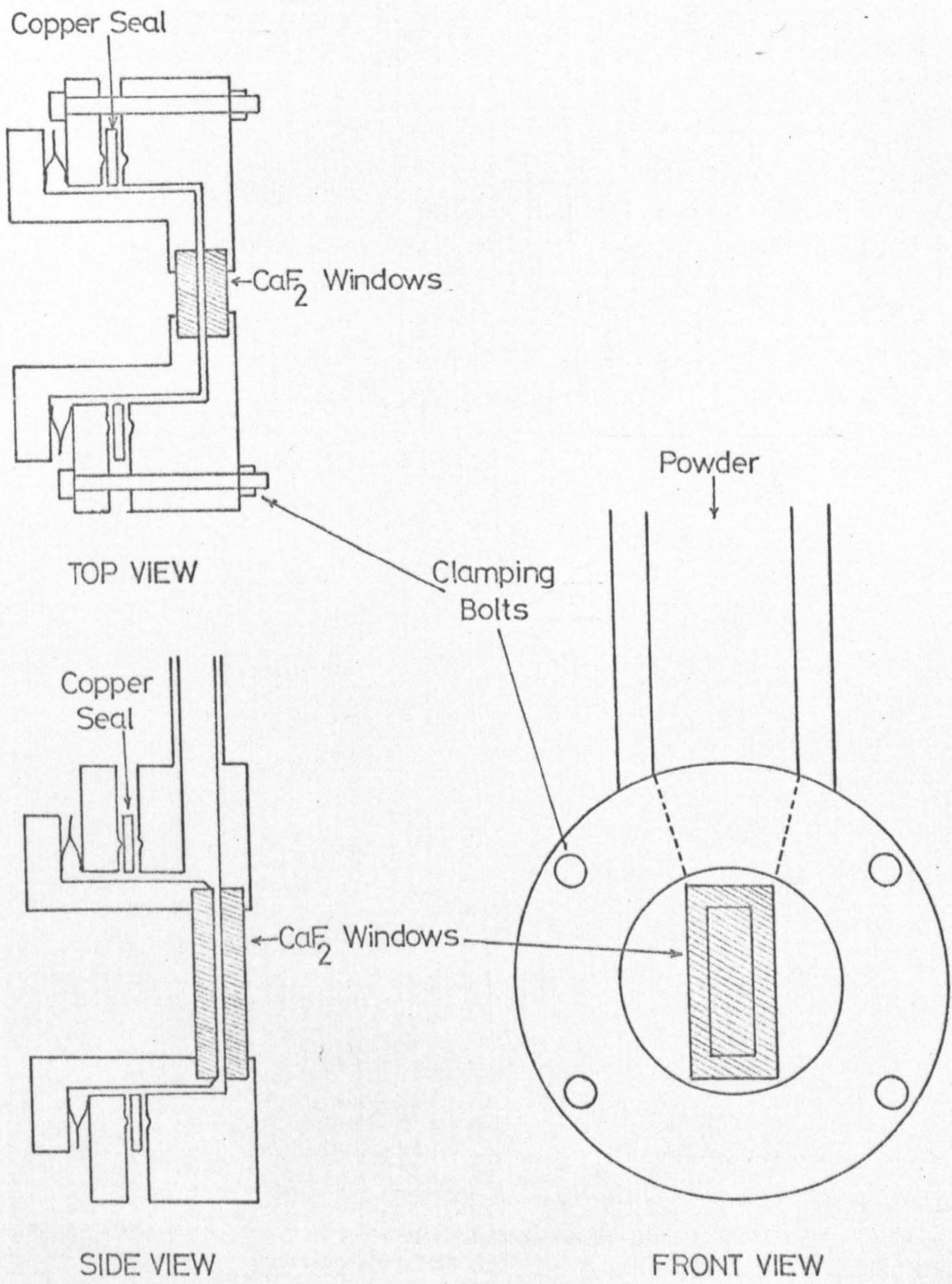


Fig 8.6 Proposed Variable Path Length Cell for use with Powders

(Actual Size)



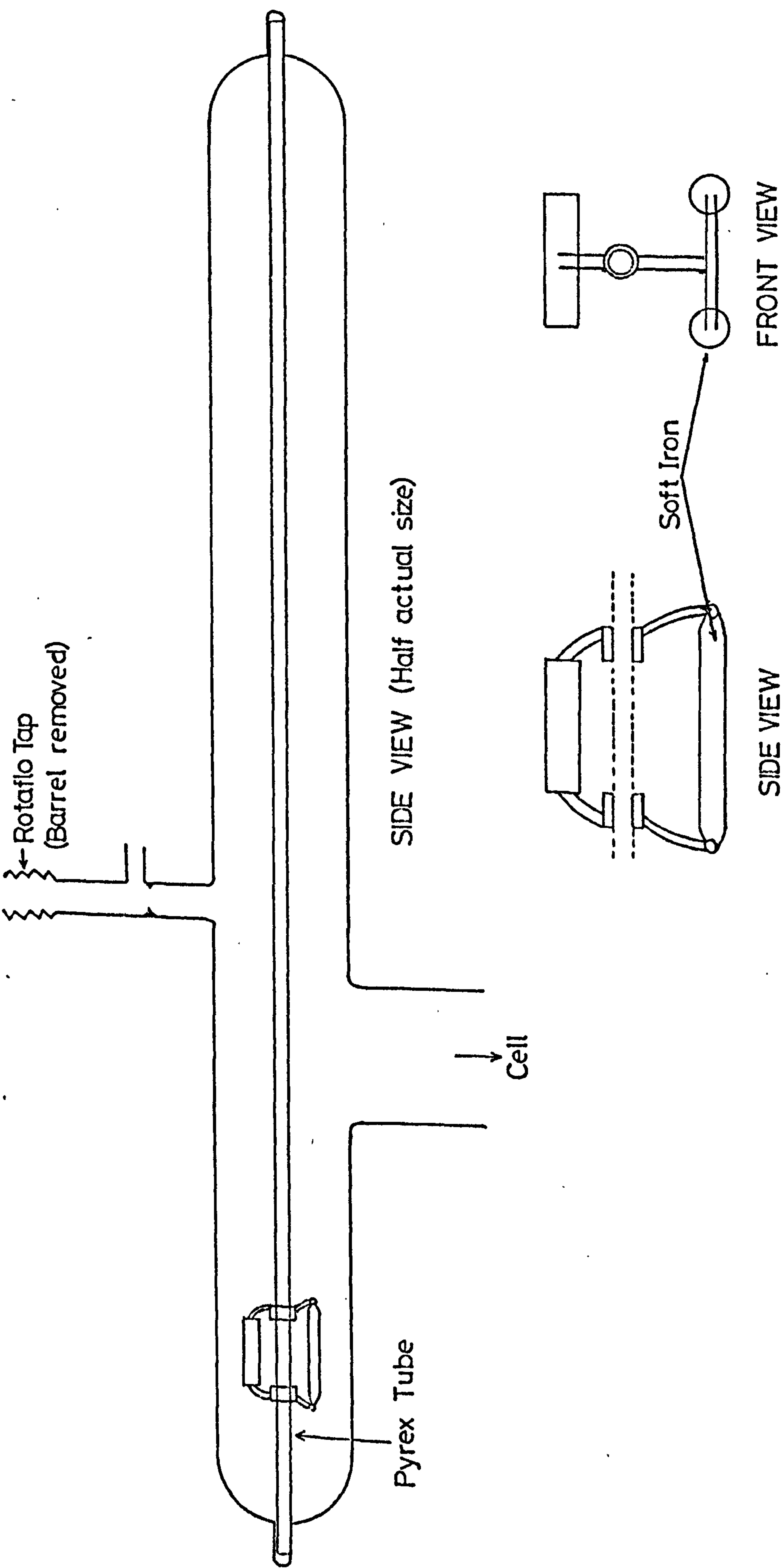


Fig 8.7 Apparatus for transferring Powders under vacuum

Truck (actual size)

APPENDIX III

SPECTRA

SPEC. 2

.....

.....  
.....  
.....

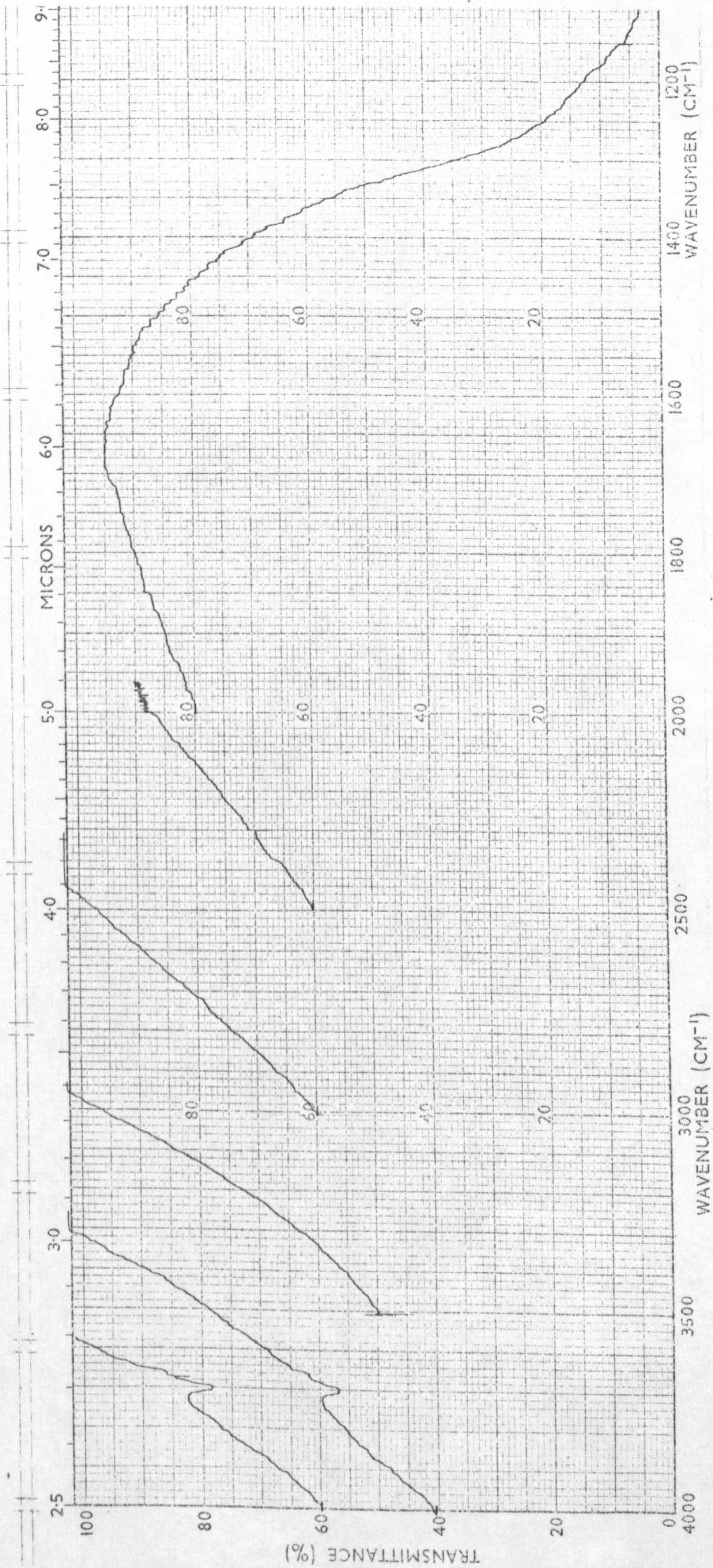
.....  
.....  
.....  
.....

.....  
.....  
.....  
.....

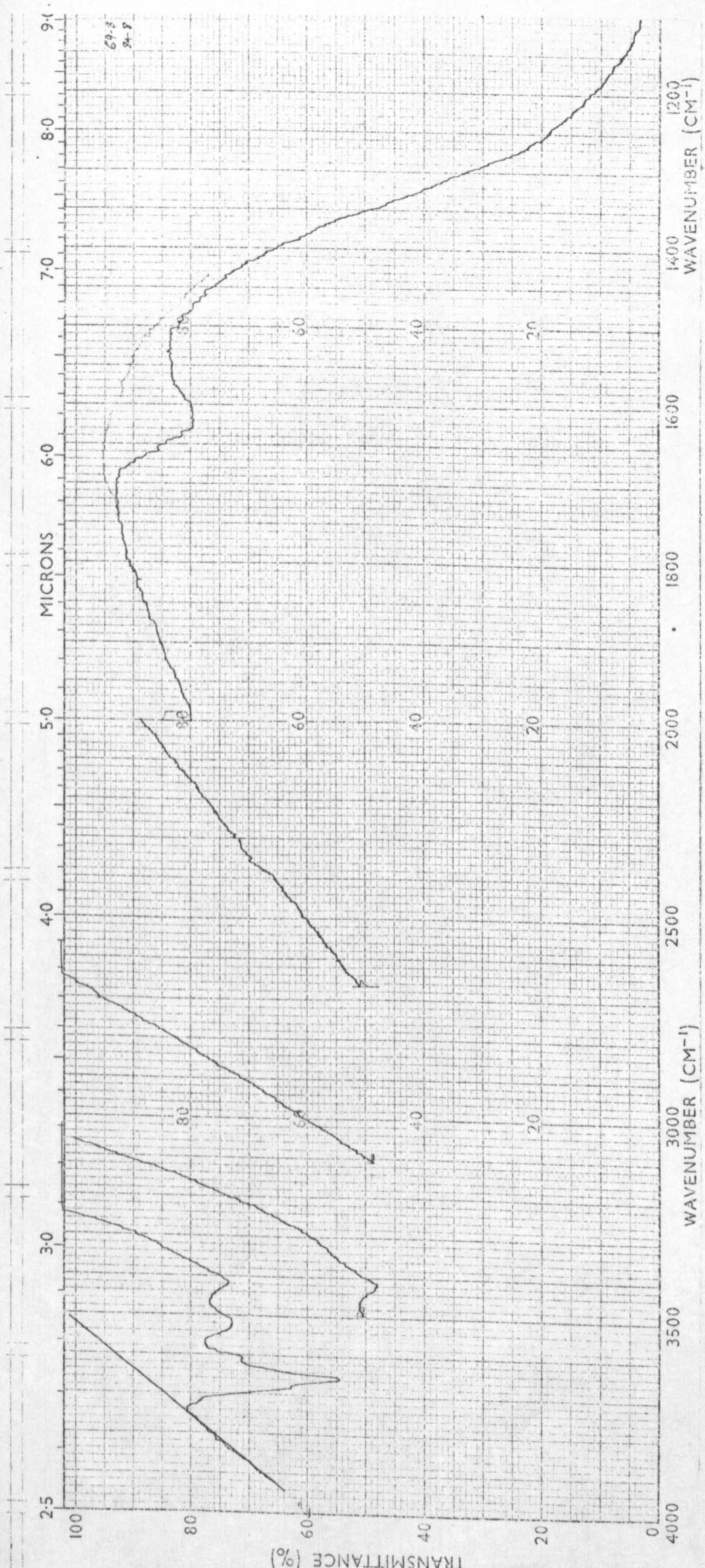
SPEC. 2

SPECTRA OF INITIAL SURFACES AS  
RECORDED ON THE SPECTROMETER

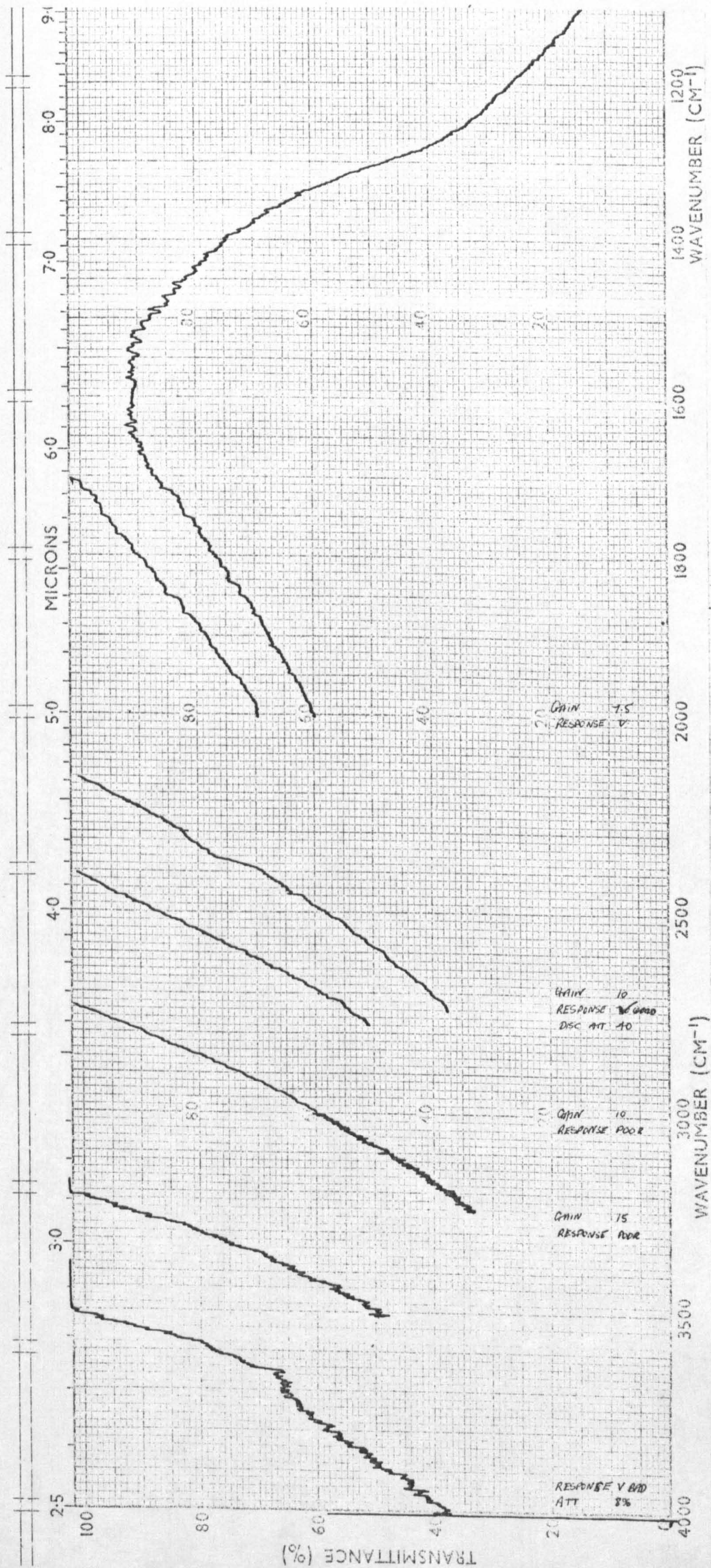
- 2.1 673 K (400°C) H<sub>2</sub>O Oxidized Surface
- 2.2 BT H<sub>2</sub>O Oxidized Surface
- 2.3 673 K (400°C) H<sub>2</sub>O Reduced Surface
- 2.4 BT D<sub>2</sub>O Reduced Surface



SPEC. 2.1 A 673 K H<sub>2</sub>O OXIDIZED SURFACE



SPEC. 2.2 A BT H<sub>2</sub>O OXIDIZED SURFACE



SPEC. 2.3 A 673 K H<sub>2</sub>O REDUCED SURFACE



SPEC. 2.4 A BT D<sub>2</sub>O REDUCED SURFACE





SPEC. 3.1

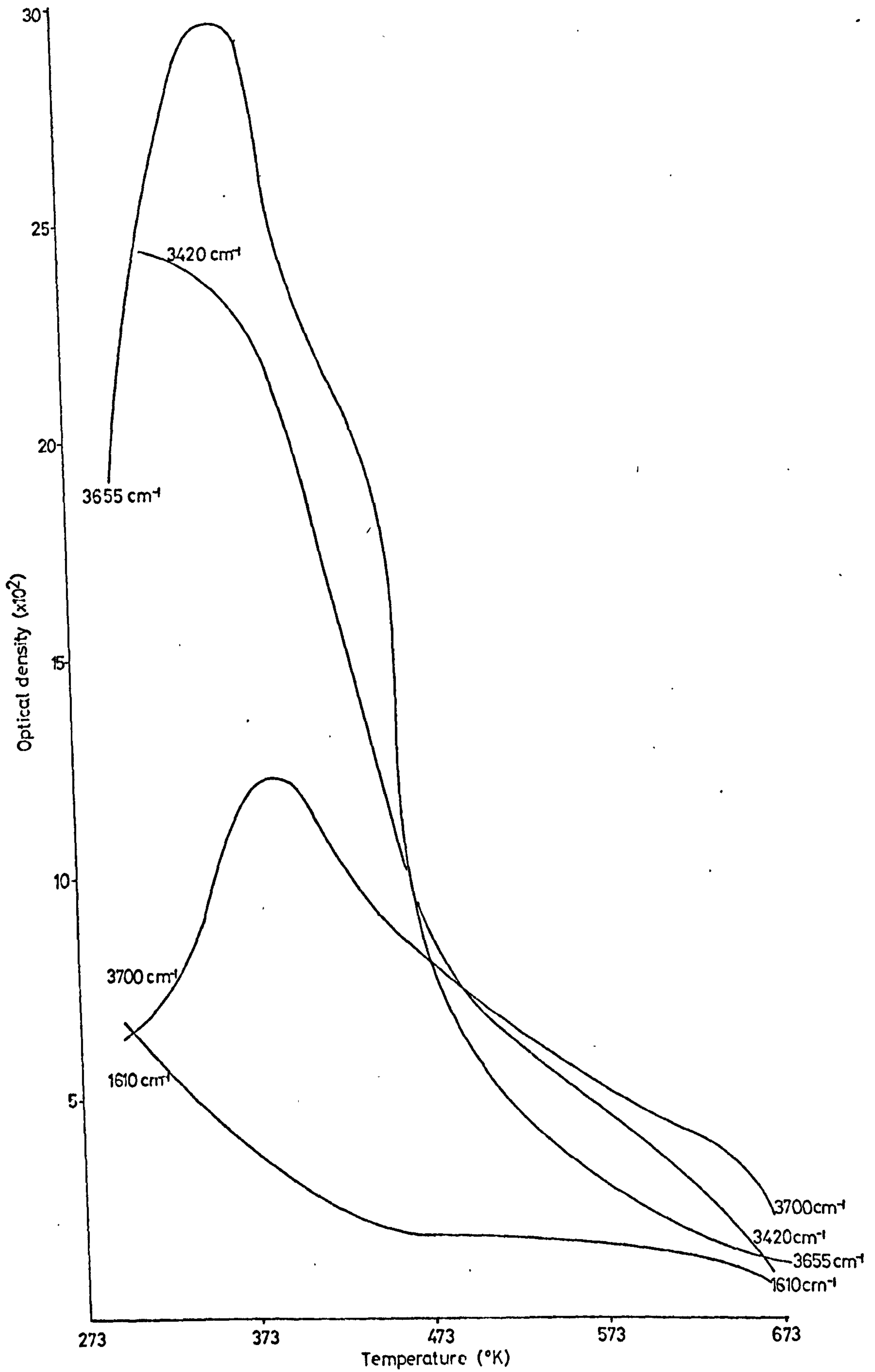
DESORPTION OF H<sub>2</sub>O FROM A BT, H<sub>2</sub>O

OXIDIZED SURFACE

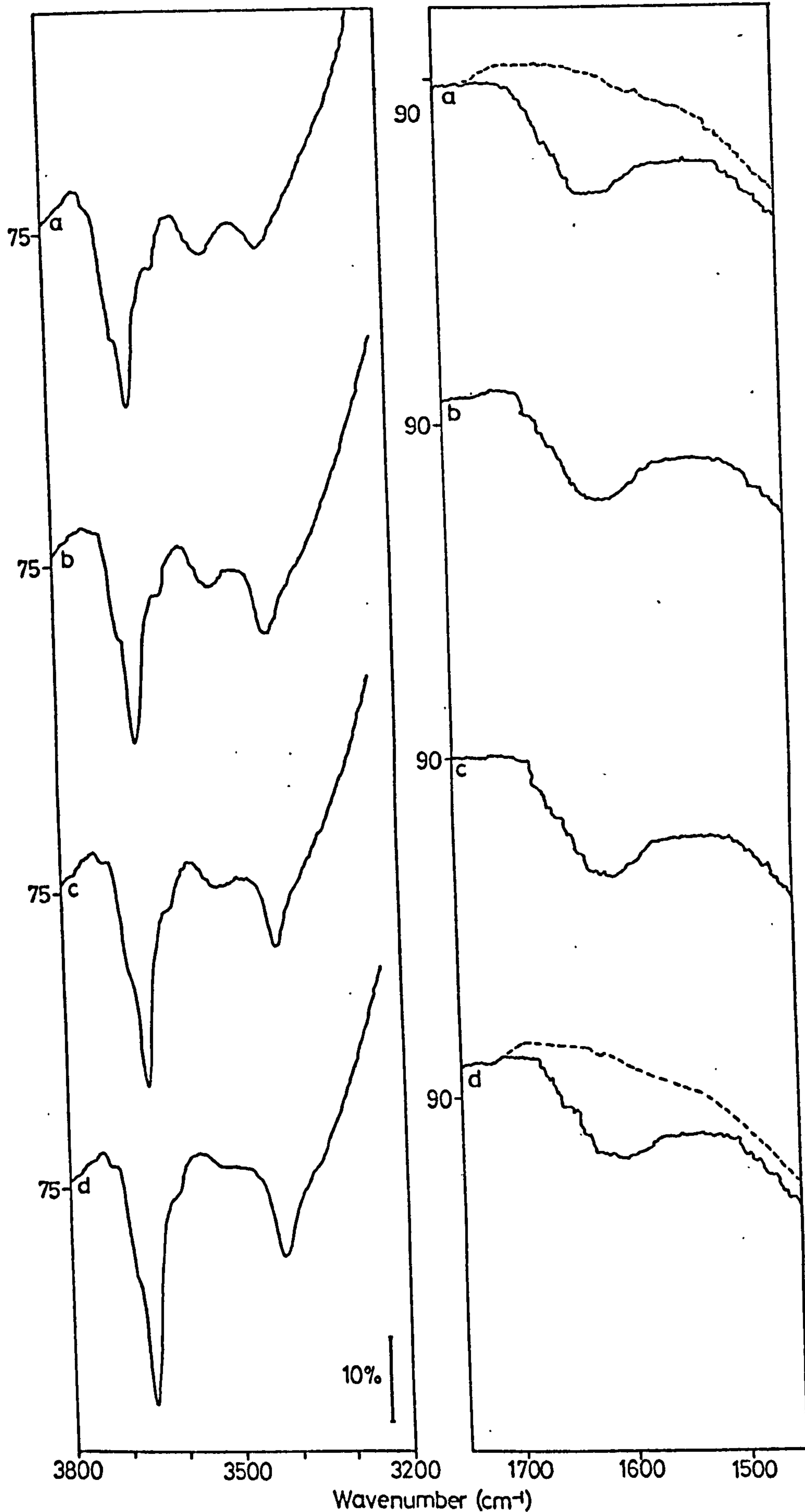
(a) Initial Surface before heating in H<sub>2</sub>O.

Spectra after heating in H<sub>2</sub>O (673 K, 5h) and evacuating  
at:-

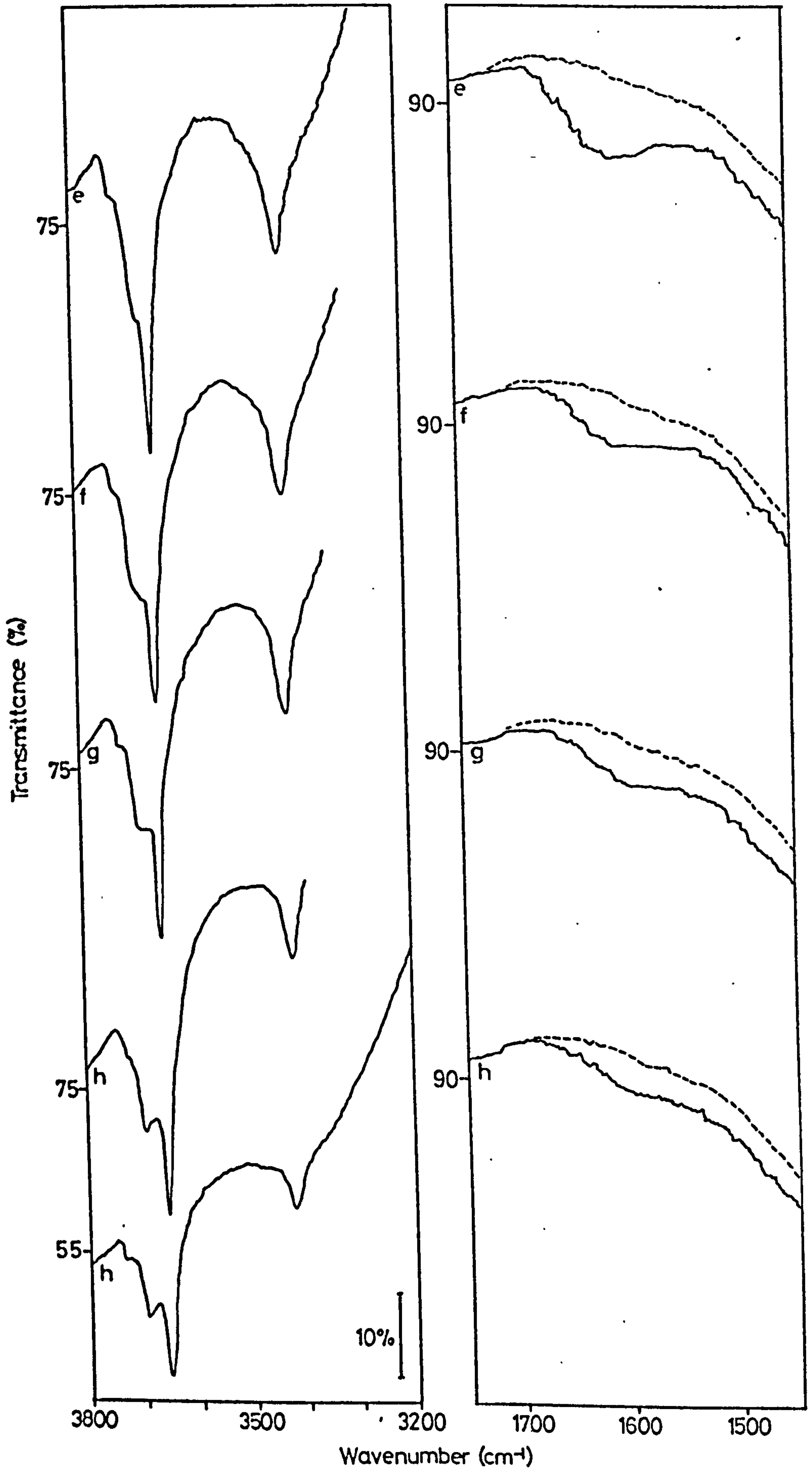
(b)	298 K, 14h	(c)	BT, ½h
(d)	331 K, 18h	(e)	368 K, 9h
(f)	393 K, 12h	(g)	423 K, 16h
(h)	455 K, 6h	(i)	461 K, 15h
(j)	473 K, 8h	(k)	481 K, 13h
(l)	503 K, 7h	(m)	523 K, 12h
(n)	573 K, 9h	(o)	623 K, 8h
(p)	663 K, 13h		



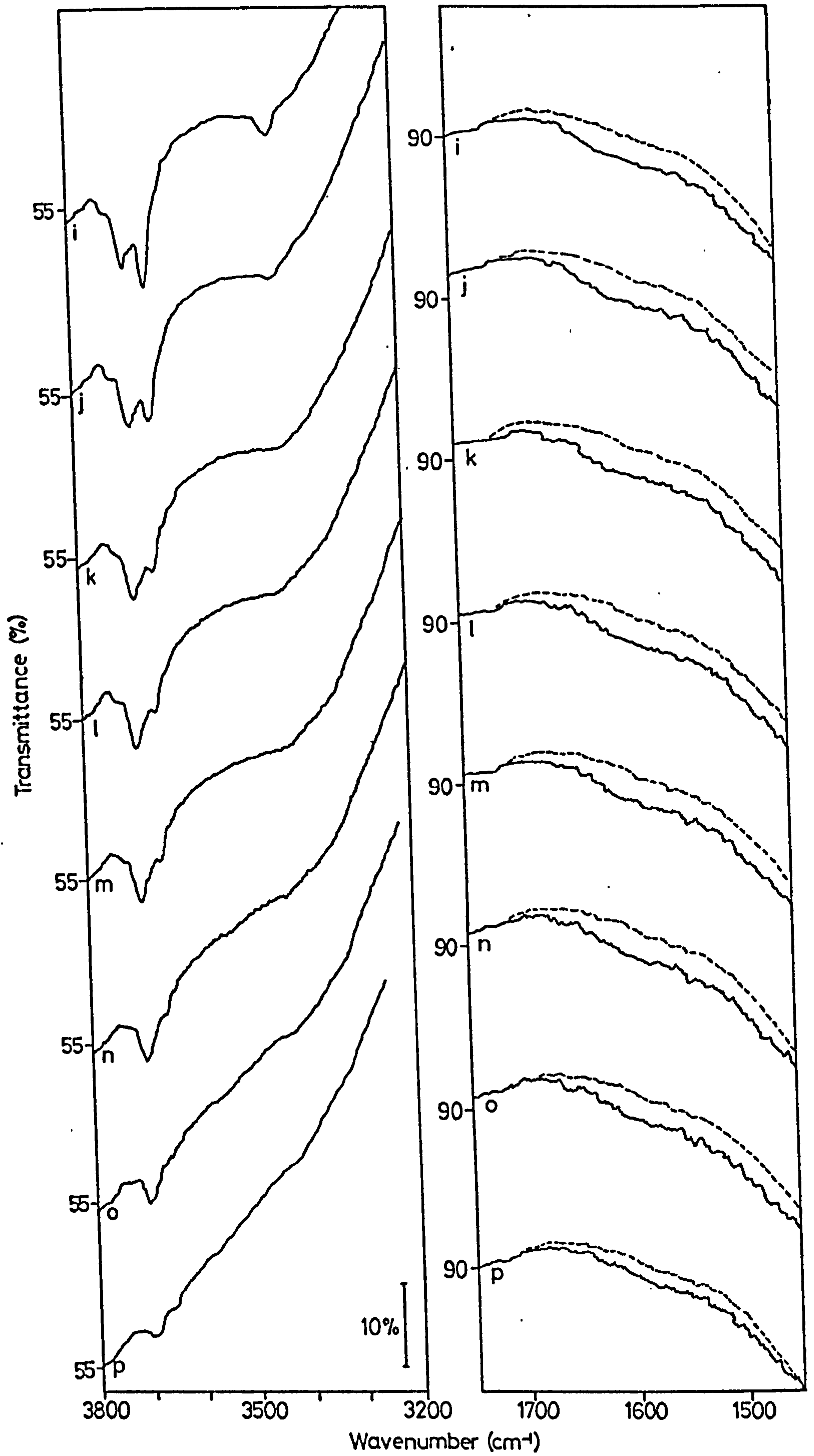
Graph 3.1 Desorption of H<sub>2</sub>O from a BT H<sub>2</sub>O Oxidized Surface



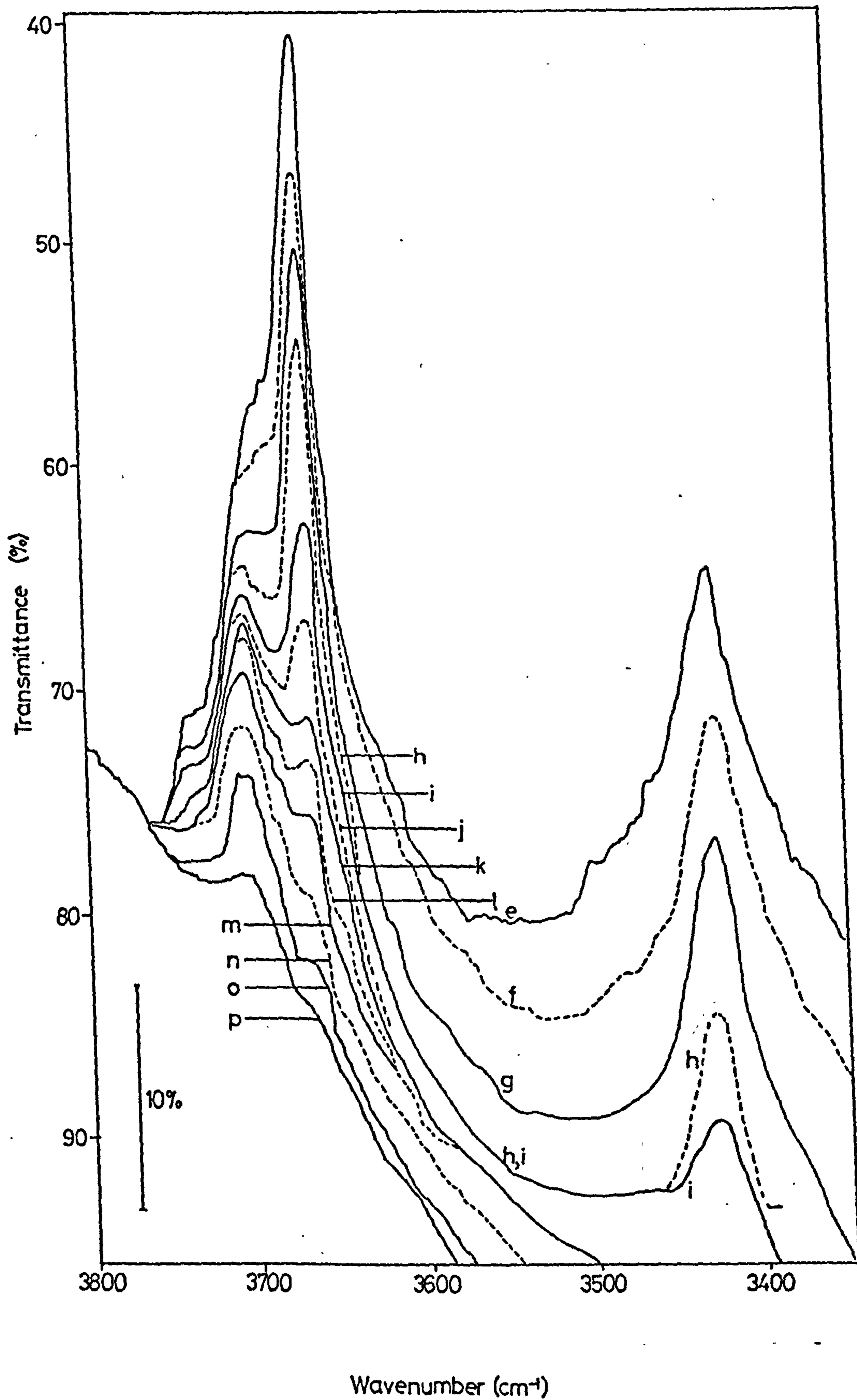
Spec. 3.1 Desorption of H<sub>2</sub>O from a BT, H<sub>2</sub>O, Oxidized Surface



Spec. 31 Desorption of H<sub>2</sub>O from a BT, H<sub>2</sub>O, Oxidized Surface



Spec. 31 Desorption of H<sub>2</sub>O from a BT, H<sub>2</sub>O, Oxidized Surface



Spec. 3.1 Desorption of H<sub>2</sub>O from a BT, H<sub>2</sub>O, Oxidized Surface

SPEC. 3.2



SPEC. 3.2

DESORPTION OF H<sub>2</sub>O FROM A BT, H<sub>2</sub>O  
OXIDIZED, SINTERED SURFACE

(a) Initial surface

Spectra after evacuating at:-

(b) 338 K, 14h

(c) 383 K, 21h

(d) 398 K, 6h

(e) 418 K, 14h

(f) 443 K, 6h

(g) 458 K, 15h

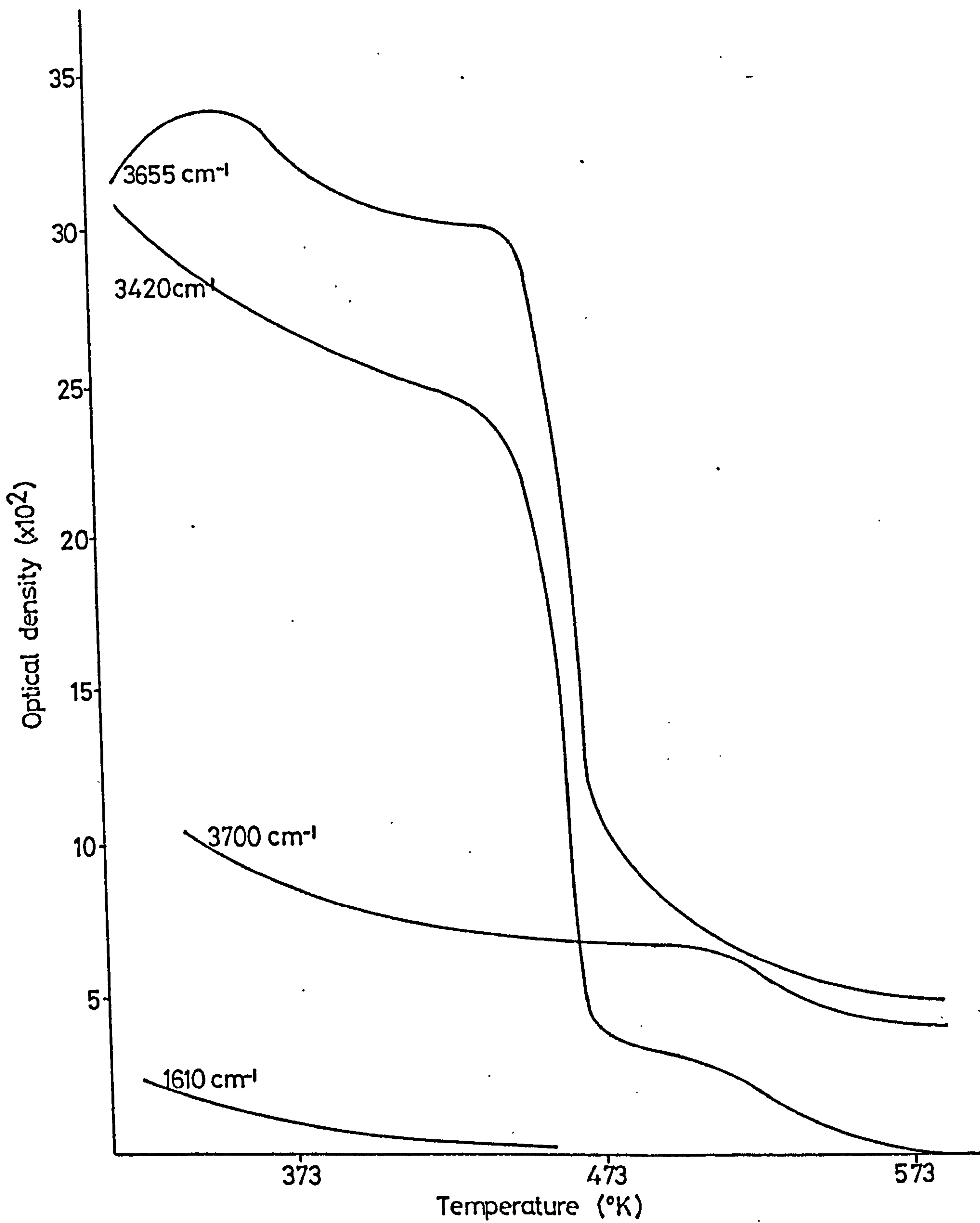
(h) 468 K, 6h

(i) 478 K, 14h

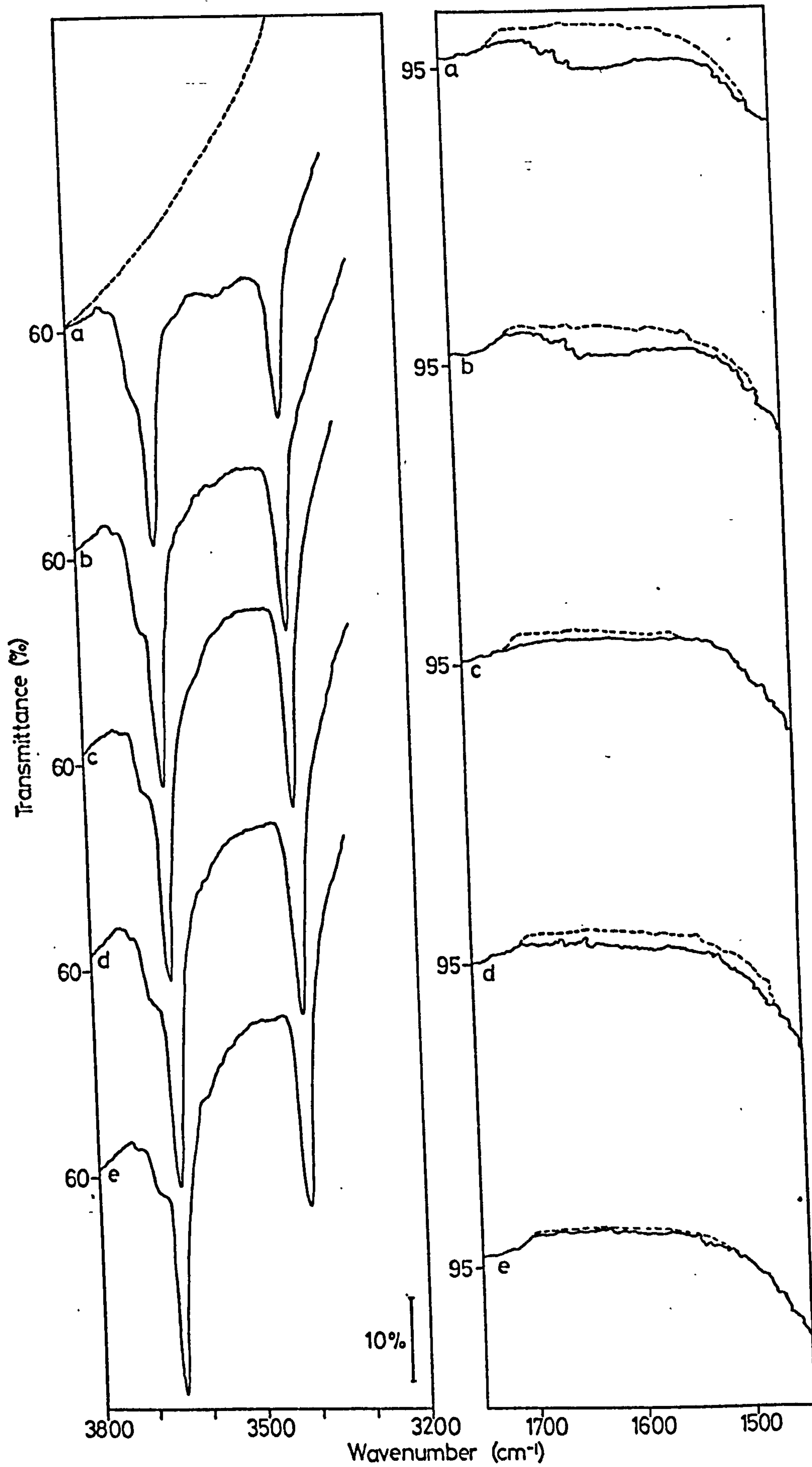
(j) 503 K, 6h

(k) 520 K, 15h

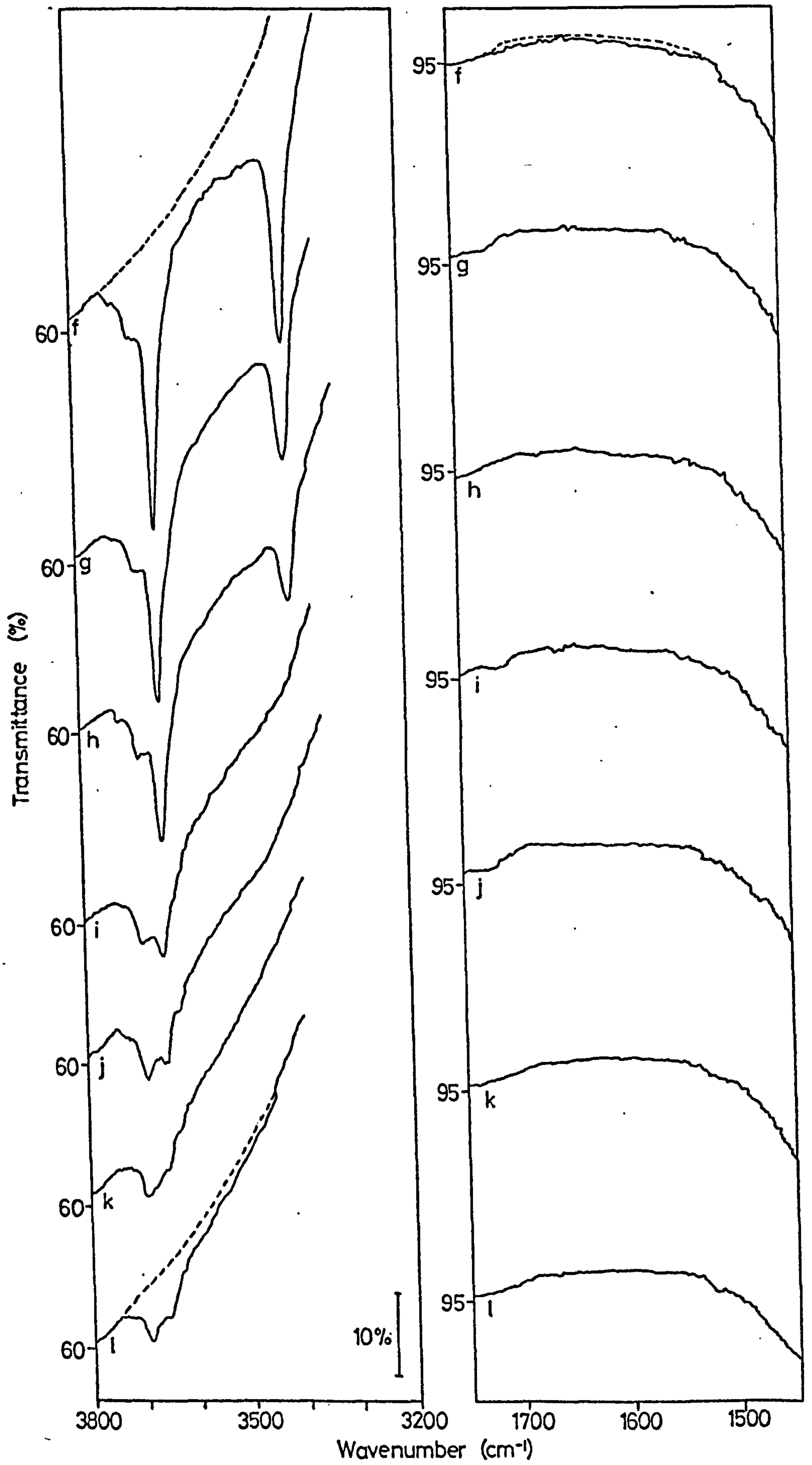
(l) 583 K, 6h



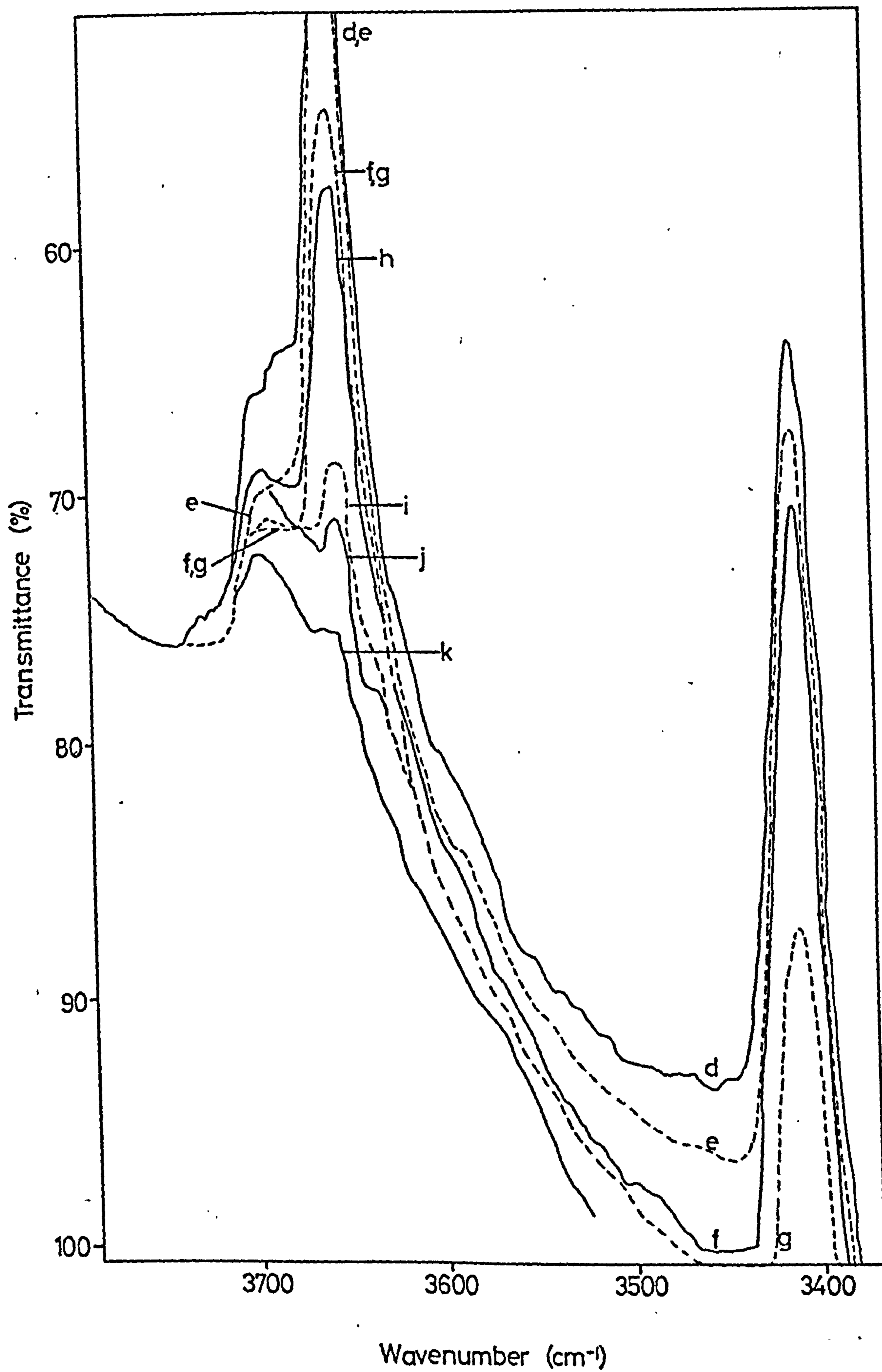
Graph 32 Desorption of H<sub>2</sub>O from a BT H<sub>2</sub>O Oxidized Sintered Surface



Spec 3.2 Desorption of H<sub>2</sub>O from a BT, H<sub>2</sub>O, Oxidized, Sintered, Surface



Spec 3.2 Desorption of H<sub>2</sub>O from a BT, H<sub>2</sub>O, Oxidized, Sintered, Surface



Spec 3.2 Desorption of H<sub>2</sub>O from a BT, H<sub>2</sub>O, Oxidized, Sintered, Surface

SPEC. 3.3

SPEC. 3.3

ADSORPTION OF H<sub>2</sub>O ONTO A 673 K (400°C)

OXIDIZED SURFACE

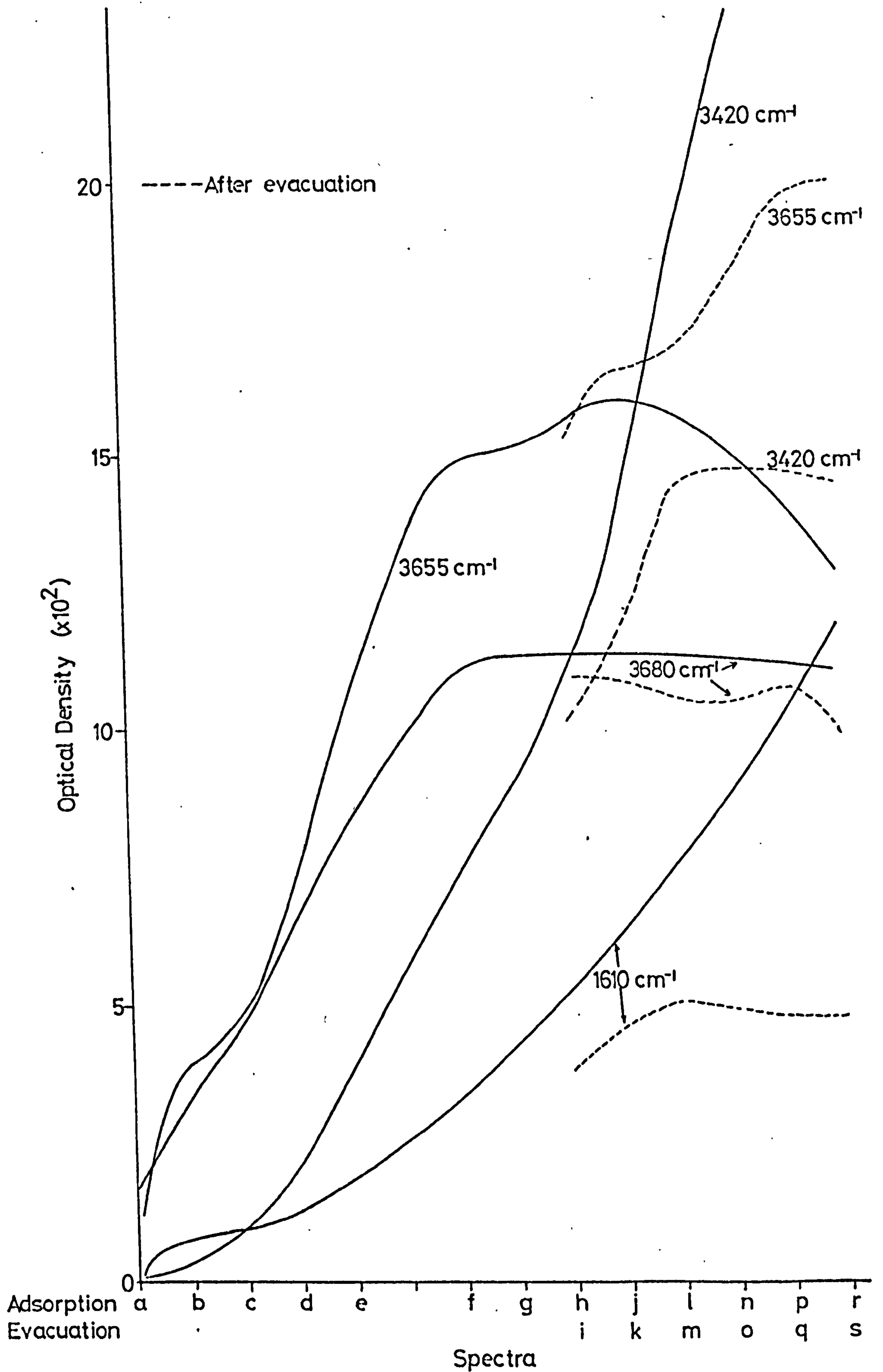
(a) Initial Surface

(b) - (h) adsorption of H<sub>2</sub>O at increasing pressures

(i) evacuation BT, 1h

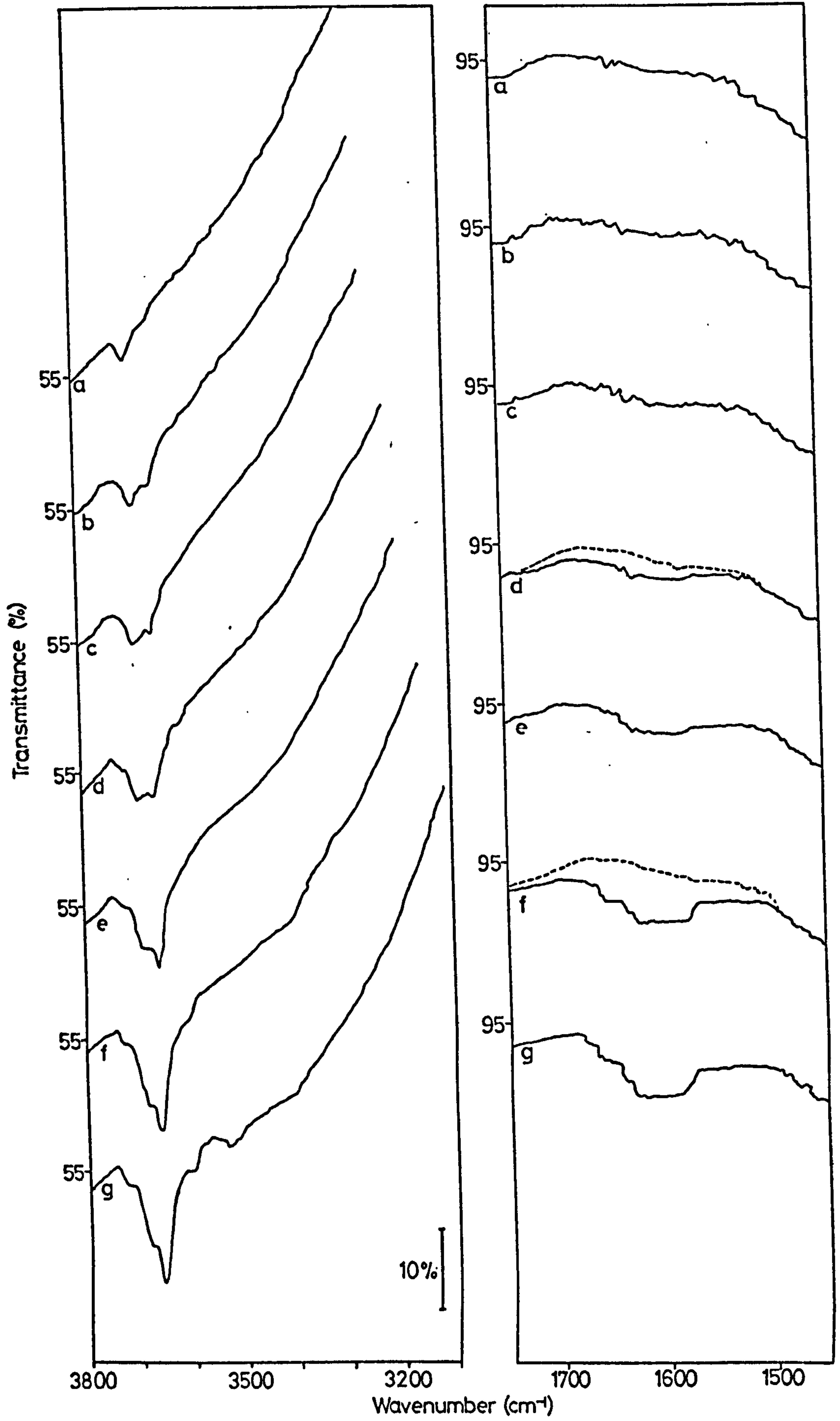
(j), (l), (n), (o), (q), (r) adsorption of H<sub>2</sub>O at increasing pressures

(k), (m), (p), (s) evacuation, BT

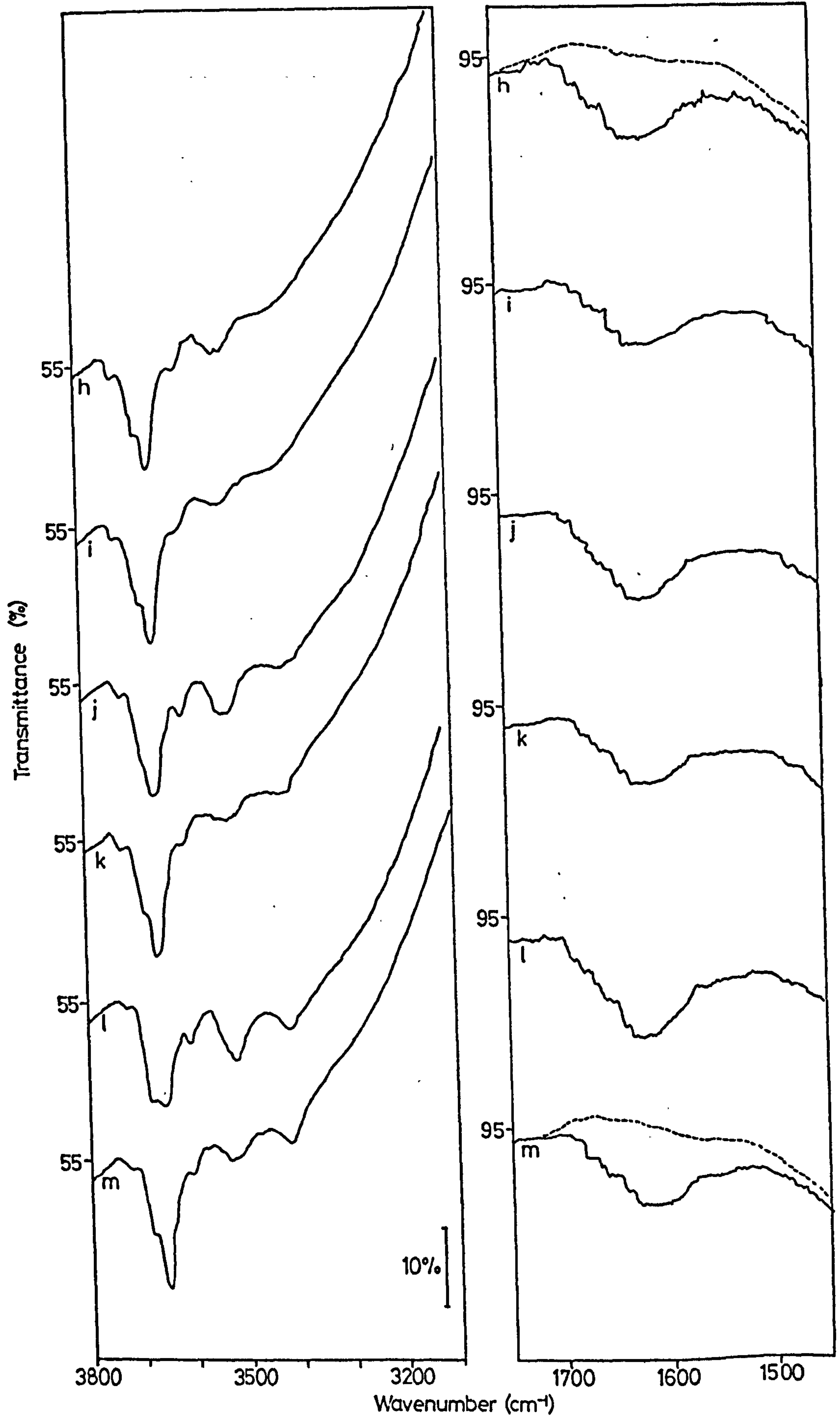


Graph 3.3 Adsorption of  $\text{H}_2\text{O}$  onto a 673 K Oxidized Surface

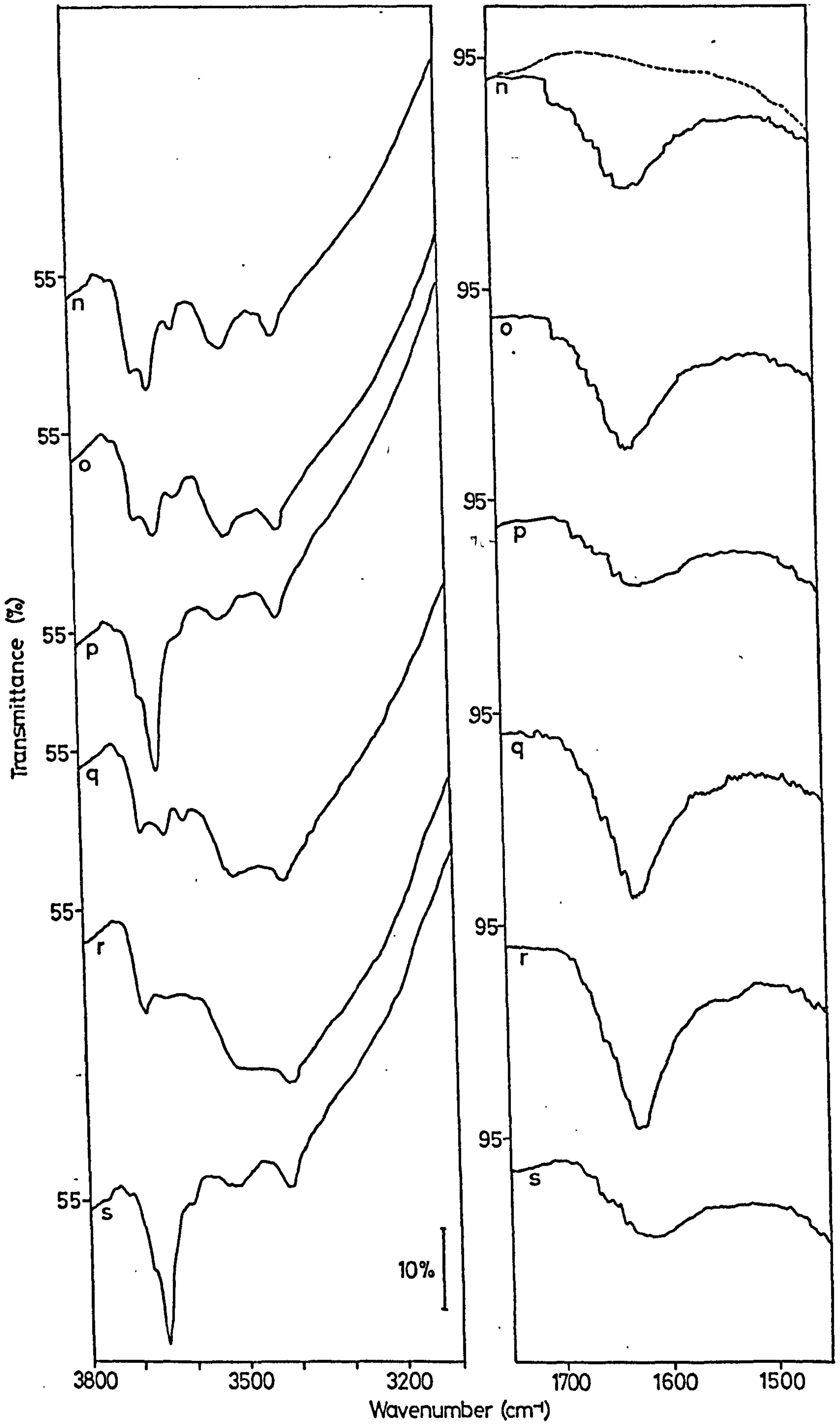




Spec 33 Adsorption of H<sub>2</sub>O onto a 673 K Oxidized Surface



Spec 33 Adsorption of  $H_2O$  onto a 673 K Oxidized Surface



Spec 33 Adsorption of H<sub>2</sub>O onto a 673 K Oxidized Surface

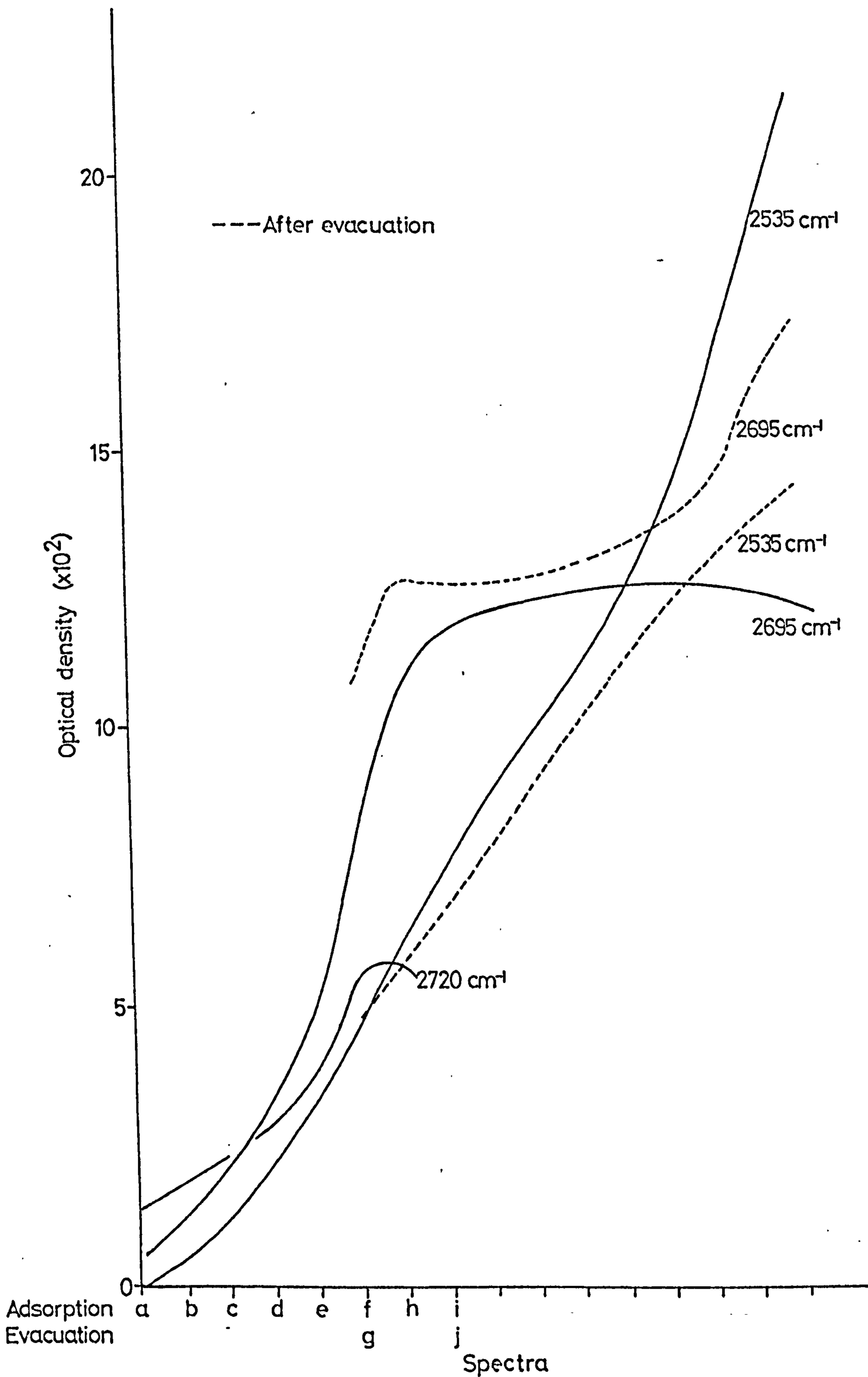
SPEC. 3.4

SPEC. 3.4

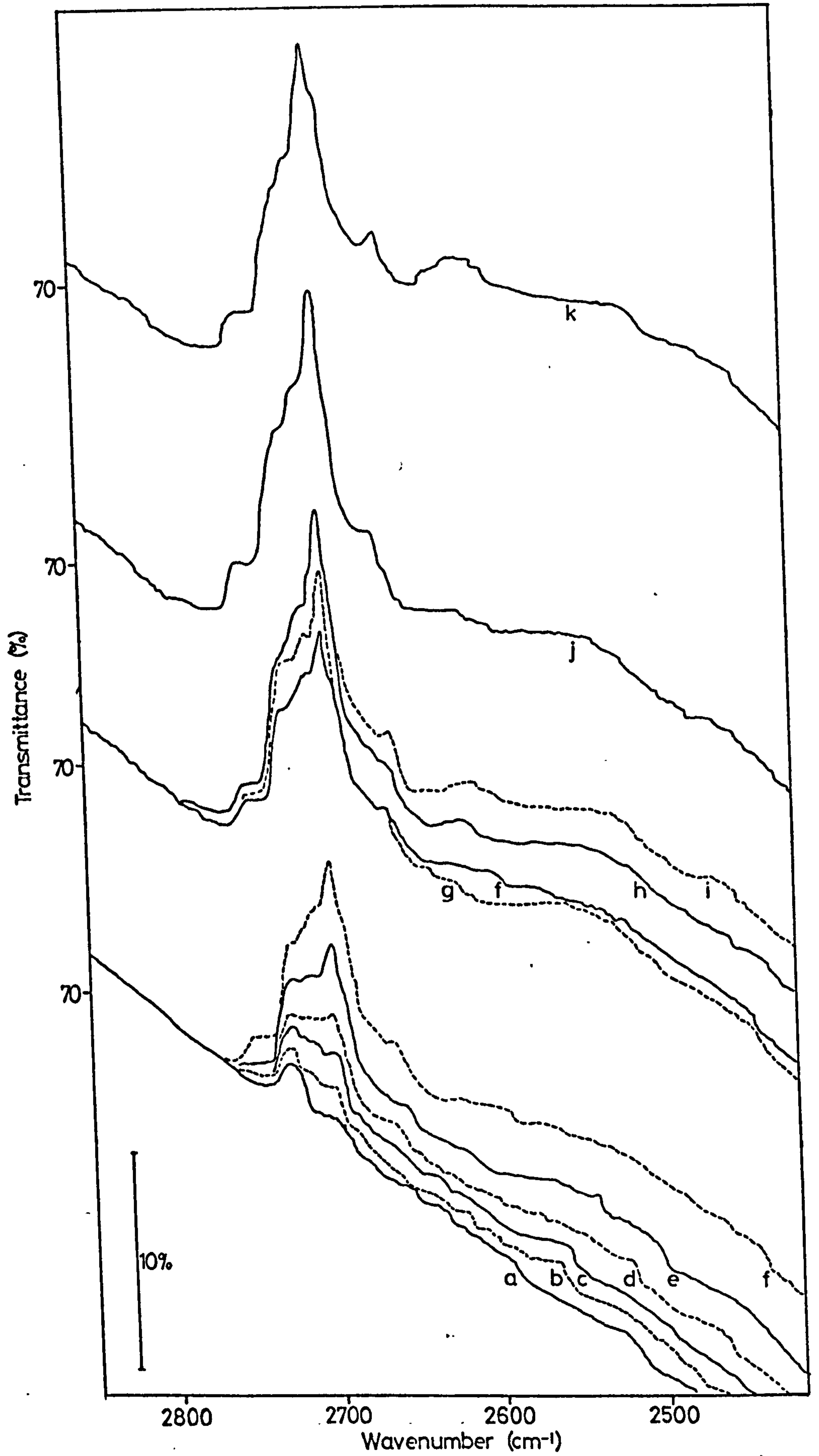
ADSORPTION OF D<sub>2</sub>O ONTO A 673 K (400°C)

D<sub>2</sub>O OXIDIZED SURFACE

- (a) Initial surface
- (b) - (i) adsorption of D<sub>2</sub>O at increasing vapour pressures
- (j) evacuation BT
- (k) disc in isolated cell 12h



Graph 3.4 Adsorption of  $\text{D}_2\text{O}$  onto a 673 K  $\text{D}_2\text{O}$  Oxidized Surface



Spec. 34 Adsorption of D<sub>2</sub>O onto a 673 K D<sub>2</sub>O, Oxidized Surface

SPEC. 3.5

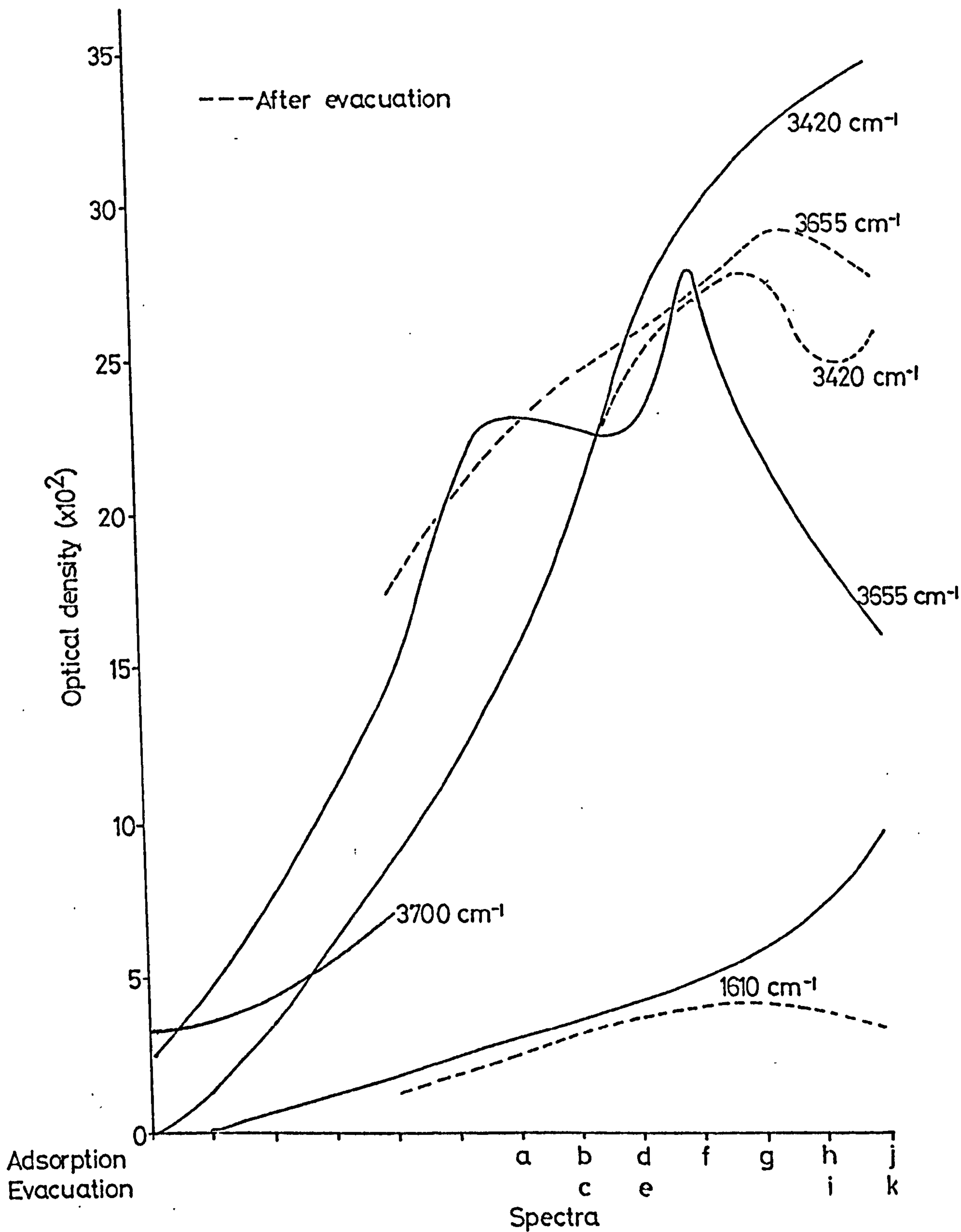


SPEC. 3.5

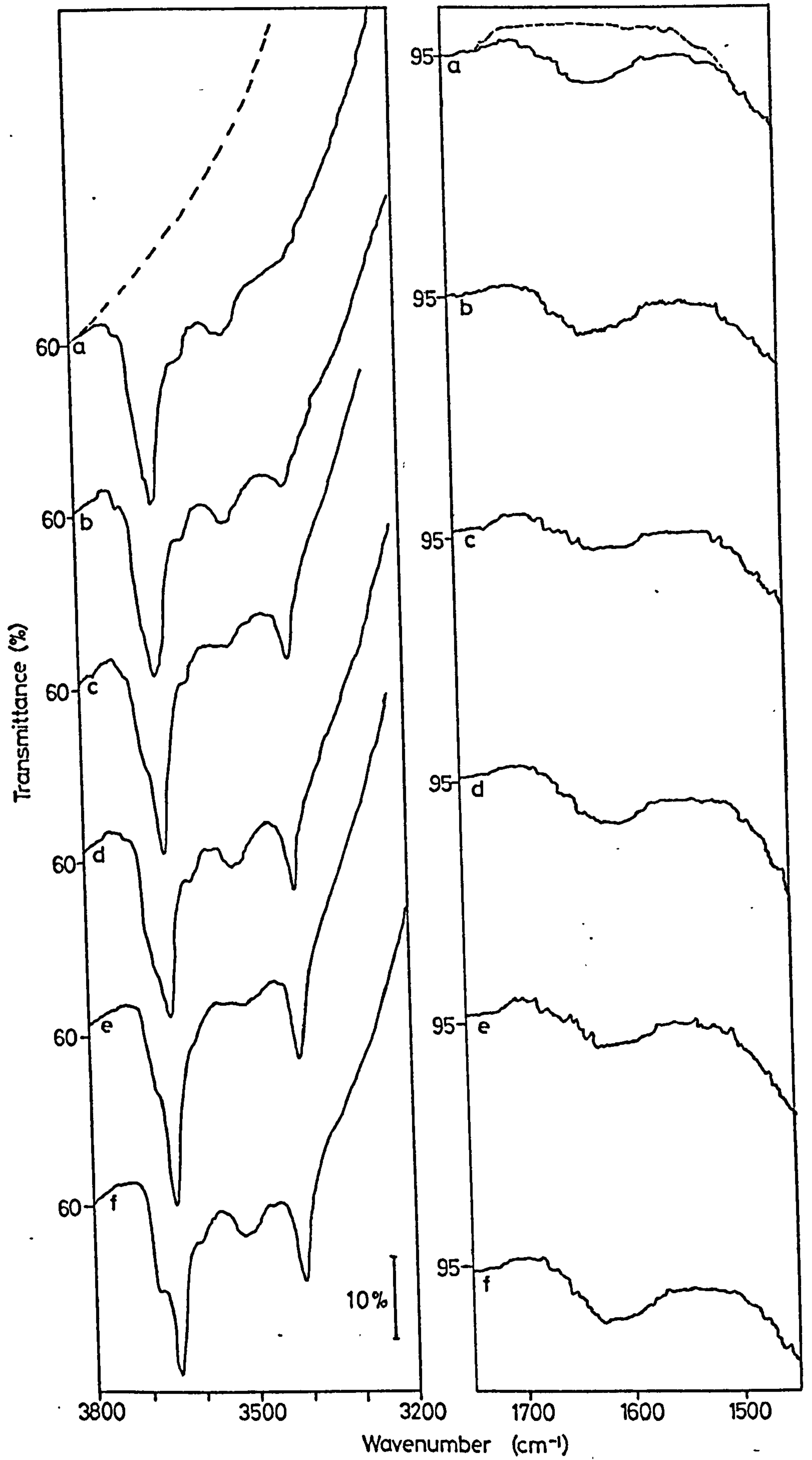
ADSORPTION OF H<sub>2</sub>O ONTO A 673 K (400°C)

H<sub>2</sub>O OXIDIZED SINTERED SURFACE

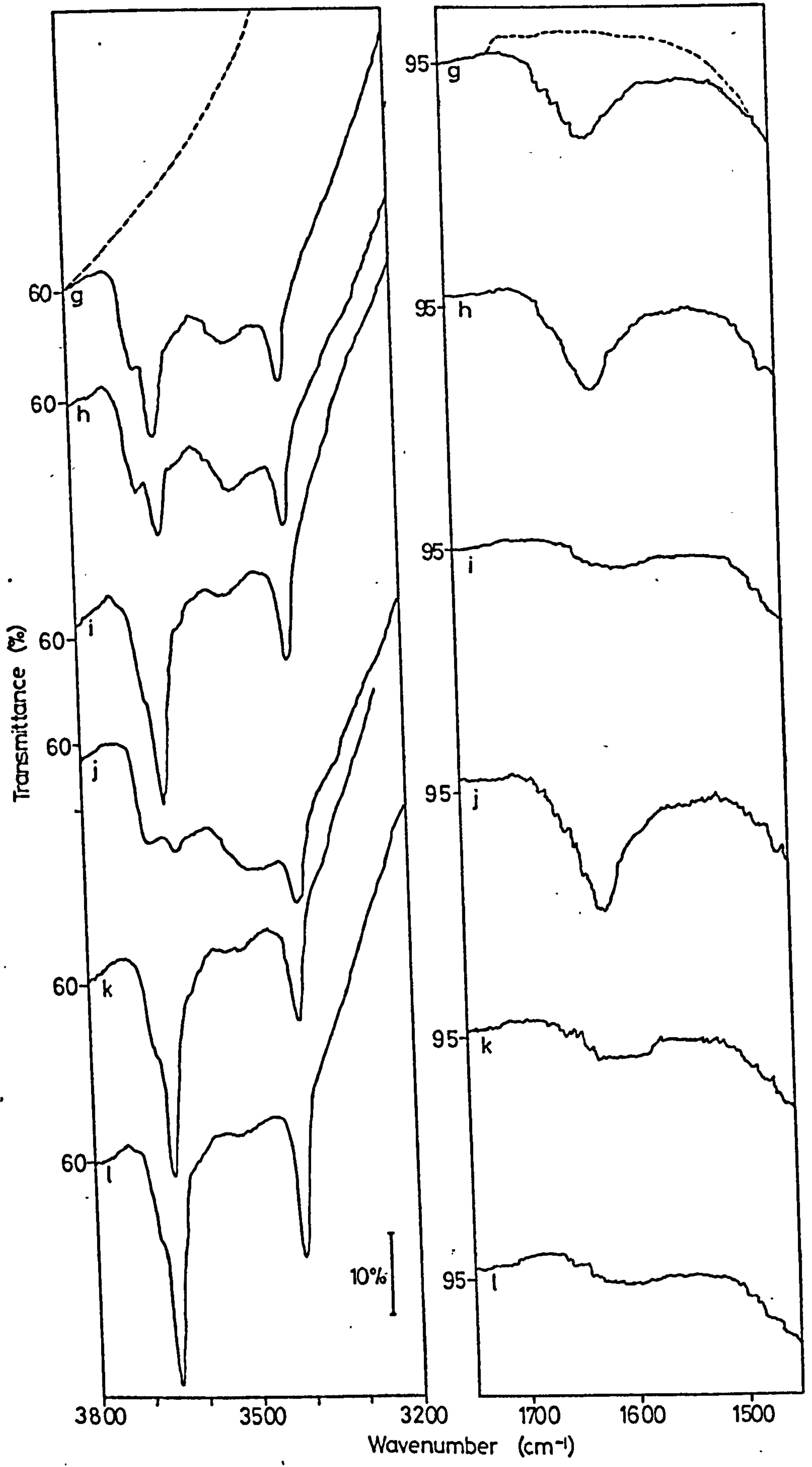
- (a) Surface after initial adsorption of H<sub>2</sub>O  
(compare spec. 3.3 g)
- (b), (d), (f), (g), (h), (j) adsorption of H<sub>2</sub>O at increasing  
vapour pressures
- (c), (e), (i), (k) evacuation, BT
- (l) disc heated in H<sub>2</sub>O (673 K, 2h) and evacuated (BT, 1h)



Graph 3.5 Adsorption of  $\text{H}_2\text{O}$  onto a 673 K Oxidized Sintered Surface



Spec 35 Adsorption of H<sub>2</sub>O onto a 673 K, H<sub>2</sub>O, Oxidized, Sintered Surface



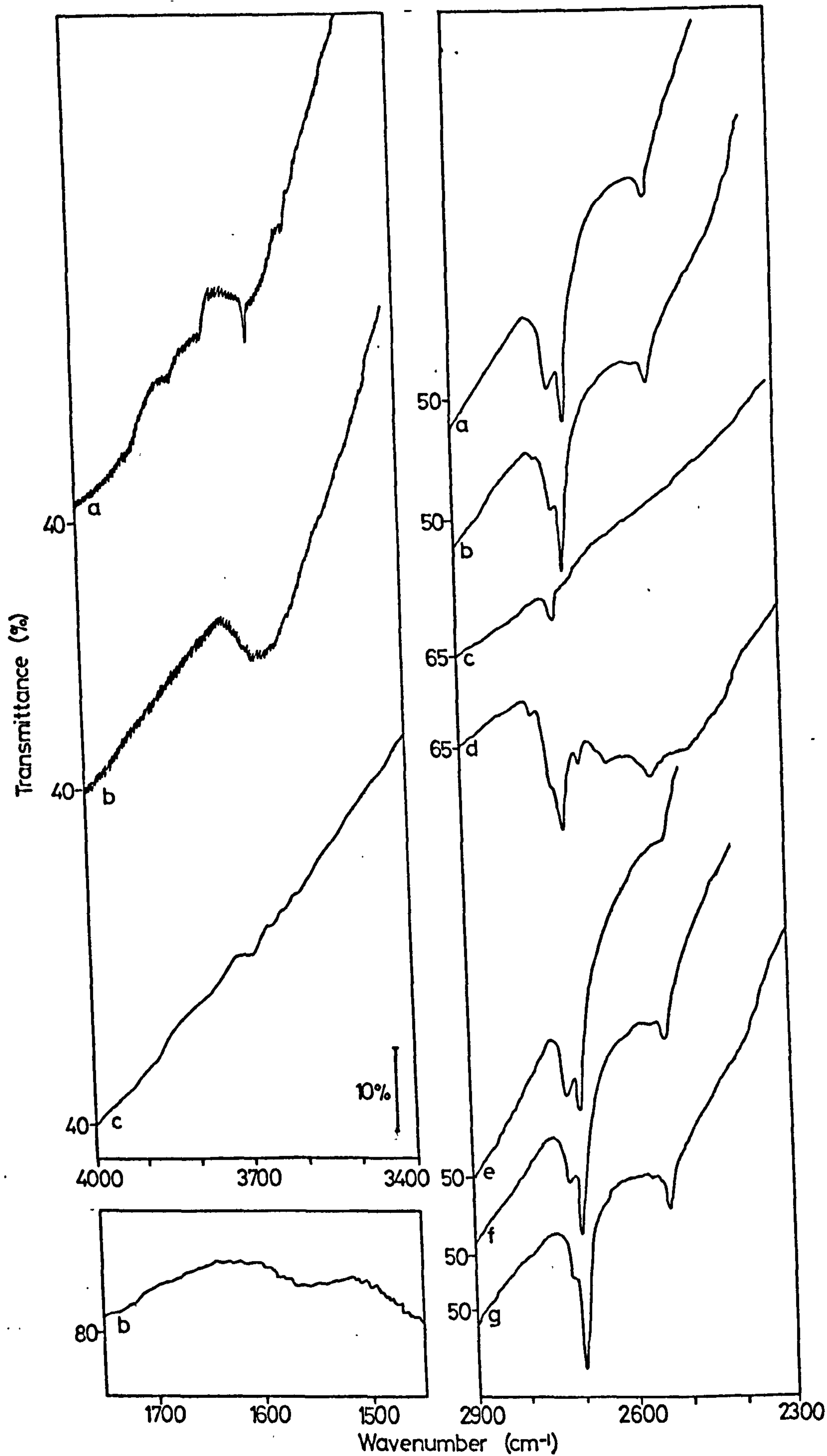
Spec 35 Adsorption of H<sub>2</sub>O onto a 673 K, H<sub>2</sub>O, Oxidized, Sintered Surface

SPEC. 3.6

SPEC. 3.6

REVERSIBILITY OF THE REDUCTION PROCESS

- (a) Initial reduced surface (see section 2.3.1 page 35 for preparation) after exposure to  $D_2O$  and evacuation
- (b) Initial surface exposed to  $D_2O$  vapour (298 K, 112h) and evacuated (BT,  $\frac{1}{2}$ h)
- (c) Surface after heating in oxygen ( $1.33 \times 10^4$  N m<sup>-2</sup>, 673 K, 1h), evacuation (673 K, 1h), oxygen ( $1.33 \times 10^4$  N m<sup>-2</sup>, 673 K, 1h) and evacuation (BT,  $\frac{1}{2}$ h)
- (d) Surface after exposure to  $D_2O$  (BT, 4h) and evacuation (298 K, 18h)
- (e) Reduction of surface (as for initial surface) evacuation (673 K, 60h), exposure to  $D_2O$  (BT,  $\frac{1}{2}$ h) and evacuation (BT,  $\frac{1}{2}$ h)
- (f) Heating in  $D_2O$  (673 K, 2h) and evacuation (BT,  $\frac{1}{2}$ h)
- (g) Heating in  $D_2O$  (673 K, 16h) and evacuation (BT,  $\frac{1}{2}$ h)



Spec 36 Reversibility of the Reduction Process

SPEC. 3.7

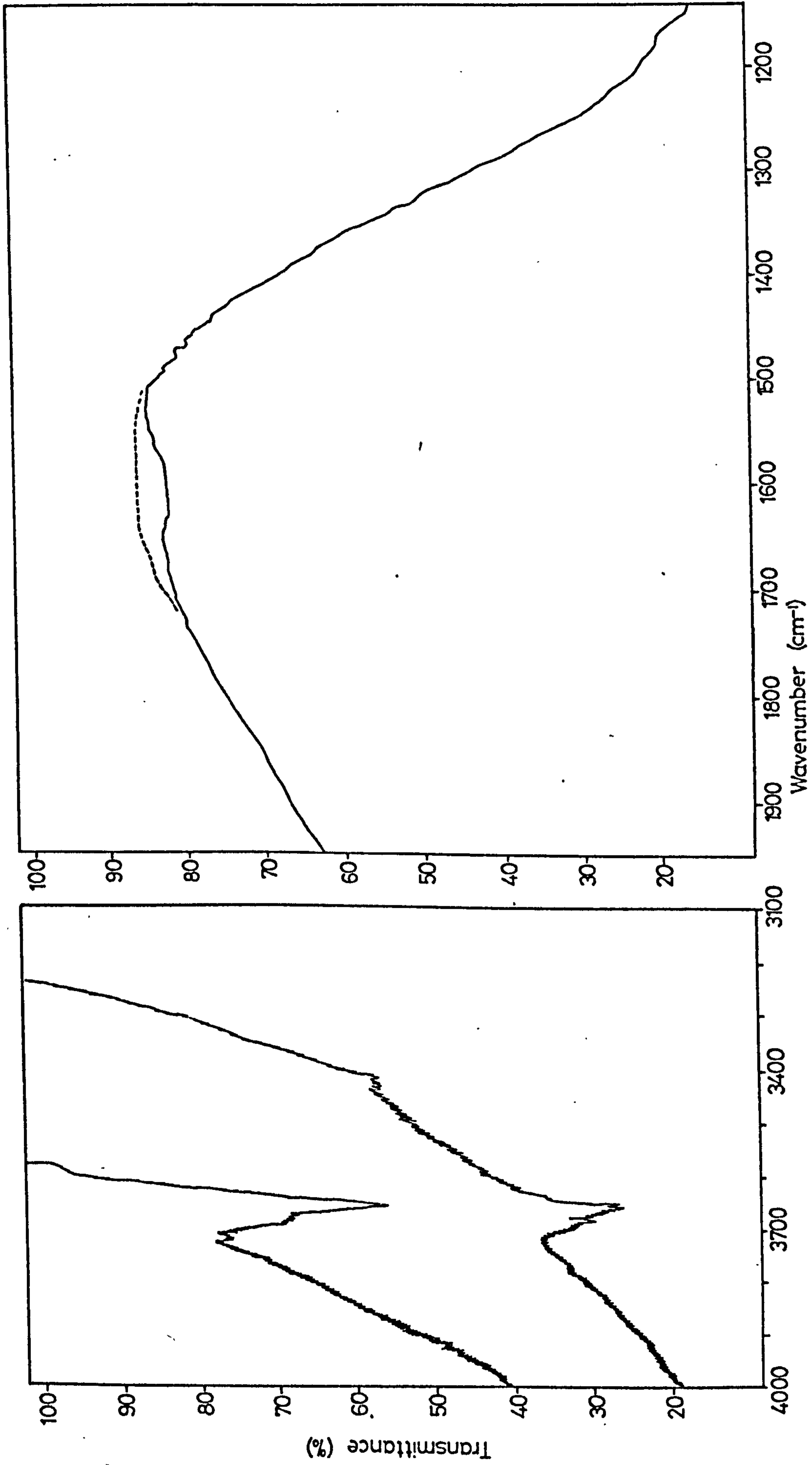


SPEC. 3.7

ADSORPTION OF H<sub>2</sub>O ONTO A 673 K (400°C)

H<sub>2</sub>O REDUCED SURFACE

Spectrum of surface after standard reduction  
procedure, adsorption of H<sub>2</sub>O vapour at BT  
and evacuation (BT, ½h)



Spec 3.7 Adsorption of H<sub>2</sub>O onto a 673 K H<sub>2</sub>O, Reduced Surface

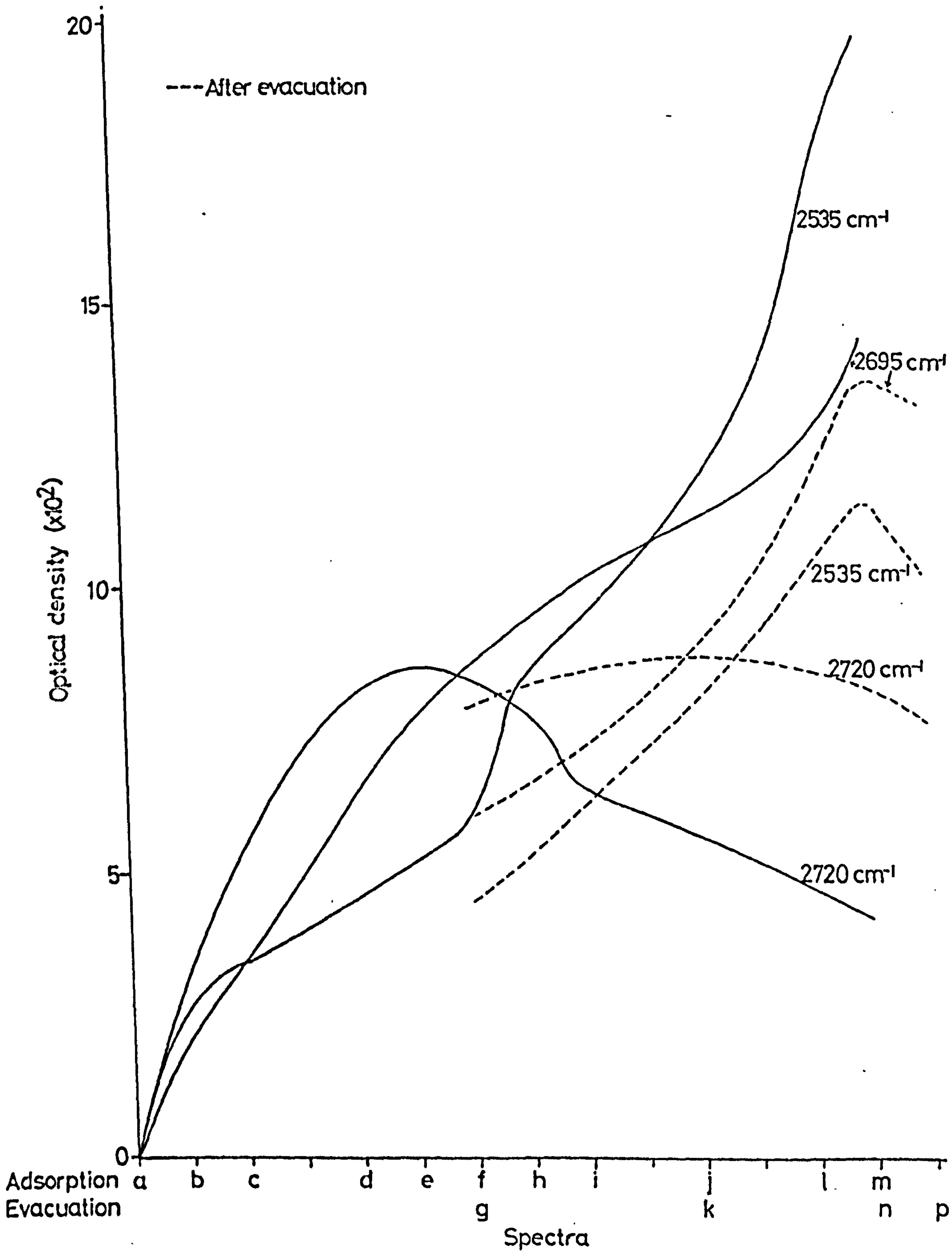
SPEC. 3.8

SPEC. 3.8

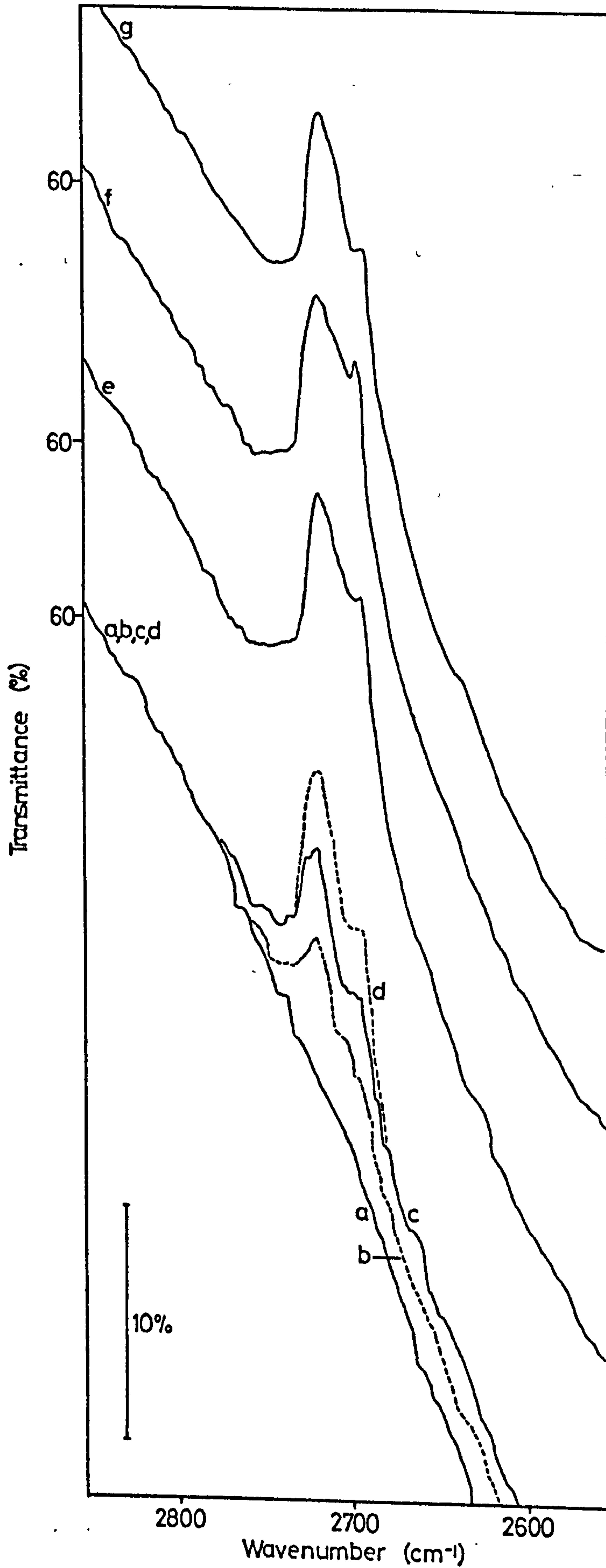
ADSORPTION OF D<sub>2</sub>O ONTO A 673 K (400°C)

H<sub>2</sub>O REDUCED SURFACE

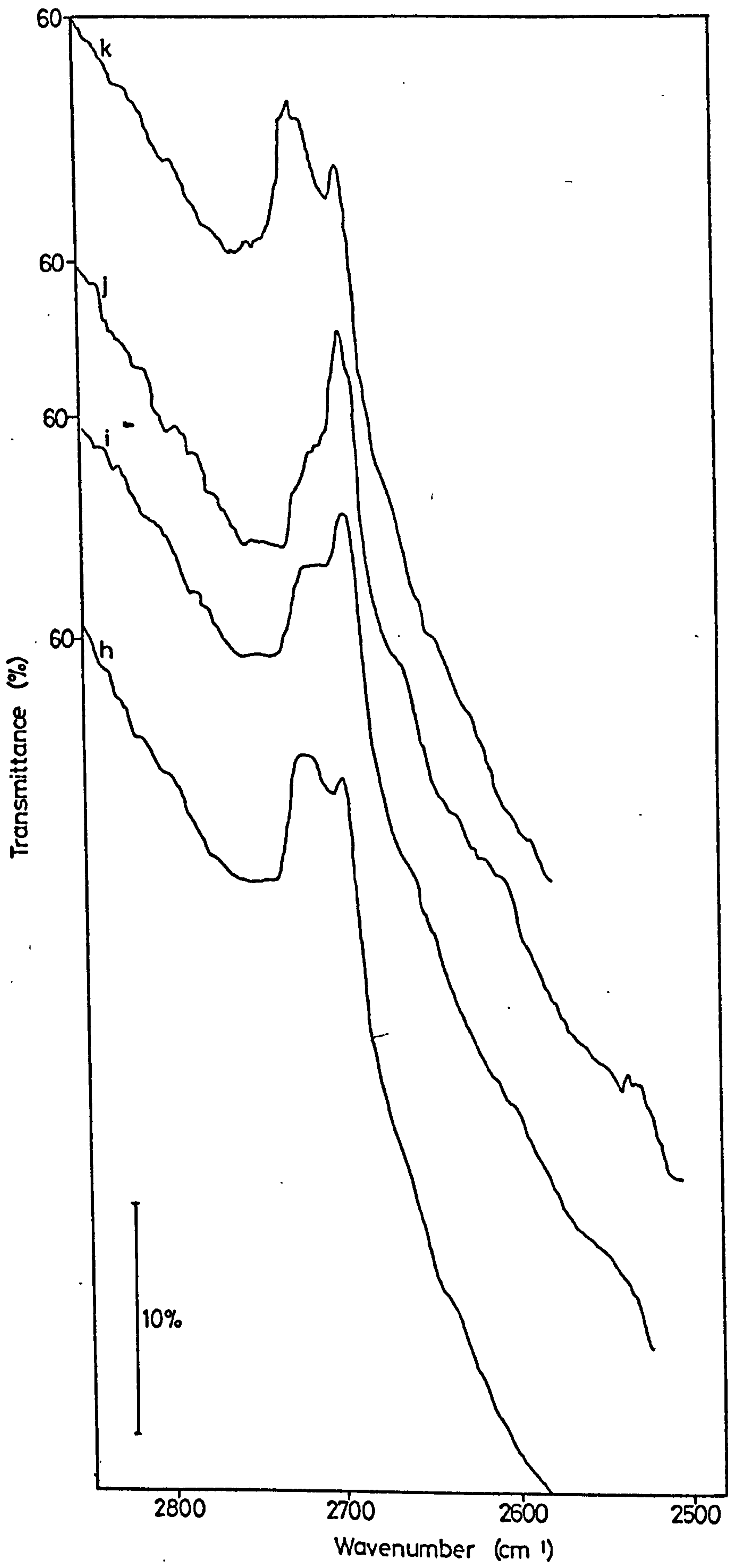
- (a) Initial surface
- (b)-(f) adsorption D<sub>2</sub>O vapour at increasing pressures
- (g) evacuation (BT, 3h)
- (h)-(j) adsorption D<sub>2</sub>O vapour
- (k) evacuation (BT, 2h)
- (l),(m) adsorption D<sub>2</sub>O vapour
- (n) evacuation (BT, 1h)
- (o) adsorption D<sub>2</sub>O at room temperature vapour pressure
- (p) evacuation (BT, 1h)
- (q) evacuation (473 K, 16h)



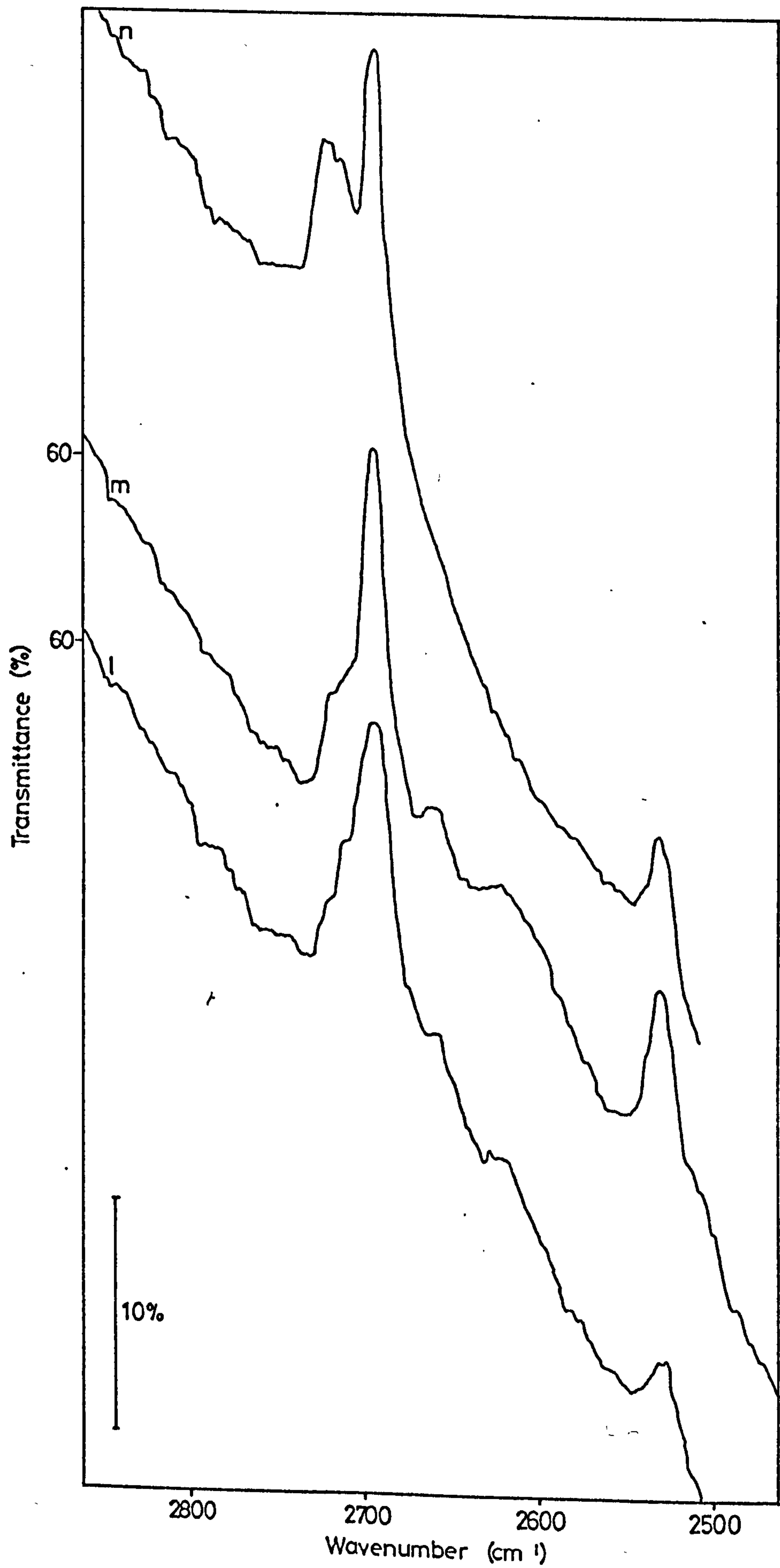
Graph 3.6 Adsorption of  $\text{D}_2\text{O}$  onto a 673 K  $\text{H}_2\text{O}$  Reduced Surface



Spec 3.8 Adsorption of D<sub>2</sub>O onto a 673 K, H<sub>2</sub>O, Reduced Surface

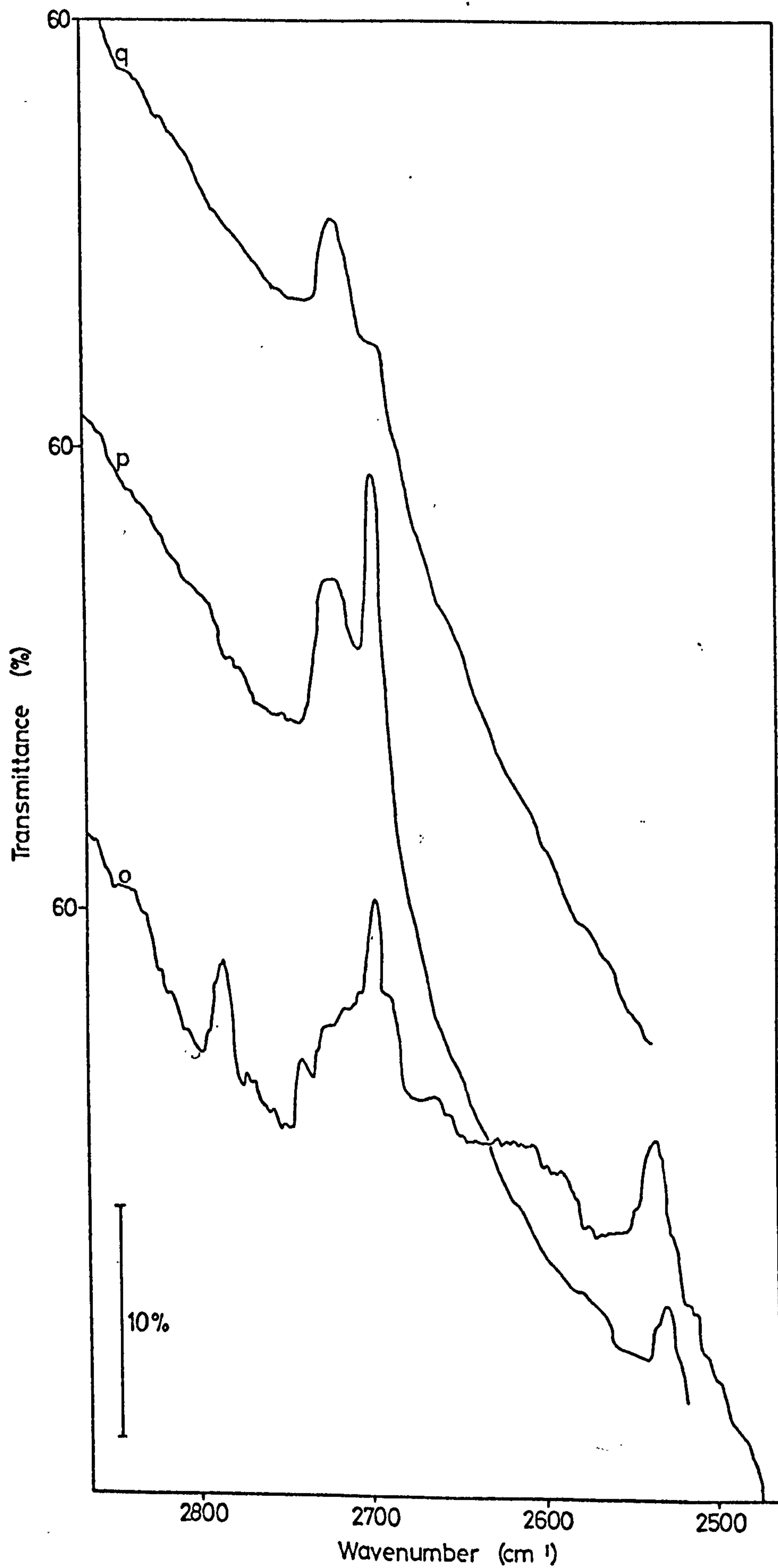


Spec 3.8 Adsorption of D<sub>2</sub>O onto a 673 K, H<sub>2</sub>O, Reduced Surface



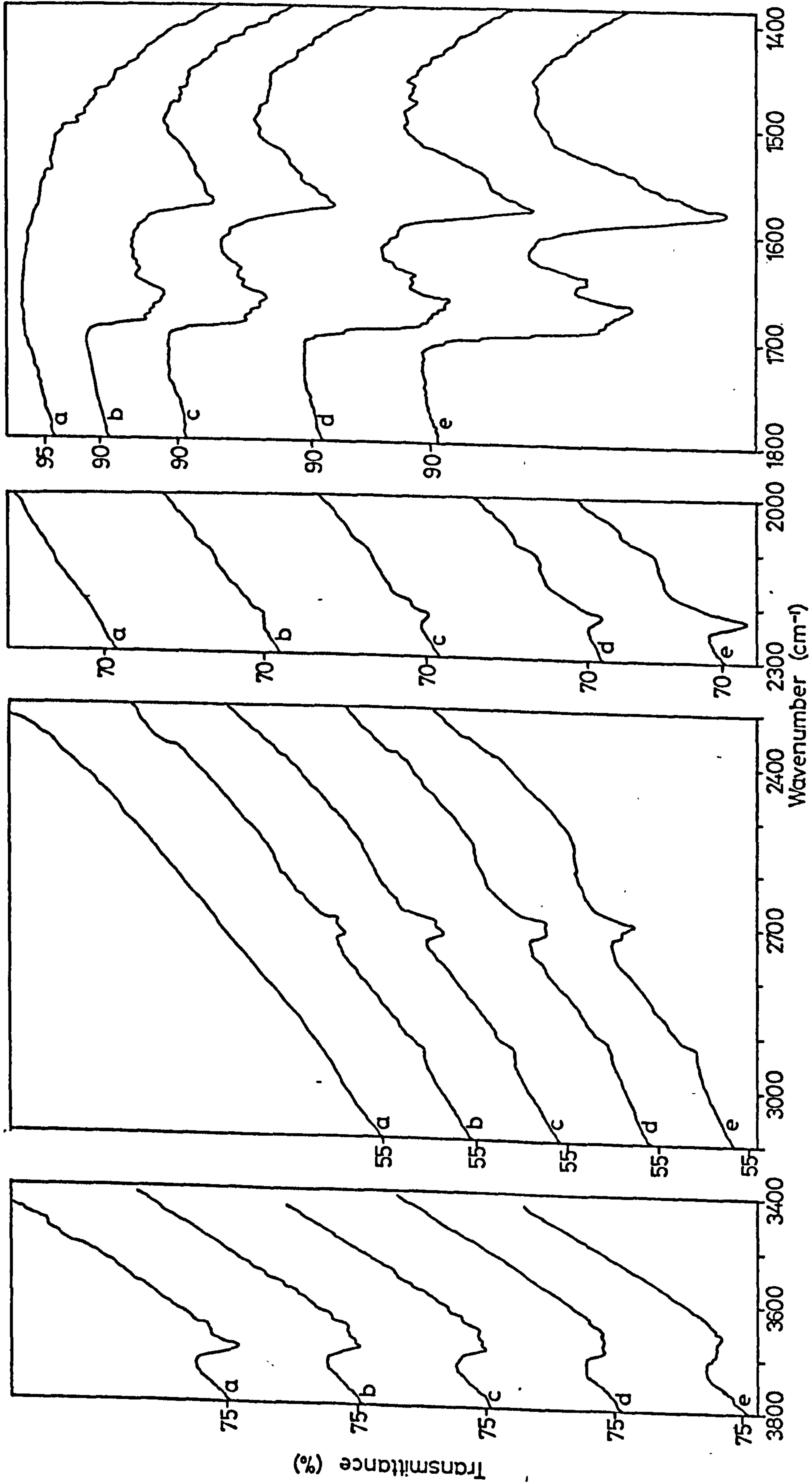
Spec 3.8 Adsorption of D<sub>2</sub>O onto a 673 K, H<sub>2</sub>O, Reduced Surface



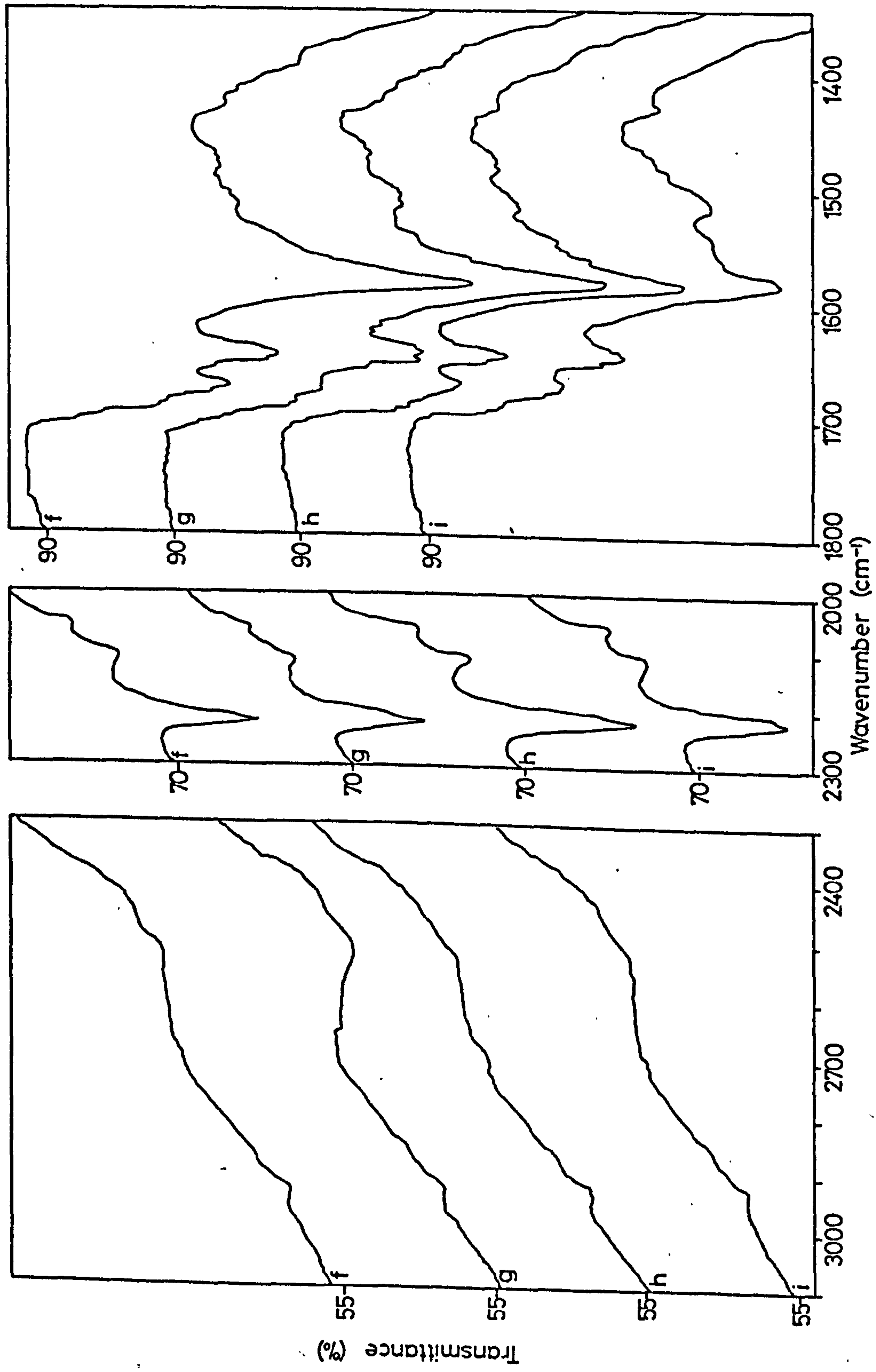


Spec 3.8 Adsorption of  $D_2O$  onto a 673 K  $H_2O$  Reduced Surface

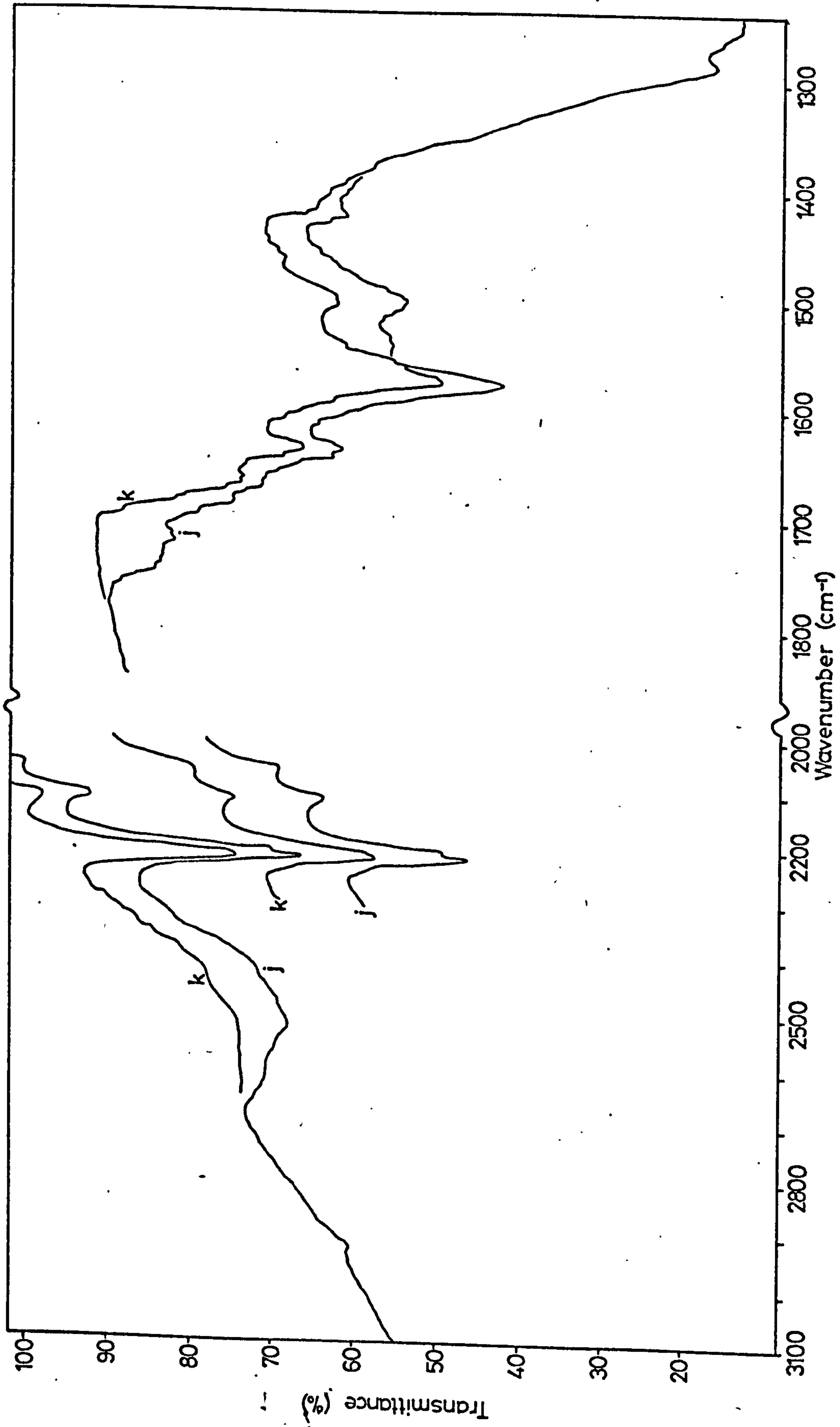
SPEC. 4.1



Spec 4.1 Adsorption of Acetone d<sub>6</sub> onto a 673 K H<sub>2</sub>O<sub>2</sub> Oxidized Surface



Spec 4.1 Adsorption of Acetone d<sub>6</sub> onto a 673 K H<sub>2</sub>O, Oxidized Surface



Spec 4.1 Adsorption of Acetone  $d_6$  onto a 673 K  $H_2O$ , Oxidized Surface

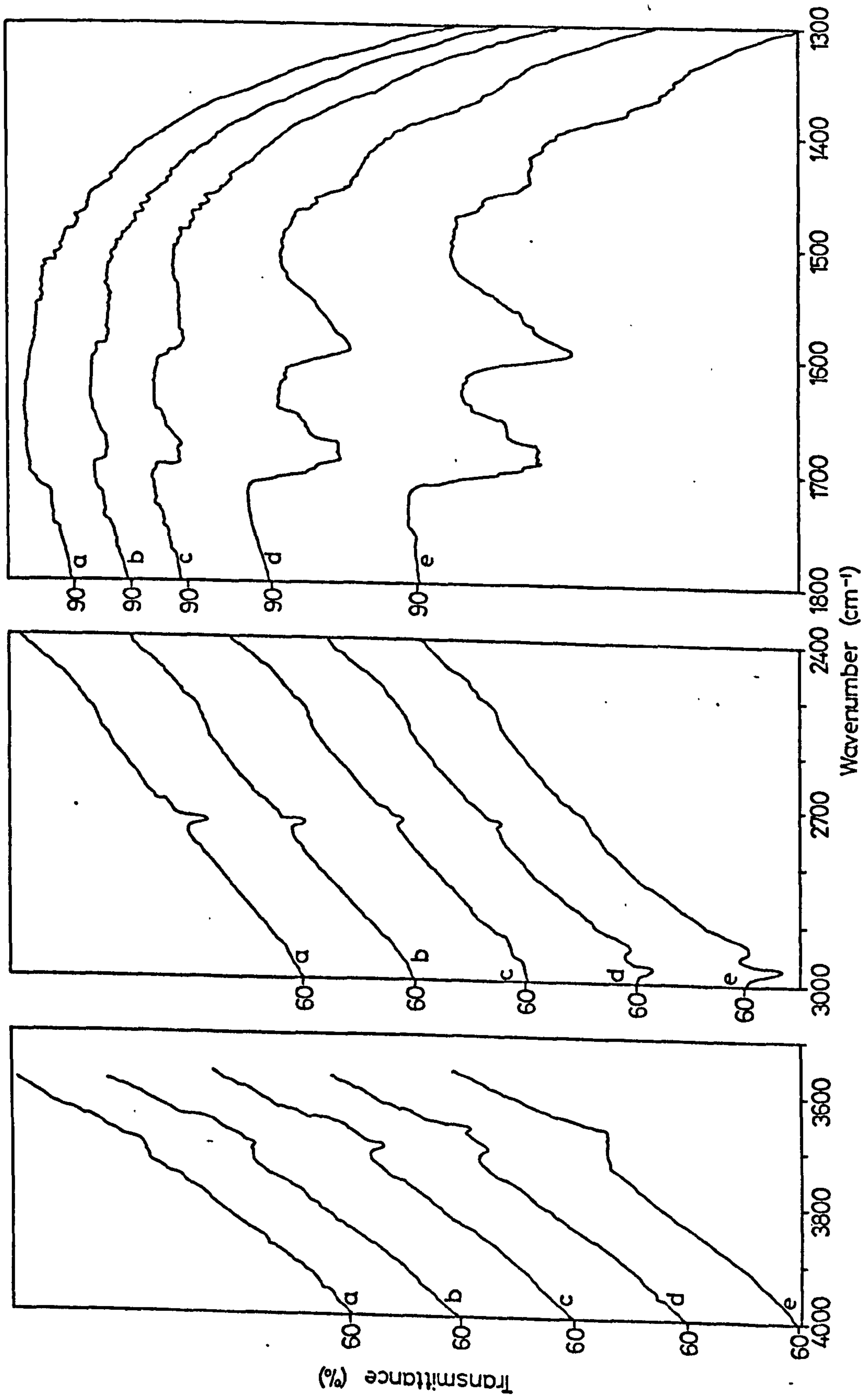
SPEC. 4.2

SPEC. 4.2

ADSORPTION OF ACETONE  $\text{h}_6$  ONTO A 673 K (400°C)

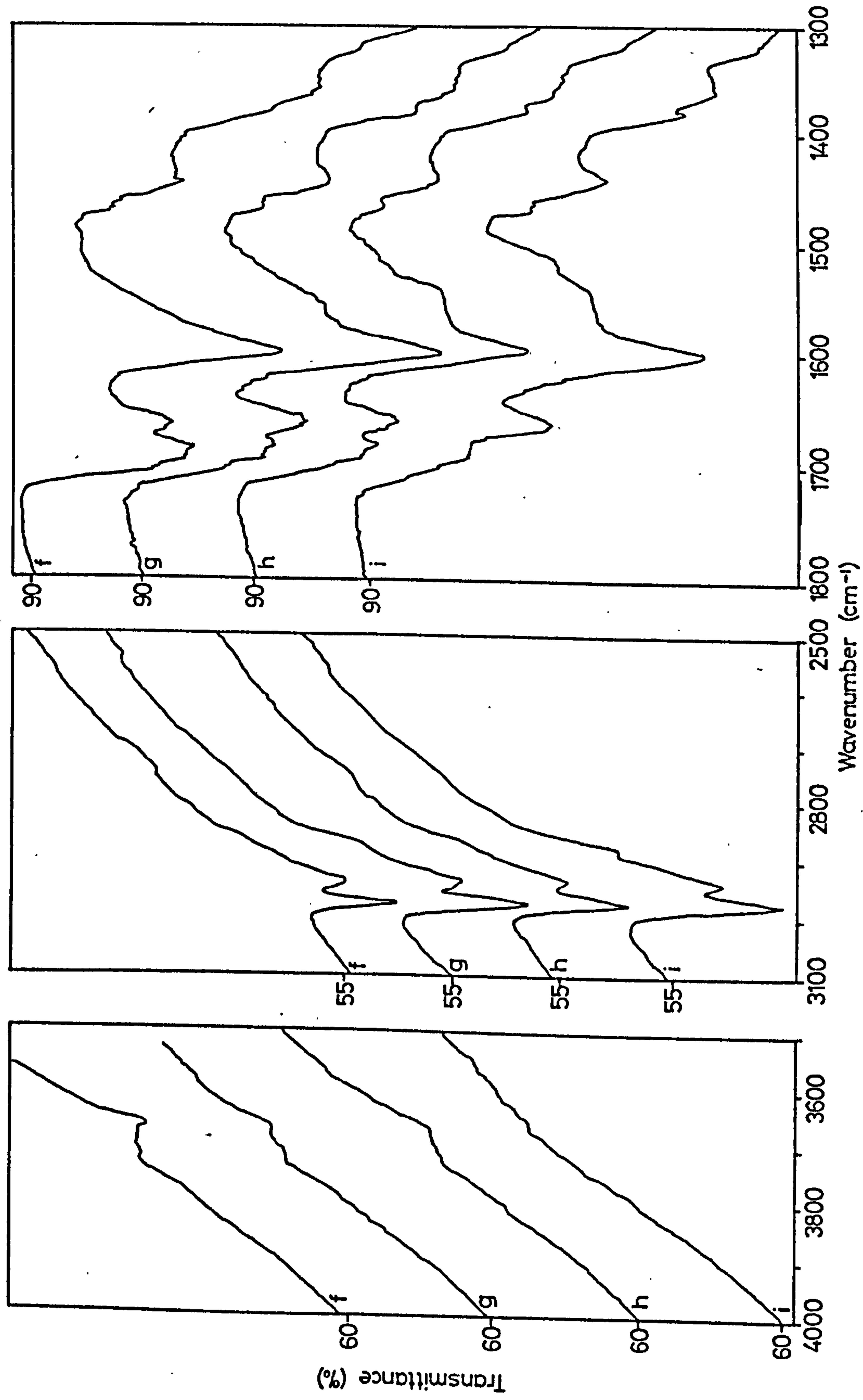
$\text{D}_2\text{O}$  OXIDIZED SURFACE

- (a) Initial surface
- (b)-(g),(i),(k) adsorption of acetone  $\text{h}_6$  at increasing vapour pressures
- (h),(j),(l) Evacuation (BT, 1h)
- (m) evacuation (298 K, 12h)
- (n) adsorption acetone  $\text{h}_6$
- (o) evacuation (BT, 1h)
- (p) exposure to  $\text{D}_2\text{O}$  vapour (298 K, 15h) and evacuation (BT, 1h)

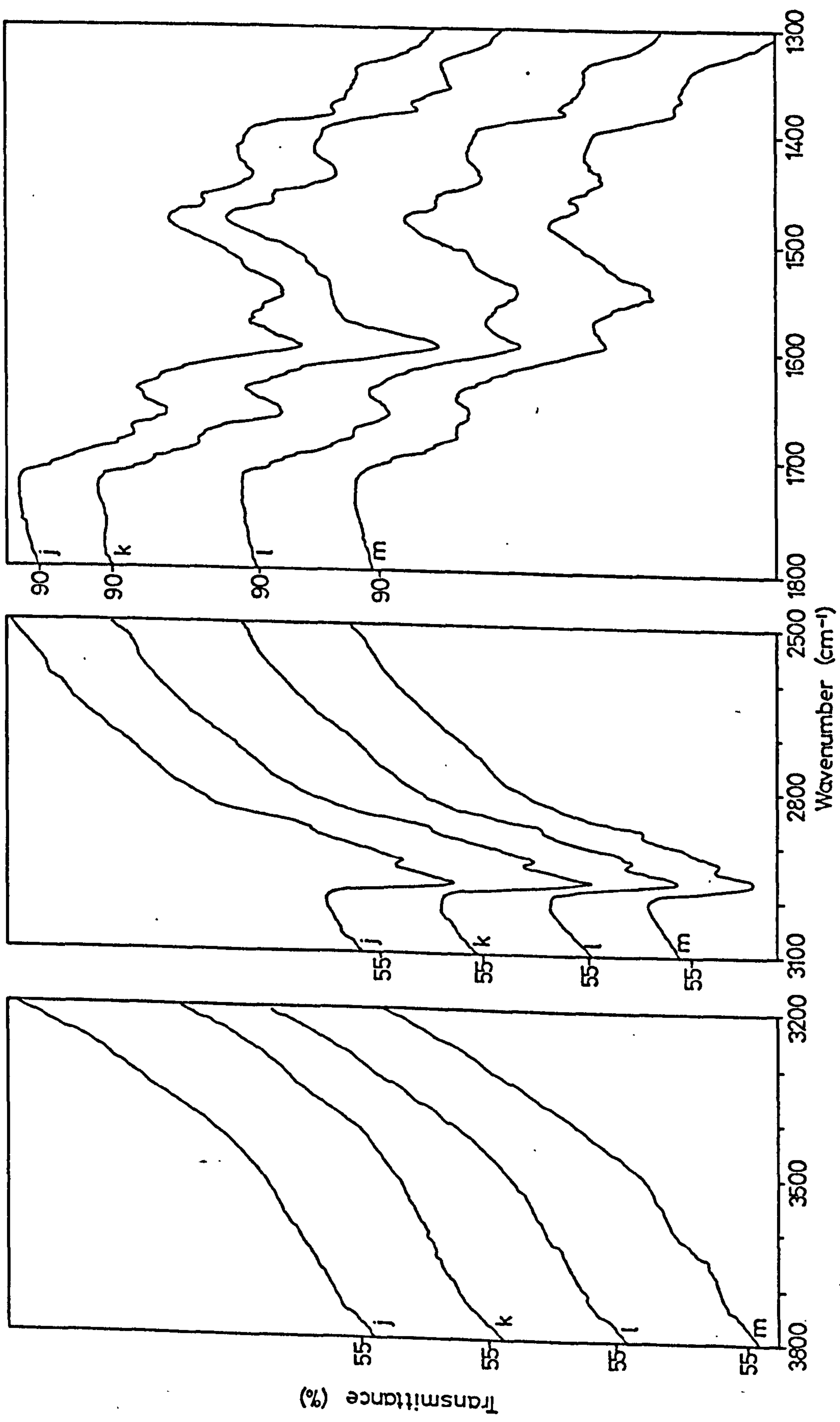


Spec 4.2 Adsorption of Acetone  $h_g$  onto a 673 K.  $D_2O$ , Oxidized Surface

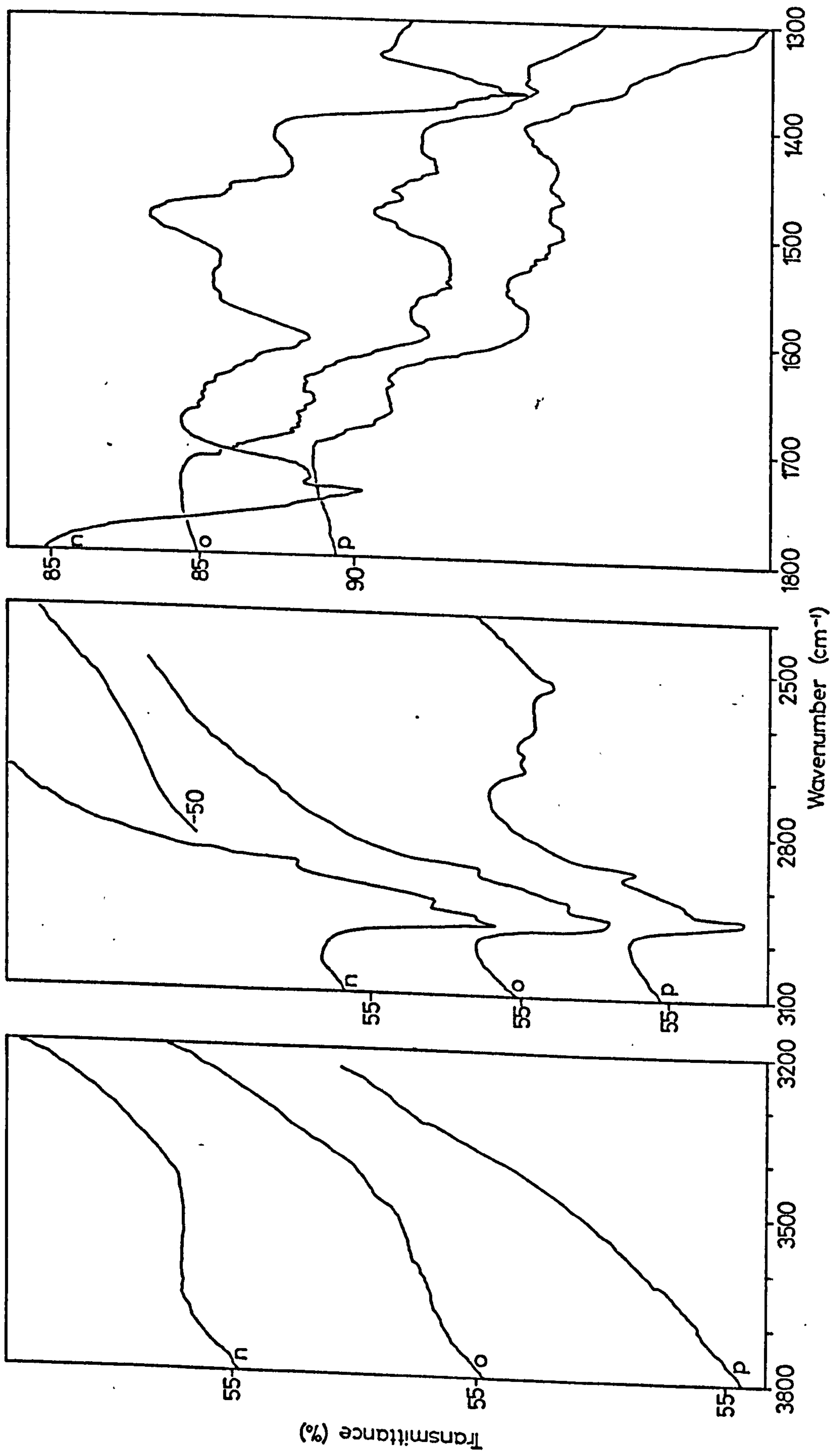




Spec 4.2 Adsorption of Acetone h<sub>6</sub> onto a 673 K. D<sub>2</sub>O, Oxidized Surface



Spec 4.2 Adsorption of Acetone h<sub>6</sub> onto a 673 K. D<sub>2</sub>O, Oxidized Surface



Spec 4.2 Adsorption of Acetone h<sub>g</sub> onto a 673 K. D<sub>2</sub>O, Oxidized Surface

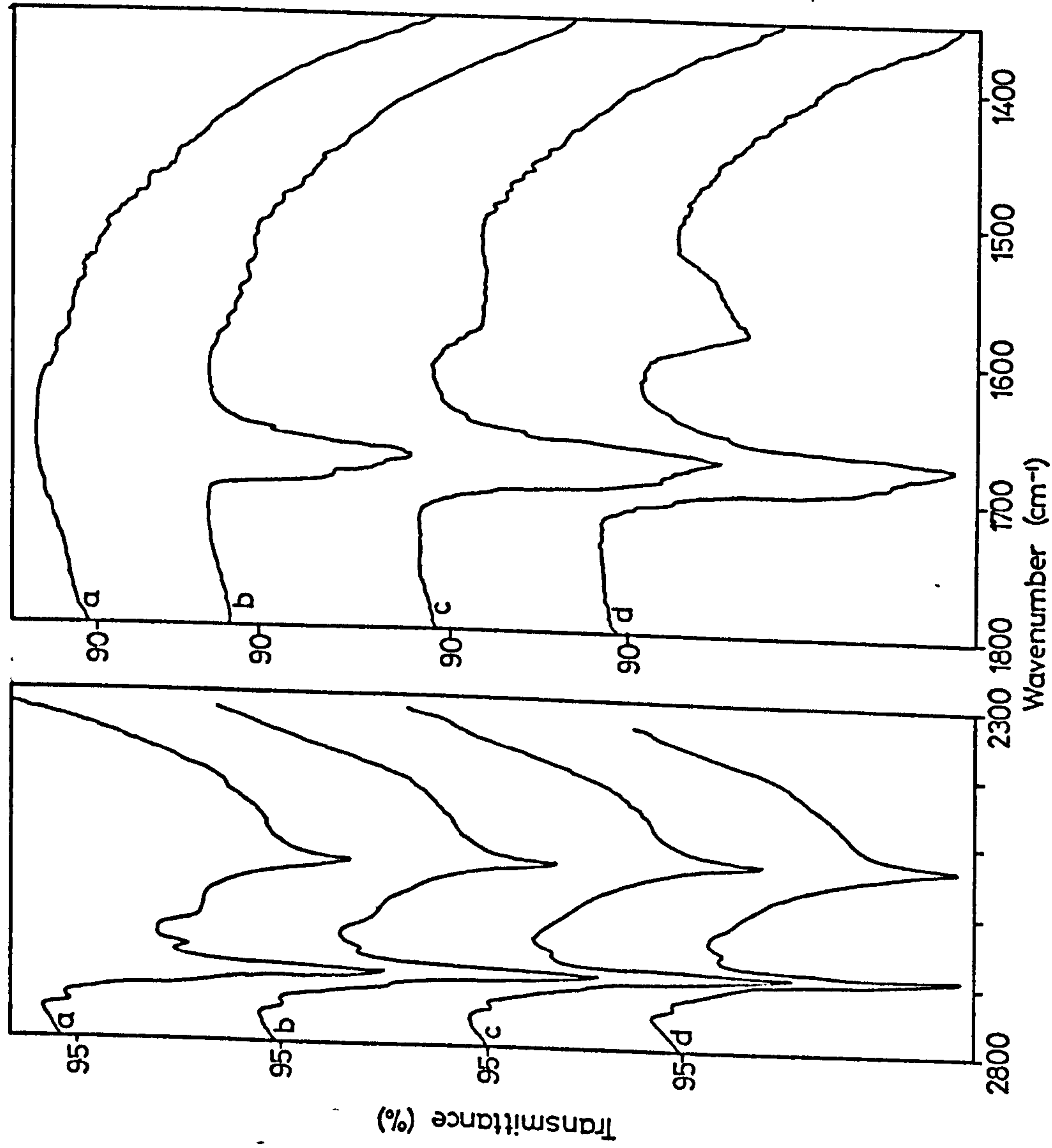
SPEC. 4.3

SPEC. 4.3

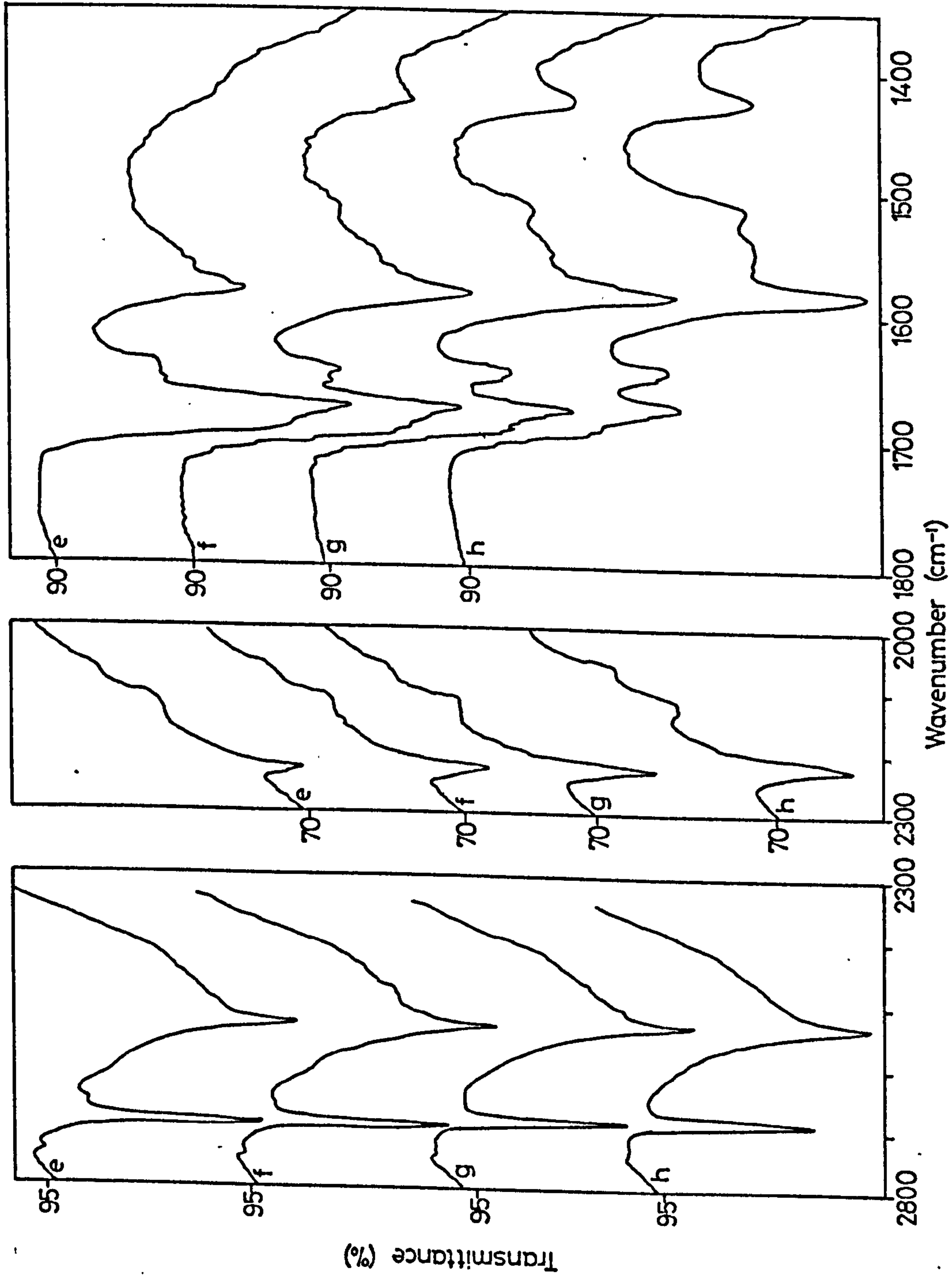
ADSORPTION OF ACETONE  $d_6$  ONTO A BT,

$D_2O$  OXIDIZED SURFACE

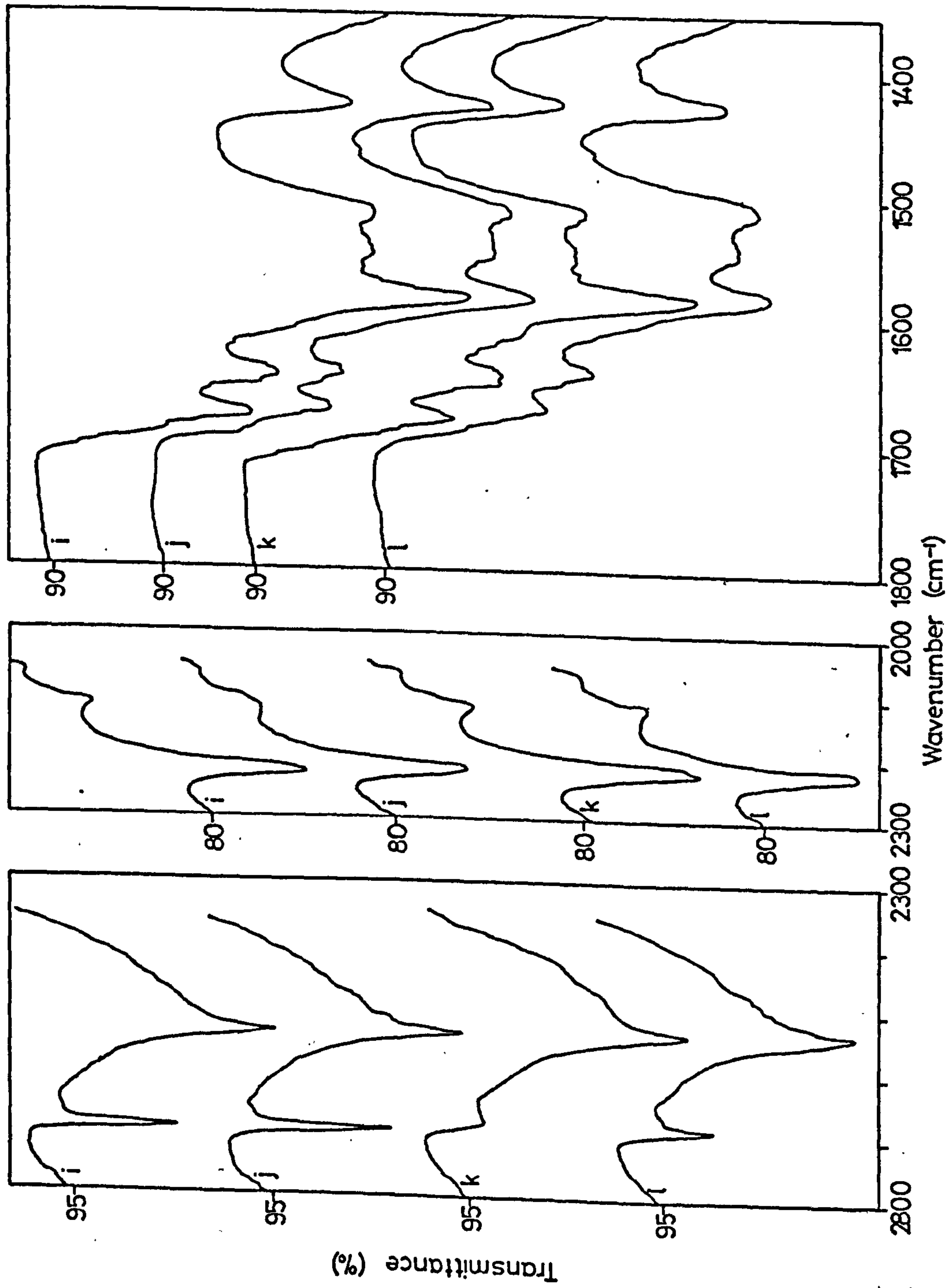
- (a) Initial surface
- (b)-(i) adsorption of acetone  $d_6$  at increasing vapour pressures
- (j) exposure disc to acetone  $d_6$  vapour in closed cell (298 K, 13h)
- (k),(m),(n) adsorption of acetone  $d_6$  at increasing vapour pressures
- (o) exposure of disc to acetone  $d_6$  vapour in closed cell (298 K, 60h)
- (p) evacuation (BT, 1h)



Spec 4.3 Adsorption of Acetone  $d_6$  onto a BT,  $D_2O$ , Oxidized Surface

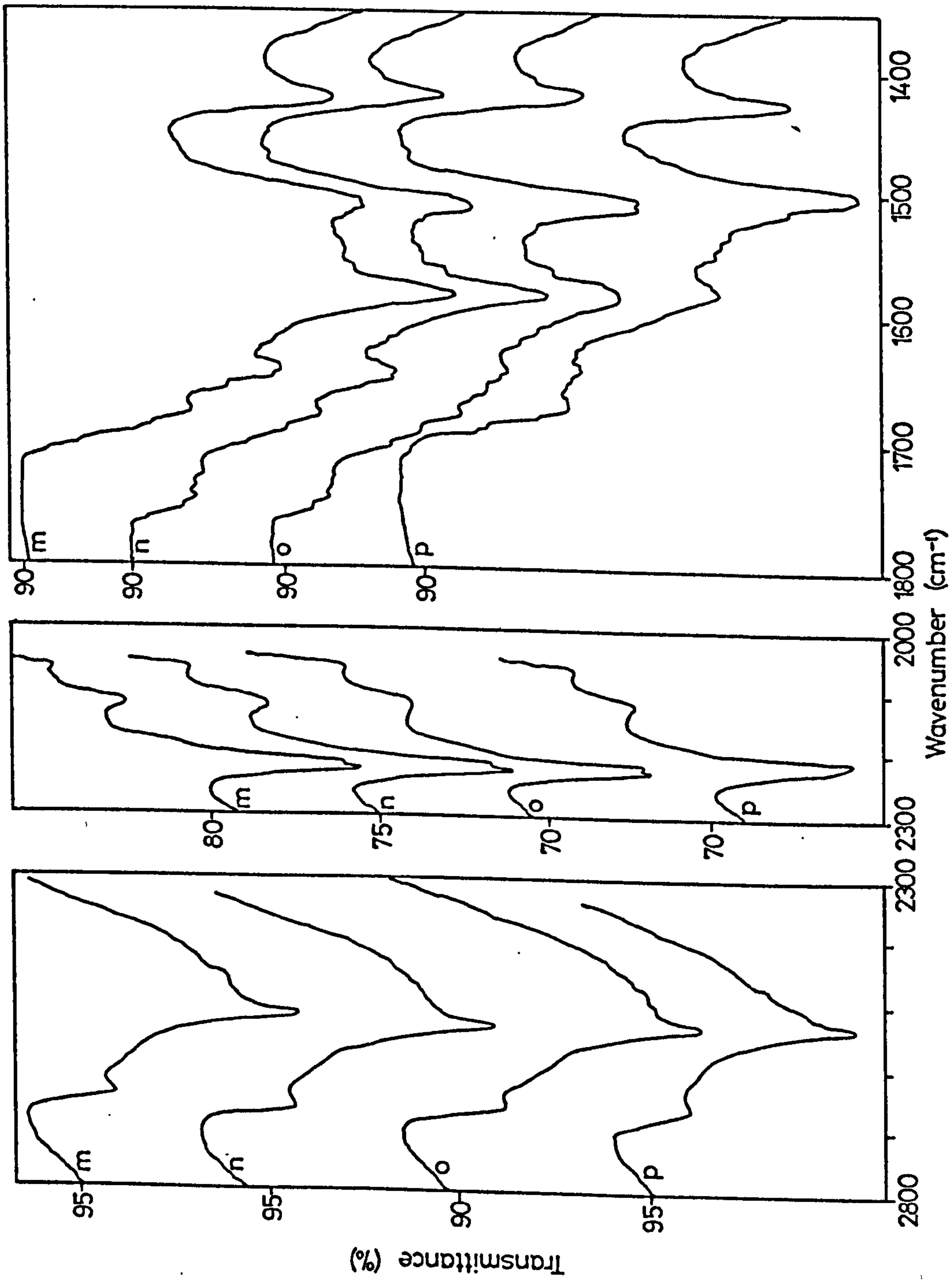


Spec 4.3 Adsorption of Acetone d<sub>6</sub> onto a BT, D<sub>2</sub>O, Oxidized Surface



Spec 4.3 Adsorption of Acetone d<sub>6</sub> onto a BT, D<sub>2</sub>O, Oxidized Surface





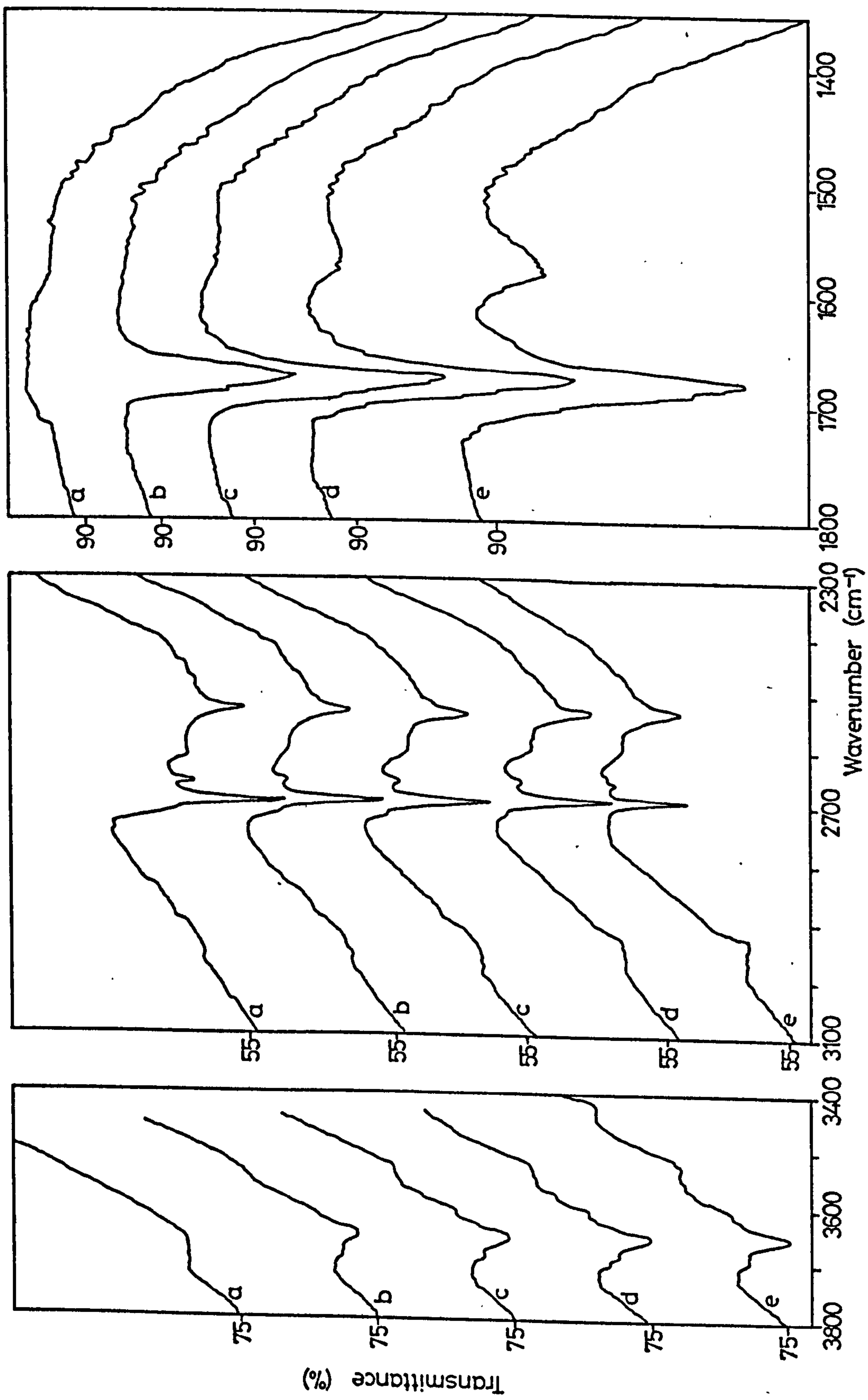
Spec 4.3 Adsorption of Acetone d<sub>6</sub> onto a BT, D<sub>2</sub>O, Oxidized Surface

SPEC. 4.4

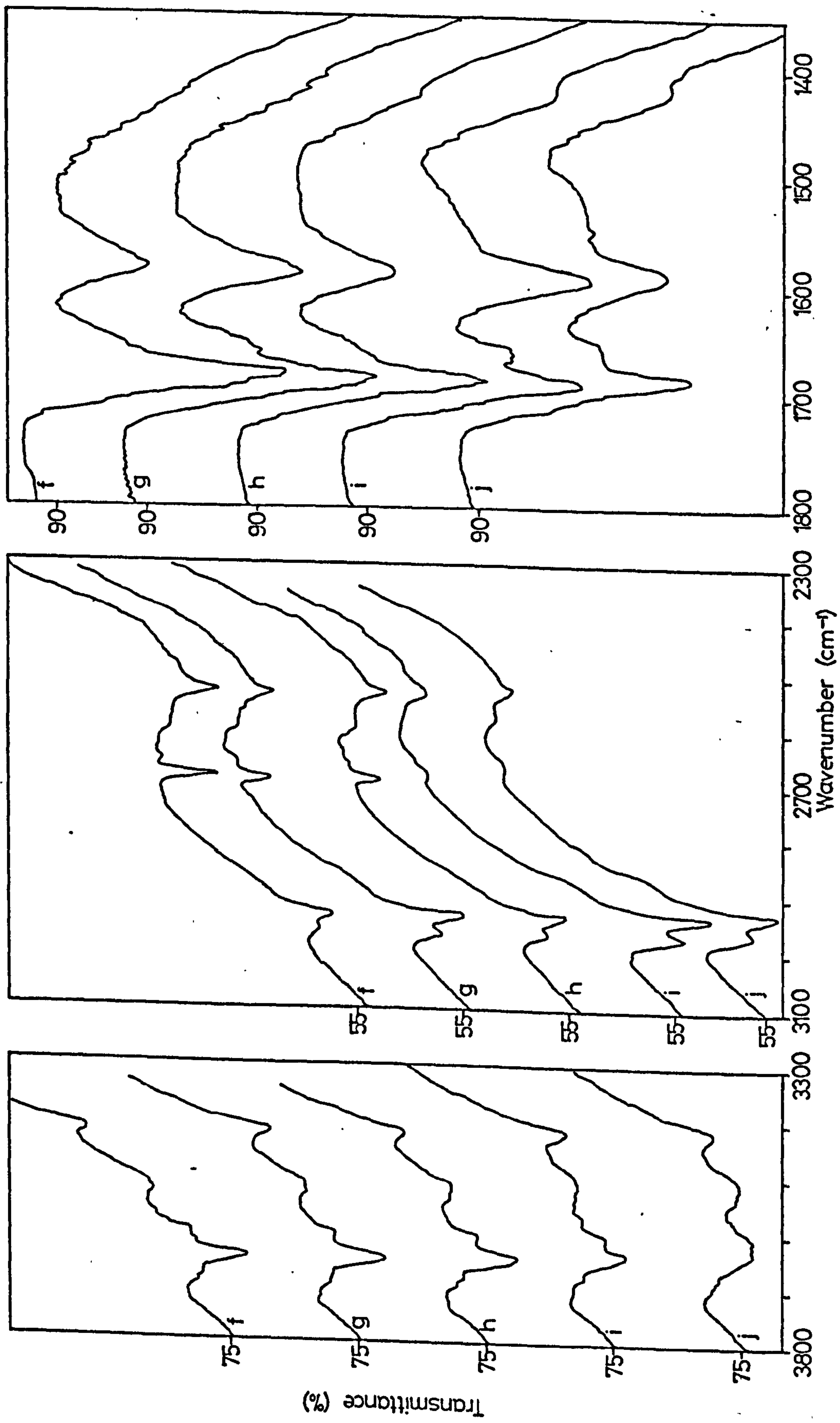
SPEC. 4.4

ADSORPTION OF ACETONE  $h_g$  ONTO A BT,  
 $D_2O$  OXIDIZED SURFACE

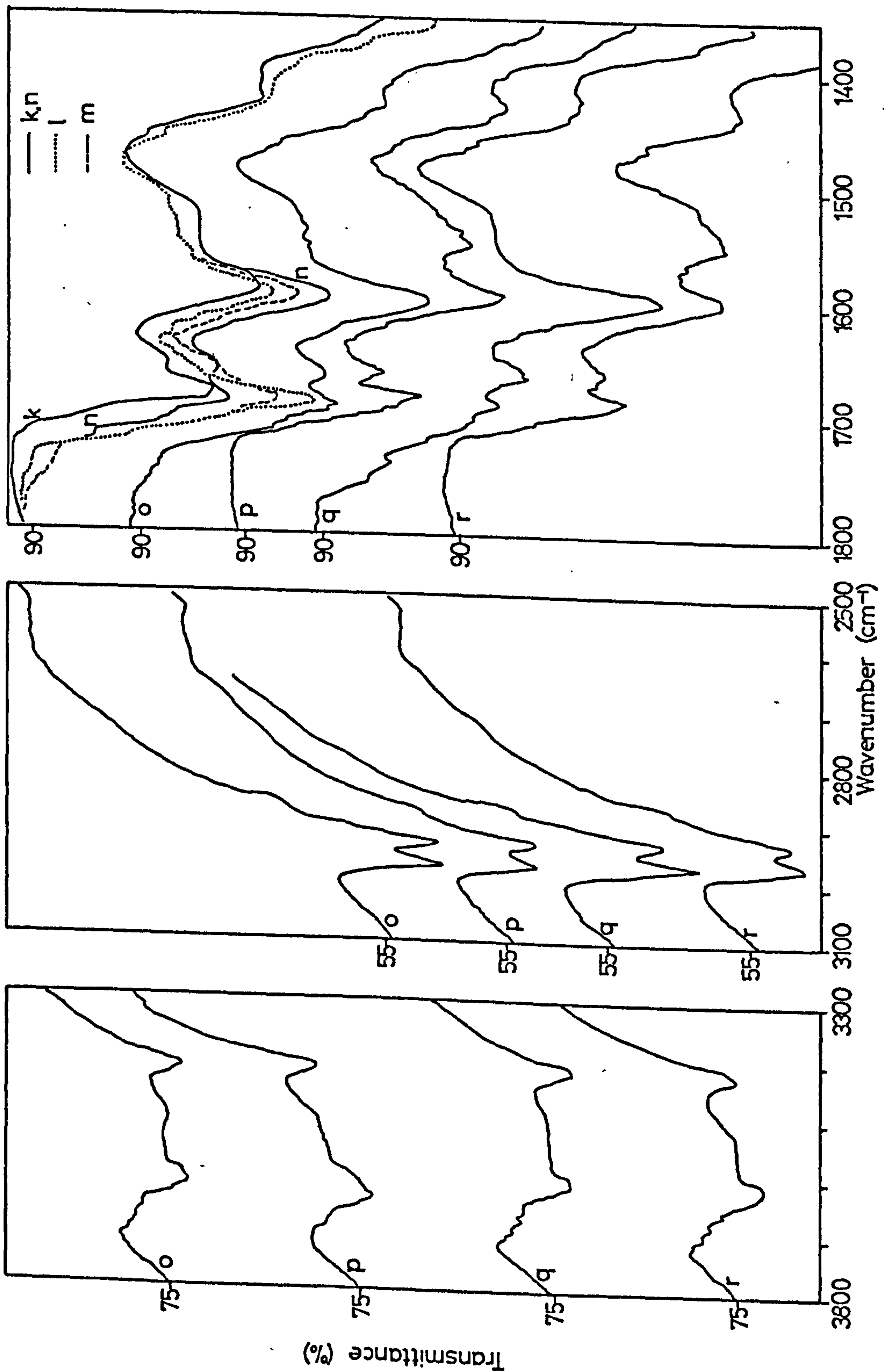
- (a) Initial surface
- (b)-(g) adsorption of acetone  $h_g$  at increasing vapour pressures
- (h) exposure of disc (g) to acetone vapour in a closed cell (298 K, 11h)
- (i) adsorption of acetone  $h_g$
- (j) exposure of disc (i) to acetone vapour in a closed cell (298 K, 62h)
- (k)-(n) adsorption of acetone  $h_g$  (k) 0 sec (l) 5 secs (m) 2 mins  
(n) 25 mins
- (o), (q) further adsorption of acetone  $h_g$
- (p) evacuation



Spec 4.4 Adsorption of Acetone h<sub>6</sub> onto a BT, D<sub>2</sub>O, Oxidized Surface



Spec 4.4 Adsorption of Acetone h<sub>6</sub> onto a BT, D<sub>2</sub>O, Oxidized Surface



Spec 4.4 Adsorption of Acetone  $h_6$  onto a BT,  $D_2O$ , Oxidized Surface

SPEC. 4.5

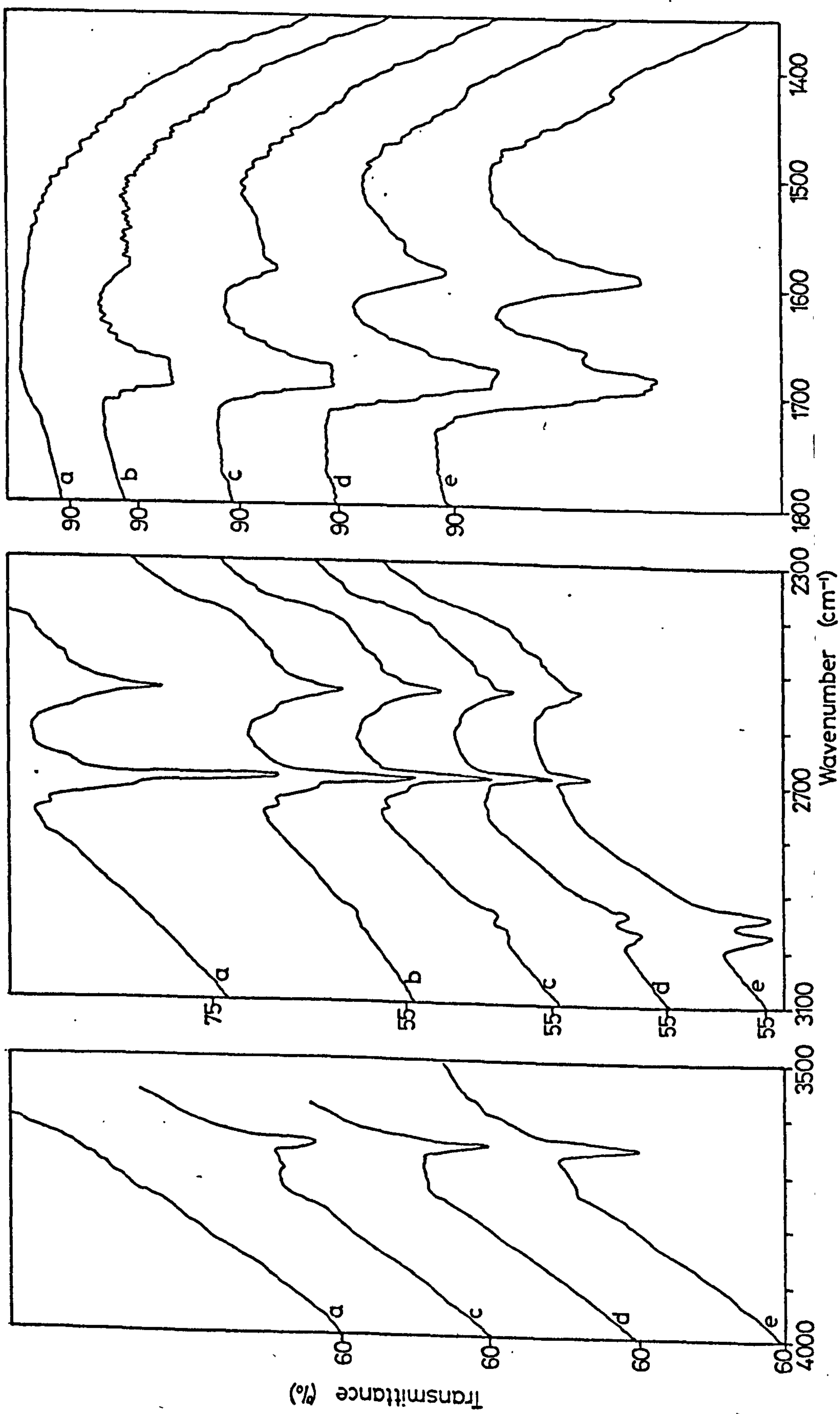
SPEC. 4.5

ADSORPTION OF ACETONE  $h_g$  ONTO A 373 K (100°C)

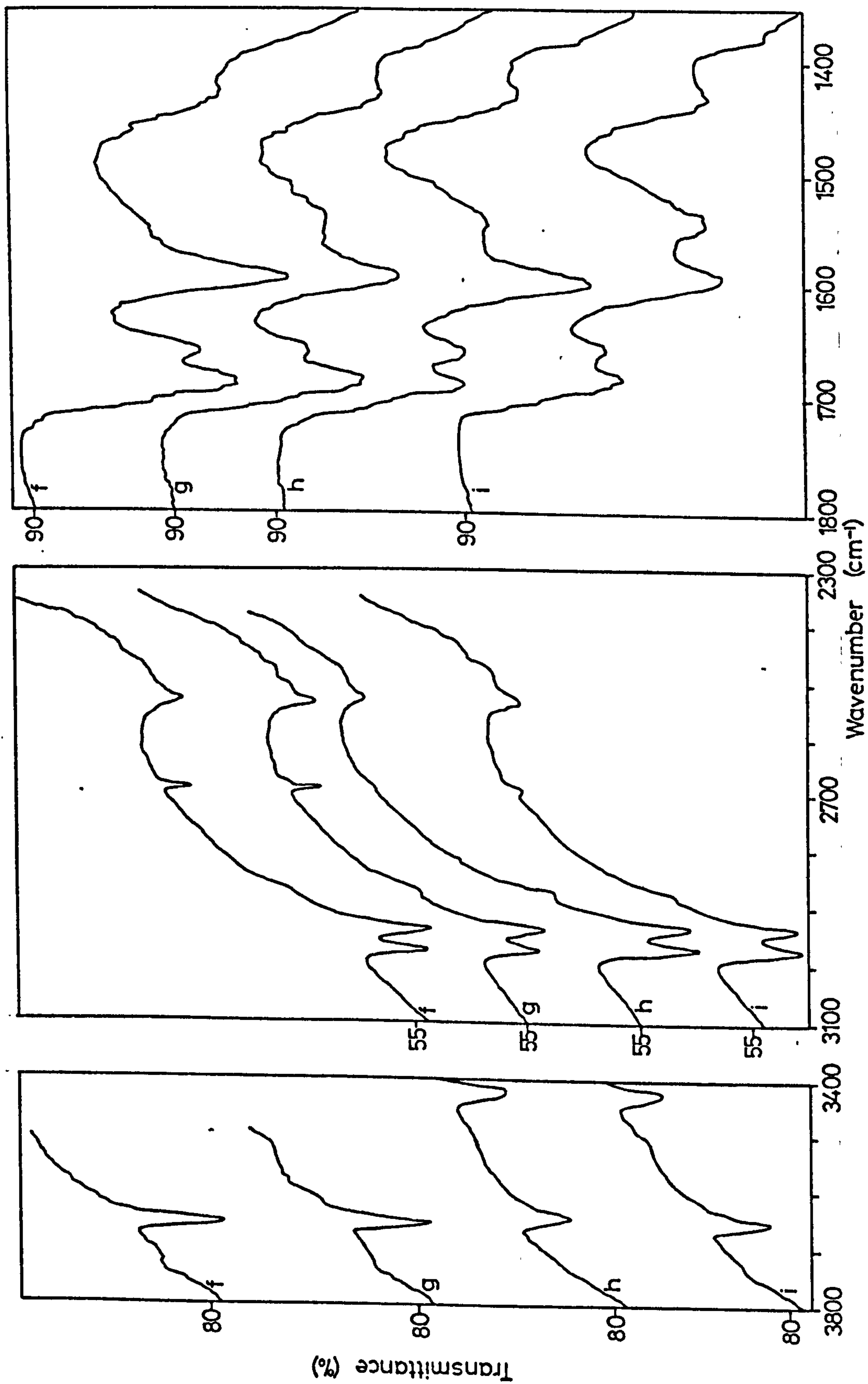
D<sub>2</sub>O OXIDIZED SURFACE

- (a) Initial surface
- (b)-(f) adsorption of acetone  $h_g$  at increasing vapour pressures
- (g) exposure of disc (f) to acetone  $h_g$  vapour in a closed cell (BT, 15h)
- (h),(j),(l) adsorption of acetone  $h_g$  at increasing vapour pressures
- (i),(k),(m) evacuation (BT)

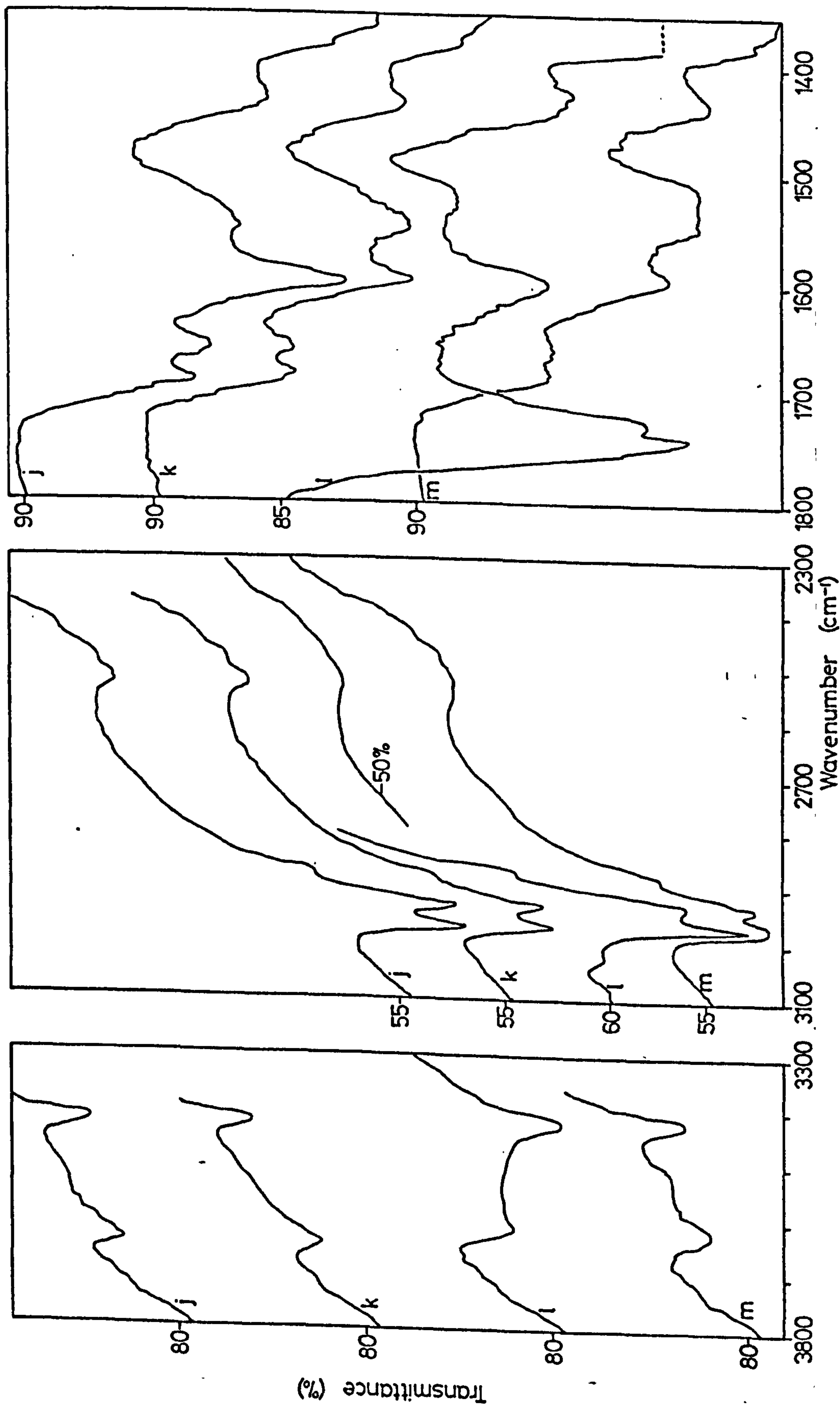




Spec 4.5 Adsorption of Acetone h<sub>g</sub> onto a 673 K D<sub>2</sub>O<sub>2</sub> Oxidized Surface



Spec 4.5 Adsorption of Acetone  $h_6$  onto a 673 K  $D_2O$  Oxidized Surface



Spec 4.5 Adsorption of Acetone  $h_6$  onto a 673 K  $D_2O$  Oxidized Surface

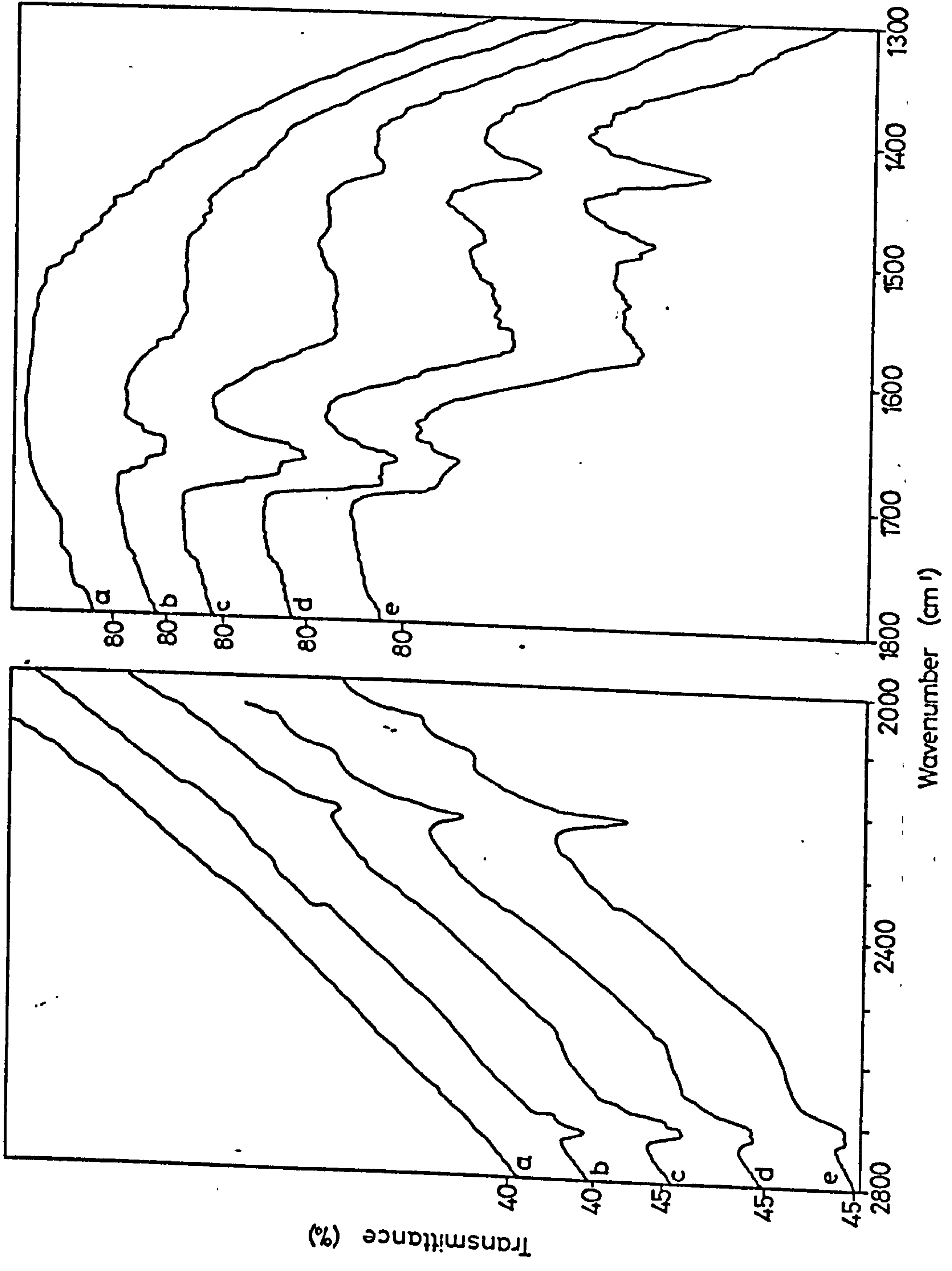
SPEC. 4.6

SPEC. 4.6

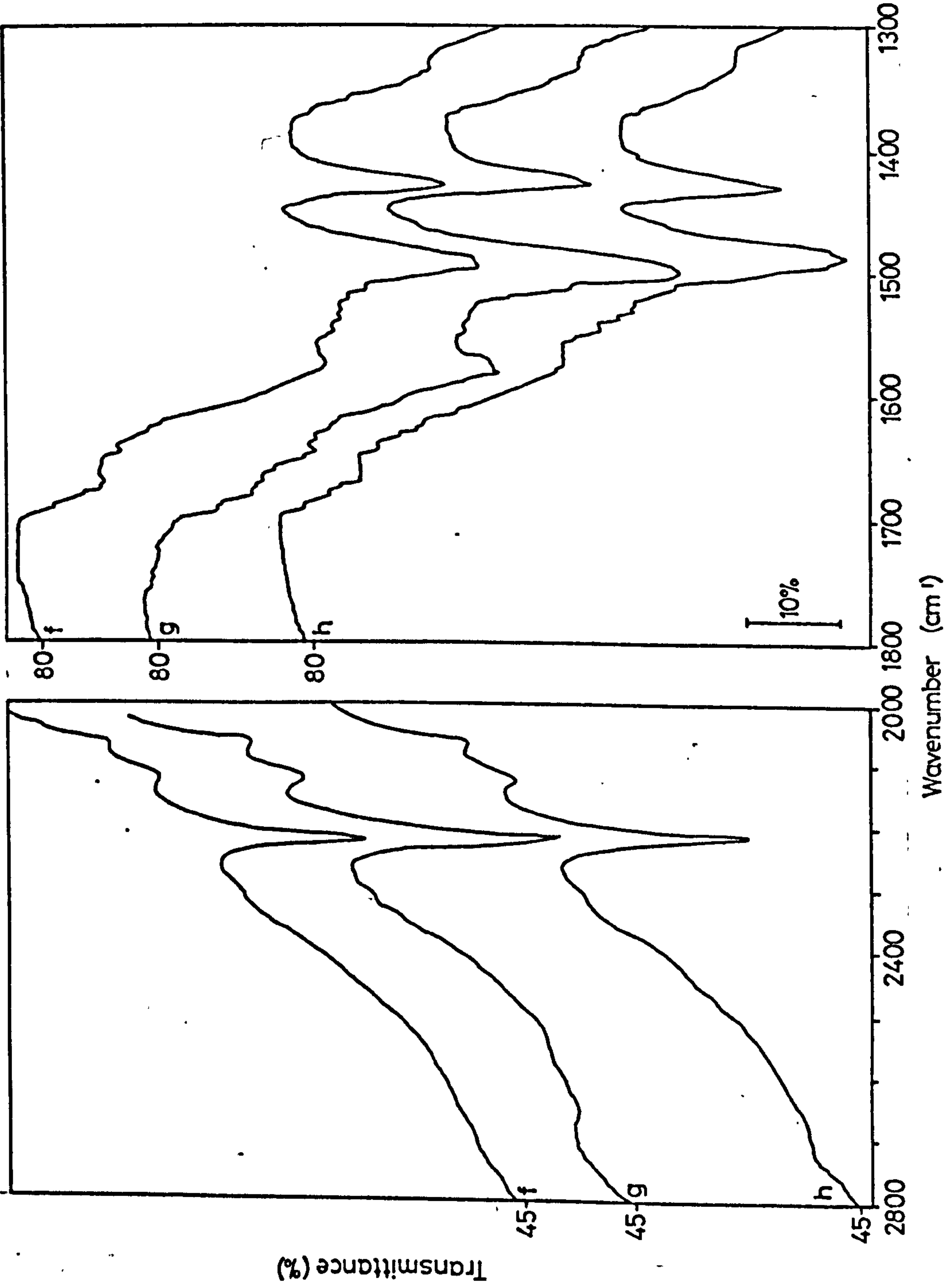
ADSORPTION OF ACETONE  $d_6$  ONTO A 673 K

REDUCED SURFACE

- (a) Initial surface
- (b)-(g) adsorption of acetone  $d_6$  at increasing vapour pressures
- (h) evacuation (BT, 1h)



Spec 4.6 Acetone d<sub>6</sub> onto a 673 K Reduced Surface



Spec 4.6 Acetone d<sub>6</sub> onto a 673 K Reduced Surface

SPEC. 4.7



SPEC. 4.7

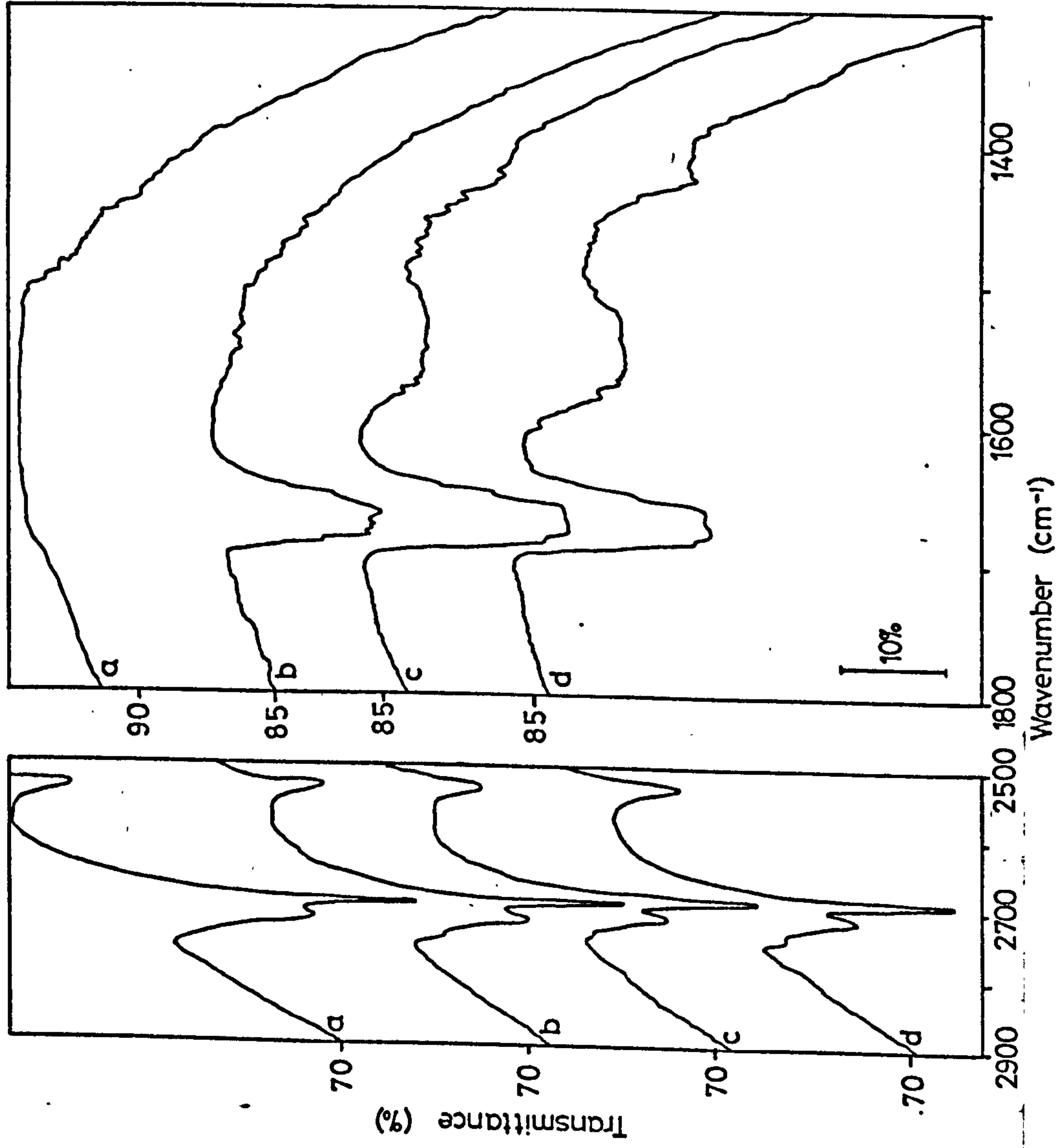
ADSORPTION OF ACETONE  $d_6$  ONTO A BT,  $D_2O$

REDUCED SURFACE

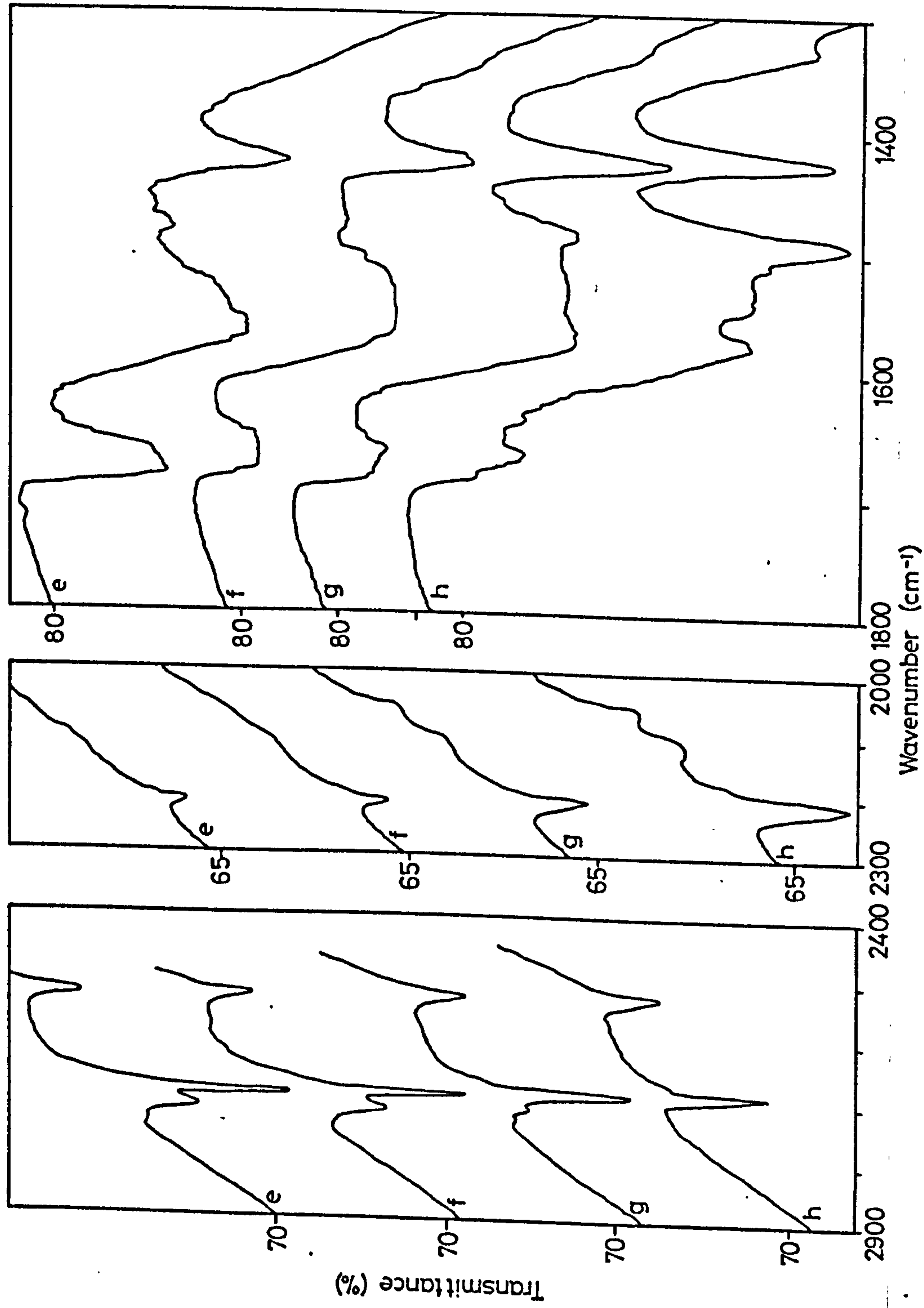
(a) Initial surface

(b)-(e), (g)-(i), (k) adsorption of acetone  $d_6$  at increasing  
vapour pressures

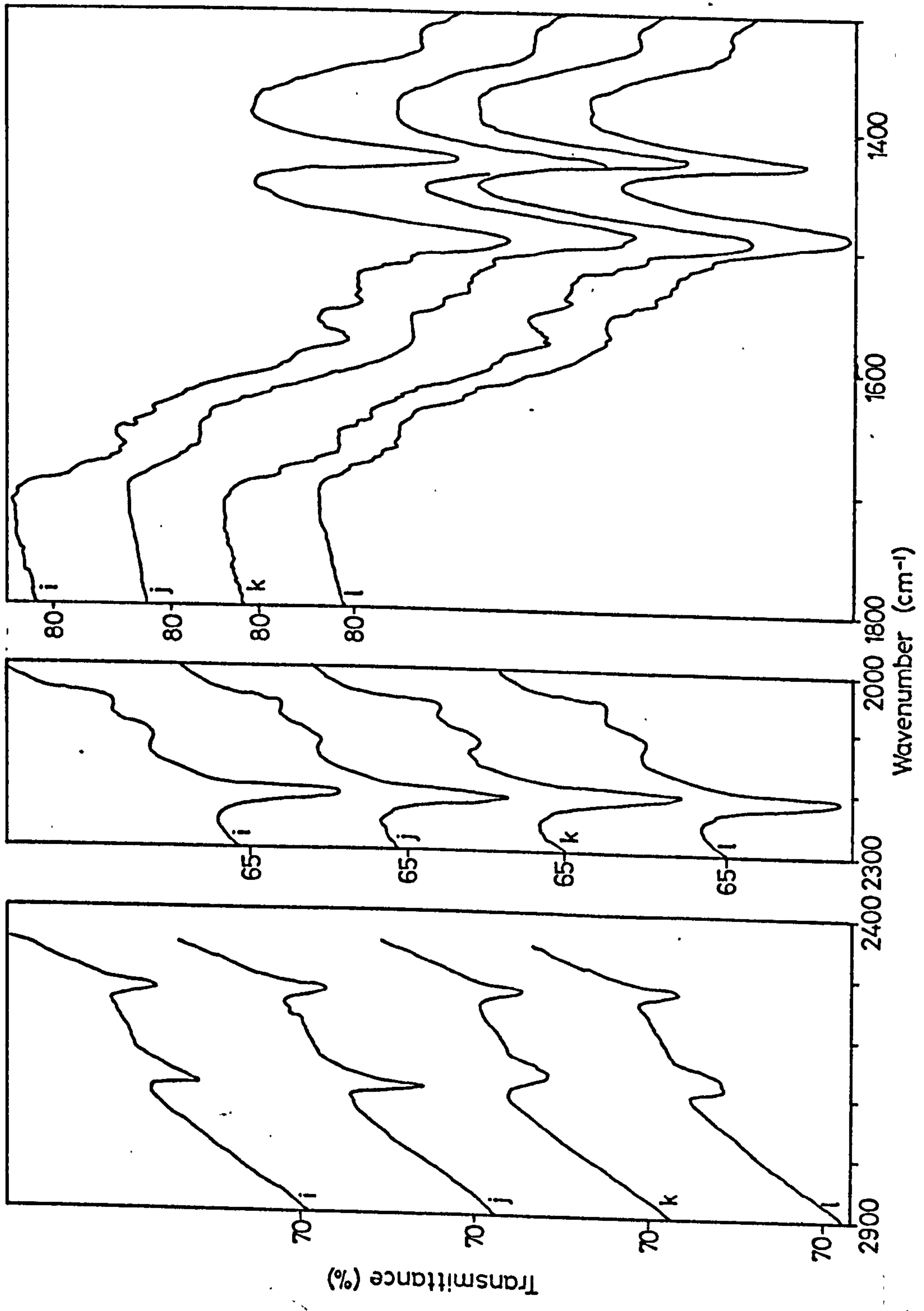
(f), (j), (l) evacuation (BT)



Spec 47 Adsorption of Acetone  $d_6$  onto a BT  $D_2O$  Reduced Surface

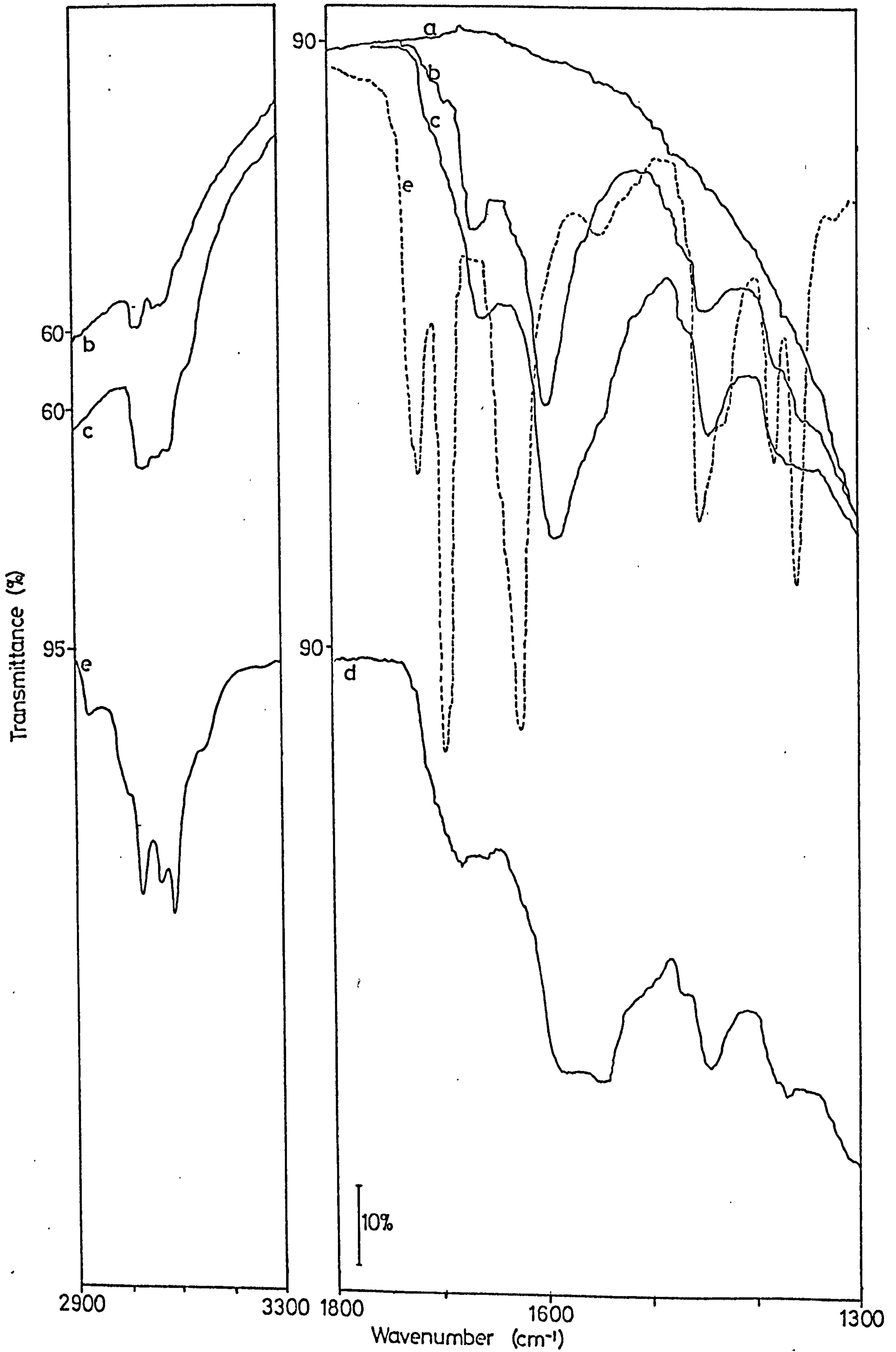


Spec 47 Adsorption of Acetone d<sub>6</sub> onto a BT D<sub>2</sub>O Reduced Surface



Spec 47 Adsorption of Acetone d<sub>6</sub> onto a BT D<sub>2</sub>O Reduced Surface

SPEC. 4.8



Spec 4.8 Adsorption of Mesityl Oxide onto a 673 K H<sub>2</sub>O Oxidized Surface

SPEC. 5.1

SPEC. 5.1

ADSORPTION OF DEUTEROACETIC ACID ONTO A

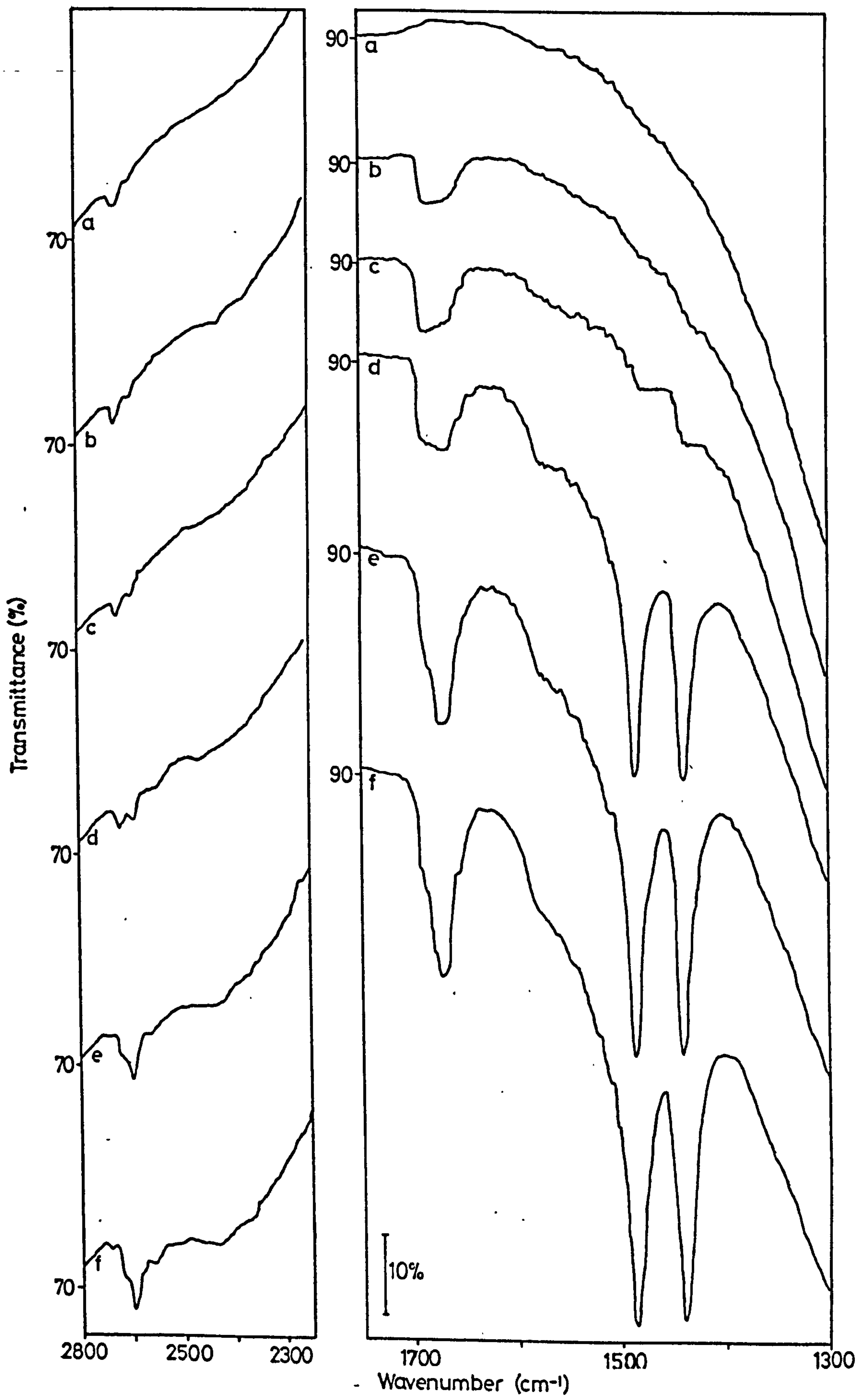
673 K, D<sub>2</sub>O, OXIDIZED SURFACE

(a) Initial surface

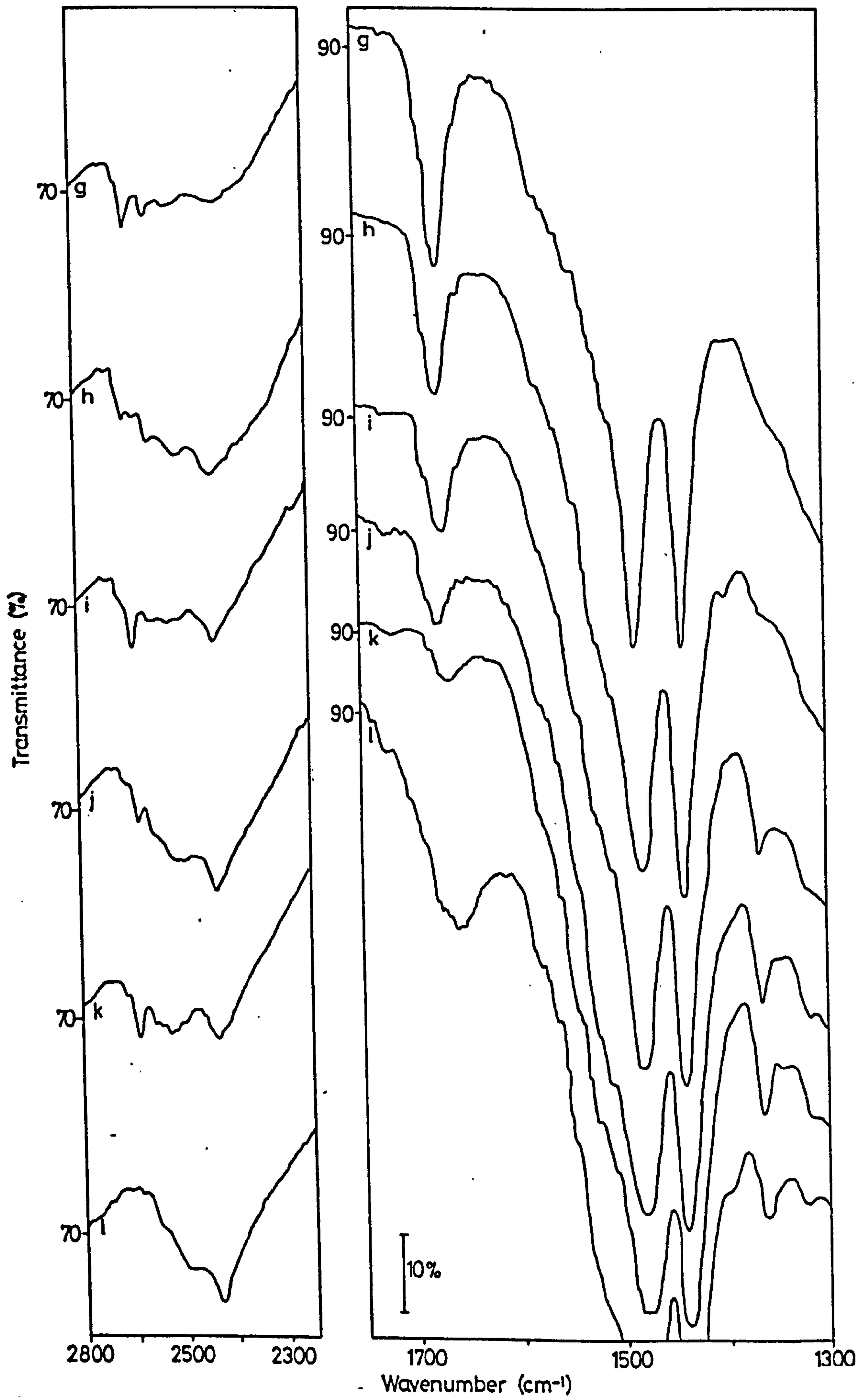
(b)-(h),(j),(l),(n),(o) adsorption deuterioacetic acid at increasing  
vapour pressures

(i),(k),(m),(p) evacuation (BT)

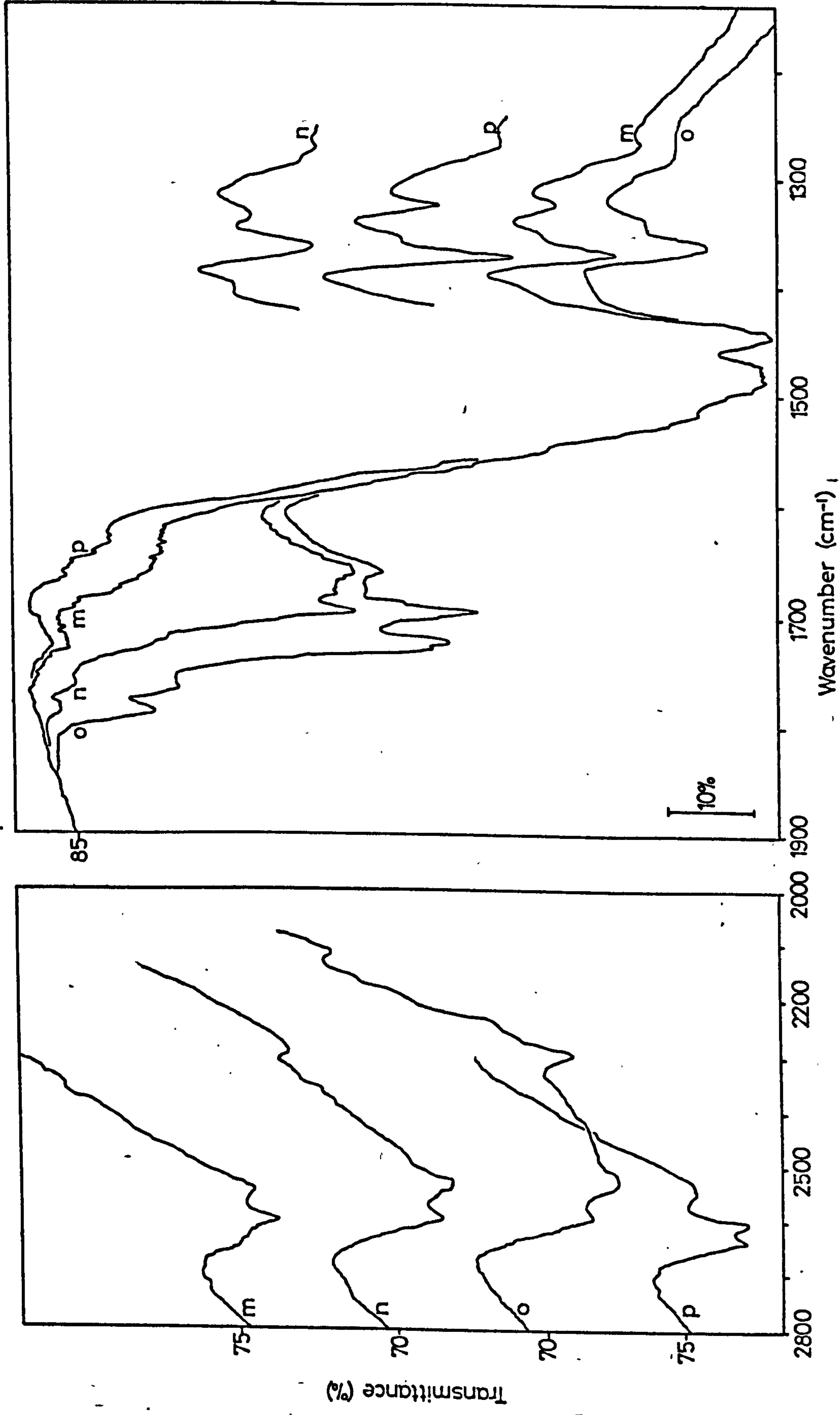




Spec 51 Adsorption of Deuteroacetic Acid onto a 673 K D O Oxidized Surface



Spec 51 Adsorption of Deuteroacetic Acid onto a 673 K D O Oxidized Surface



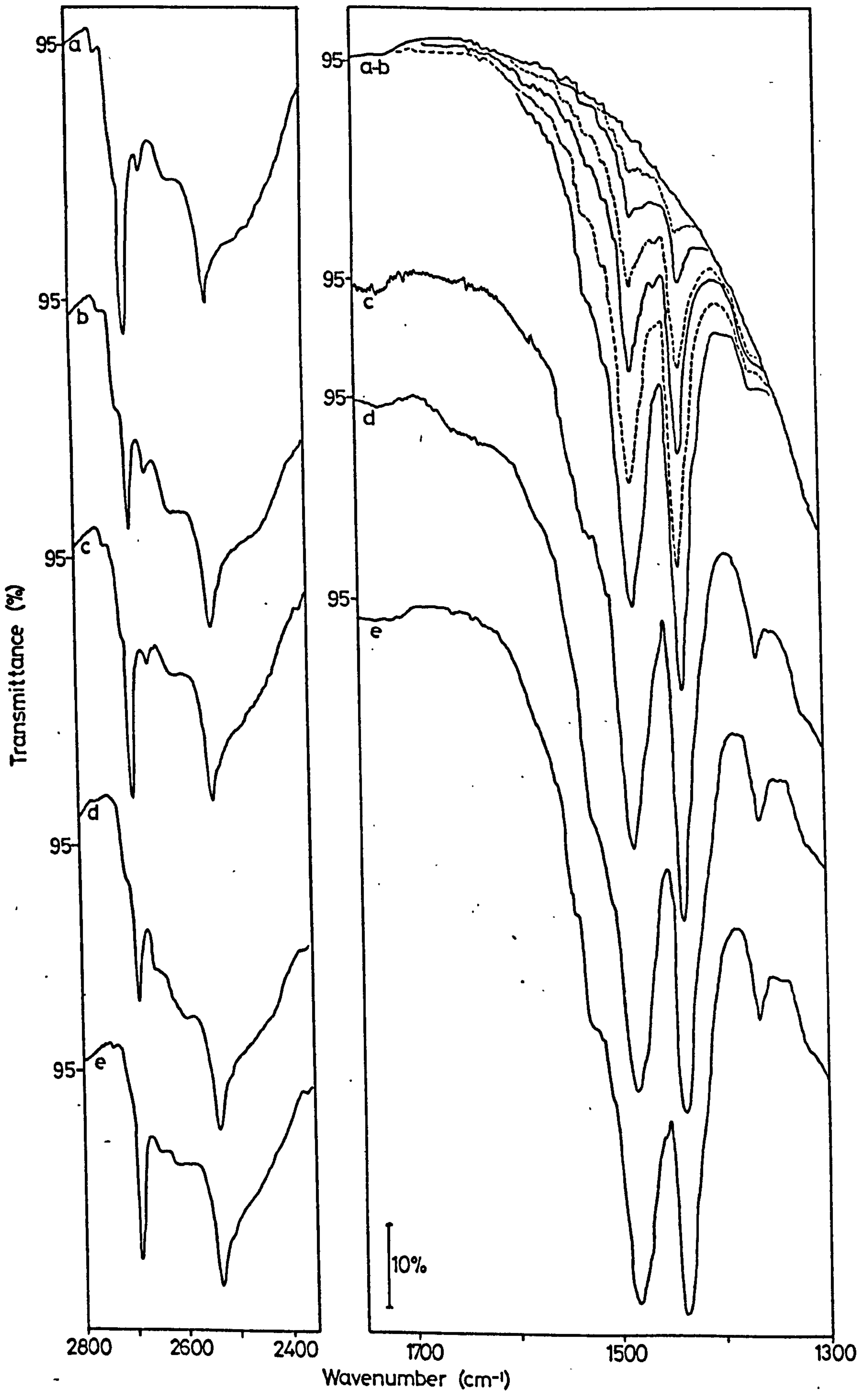
Spec 51 Adsorption of Deuteroacetic Acid onto a 673 K D O Oxidized Surface

SPEC. 5.2

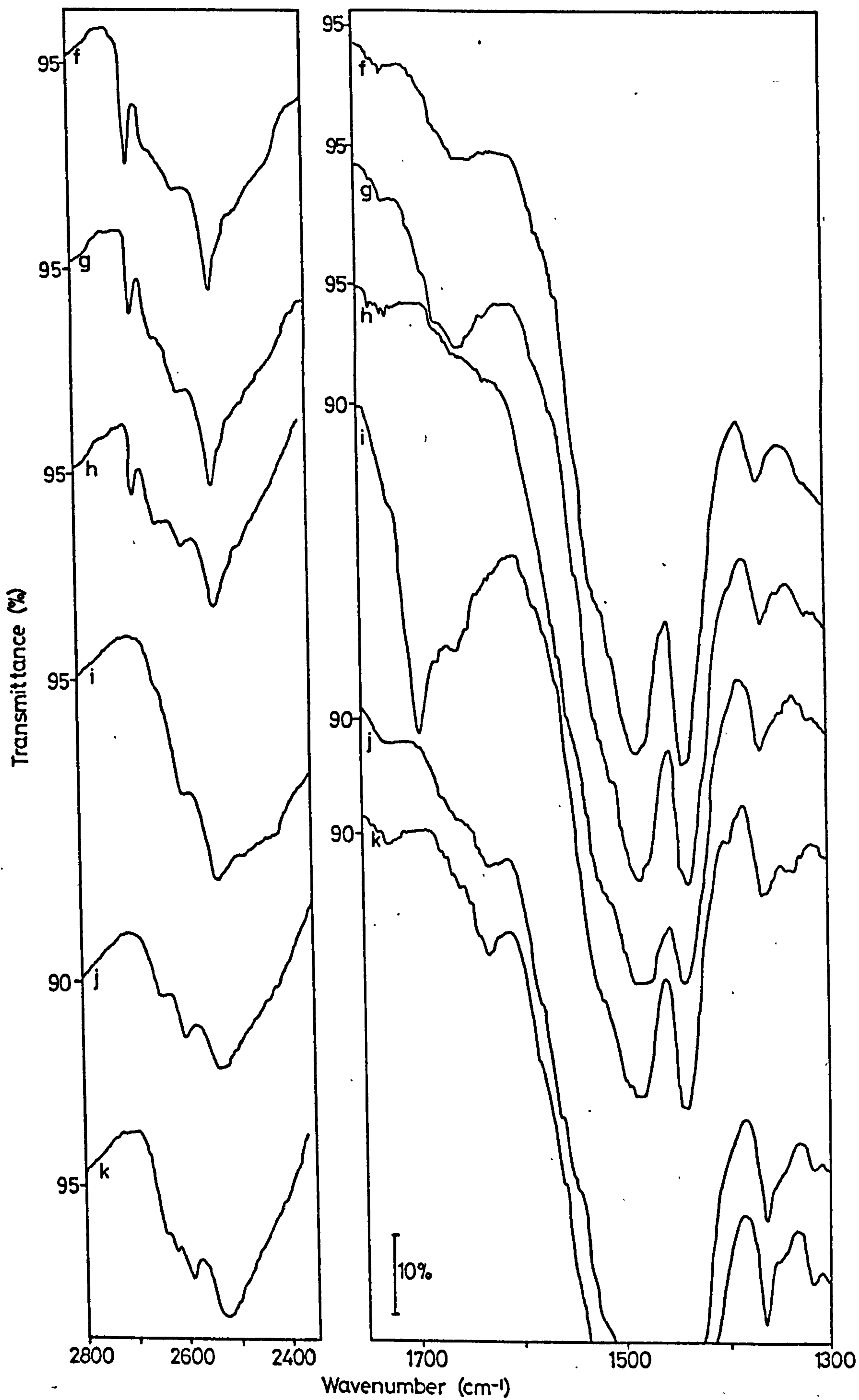
SPEC. 5.2

ADSORPTION OF DEUTEROACETIC ACID ONTO A  
BT, D<sub>2</sub>O, OXIDIZED SURFACE

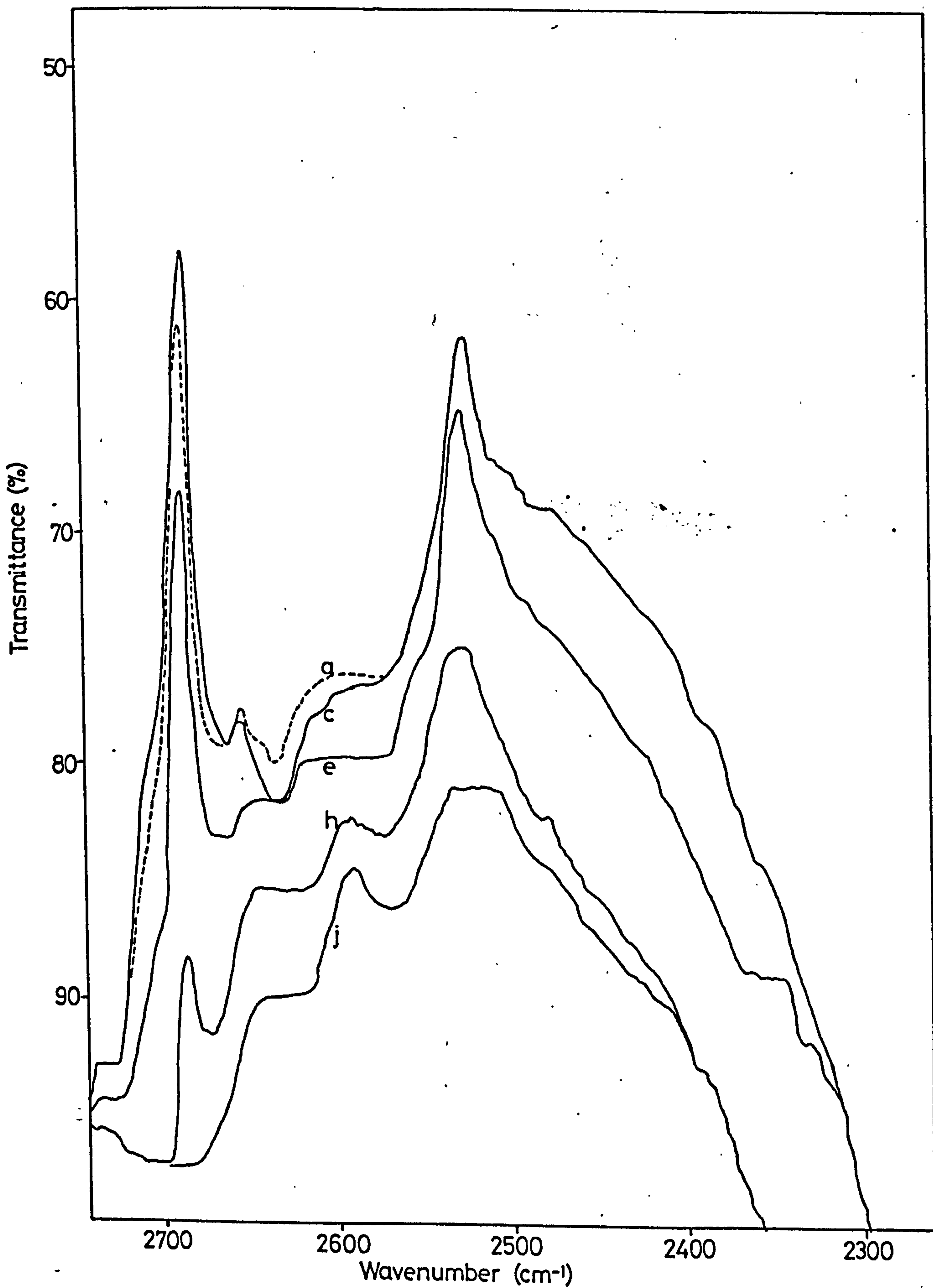
- (a) Initial surface
- (b),(d),(f),(g),(i) adsorption deuterioacetic acid at increasing  
vapour pressures
- (c),(e),(h),(j) evacuation (BT)
- (k) adsorption D<sub>2</sub>O (BT, ½h) and evacuation (BT, ½h)



Spec 5.2 Adsorption of Deuteroacetic Acid onto a BT D<sub>2</sub>O Oxidized Surface



Spec 5.2 Adsorption of Deuteroacetic Acid onto a BT D<sub>2</sub>O Oxidized Surface



Spec 5.2 Adsorption of Deuteroacetic Acid onto a BT D<sub>2</sub>O Oxidized Surface



SPEC. 5.3

SPEC. 5.3

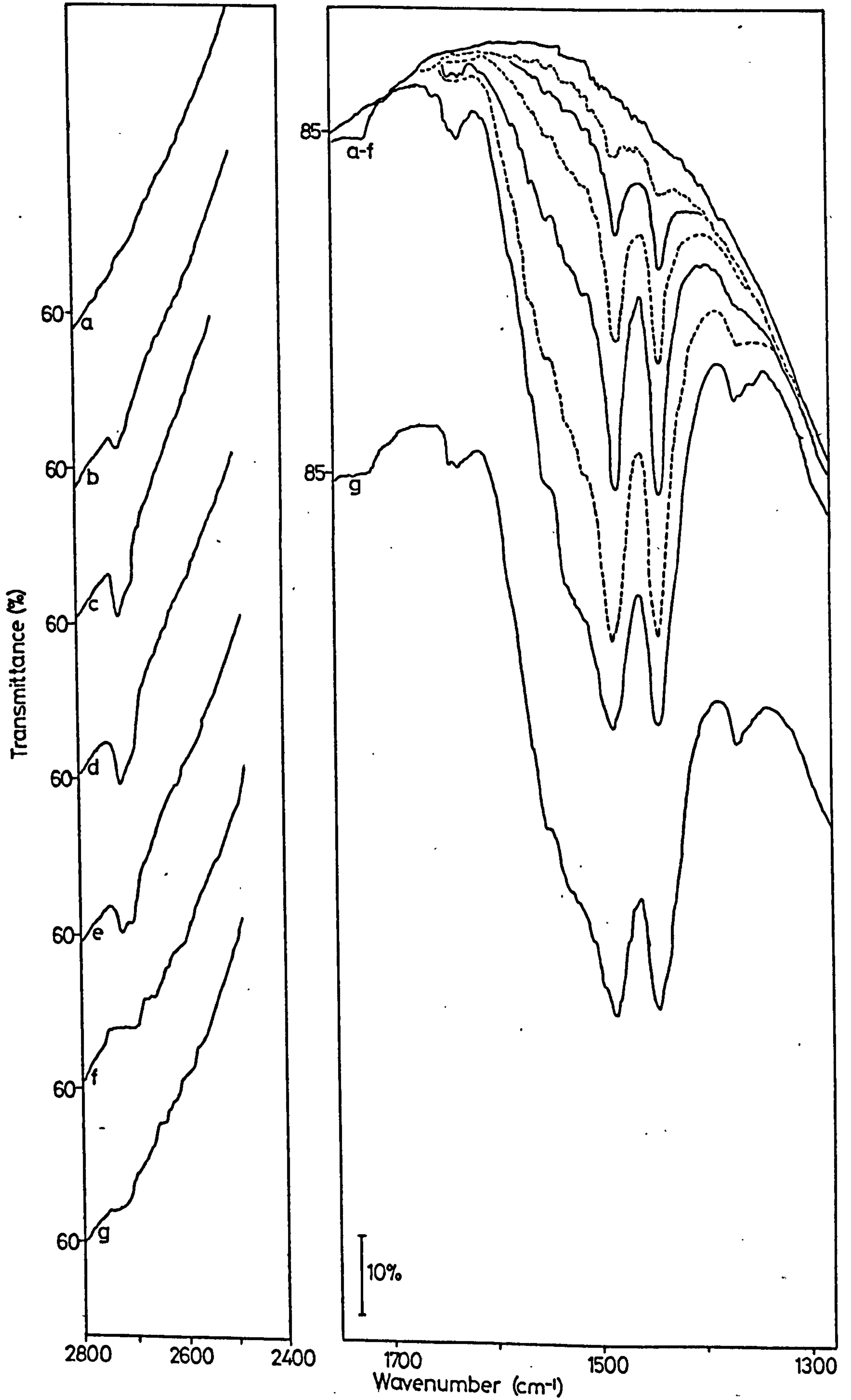
ADSORPTION OF DEUTEROACETIC ACID ONTO A 673 K,

D<sub>2</sub>O REDUCED SURFACE

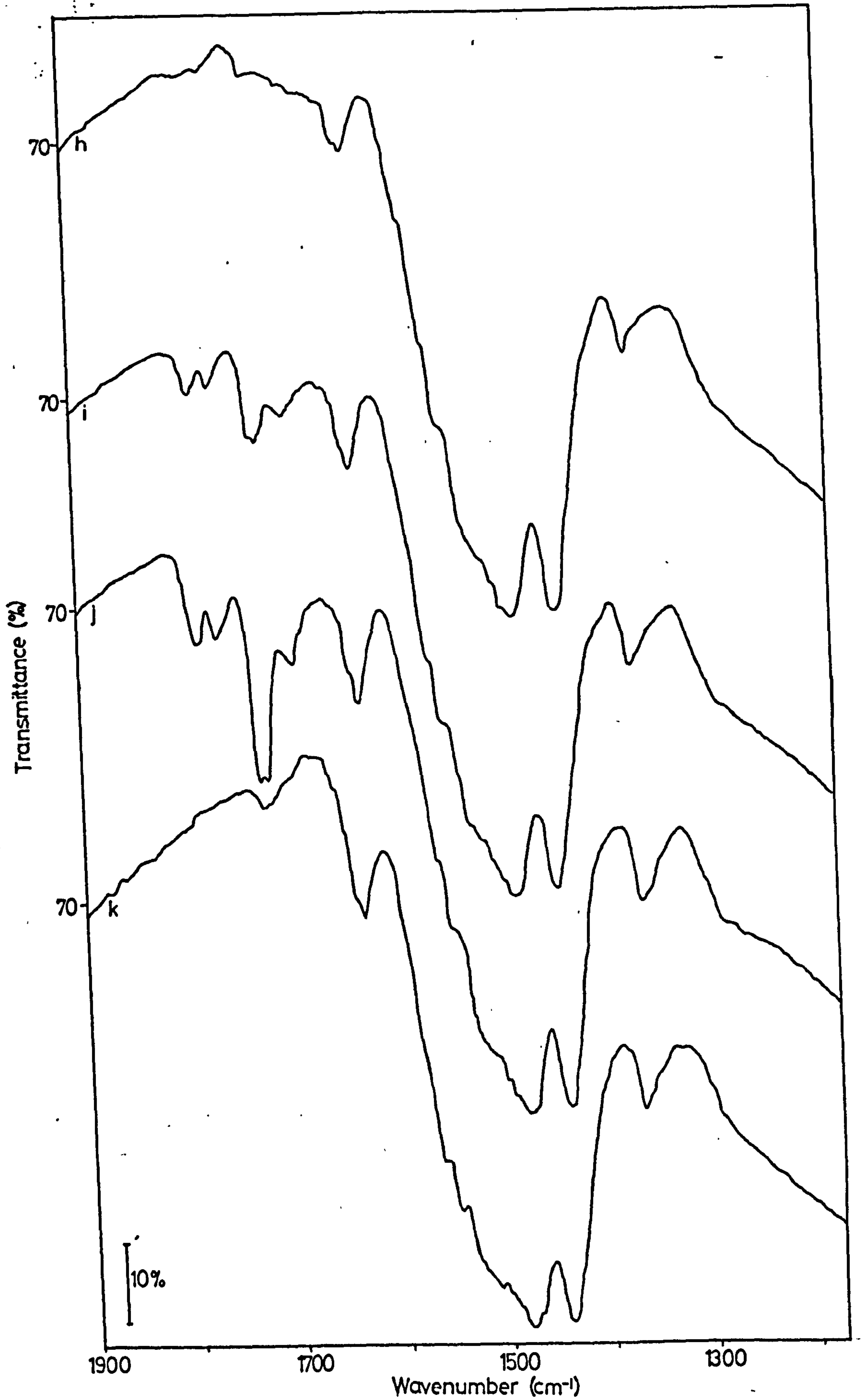
(a) Initial surface

(b)-(f),(h),(i),(j) adsorption of deuterioacetic acid at  
increasing vapour pressures

(g),(k) evacuation (BT, lh)



Spec 53 Adsorption of Deuteroacetic Acid onto a 673 K D<sub>2</sub>O Reduced Surface



Spec 5.3 Adsorption of Deuteroacetic Acid onto a 673 K D<sub>2</sub>O Reduced Surface

SPEC. 5.4

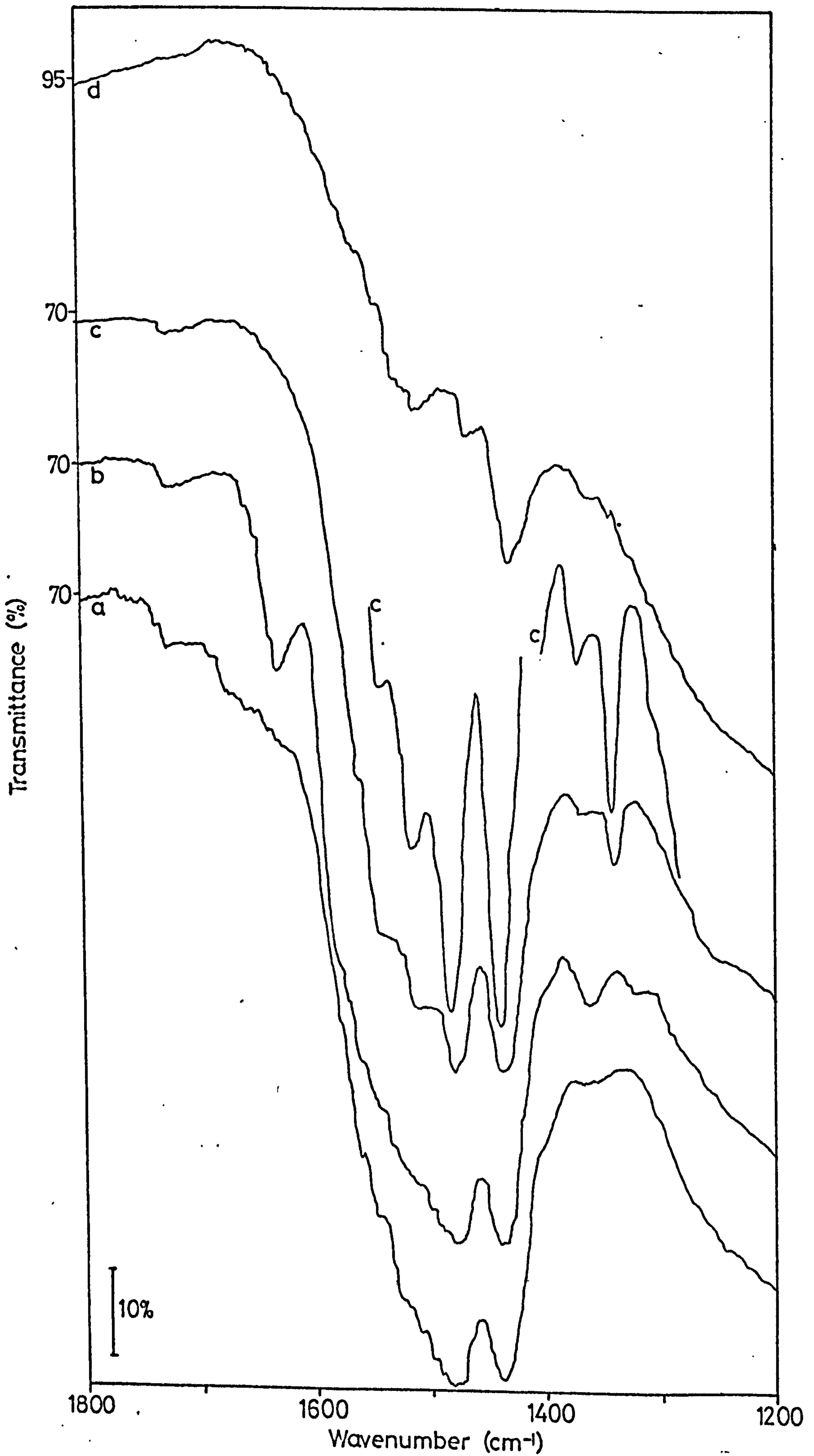
SPEC. 5.4

DESORPTION OF DEUTEROACETIC ACID FROM AN  
OXIDIZED SURFACE

- (a) 673 K, H<sub>2</sub>O surface after dosing on deuterioacetic acid  
vapour and evacuating at BT

Evacuation:-

- (b) 463 K, 1½h  
(c) 523 K, 2h  
(d) 616 K, 1½h



Spec 5.4 Desorption of Deuteroacetic Acid from an Oxidized Surface

SPEC. 6.1



SPEC. 6.1

ADSORPTION OF HEXAFLUOROACETONE ONTO A

673 K, D<sub>2</sub>O, OXIDIZED SURFACE

Adsorption of hexafluoroacetone

- (a) Initial surface
- (b)-(d) increasing pressures hexafluoroacetone

Evacuation

- (e) 423 K, 3h; (f) 473 K, 4h; (g) 543 K, 2½h;
- (h) 543 K, 20h;

Adsorption of D<sub>2</sub>O

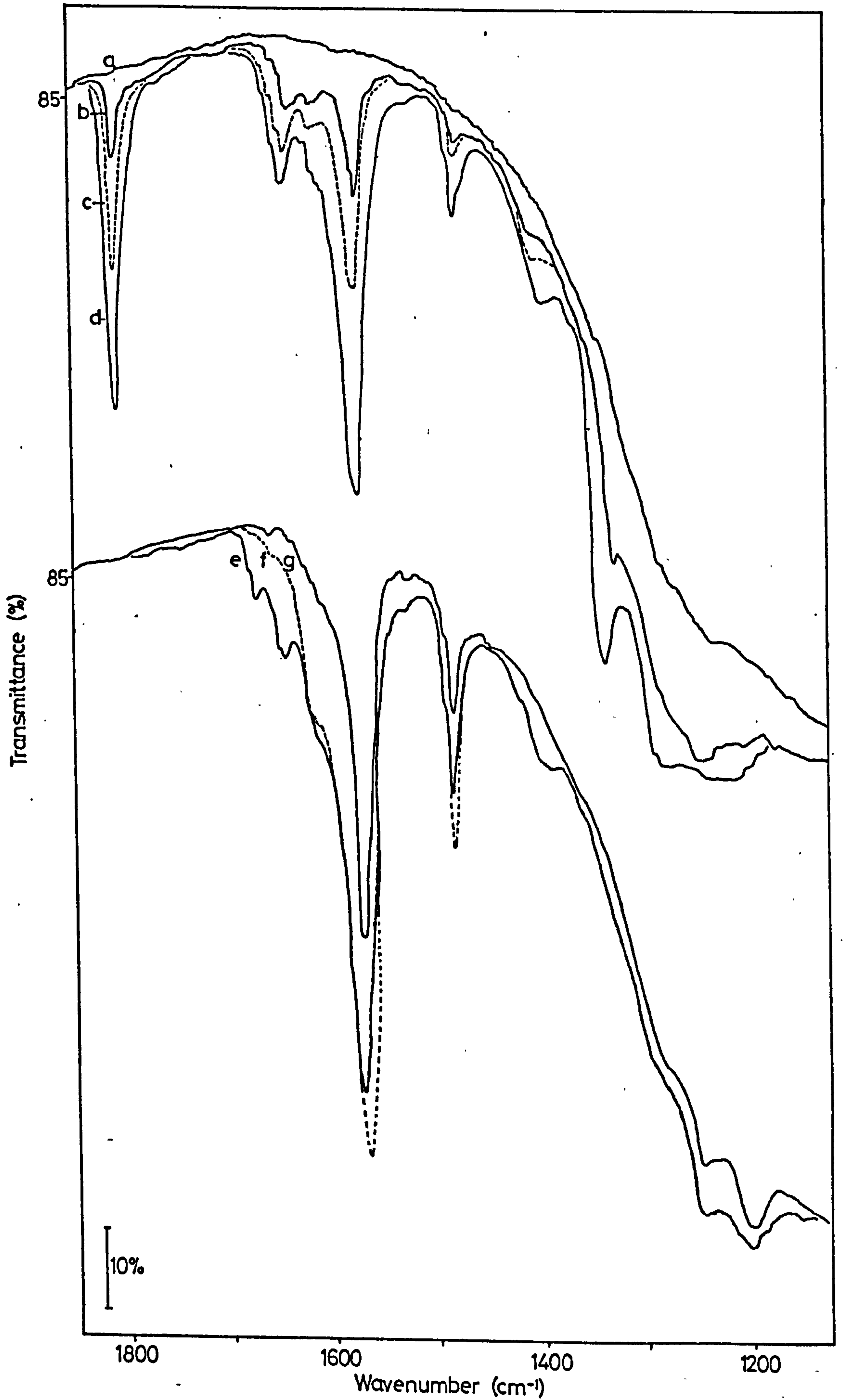
- (i) Exposure disc to D<sub>2</sub>O vapour (BT, 2½h) and evacuation

Evacuation

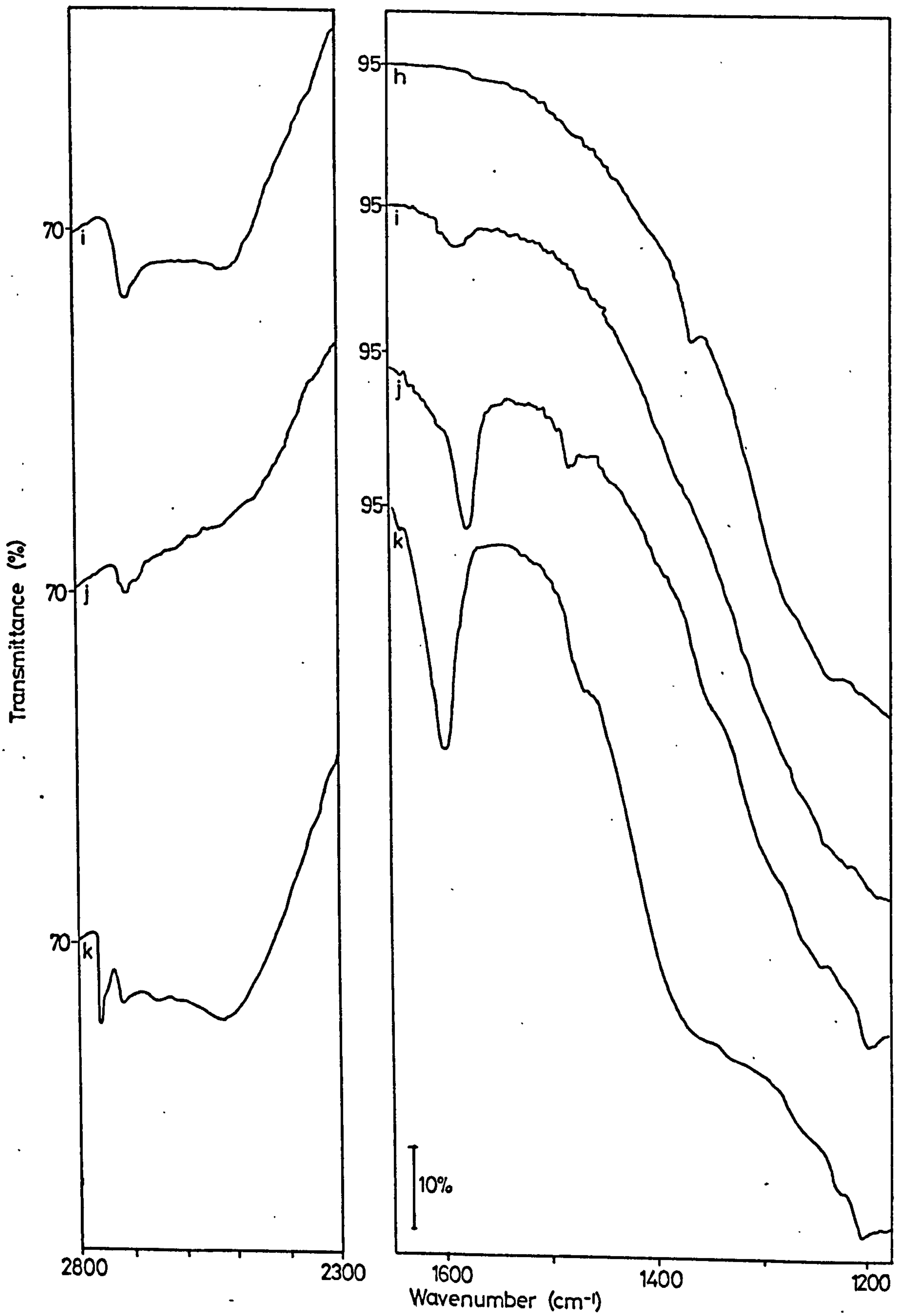
- (j) 363 K, 11h, 443 K, 1h

Adsorption of D<sub>2</sub>O

- (k) Exposure disc to D<sub>2</sub>O vapour (473 K, 15h) and evacuation (BT, 1h)



Spec 6.1 Adsorption of Hexafluoroacetone onto a 673 K Oxidized Surface



Spec 6.1 Adsorption of Hexafluoroacetone onto a 673 K Oxidized Surface

SPEC. 6.2

SPEC. 6.2

ADSORPTION OF HEXAFLUOROACETONE ONTO A  
BT, D<sub>2</sub>O, OXIDIZED SURFACE

Alternate adsorption and evacuation

- (a) Initial surface
- (b) adsorption of hexafluoroacetone
- (c) evacuation BT, 1h
- (d),(e) adsorption hexafluoroacetone
- (f) evacuation 373 K, 12h
- (g)-(j) adsorption at increasing pressures of hexafluoroacetone
- (k) evacuation 423 K, 2h
- (l),(m) adsorption at increasing pressures of hexafluoroacetone
- (n) evacuation 407 K, 13h
- (o) adsorption hexafluoroacetone

Evacuation to remove 1580, 1480 cm<sup>-1</sup> bands

- (p) 473 K, 2h (q) 473 K, 15h (r) 513 K, 2h (s) 543 K, ½h
- (t) 543 K, 2h (u) 543 K, 6h (v) 543 K, 20h

Adsorption of D<sub>2</sub>O

- (w) exposure to D<sub>2</sub>O vapour (7h) and evacuation (1½h)

SPEC. 6.2 Continued

SPEC. 6.2 Continued

Evacuation

(x) 473 K, 12h

Adsorption of hexafluoroacetone

(y) exposure to vapour

Evacuation

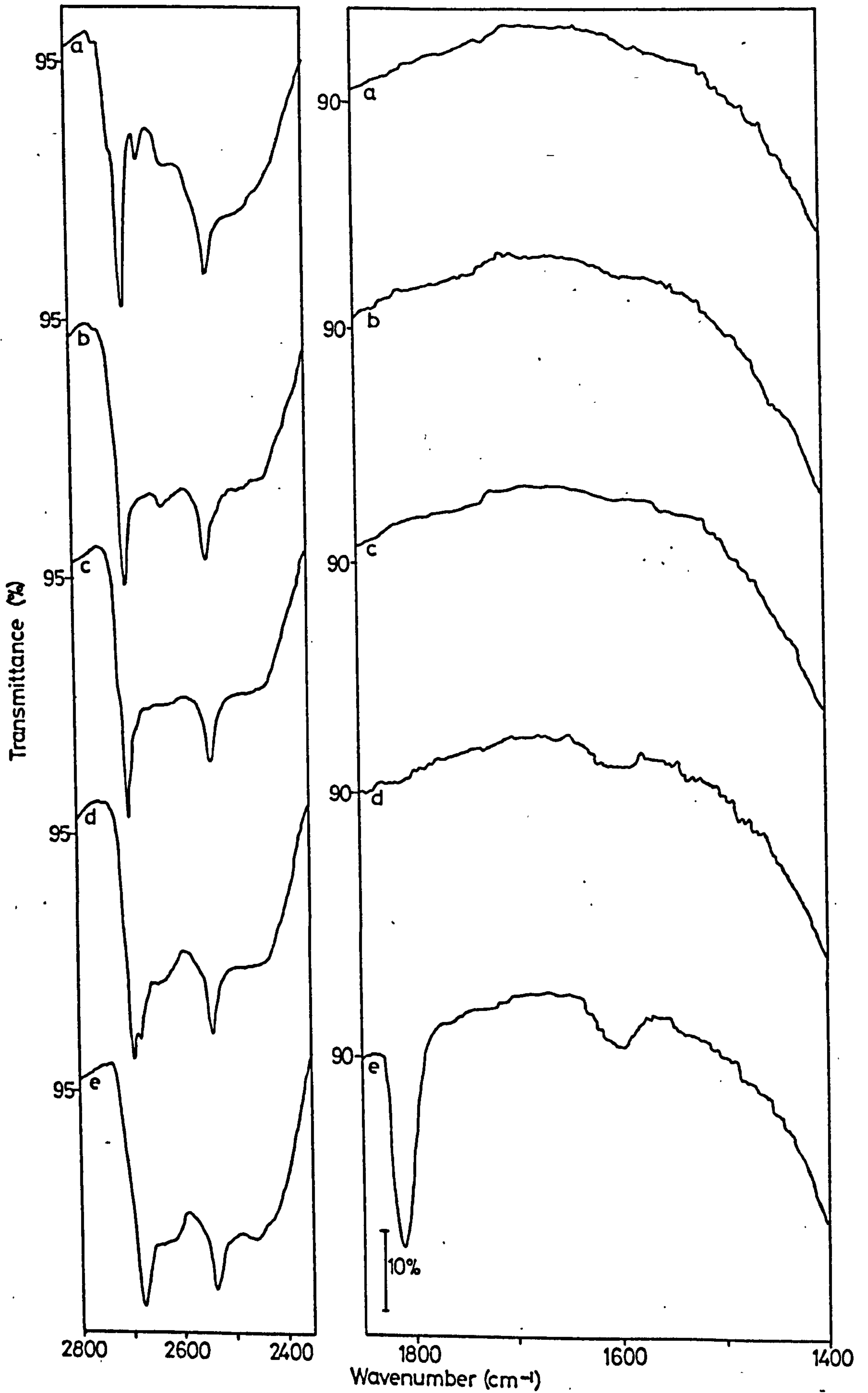
(z) 453 K, 6h

Adsorption of D<sub>2</sub>O

(a<sup>1</sup>) exposure of disc to D<sub>2</sub>O vapour (BT, ½h) and  
evacuation (BT, ½h)

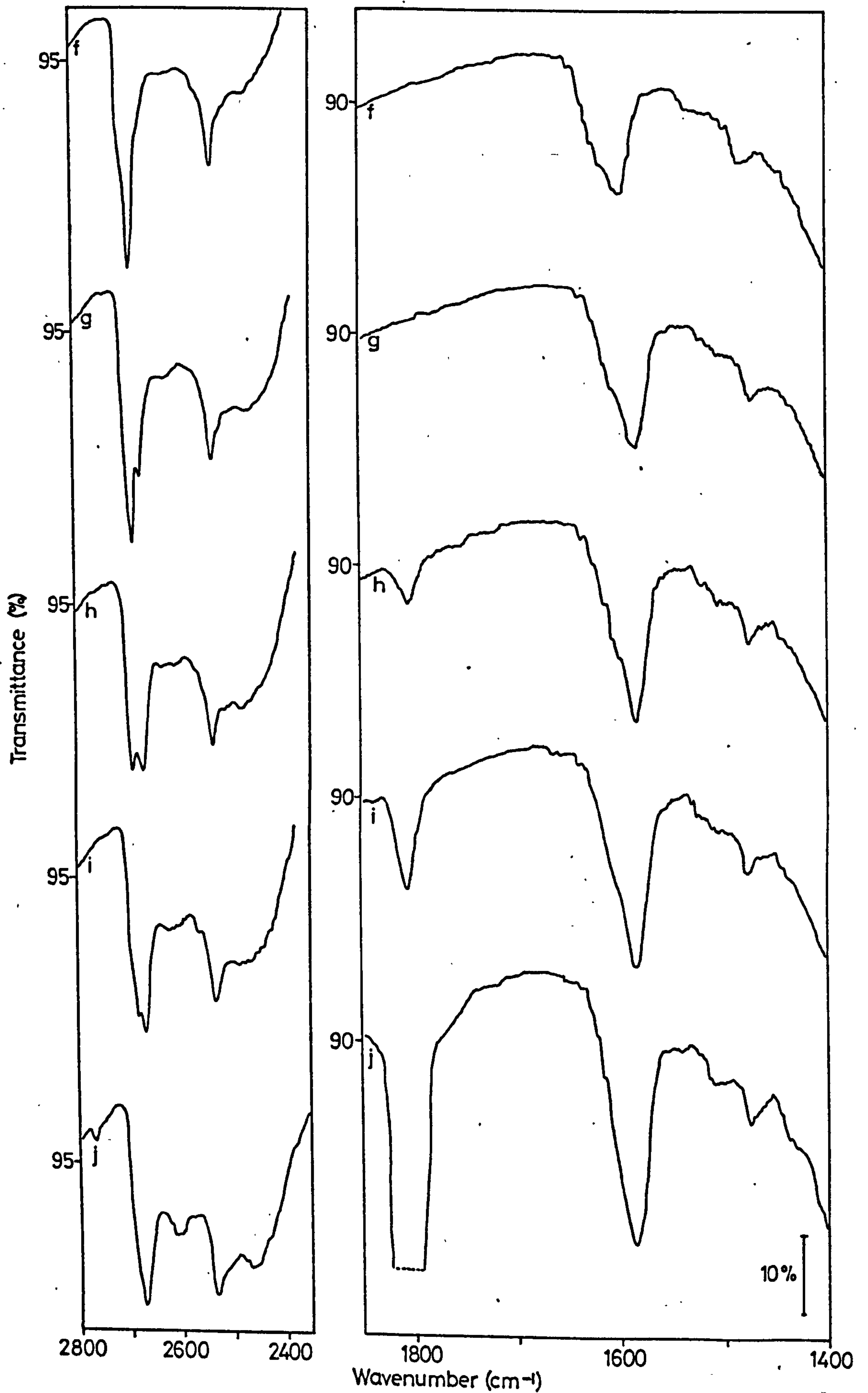
Evacuation

(b<sup>1</sup>) 453 K, 2h

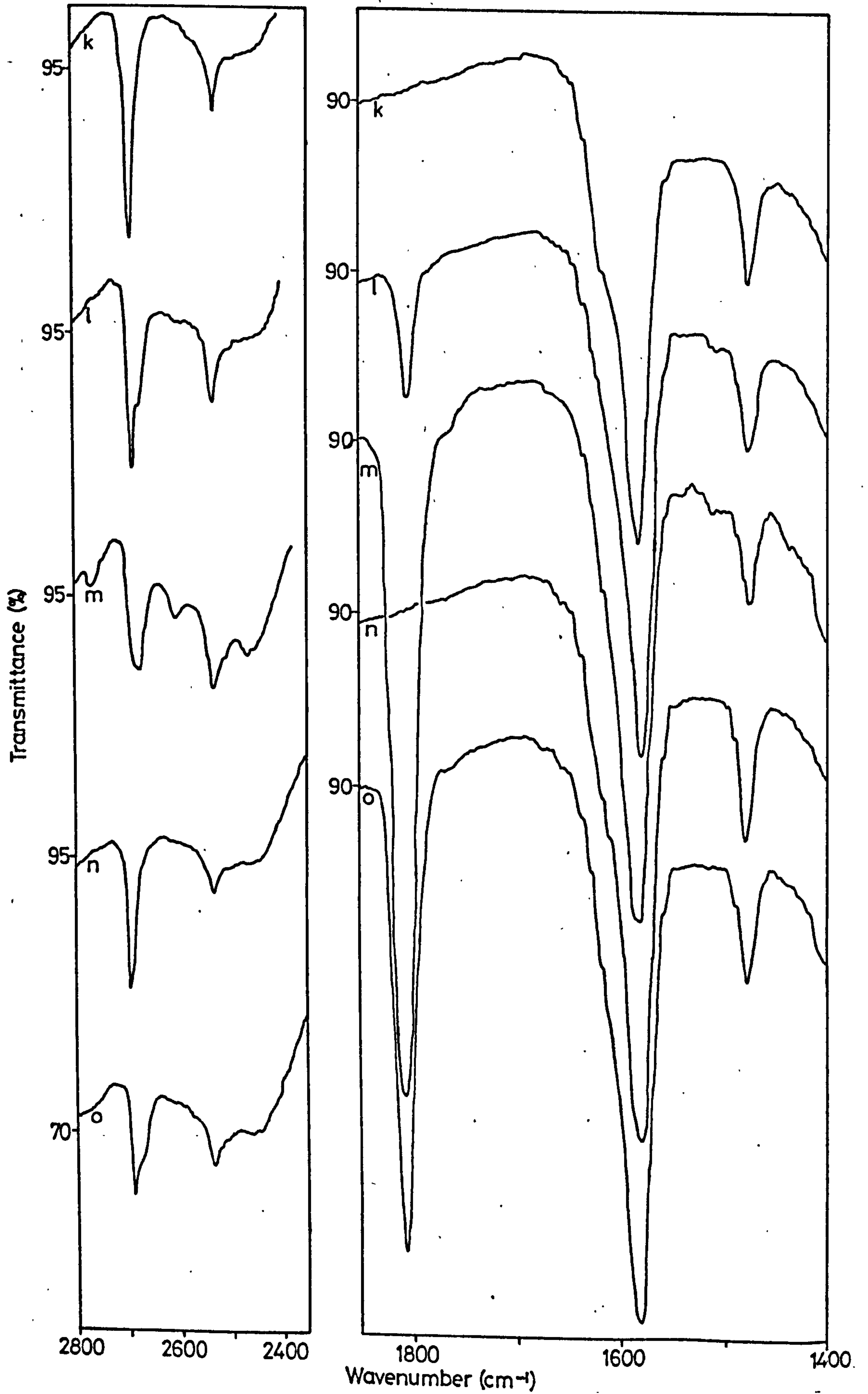


Spec 6.2 Adsorption of Hexafluoroacetone onto a BT D<sub>2</sub>O Oxidized Surface

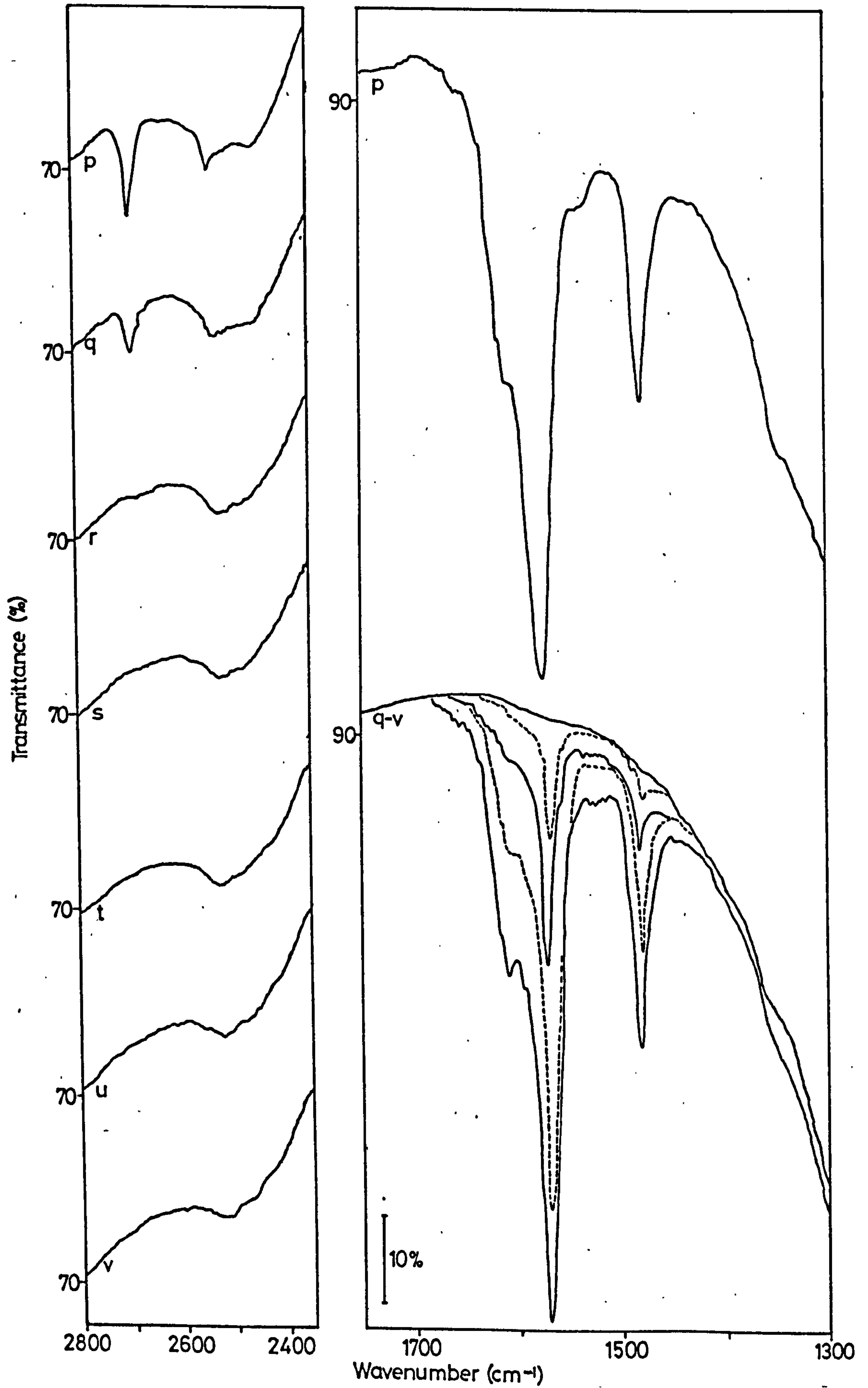




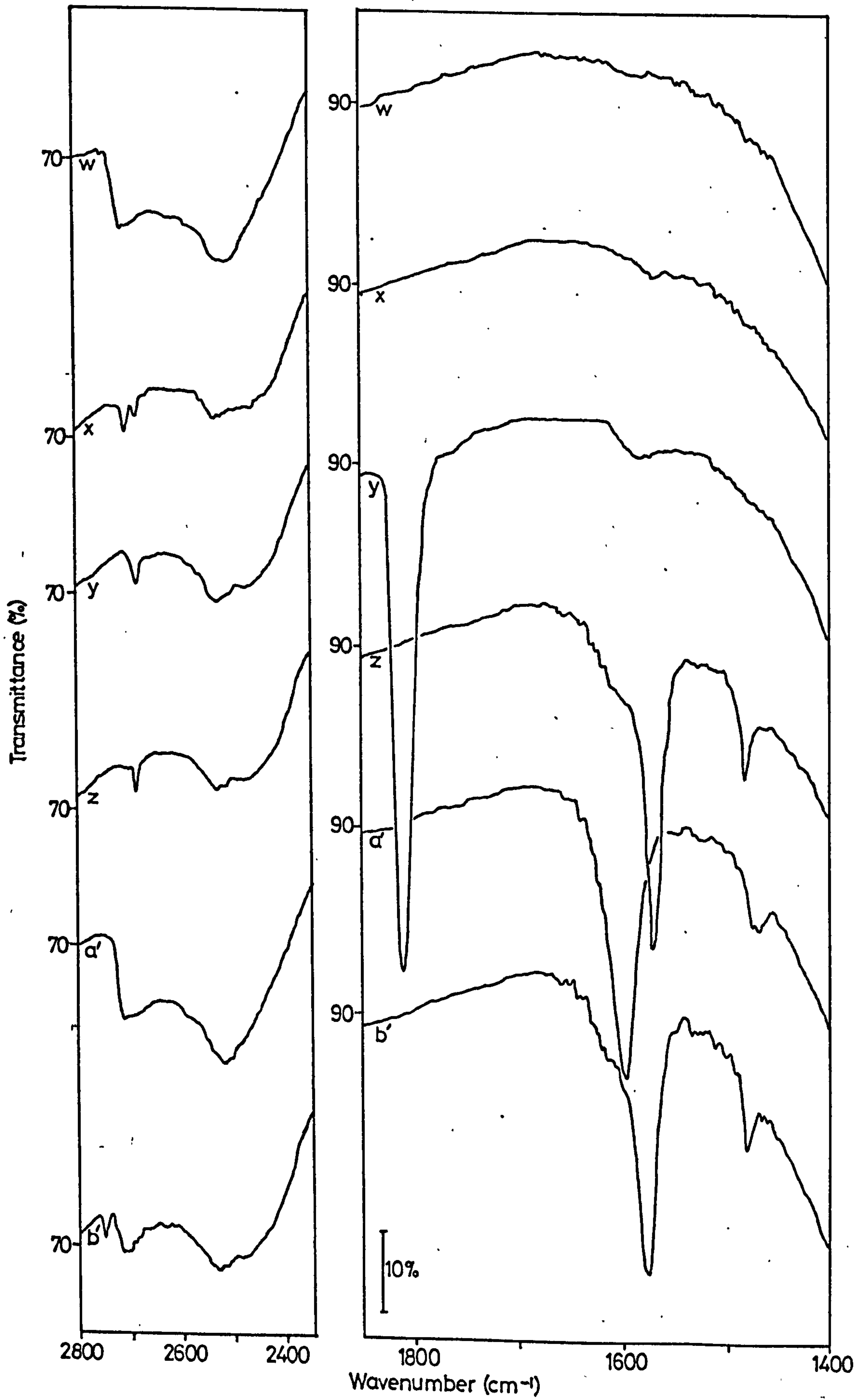
Spec 6.2 Adsorption of Hexafluoroacetone onto a BT D<sub>2</sub>O Oxidized Surface



Spec 6.2 Adsorption of Hexafluoroacetone onto a BT D<sub>2</sub>O Oxidized Surface



Spec 6.2 Adsorption of Hexafluoroacetone onto a BT D<sub>2</sub>O Oxidized Surface



Spec 6.2 Adsorption of Hexafluoroacetone onto a BT D<sub>2</sub>O Oxidized Surface

SPEC. 6.3

SPEC. 6.3

ADSORPTION OF HEXAFLUOROACETONE ONTO A

673 K, D<sub>2</sub>O, REDUCED SURFACE

Adsorption of hexafluoroacetone

- (a) Initial surface
- (b)-(f) exposure to increasing pressures

Adsorption of D<sub>2</sub>O and evacuation

- (g) BT, 1h (h) 473 K, 18h (i) 573 K, ½h

Adsorption of hexafluoroacetone

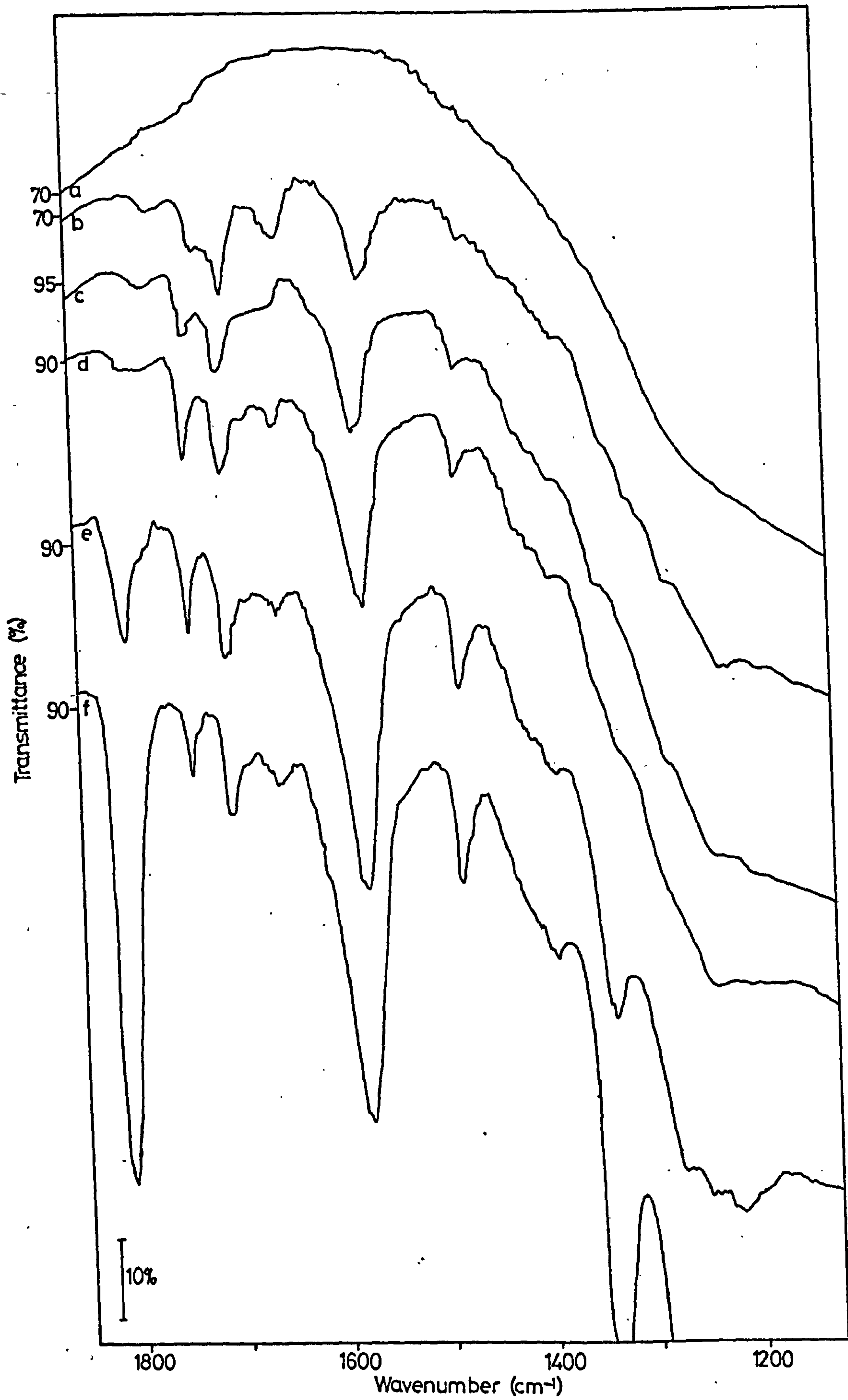
- (j) exposure to vapour

Evacuation

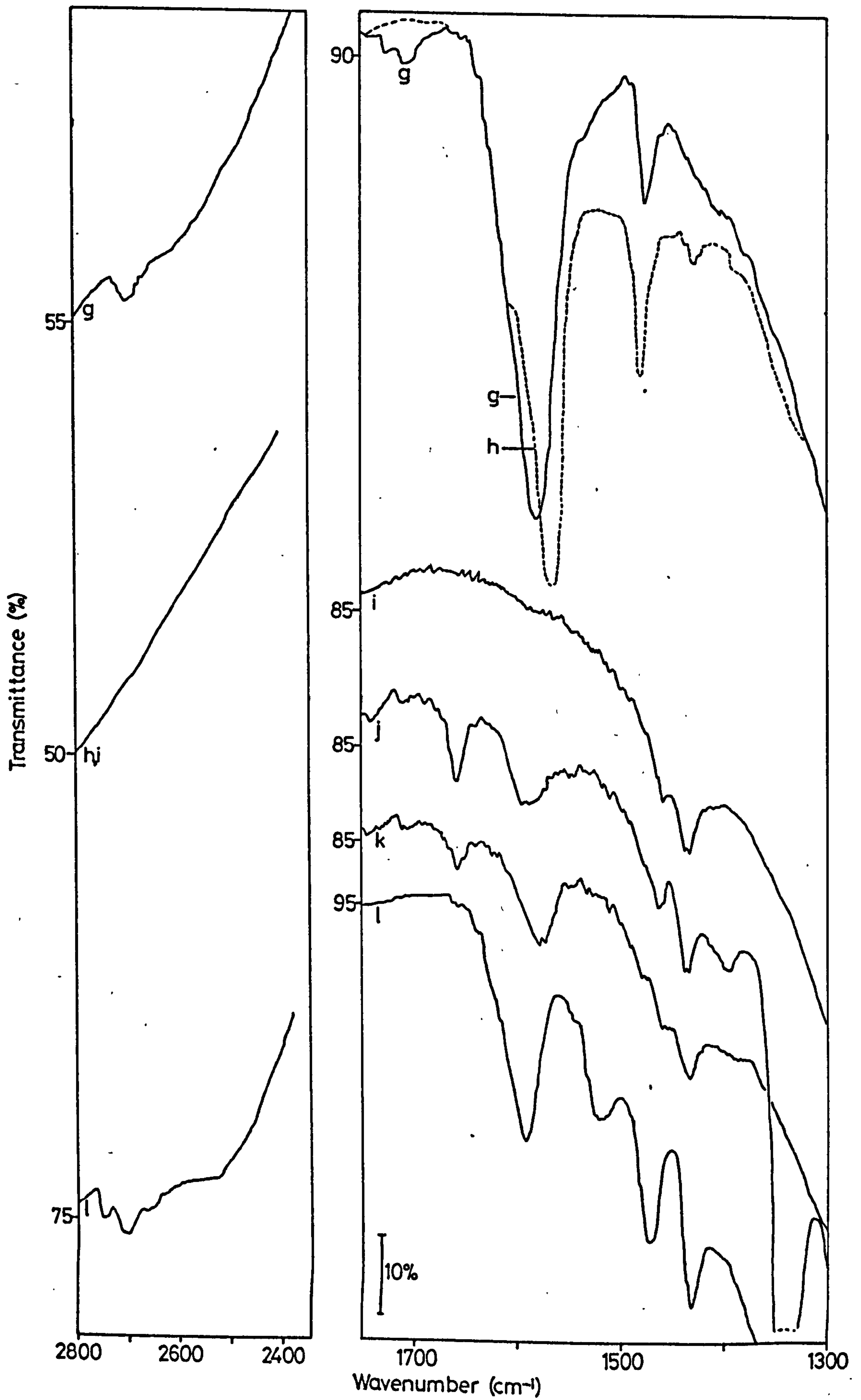
- (k) BT, 1h

Adsorption of D<sub>2</sub>O

- (l) disc exposed to D<sub>2</sub>O (473 K, 16h) and evacuated (BT, ½h)



Spec 6.3 Adsorption of Hexafluoroacetone onto a 673 K Reduced Surface



Spec 6.3 Adsorption of Hexafluoroacetone onto a 673 K Reduced Surface



SPEC. 6.4

SPEC. 6.4

ADSORPTION OF HEXAFLUOROACETONE ONTO A

BT, D<sub>2</sub>O, REDUCED SURFACE

Adsorption of hexafluoroacetone

- (a) Initial surface
- (b)-(e) exposure of the disc to increasing vapour pressures

Evacuation

- (f) BT, 1h

Adsorption of D<sub>2</sub>O

- (g) Exposure to D<sub>2</sub>O vapour (BT, 2h) and evacuation (BT, 1h)

Evacuation

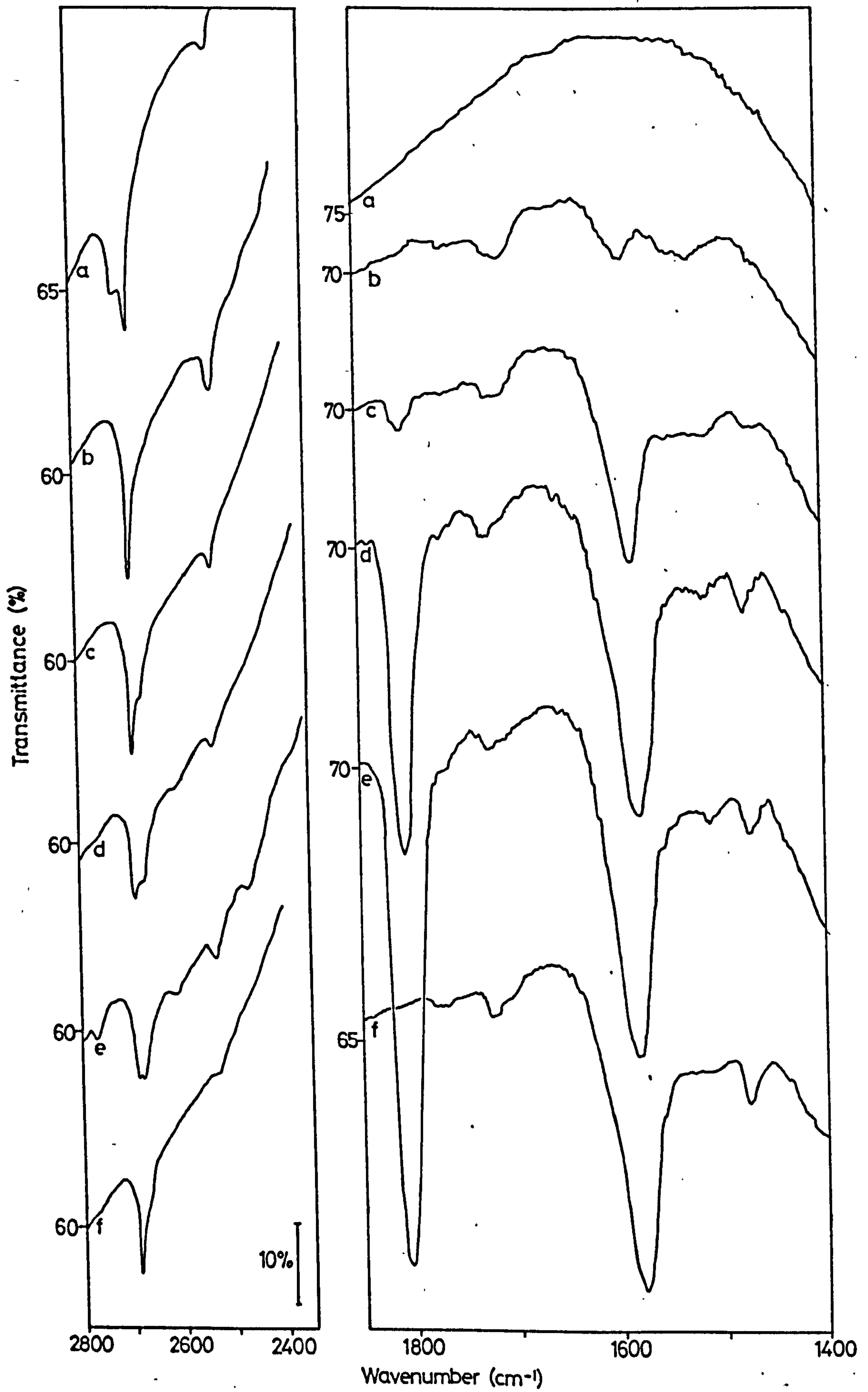
- (h) 588 K, 1h

Adsorption of D<sub>2</sub>O

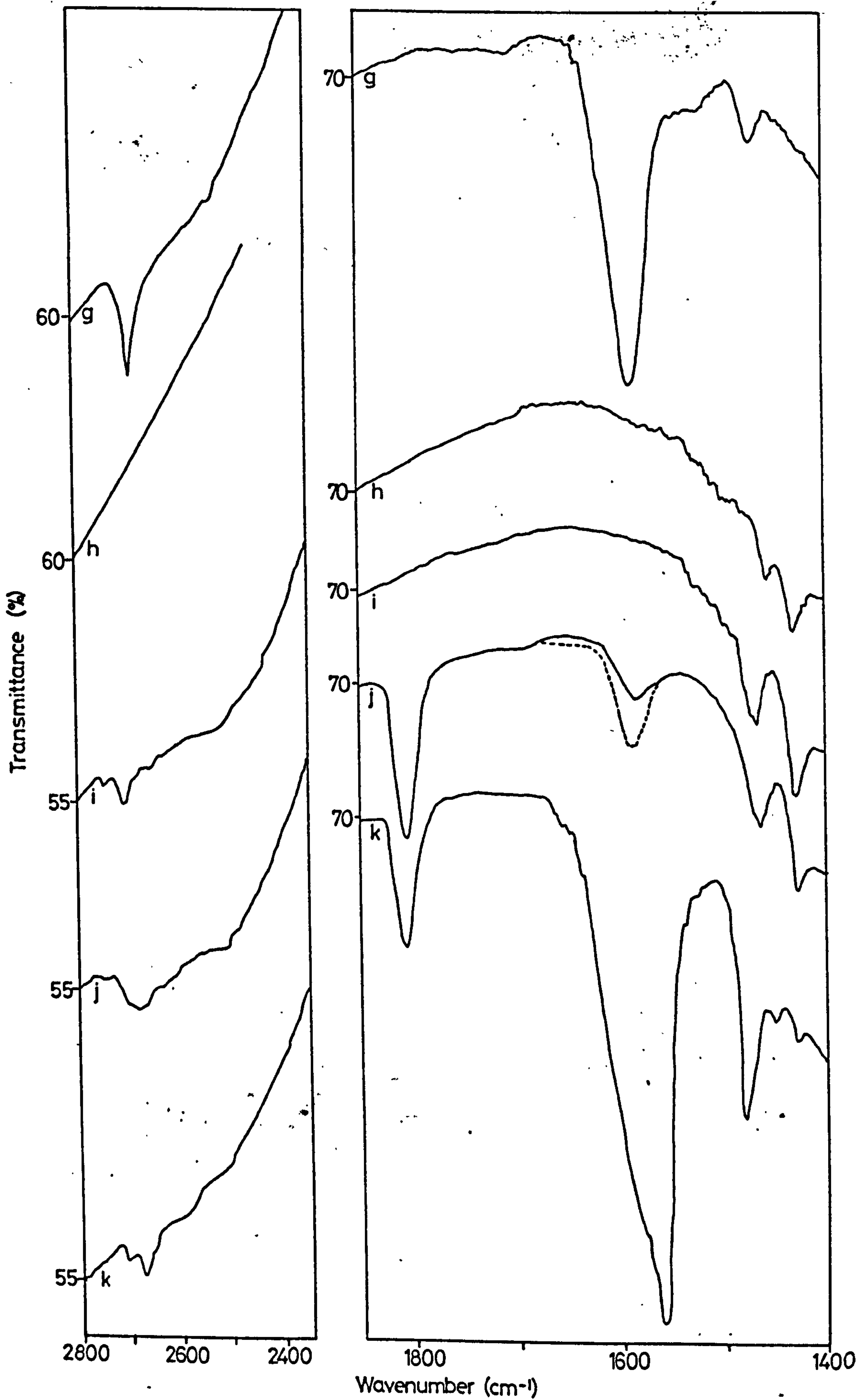
- (i) exposure to D<sub>2</sub>O vapour (473 K, 14h) and evacuation (BT, 1h)

Adsorption of hexafluoroacetone

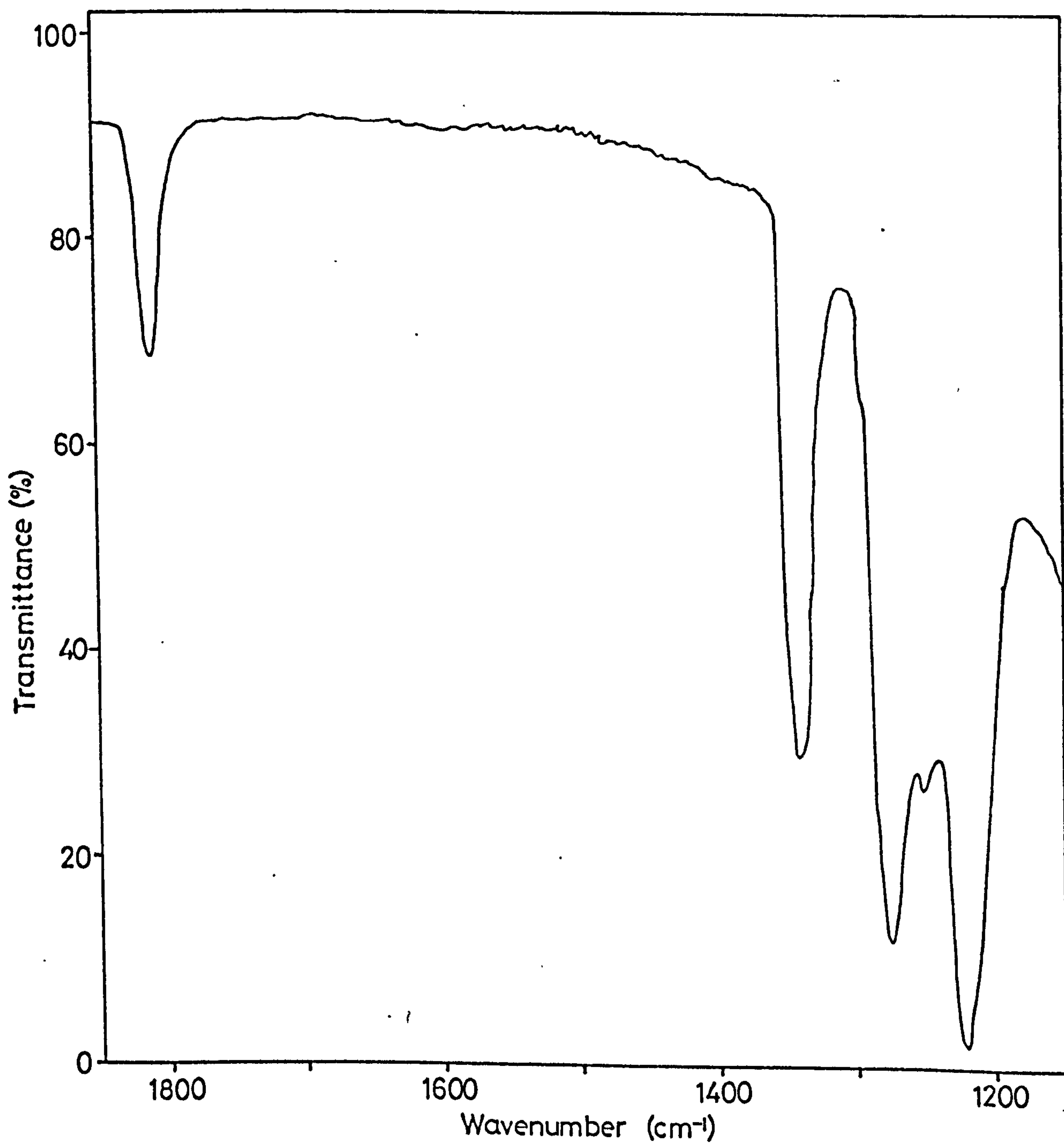
- (j) exposure of disc to vapour (BT)
- (k) exposure of disc to vapour (473 K, 1h)



Spec 64 Adsorption of Hexafluoroacetone onto a BT D<sub>2</sub>O Reduced Surface



Spec 6.4 Adsorption of Hexafluoroacetone onto a BT D<sub>2</sub>O Reduced Surface



Spec 6.5 Hexafluoroacetone vapour

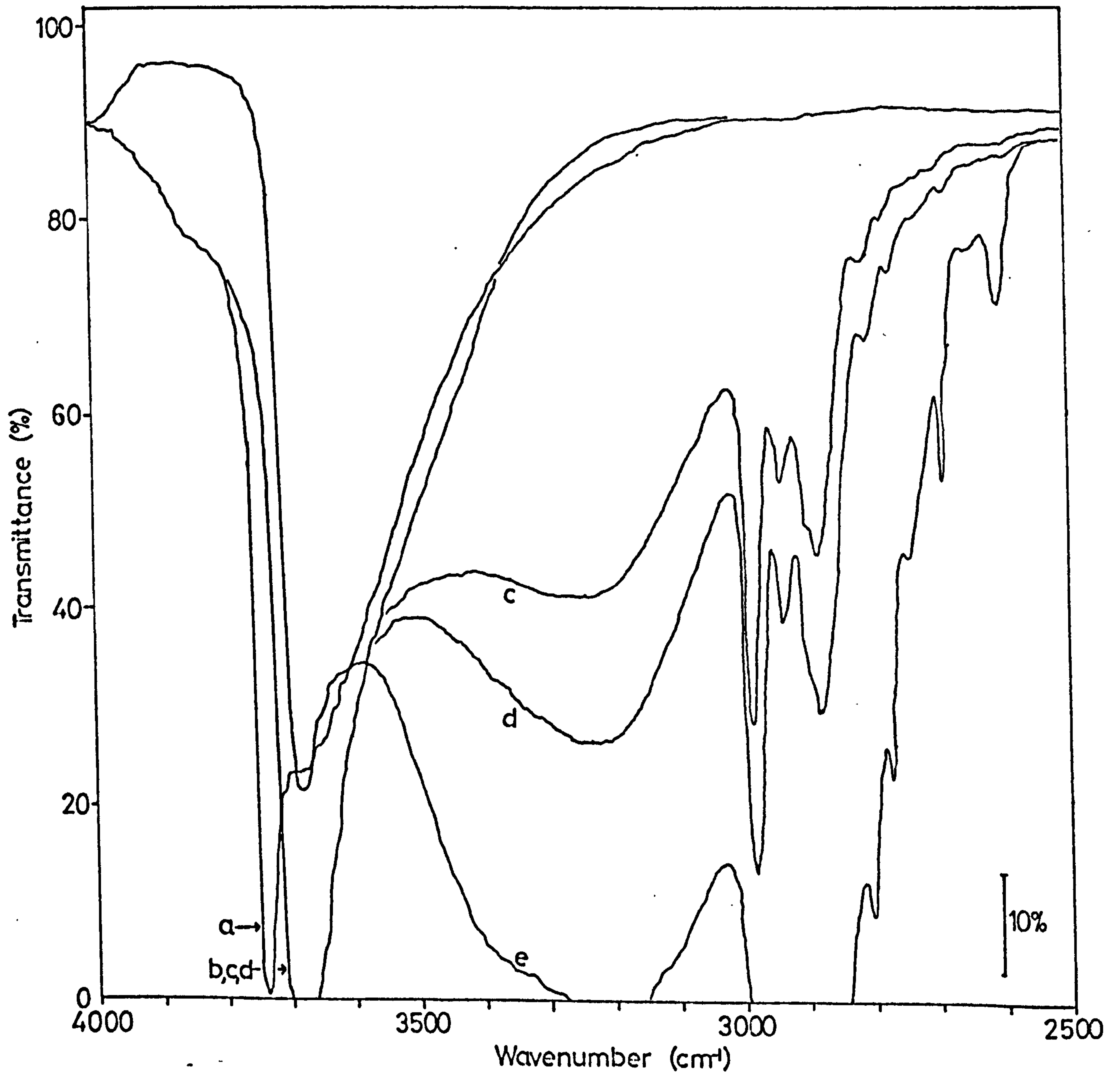
SPEC. 8.1

SPEC. 8.1

ADSORPTION OF DIETHYL ETHER ONTO SILICA

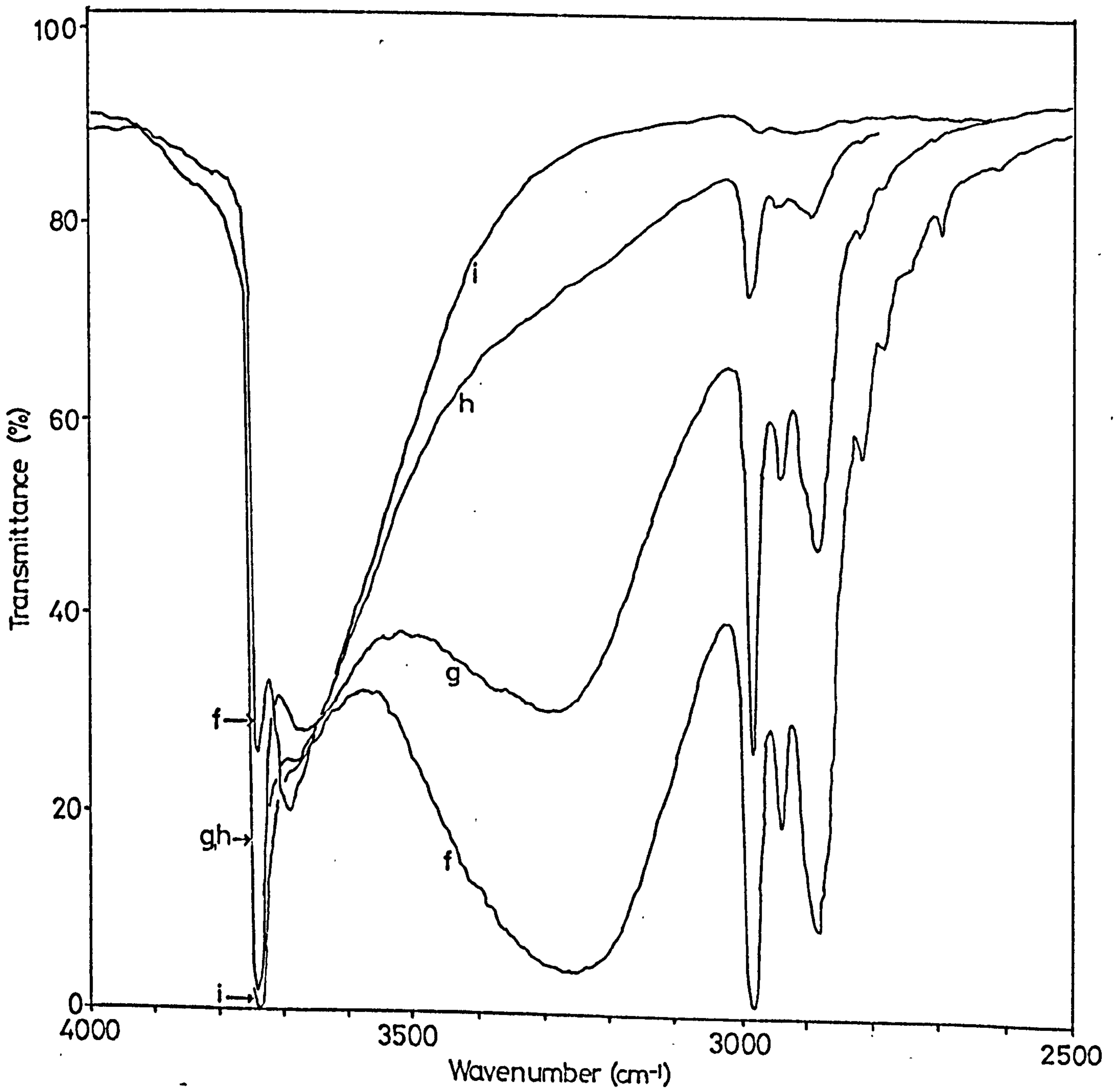
Spectra of silica after

- (a) initial treatment in flow of oxygen (673 K, 2h) and evacuation.
- (b) Immersion in carbon tetrachloride.
- (c)-(e) Contact with increasing concentrations of ether in carbon tetrachloride.
- (f)-(h) evacuation of solution.
- (i) final surface.



Spec 8.1 Adsorption of Ether onto Silica





Spec 8.1 Adsorption of Ether onto Silica

APPENDIX IV

REFERENCES

## REFERENCES

- 1 P. Jackson, Ph.D. Thesis, University of Nottingham, 1969.
- 2 J. Ramsbotham, Ph.D. Thesis, University of Nottingham, 1971.
- 3 C.N. Barwell, Fundamentals of Molecular Spectroscopy, McGraw-Hill, London, 1966.
- 4 G.M. Barrow, Introduction to Molecular Spectroscopy, McGraw-Hill, London, 1962.
- 5 M.L. Hair, Infrared Spectroscopy in Surface Chemistry, Marcell Dekker, New York, 1967.
- 6 L.H. Little, Infrared Spectra of Adsorbed Species, Academic Press, London, 1966.
- 7 C.H. Rochester, To be published.
- 8 R.J.H. Clark, Chemistry of Titanium and Vanadium, Elsevier, Amsterdam, 1969 Ch9.
- 9 British Titan Products Co. Ltd., Information Booklet.
- 10 P. Jackson and G.D. Parfitt, Trans. Faraday Soc. 1971, 67, 2469.
- 11 P. Jones and J.A. Hockey, Trans. Faraday Soc. 1971, 67, 2669.
- 12 C.H. Moore, Jr. Mining Trans. 1949, 184, 194.
- 13 F.A. Grant, Rev. Mod. Phys. 1959, 31, 646.
- 14 K.P. Wagstaff, Ph.D. Thesis, University of Nottingham, 1970.
- 15 W.H. Baur, Acta. Cryst. 1956, 9, 515.
- 16 R.D. Iyengar, M. Codell, J.S. Karra, J. Turkevich, J. Amer. Chem. Soc. 1966, 88, 5055.
- 17 P.C. Richardson, R. Rudham, A.D. Tullet, K.P. Wagstaff., J.C.S. Faraday I, 1972, 68, 2203.
- 18 R.G. Breckemridge and W.R. Hosler, Phys. Rev., 1953, 91, 793.

- 19 J.B. Goodenough, *Bull. Soc. Chim. France*, 1965, 1200.
- 20 Y.L. Sandler, *J. Physical Chem.*, 1954, 58, 54.
- 21 L.A. Bursill, B.G. Hyde, O. Teresaki, D. Watanabe, *Phil. Mag.*, 1969, 20, 347.
- 22 F. Garcia-Moliner, *Cat. Rev.*, 1968, 2, 1.
- 23 A. Clark, *The Theory of Adsorption and Catalysis*, Academic Press, New York, 1970.
- 24 Th. Wolkenstein, *Adv. Catalysis*, 1960, 12, 189.
- 25 D.A. Dowder, N. Mackenzie, B.M.W. Trapnell, *Proc. Roy. Soc. A.*, 1956, 237, 245.
- 26 P.C. Richardson and R.D. Rossington, *J. Cat.*, 1969, 14, 175.
- 27 P.C. Gravelle, F. Juillet, P. Meriaudeau, S.J. Teichner, *Disc. Faraday Soc.*, 1971, 52, 140.
- 28 C. Naccache, P. Meriaudeau, M. Che and A.J. Tench, *Trans. Faraday Soc.*, 1971, 67, 506.
- 29 M. Che, C. Naccache, and B. Imelik, *J. Cat.*, 1972, 24, 328.
- 30 E.N. Figurovskaya, *Kinetics and Catalysis (USSR)*, 1969, 10, 374.
- 31 V.F. Kiselev, *Bull. Acad. Sci. USSR.*, 1967, 176, 657.
- 32 A.J. Tyler, F.H. Hambleton and J.A. Hockey, *J. Catalysis*, 1969, 13, 35.
- 33 D. Kunath and A. Reklat, *Z. Chem.*, 1971, 11, 361.
- 34 A.V. Kiselev, V.A. Lokutsievskii and V.I. Lygin, *Russ. J. Phys. Chem.*, 1971, 45, 1510.
- 35 E. Gallei and G.A. Parks, *J. Coll. Int. Sci.*, 1972, 38, 650.
- 36 G.L. Haller and R.W. Rice, *J. Physic. Chem.*, 1970, 74, 4386.
- 37 N. Takezawa, *Bull. Soc. Chem. Japan*, 1971, 44, 3177.
- 38 G. Kortum and H. Delfs, *Spectrochim Acta.*, 1964, 20, 405.
- 39 P.J. Hendra, 'Chemisorption and Catalysis', Ed. P. Hepple, Institute of Petroleum, London, 1971, p80.

- 40 P.J. Hendra, J.R. Horder, and E.J. Loader, Chem. Comm., 1970, 563.
- 41 P. Jones and J.A. Hockey, Trans. Faraday Soc., 1971, 67, 2679.
- 42 P Jones and J.A. Hockey, J.C.S. Faraday I, 1972, 68, 907.
- 43 B.H. Soffer, J. Chem. Phys., 1961, 35, 940.
- 44 M. Primet, P. Pichat, M.V. Matieu, J. Phys. Chem., 1971, 75, 1216.
- 45 G.D. Parfitt, J. Ramsbotham, C.H. Rochester, Trans. Faraday Soc., 1971, 67, 841.
- 46 N.D. Parkyns, 'Chemisorption and Catalysis', ed. P. Hepple, Institute of Petroleum, London, 1971.
- 47 M. Primet, P. Pichat, and M.V. Matieu, J. Phys. Chem., 1971, 75, 1221.
- 48 G.D. Parfitt, J. Ramsbotham, C.H. Rochester, Trans. Faraday Soc., 1971, 67, 1500.
- 49 M. Primet, J. Bandiera, C. Naccache and M.V. Matieu, J. Chim. Phys., 1970, 67, 535.
- 50 M. Primet, J. Bandiera, C. Naccache and M.V. Matieu, J. Chim. Phys., 1970, 67, 1030.
- 51 P. Jackson and G.D. Parfitt, J.C.S Faraday I, 1972, 68, 896.
- 52 G.D. Parfitt, J. Ramsbotham, C.H. Rochester, Trans. Faraday Soc., 1971, 67, 3100.
- 53 M. Primet, J. Basset, M.V Matieu, M. Pettre, J. Phys. Chem., 1970, 74, 2868.
- 54 M. Primet, M. Che, C Naccache and M.V. Matieu, J. Chim. Phys., 1970, 67, 1629.
- 55 G.D. Parfitt, J. Ramsbotham, C.H. Rochester, J.C.S. Faraday I, 1972, 68, 17.
- 56 P. Jackson and G.D. Parfitt, J.C.S Faraday I, 1972, 68, 1443.
- 57 A.F. Sherwood and S.M. Rybika, J. Oil Colour Chemists' Assoc., 1966, 49, 648.

- 58 A.V. Kiselev and A.V. Uvarov, *Surface Sci.*, 1967, 6, 399.
- 59 F. Bozon-Verduraz, *J. Cat.*, 1970, 18, 12.
- 60 A. Buckland, J. Ramsbotham, C.H. Rochester and M.S. Scurrrell, *J. Phys. E.*, 1971, 4, 146.
- 61 D.R. Ashmead and R. Rudham, *Chem. and Ind.*, 1962, 401.
- 62 H.H. Read, 'Rutleys Mineralogy' 25th Ed., George Allen & Urwin Ltd., a) p311 b) p90 c) 124, London, 1962.
- 63 K.E. Lewis and G.D. Parfitt, *Trans. Faraday Soc.*, 1966, 62, 204.
- 64 M. Ceccaldi, M. Goldman and E. Roth, *Colloquium Spectroscopicum Inter. VI* (Amsterdam 1956) Pergamon Press.
- 65 C.G. Armistead, A.J. Tyler, F.H. Hambleton, S.A. Mitchell and J.A. Hockey, *J. Phys. Chem.*, 1969, 73, 3947.
- 66 J.B. Peri, *J. Phys. Chem.*, 1965, 69, 220.
- 67 H.P. Boehm, *Disc. Faraday Soc.*, 1971, 52, 264.
- 68 K. Atherton, G. Newbold and J.A. Hockey, *Disc. Faraday Soc.*, 1971, 52, 33.
- 69 P.J. Anderson, R.F. Horlock and J.F. Oliver, *Trans. Faraday Soc.*, 1965, 61, 2754.
- 70 R.E. Day, *Thesis*, Nottingham, 1966.
- 71 G. Munuera and F.S. Stone, *Disc. Faraday Soc.*, 1971, 52, 205.
- 72 R.I. Bickley and R.K.M. Jayanty, *Disc. Faraday Soc.*, 1971, 52, 226.
- 73 J.C.R. Waldsax, M.J. Jaycock, *Disc. Faraday Soc.*, 1971, 52, 231.
- 74 T. Morimoto, M. Nagao and T. Omori, *Bull. Chem. Soc. Japan*, 1969, 42, 943.
- 75 P.J. Anderson and P.L. Morgan, *Trans. Faraday Soc.*, 1964, 60, 930.

- 76 M.L. Hair and W. Hertl, J. Phys. Chem., 1970, 74, 91.
- 77 F Freund, J. Amer. Ceram. Soc., 1967, 50, 493.
- 78 T.A. Ford and Michael Falk, J. Mol. Structure, 1969, 3, 445.
- 79 K. Nakamoto, M. Margoshes and R.E. Rundle, J. Amer. Chem. Soc., 1955, 77, 6480.
- 80 O. Glenster and E. Hartert, Z. anorg. Chem., 1956, 283, 111.
- 81 G.C. Pimentel and A.L. McClellan, The Hydrogen Bond (W.H. Freeman and Company, San Francisco, 1959).
- 82 M. van Thiel, E.D. Becker and G.C. Pimentel, J. Chem. Phys., 1957, 27, 486.
- 83 E. Cartmell and G. Fowles, Valency and Molecular Structure, Butterworths, London, 1961.
- 84 R.E. Day, G.D. Parfitt and J. Peacock, To be published.
- 85 A.V. Kiselev and A.V. Uvarov, Surface Sci., 1967, 6, 399.
- 86 P.A. Elkington and C. Curhoy, J. Colloid Interface Sci., 1961, 28, 331.
- 87 P. Fink, Rev. Roumaine Chim., 1969, 14, 811.
- 88 A.V. Deo, T.T. Chuang, I.G. Dalla Lana, J. Phys. Chem., 1971, 75, 234.
- 89 H. Winde, Z. Chem., 1970, 10, 64.
- 90 A.A. Kadushin, Yu.N. Rufov and S.Z. Roginski, Kinetics and Catalysis (USSR), 1967, 8, 1147.
- 91 A.A. Kadushin, Yu.N. Rufov and S.Z. Roginski, Bull. Acad. Sci. (USSR), 1968, 697.
- 92 A.A. Kadushin and S.Z. Roginski (CA 74 35116x), Probl. Kinet. Katal., 1970, 14, 166.

- 93 V.Ya. Danyushevskii, L.I. Lafer, V.I. Yakerson, A.M. Rubenshtein, L.A. Gorskaya, Bull. Acad. Sci. (USSR), 1970, 789.
- 94 R. Rudham, Private Communication.
- 95 I.R. Shannon, I.J.S. Lake and C. Kemball, Trans. Faraday Soc., 1971, 67, 585.
- 96 R. Fujii, J. Chem. Soc. Japan, Pure Chem. Sect., 1948, 69, 151.
- 97 J.D. Roberts and M.C. Caserio, Basic Principles of Organic Chemistry, (W.A. Benjamin, inc. New York, 1965).
- 98 I.L. Finar, Organic Chemistry Vol. I, (Longmans, Green and Co. Ltd., London, 1967).
- 99 D. Schartz and B. Larsen, J. Less-Common Metals, 1963, 5, 365.
- 100 B.P. Susz and A. Lachavanne, Helv. Chim. Acta., 1958, 41, 634.
- 101 W.M. Craven and N. Peterson, J. Inorg. Nuclear Chem., 1969, 31, 1743.
- 102 Ram. Chand Paul and S.L. Chada, J. Inorg. Nuclear Chem., 1969, 31, 1679.
- 103 P. Chalanden and B.P. Susz, Helv. Chim. Acta., 1958, 41, 697.
- 104 L.J. Bellamy, Advances in Infrared Group Frequencies (Methuen, London 1968).
- 105 R.G. Greenler, J. Chem. Phys., 1962, 37, 2094.
- 106 K.K. Ito and H.J. Bernstein, Canad. J. Chem., 1956, 34, 170.
- 107 G. Dellepiane and J. Overend, Spectrochim. Acta., 1966, 22, 593.
- 108 R. Mecke and K Noack, Chem. Ber., 1960, 93, 210.
- 109 E.C. Craven and W.R. Ward, J. Appl. Chem., 1960, 10, 18.
- 110 K. Noack, Spectrochim. Acta., 1962, 18, 703.
- 111 M.J. Jaycock and J.C.R. Waldsax, J. Chem. Soc., Farad. Trans. I, 1974, 70, 1501.



- 112 H. Miyata, Y. Toda, Y. Kubokawa, *J. Cat.*, 1974, 32, 155.
- 113 Nakamoto, *Infrared of Inorganic Coordination Compounds*, Wiley, 1963.
- 114 S.D. Ross, *Inorganic Infrared and Raman Spectra*, McGraw Hill, 1972.
- 115 A.I. Grigor'ev, *Russ. J. Inorg. Chem.*, 1963, 8, 409.
- 116 D.A. Edwards and R.N. Hayward, *Canad. J. Chem.*, 1968, 46, 3443.
- 117 M.J.D. Low, H. Jacobs and N. Takezawa, *Water, Air and Soil Pollution*, 1973, 2, 61.
- 118 S. Hayashi, T. Takenaka and R. Gotoh, *Bull. Inst. Res. Kyoto Univ.*, 1969, 47, 378.
- 119 G. Munuera, *J. Cat.*, 1970, 18, 19.
- 120 J.V. Evans and T.L. Whateley, *Trans. Faraday Soc.*, 1967, 63, 2769.
- 121 B.J. Fontana and J.R. Thomas, *J. Phys. Chem.*, 1961, 65, 480.
- 122 B.J. Fontana, *J. Phys. Chem.*, 1963, 67, 2360.
- 123 B.J. Fontana, *J. Phys. Chem.*, 1966, 70, 1801.
- 124 M.J.D. Low and M. Hasegawa, *J. Colloid. Int. Sci.*, 1968, 26, 95.
- 125 M. Hasegawa and M.J.D. Low, *J. Colloid Int. Sci.*, 1969, 29, 593.
- 126 M. Hasegawa and M.J.D. Low, *J. Colloid. Int. Sci.*, 1969, 30, 378.
- 127 D.M. Griffiths, K. Marshall, and C.H. Rochester, *J.C.S. Faraday I*, 1974, 70, 400.
- 128 K. Marshall and C.H. Rochester, *J.C.S. Faraday I*, 1975, 71, 1754.
- 129 M.L. Hair and W. Hertl, *J. Phys. Chem.*, 1970, 74, 91.
- 130 G.A. Galkin, A.V. Kiselev and V.I. Lygin, *Russ. J. Phys. Chem.*, 1967, 41, 20.
- 131 H. Arai, Y. Saito and Y. Yoneda, *J. Catalysis*, 1968, 10, 128.
- 132 M.F. Lappert, *J. Chem. Soc.*, 1962, 542.

- 133 D. Cook, *Can. J. Chem.*, 1963, 41, 522.
- 134 M.L. Hair and I.D. Chapman, *J. Phys. Chem.*, 1965, 69, 3949.
- 135 C.G. Krespan and W.J. Middleton, *Fluorine Chem. Rev.*, 1967, 1, 145.
- 136 E.L. Pace, A.C. Plaush and H.V. Samuelson, *Spectrochem. Acta.*, 1966, 22, 993.
- 137 W.J. Middleton and R.V. Lindsey, *J. Amer. Chem. Soc.*, 1964, 86, 4948.
- 138 J.H. Prager and P.H. Ogden, *J. Org. Chem.*, 1968, 33, 2100.
- 139 G.C. Nicholson and P.H. Ogden, *J. Inorg. Nucl. Chem.*, 1968, 30, 2617.
- 140 P. Sartori and M. Weidenbruch, *Chem. Ber.*, 1967, 100, 2049.
- 141 C.H. Rochester- Private Communication.
- 142 K.M. Marshall, Thesis, University of Nottingham, 1975.